Dielectric and Precursor Analysis to Study Metabolic Effects on CHO Cell Viability and Antibody Glycosylation

by

Katrin Braasch

A Thesis submitted to the Faculty of Graduate Studies of
The University of Manitoba
in partial fulfillment of the requirements of the degree of

DOCTOR OF PHILOSOPHY

Department of Microbiology
University of Manitoba
Winnipeg

ACKNOWLEDGMENTS

I would like to thank my supervisor, Dr. Michael Butler, for his constant support and guidance throughout my Grad Studies, as well as all the opportunites. I would also like to thank Dr. Deborah Court and Dr. David Levin, members of my advisory committee, for their helpful advice and support. Furthermore a thank you to my external examiner, Dr. Michael Kallos, for his criticism and advise to improve this thesis. In addition, I would like to thank the following people:

- Dr. Douglas Thomson, Dr. Gregory Bridges, Dr. Marija Nikolic-Jaric, Elham Salimi, Dr. Tim Cabel, Ashlesha Bhidea, Bahareh Saboktakin Rizi, Kaveh Mohammad, and Samaneh Afshar for their insight, collaboration and support with the dielectric portion of this project.
- Vincent Jung and Dr. Maureen Spearman for their technical support and helpful advice.
- To all members of the Butler lab, past and present, that I had the opportunity to work with: Natalie Krahn, Sarah Chan, Dr. Ben Dionne, Dr. Venkata Tayi, Neha Mishra, Carina Villacres, Viridiana Urena Ramirez, Bo Liu, Alan Froese, Teslin Sandstrom and Rachel Rudney. Thank you for your support and constant discussion.

I am also grateful to my husband, Paul, and my family for their encouragement and support throughout this time.

The work for this thesis was supported by a Natural Science and Engineering Research Council network research grant. A Manitoba Graduate Scholarship and a Faculty of Science Graduate Scholarship are also gratefully acknowledged.

ABSTRACT

The main goal in biopharmaceutical production is achieving high volumetric productivity while maintaining product quality (i.e. glycosylation). The objectives of this project were to explore the use of dielectric analysis in the early detection of cell demise and to analyze the impact of nucleotide / nucleotide sugar precursor feedings in biopharmaceutical production and glycosylation.

Measurements of changes in the polarizability of individual cells can be performed in a dielectrophoretic (DEP) cytometer designed at the University of Manitoba. In this instrument the trajectory of individual cells was tracked according to their polarizability and recorded as a force index (FI). The identified sub-populations from a batch bioreactor and apoptosis-induced cultures were correlated with the fluorescent markers of apoptosis analyzed in a flow cytometer. Discrete cell sub-populations were identified as cells passed through the various stages of apoptosis. In the batch and the starvation culture the early changes in the measured FI of cells correlated with the Annexin V fluorescent assay associated with early phase apoptosis. For the oligomycin and staurosporine cultures changes in the FI could be correlated to modifications in the mitochondrial metabolism linked with early apoptosis for both inducers.

In fed-batch experiments 10 mM galactose alone or 20 mM galactose in combination with 1 mM uridine or 1 mM uridine + 8 μM $MnCl_2$ was added to the basal and feed medium for two CHO cell lines to determine their impact on the biopharmaceutical production and the glycosylation process. The results showed that the addition of all three precursors combined increased UDP-Gal, which increased and maintained the galactosylation index during the bioprocess for CHO-EG2 and CHO-DP12 cultures by 25.4% and 37.9%, respectively, compared to the non-supplemented fed-batch culture. In both cell lines saturation was reached when a

further increase in the UDP-Gal concentration did not increase the galactosylation. A negative impact on cell growth was observed with the uridine addition in the CHO-EG2 culture, which was linked to the CHO-EG2 cell line being $DHFR^{-/-}$.

This work presents a dielectric detection method to monitor early changes in the cell metabolism and information for shifting and maintaining galactosylation during biopharmaceutical production.

LIST OF ABBREVIATION

7-AAD	7-aminoactinomycin
ADCC	Antibody-dependent cellular cytotoxicity
ADP	Adenosine diphosphate
AEC	Adenylate Energy Charge (ATP + 0.5 ADP)/(ATP + ADP + AMP)
AMP	Adenosine monophosphate
ATP	Adenosine triphosphate
CDC	Complement-dependent cytotoxicity
CDP	Cytidine diphosphate
CHO	Chinese hamster ovary
CTP	Cytidine triphosphate
DEP	Dielectrophoresis
ELISA	Enzyme linked Immuno Sorbent Assay
EDTA	(Ethylene dinitrilo)-tetraacetic acid
FI	Fucosylation index
GDP	Guanosine diphosphate
GI	Galactosylation index
GTP	Guanosine triphosphate
HILIC	Hydrophilic interaction liquid chromatography
HPLC	High performance liquid chromatography
IVCD	Integral viable cell density
NTP	Nucleotide triphosphate
NTP ratio	(ATP + GTP)/((UDP-GlcNAc + CTP) + UTP)

NTP/U ratio	NTP ratio/ U-ratio
PBS	Phosphate-buffered saline
PS	Phosphatidylserine
q_G	Specific glucose consumption rate
q_L	Specific lactate production rate
SI	Sialylation index
UDP-Glc	Uridine diphosphate-glucose
UDP-GalNac	Uridine diphosphate-N-acetylgalactosamine
UDP-GlcNac	Uridine diphosphate-N-acetylglucosamine
UDP-GNac	Sum of UDP-GalNac and UDP-GlcNac
U-ratio	UTP/UDP-GNac
UTP	Uridine triphosphate
$Y_{Lac/Glc}$	Yield coefficient; moles of lactate produced per mole of glucose utilized
μ_{max}	Maxium growth rate

TABLE OF CONTENTS

Section B

Nucleotide sugar precursor feeding for manipulation of glycosylation

LIST OF FIGURES

LIST OF TABLES

LIST OF COPYRIGHT MATERIAL

Abu-Absi, S., Xu, S., Graham, H., Dalal, N., Boyer, M., Dave, K. (2014), Cell culture process operations for recombinant protein production: in Mammalian Cell Cultures for Biologics Manufacturing (ed. Weichang Zhou and Anna Kantardjief), 139: 35-68. Advances in Biochemical Engineering / Biotechnology. Springer. [Figure 2, p. 38; Figure 4, p. 40]

Braasch, K, Nikolic-Jaric, M, Cabel, T, Salimi, E, Bridges, GE, Thomson, DJ, Butler, M. (2013), The changing dielectric properties of CHO cells can be used to determine early apoptotic events in a bioprocess. Biotechnology and Bioengineering 110 (11): 2902-2914.

Braasch, K., Villacres, C., and Butler, M. (2015), Evaluation of quenching and extraction methods for nucleotide / nucleotide sugar analysis: in Glyco-Engineering: Methods and Protocols (ed. Alexandra Castilho), Methods in Molecular Biology. Humana Press.

Butler, M., Spearman, M. and Braasch, K. (2014), Monitoring cell growth, viability and apoptosis: in Animal Cell Biotechnology – Methods and Protocols (ed. Ralf Poertner), 1104: 169-192. Methods in Molecular Biology. Humana Press.

Dwek, R. A., Butters, T. D., Platt, F., Zitzmann, N. (2002) Targeting glycosylation as a therapeutic approach. Nature Reviews Drug Discovery. 1: 65-75. [Figure 1]

Freeze, H. H., Elbein, A. D. (2009), Glycosylation Precursors. In: Varki, A., Cummings, R. D., Esko, J. D., et al., editors. Essentials of Glycobiology. 2nd edition. Cold Spring Harbor (NY): Cold Spring Harbor Laboratory Press. Chapter 4 [Figure 4.1]

Wesolowski, J., Alzogaray, V., Reyelt, J., Unger, M., Juarez, K., Urrutia, M., Cauerhff, A., Danquah, W., Rissiek, B., Scheuplein, F., Schwarz, N., Adriouch, S., Boyer, O., Seman, M., Licea, A., Serreze, D. V., Goldbaum, F. A., Haag, F., Koch-Nolte, F. (2009), Single

domain antibodies: promising experimental and therapeutic tools in infection and immunity. Medical Microbiology and Immunology. 198: 157-174. [Figure 1, p. 158]

Yeo, J. H. M., Lo, J. C. Y., Nissom, P. M., Wong, V. V. T. (2006), Glutamine or glucose starvation in hybridoma cultures induces death receptor and mitochondrial apoptotic pathways. Biotechnology Letters. 28: 1445-1452. [Figure 5, p.1451]

Chapter 1

Introduction[*]

1.1 Biopharmaceuticals

Biopharmaceuticals are proteins or nucleic acid based products with pharmaceutical qualities that are produced in an engineered biological source (Walsh, 2002). Many of the biopharmaceuticals produced are glycoproteins. Animal cell cultures have been used in the bioprocesses of these biopharmaceuticals because of their capacity to perform the post-translational modifications needed of these glycoproteins (Varki et al., 2008). Among mammalian cell cultures, Chinese hamster ovary (CHO) cells are the most commonly used for the production of recombinant glycoproteins as they have been well characterized, and are known to produce human-like glycosylation (Durocher and Butler, 2009; Ghaderi et al., 2012).

[#]Within the last decade there has been a rapid and increasing demand for the large-scale production of glycoproteins – especially antibodies – from mammalian cell culture processes (Butler, 2005). This demand is driven by the application of these molecules as biopharmaceuticals for unmet medical needs (Walsh, 2010). To meet this high demand significant improvements have been made in cell line engineering including the development of

---

[*] Partial content of this chapter was included in several papers (see specific indication when section is a direct copy):
[#]Braasch, K., Nikolic-Jaric, M., Cabel, T., Salimi, E., Bridges, G.E., Thomson, D.J., and Butler, M. (2013), The changing dielectric properties of CHO cells can be used to determine early apoptotic events in a bioprocess. Biotechnology and Bioengineering. 110 (11): 2902-2914.
[$]Butler, M., Spearman, M. and Braasch, K. (2014), Monitoring cell growth, viability and apoptosis: in Animal Cell Biotechnology – Methods and Protocols (ed. Ralf Poertner), 1104: 169-192. Methods in Molecular Biology. Humana Press.
[~]Braasch, K., Villacres, C., and Butler, M. (2015), Evaluation of quenching and extraction methods for nucleotide / nucleotide sugar analysis: in Glyco-Engineering: Methods and Protocols (ed. Alexandra Castilho), 1321: 361-372. Methods in Molecular Biology. Humana Press.

mammalian expression vectors (Bebbington et al., 1992; Lucas et al., 1996) and the addition of anti-apoptotic genes (Kim and Lee, 2002; Mastrangelo et al., 2000; Tey et al., 2000) to enhance specific and volumetric productivity. In media development the ability to formulate media based on the cells metabolic needs and the addition of sodium butyrate (Mimura et al., 2001) as well as other small chemicals has shown to increase the recombinant protein production in a bioprocess. Most importantly all of these developments in bioprocess techniques have improved the recombinant protein titers achieved. By changing from batch to optimized fed-batch processes cells stay metabolically active over extended periods of culture time increasing volumetric productivity up to 1-5 g/L for antibodies (De Jesus and Wurm, 2011; Lim et al., 2010).

While these improvements increase cell specific and volumetric productivity the monitoring of cell density and viability during a bioprocess is still pivotal. In a bioprocess the cell density and viability are used as indicators to determine the optimal point to starting feeding in a fed-batch culture and to determine the end point of a culture. Monitoring the cell viability in a bioprocess is especially important in connection to the biopharmaceutical produced in the process. As the cell viability decreases cells in the culture will lyse releasing enzymes that can degrade the proteins or their glycan structures produced in the bioprocess (Winchester, 2005). This will affect not only the volumetric productivity but also the product quality negatively.

The attached glycan structures of glycoproteins have been shown to affect their physiological and pharmacological properties (Butler, 2009) important in regards to their specific application. Because of this impact of the glycan structure – especially in antibodies (Koide et al., 1977) – different pathways have been explored to change the glycosylation to optimize the function of the particular glycoprotein. The knockout or addition of genes that play a role in glycosylation has resulted in changes in the glycan profile of these cells (Wong et al., 2006;

Wong et al., 2010). However, even the simple addition of precursors has shown an impact on the final glycan profile (Wong et al., 2010; Hills et al., 2001).

For many decades the main problem was the overall low productivity in mammalian cell processes. These problems have been solved and processes are consistently achieving high final titers. Now the focus is shifting to the production of biopharmaceuticals with improved effector functions. Because the effector function of glycoproteins is based on their glycan structure different strategize to optimize the glycosylation in a bioprocess are currently explored. Overall it is important in a bioprocess to not only achieve high volumetric productivity by extending the culture run but also to ensure the desired high and consistent quality in the final product.

1.2 Antibodies

Antibodies not only play a significant part in our immune system but they also make up a very important portion of the biopharmaceutical glycoproteins produced. The first therapeutic monoclonal antibody, Orthoclone OKT3, was approved in 1986 (Ecker et al., 2015). Since the release of this antibody many other therapeutic monoclonal antibodies or related products have been introduced to the market to treat a variety of diseases. In 2013 antibodies represented half of the overall sales of biopharmaceutical products (Ecker et al., 2015). This sale revenue represented a 90% increase compared to sales in 2008, while the sales of other recombinant proteins experienced a much smaller increase of only ~26% (Ecker et al., 2015). As of late 2014, 47 monoclonal antibodies have been approved as therapeutic agents (Ecker et al., 2015). Hence, antibodies have become the largest portion of therapeutic glycoproteins because of their unique ability to be used in therapeutic and diagnostic applications. Thirty-one of the antibodies on today's market are full-length monoclonal antibodies with a size of ~150 kDa. Smaller

antibodies or antibody fragments are currently becoming of interest due to their potential increased ability to penetrate tissue and tumors making them better for diagnostic purposes. For example, a camelid single domain antibody (sdAb) linked to a human Fc region (cHCAb ~80 kDa) has shown improvements in tumor penetration (Bell et al., 2010).

1.2.1 Antibody DP12

The CHO-DP12 (CHO-K1) cell line produces a regular full-length recombinant human anti-IL-8 antibody (~150 kDa) that inhibits the binding of interleukin 8 (IL-8) to human neutrophils (Figure 1.1a). The IgG antibody has one glycosylation site in the Fc region (CH2 domain).

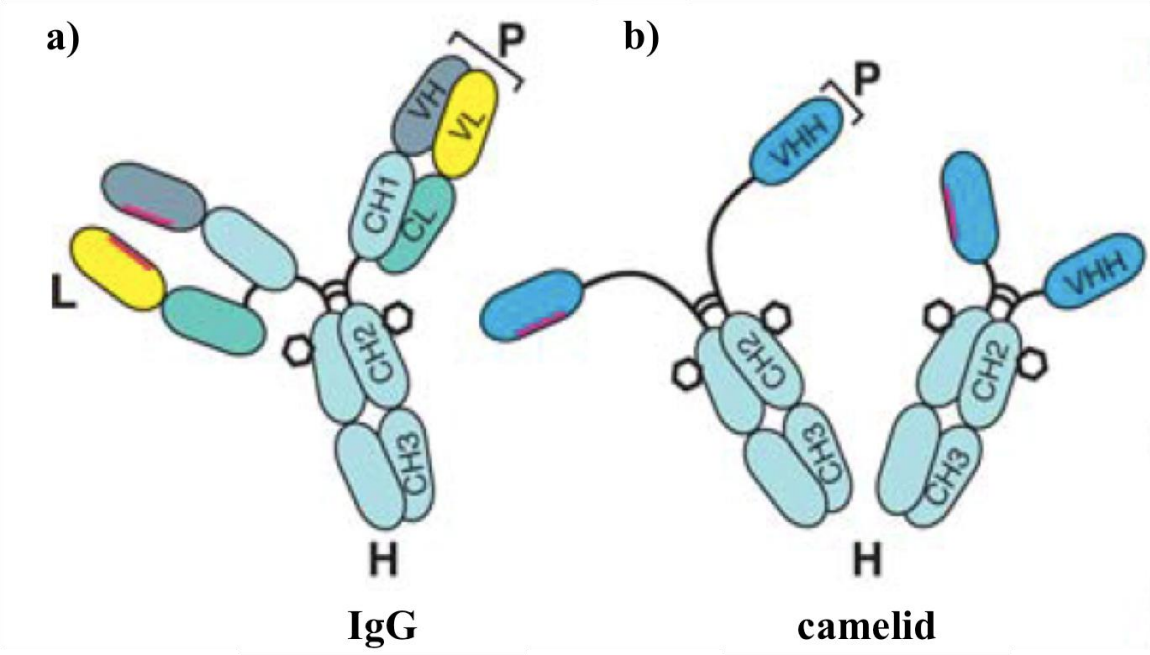

Figure 1.1: Comparison of the regular IgG (DP12) and the camelid (EG2) antibody. (adapted from Wesolowski et al., 2009; p. 158).

1.2.2 Antibody EG2

The CHO-EG2 (CHO-DG44) cell line produces a chimeric antibody consisting of a camelid single domain variable heavy chain (sdHC) fused with a human Fc (~80 kDa) (Bell et al., 2010) (Figure 1.2b). The single domain derived from a camelid heavy chain antibody (HCAb) binds to the epidermal growth factor receptor, which is usually overexpressed in tumors (Sebastian et al., 2006). The sdHc is derived from a camelid antibody, which is unique in that it contains no light chains (Hamers-Castermann et al., 1993). That makes the sdHC the smallest antibody-binding fragment with a size of 12 – 15 kDa (Bell et al., 2010). The human Fc portion is fused to the sdHC to reduce immunogenicity and to ensure proper antibody-dependent cellular cytotoxicity (ADCC) and complement-dependent cytotoxicity (CDC) activity. Like the CHO-DP12 antibody this antibody has the usual glycosylation site in the Fc region.

1.3 Mammalian cell culture

To this date ~94 % of all antibodies on the market are produced in mammalian cells (Ecker et al., 2015). While mammalian cells are more difficult to grow and usually produce lower titers than bacterial cells they are continuing to be the preferred production vessel for antibodies and other glycoproteins. The main reason for this is the availability of post-translational modifications in mammalian cells not available in prokaryotes. Over the years cell culture engineering has improved so that new and improved growth media, culture conditions and strains can compensate for some of the previous shortcomings observed in mammalian cell culture.

1.3.1 Batch and fed-batch culture

Two of the most common culture modes for biopharmaceutical production in mammalian cells are the batch and fed-batch processes.

The batch process is the most common and basic approach in biopharmaceutical production (Figure 1.2 a). Cells are inoculated in media and left to produce the product of interest up to a predetermined point in time at which the entire culture is harvested and prepared for downstream processing. During the time of the culture no additional media is added to the bioreactor. The culture may initially present a lag phase in which little to no growth is observed. The presence and length of the lag phase depends on the condition of the cells used for inoculation. The cells then exhibit an exponential growth phase in which the cells usually double within 15-25 hours (Butler, 1988). Towards the end of the exponential growth phase the doubling slows down and the culture will enter the stationary phase in which growth is halted while production is still ongoing. During a regular batch culture the stationary phase is fairly short and more a transition phase into the decline or death phase. Most often the viability in this type of culture declines due to the cells running out of key nutrients such as glucose, glutamine or amino acids (Butler and Jenkins, 1989; Dalili et al., 1990). However, it is also possible that cell death occurs due to the accumulation of metabolic waste products (i.e. lactate and ammonia) (Doyle and Butler, 1990; Duval et al., 1992). Overall the production time is limited and production downtime between batches due to clean up of the bioreactors can further decrease production time. In addition, it has been observed that glycosylation decreases over the time of a batch culture – most likely also due to the nutrient limitation (Curling et al., 1990, Hayter et al. 1992, Nyberg et al., 1999).

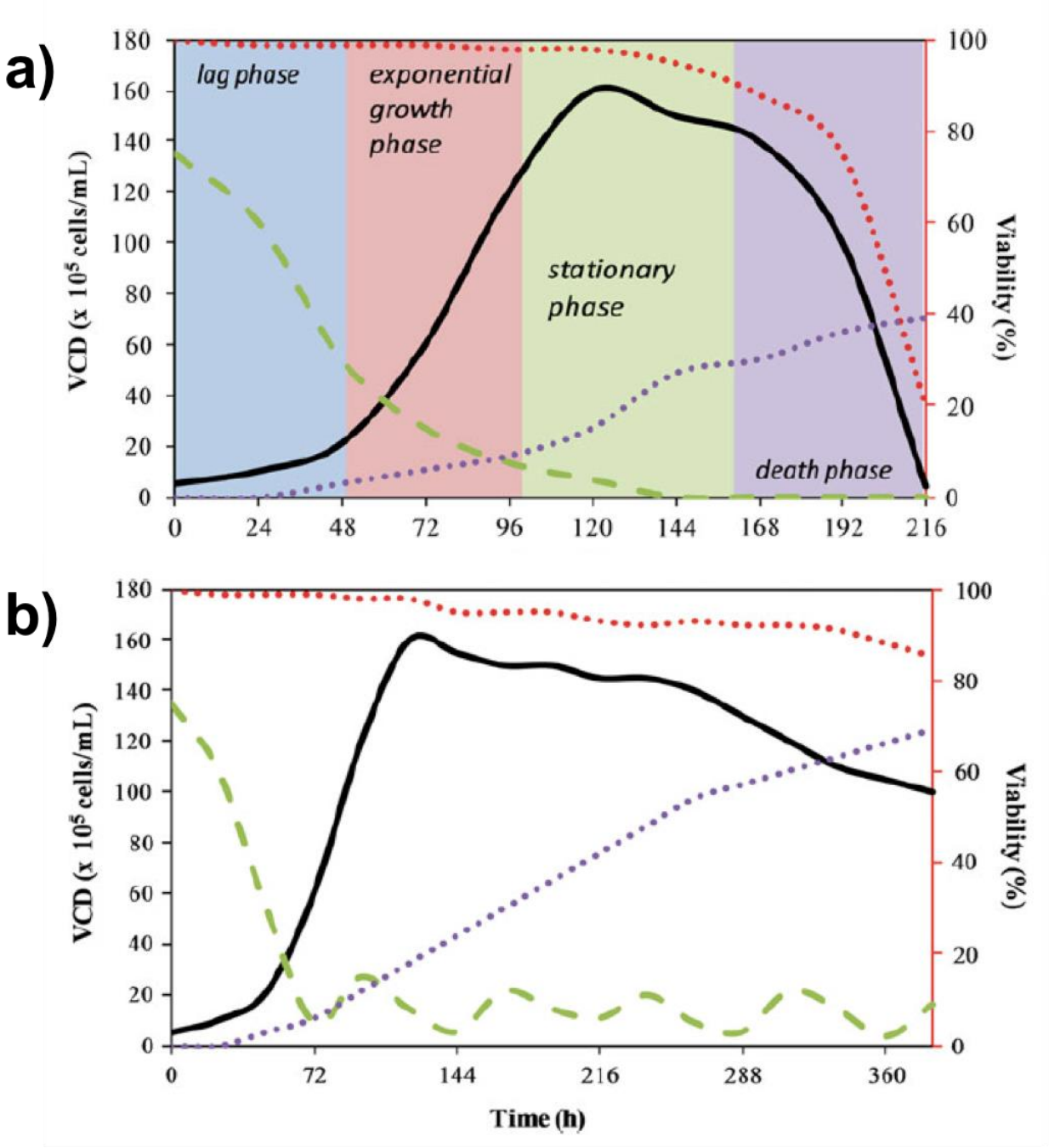

Figure 1.2: Examples of the time course of a regular **a)** batch and **b)** fed-batch growth including lag phase, exponential growth, stationary and death phase. This graph shows the representative viable cell density (VCD) (——), viability (·····), glucose (– –), and lactate concentrations (·····). (taken from Abu-Absi et al., 2014; p. 38/40)

The fed-batch process starts out like the batch process (Figure 1.2 b). However, unlike in the batch culture additional feedings (e.g. media, concentrated supplements) occur in the fed-batch culture at designated time points. The strategic addition of key nutrients (i.e. glucose, amino acids) prolongs the overall culture time so that a higher volumetric productivity can be achieved. However, the addition of extra nutrients also increases the overall accumulation of metabolic waste products (e.g. lactate, ammonia) in the culture, which could lead to cell demise. Hence, proper care must be taken to optimize the feeding strategy. Overall, the fed-batch processes run longer resulting in higher overall production and cost efficiency. Furthermore, the longer running / production times decrease the frequency at which the bioprocess ends and the bioreactor needs to be cleaned prior to starting up a new run. The cleaning process takes time during which production does not happen. Hence, when running fed-batch cultures the bioreactor is not in operation, due to cleaning, less often compared to bioreactors run in batch mode.

The culture mode of choice will depend on the recombinant protein in production and the overall yield required during production.

1.3.2 Growth media

The growth medium used for the cell culture process has a significant impact on the biopharmaceutical production. A good growth medium allows for optimal growth and a high product titer with consistent protein quality.

Mammalian cells have more needs for nutrients and growth factors than bacterial cells. This means that media development has been a lot more difficult to ensure that all nutritional requirements are met. Because of these distinct requirements mammalian cells were cultured

using media with fetal bovine serum (FBS) or bovine serum albumin (BSA) (Butler, 2005). While both supplements support growth and productivity in cell culture, their use also comes with some fundamental problems. On the one hand supplies of FBS and BSA have shown to have a high batch-to-batch variability due to their isolation from livestock. On the other hand FBS, BSA and other components derived from animal sources have been associated with viral and prion contaminations. For both of these reasons media with any animal derived components is not appropriate for the use in biopharmaceutical production. Therefore, it is of upmost importance to eliminate any animal derived components from the media.

In recent years FBS and BSA have been replaced with yeast or plant derived hydrolysates (i.e. pea, cotton), which have shown to support cell growth (Sung et al., 2004). The batch-to-batch variability found in such hydrolysates however is an issue because it can cause batch-to-batch variability in the final product, which is not desired. However, improvements in the hydrolysis process and final clean-up have reduced this variability (Siemensma et al., 2010; Chun et al., 2007). While this improvement is important in the overall use of those hydrolysates there is a push to identify the bioactive components in the hydrolysates that are necessary for growth. The identification of these components would allow for the production of a chemically defined medium that would be of consistent quality. By being able to design a chemically defined medium and change individual components it will also allow us to get more insight into the overall cell metabolism. This will also give better insight into the overall needs of individual cell lines and their specific products.

At the moment media containing yeast or plant hydrolysates added to a basal medium are quite commonly used. In addition, specific components such as pluronic F68, sodium butyrate,

and nucleotide / nucleotide sugar precursors can be added to the medium to improve cell viability, productivity and product quality in the cell culture.

1.3.3 Monitoring of cell culture

During a bioprocess several parameters in the cell culture can be monitored. These parameters can include but are not limited to cell density, viability, glucose consumption, lactate production and product concentration. Some of these factors are monitored daily or even more often (e.g. cell density and viability) while others are monitored less frequently or determined at the end of a run.

The monitoring can be helpful during process development to determine key nutrients or factors affecting the culture. This can help to improve the bioprocess by optimizing the basal or feed medium.

In industrial processes one of the main attributes monitored is the viable cell density and viability of a culture to observe the overall progression of the culture or to make key decision on feeding strategies or when to terminate a culture. In addition, extracellular media components such as glucose, lactate, glutamine and glutamate can be analyzed to take into consideration.

1.4 Apoptosis

#Most mammalian cells in a bioprocess lose viability as a result of programmed cell death, or apoptosis (Kerr et al., 1972), initiated by a variety of triggers such as oxidative stress, starvation, and ER stress (Limoli et al., 1998; Rao et al., 2006; Simon and Karim, 2002). Even though the cell membrane is intact at the onset of apoptosis, once a cell commits to the programmed death the process cannot be reversed. Therefore, it is reasonable to include all cells

consigned to apoptosis into a non-viable count. With the aim of increasing volumetric productivity and maintaining a constant product quality, indicators of early events leading to apoptosis are highly desirable in cell bioprocesses because these initial stages may be reversible by appropriate intervention -- e.g. nutrient feeding (Geske et al., 2001). While the mid-stages of apoptosis indicate the end of production from the cells, late stages may cause harm as lysed cells release proteinases and glycosidases into the medium with potential to degrade the glycoprotein product (Winchester, 2005).

#One of the earliest indications of apoptosis in a mammalian cell is the presentation of phosphatidylserine on the cell surface (Martin, 1995). In addition cells shrink (Bortner and Cidlowski, 2002; Bortner and Cidlowski, 2003; Kerr et al., 1972) due to ionic cell content regulation (Panayiotidis et al., 2006) and chromatin condensation (Kerr et al., 1972). Early pro-apoptotic signals trigger a cascade of caspase activity within the cells (Budihardjo et al., 1999). Finally, the late stage of apoptosis is characterized by DNA fragmentation and loss of membrane integrity. The phases of apoptosis can be detected by offline measurements of a sample from a bioreactor using fluorescent markers with a flow cytometer. Specific markers are available for early, mid and late stages of apoptosis.

Apoptosis can be triggered in cells by internal or external stimuli. Internal stimuli such as DNA abnormalities cause the intrinsic pathway while the extrinsic pathway is initiated by external stimuli such as the removal of nutrients (Figure 1.3).

1.4.1 Intrinsic (mitochondrial) pathway

Internal stimuli such as oxidative stress, high concentration of cytosolic Ca^{2+}, genetic damage or the lack of growth factors can trigger the intrinsic pathway ((Limoli et al., 1998; Rao et al., 2006; Simon and Karim, 2002; Vermes et al., 2002). The Bcl-2 family, consisting of pro-

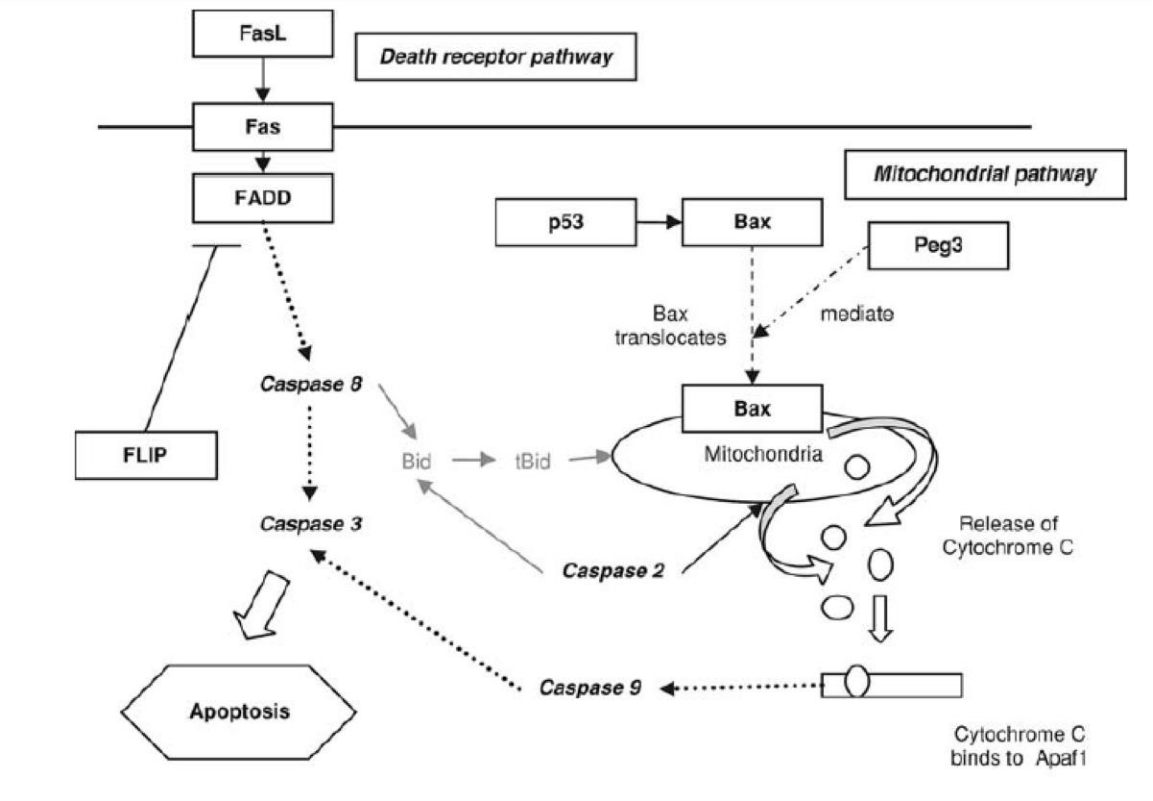

Figure 1.3: Overview of the intrinsic and extrinsic signaling pathway of apoptosis. (taken from Yeo et al., 2006; p. 7)

apoptotic and anti-apoptotic members, plays a big role in the regulation of this pathway (Green and Reed, 1998). If a pro-apoptotic member of the bcl-2 family, such as Bak and Bax, attaches to the outer mitochondrial membrane it promotes the release of cytochrome c by forming a pore after the molecules oligomerize (Caro-Maldonado, 2011). It is believed that this release causes the cell to commit to apoptosis (Adams, 2003; Arden and Betenbaugh, 2004). In the cytosol cytochrome c forms a complex with procaspase-9 and Apaf-1 to form a multiprotein complex

(Caro-Maldonado, 2011). This complex is called the apoptosome and contains procaspase-9 that is activated as part of the apoptosome (Adams and Cory, 2001; Liu et al., 1996). The activated initiator caspase-9 then activates so called executioner caspases thereby continuing the apoptosis pathway.

1.4.2 Extrinsic (receptor mediated) pathway

In the extrinsic pathway the trigger for the initiation of apoptosis comes from outside the cell and is receptor-mediated. One of the receptors that is part of the extrinsic pathway is the tumor necrosis factor receptor (TNFR1). The tumor necrosis factor (TNF) produced by cells in response to extrinsic stimuli – such as nutrient deprivation, waste accumulation and oxygen limitation – binds to the receptor (Al-Rubeai et al., 1990; Chung et al., 1998; Singh et al., 1994; Singh et al., 1997). This binding then leads to a conformational change in the death domain, which will recruit the Fas-associated death domain (FADD). This attachment is followed by the attachment of two procaspase-8 molecules to the complex (Kischkel et al., 2001; LeBlanc and Ashkenazi, 2003). When those two pro-caspase molecules are held in close proximity to each other they can cleave the polypeptide chain from the other molecule to activate each other. Like caspase-9, caspase-8 then activates executioner caspases to carry out the programmed cell death (Boatright and Salvesen, 2003).

In addition, the caspase-8 molecule can initiate the intrinsic pathway via the bcl-2 homolog, Bid, which will interact with the pro-apoptotic Bax protein needed for the initiation of that pathway (Scorrano et al., 2003).

1.5 Cell Culture Density and / or Viability Determination

As mentioned above the monitoring of the cell culture density and / or viability is an important aspect in the overall monitoring of a cell culture. #The measurement of viable cells is important because these are the metabolically active producer cells. However, the concept of "viability" is complex and depends critically on the cell characteristics used to define it (Browne and Al-Rubeai, 2011). Commonly used assays, such as the trypan blue exclusion method, associate loss of viability with a loss of cell membrane integrity as measured by the uptake of high molecular weight dyes. However, this marks the end of apoptosis, the primary cause for cell death in a bioprocess. Cells going through apoptosis will eventually lyse due to secondary necrosis. The lysed cells will then release enzymes into the medium that can cause damage to the already produced glycoproteins (Winchester, 2005). Hence the determination of an early decline in cell viability is important. Various direct or indirect methods have been shown to be successful in detecting specific metabolic changes that precede the late stages in apoptosis and can be predictive of the reduced ability of cells to grow and divide when they enter senescence.

1.5.1 Coulter Counter

The Coulter counter registers electronically the presence of particles at a predetermined size and is a rapid method that can give the total cell density of a cell suspension. It has been used in the past for quick cell counts. The counter works by taking up a predetermined volume of a diluted sample through a small aperture (diameter of 70 μm). Around the aperture is an electric field, which is interrupted in the event of a cell passing through the electric sensing field. This interruption is then counted as an event. The counted events are then converted to a total cell count via an equation taking the sample dilution and volume measured into consideration. In

the case that several cells are in the sensing field at the same time the event is only counted as a single event. This means that the sample has to be sufficiently diluted to avoid artificially low counts (Butler et al., 2014).

1.5.2 Image-based analysis

Several systems are available to analyze a cell sample (stained or unstained) based on a picture taken by a camera. The picture can be transferred to a computer and a software system for further analysis in regards to cell density, viability, cell diameter and aggregation.

Quite often the image-based analysis is used with the addition of exclusion dyes, which allow for the determination of viability in a cell sample. The most commonly used method is the trypan blue exclusion method. Trypan blue is a high molecular weight dye that will only be able to enter a cell once its membrane integrity has been compromised. Therefore, 'viable cells' will remain colourless while 'dead cells' will take up the dye and stain blue. The software is then able to detect and differentiate the cells based on the light intensity that passes through them to calculate viability.

1.5.3 Flow cytometer

The flow cytometer is a laser-based technology that enables users to analyze suspended cell samples. Flow cytometer measurements can be very precise in detecting the different stages in the apoptotic pathway when stage-specific structures and proteins are fluorescently labeled. By combining different fluorescent labels a good overview of the cell's apoptotic stage can be determined.

[$]In the early stage of apoptosis cells lose their ability to maintain membrane phospholipid asymmetry. Because of this phosphatidylserine (PS) is increasingly exposed on the outer leaflet of the plasma membrane of the cell and not on the inner membrane surface as normally expected (Al Rubeai and Emery, 1993). The exposed PS molecule can be labelled with an Annexin-V molecule conjugated with a fluorescent dye, such as fluorescein isothiocyanate (FITC) (Al Rubeai and Emery, 1993) or R-phycoerythrin (PE). In addition the cell sample is stained with propidium iodide (PI) or 7-aminoactinomycin D (7-AAD) to further distinguish microscopically between early-apoptotic and necrotic cells, which may also be stained by Annexin-V due to membrane injuries allowing the Annexin-V label to enter the cell and stain PS there (Vermes et al., 1995).

In addition, several caspase proteins play a role in the apoptotic pathway by initiating the apoptotic cascade, causing cellular breakdown and by being involved in the maturation and inactivation of cytokines. These can be detected by fluorescently labeling the activated caspase proteins by either an antibody against a fragment of the specific caspase (Ishaque et al., 2003) or by using an inhibitor of multiple caspases such as sulforhodamine-valyl-alanyl-aspartyl-fluoromethyl-ketone (SR-VAD-FMK) (Ekert et al., 1999). In both cases the antibody or SR-VAD-FMK are fluorescently labelled using a fluorochrome.

The fluorescent assays mentioned above and other assays to monitor viability and apoptosis are available as individual stains or commercial kits (e.g. Millipore). The availability of these assays allows for a fairly simple staining procedure for cell samples to determine their progression through apoptosis.

1.5.4 Dielectric based analysis

Dielectric based measurements refer to the monitoring of the cells behavior in an electric field. These measurements are based on the electric properties cells possess and the change in these properties throughout a bioprocess. The dielectric measurements can either be bulk dielectric measurements when a certain volume fraction of a homogenous culture is measured or a single cell dielectric measurement when individual cells are observed.

1.5.4.1 Dielectric properties of mammalian cells

A healthy cell has a well-balanced ionic content that is actively maintained by the cells. Changes in the ionic content, membrane capacitance and mitochondrial capacitance have been correlated to physiological and metabolic changes within the cells (Demierre et al., 2008; Duncan et al., 2008; Flanagan et al., 2008; Gagnon, 2011; Huang et al., 1992; Pethig et al., 2010). In addition, a number of studies have connected the ionic flux over the cell membrane with the onset of programmed cell death (Bortner et al., 2012; Bortner and Cidlowski, 2002; Bortner and Cidlowski, 2003) and found that changes in the ionic composition of the cell are linked to early stages of apoptosis (Labeed et al., 2006). Therefore, methods based on dielectric measurements are particularly promising for identifying emerging subpopulations of apoptotic cells.

1.5.4.2 Bulk dielectric measurement

In bulk dielectric measurements the probe measures the electrical capacitance of all cells within the electric field of the probe (Carvell and Dowd, 2006). #A sterilizable capacitance probe commercialized as a "biomass monitor" has been available over the last decade. Hence, the bulk capacitance and the conductance of yeast and mammalian cell cultures can be monitored

by a dielectric probe positioned within the bioreactor (Ansorge et al., 2010; Ducommun et al., 2002; Knabben et al., 2010; Opel et al., 2010; Tibayrenc et al., 2011).

The monitored capacitance of the bulk cell suspension, C, is a function of the effective dielectric permittivity of the suspension, ε, which is in turn a function of the biovolume. The dominant response of the cell to an electrical field is charge polarization, which diminishes as the frequency of the field increases between 0.1 and 20 MHz, resulting in a large decrease in dielectric permittivity, $\Delta\varepsilon$, around the critical frequency f_C (Figure 1.4). For these measurements it is assumed that the cell membrane capacitance is constant (Foster and Schwan, 1989; Maxwell, 1881; Schwan, 1957). $\Delta C \propto \Delta\varepsilon$ allows for the biovolume to be monitored using differences in bulk suspension capacitance for two frequencies from the opposite ends of the range 0.1 – 20 MHz (Harris et al., 1987; Opel et al., 2010). It is also expected that $\Delta\varepsilon$ should only depend on the number of cells, N, and their average radius, R. However, this simplified relationship has been shown to deviate when there are changes in the physiological or metabolic state of mammalian cells as they lose viability in the stationary and decline phases of a bioprocess (Opel et al., 2010). In recent years, dielectric spectroscopy has been used successfully for cell density and viability measurements with the advantage of constant monitoring that could enable early corrective action to maximize cell viability (Ducommun et al., 2002).

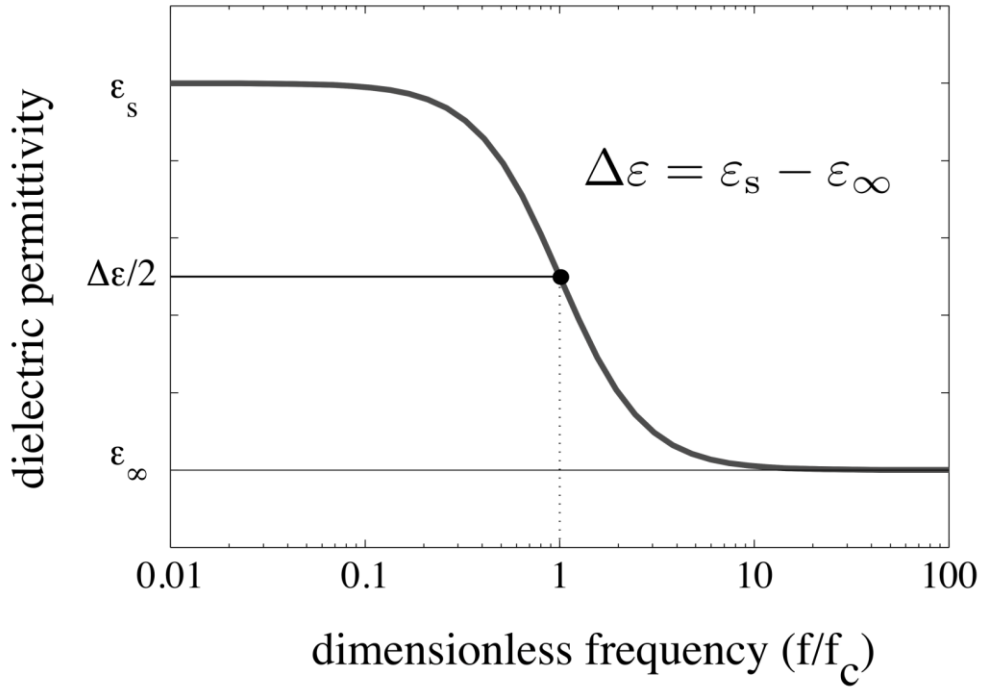

Figure 1.4: β-dispersion, schematic plot. Charge accumulation on the membranes occurs over a finite amount of time, resulting in a large drop in dielectric permittivity, $\Delta\varepsilon$ (from permittivity, ε_s, at low to permittivity, ε_∞, at high frequencies) at the critical frequency, f_C. Values are plotted for dimensionless frequency, f/f_C (Braasch et al., 2013; p. 2).

1.5.4.3 Single cell dielectric measurement

The prototype dielectrophoretic (DEP) cytometer developed at the University of Manitoba (Nikolic-Jaric et al., 2013) probes dielectric properties of individual cells by independently detecting and actuating the cells as they flow through a microfluidic channel.

#The cells are actuated by a DEP force resulting from the AC signal, with a frequency from 0.1 to 6 MHz, applied through the set of actuation electrodes (Nikolic-Jaric et al., 2013). Cells respond to the applied electric field by polarization, which can be defined in terms of variations in charge distribution. This results in a vertical displacement of the cells between the two detection sites (D1 and D2) and is translated into an electronic signature, S, as shown in

Figure 1.5. The peaks, P_1 and P_2, depend on the vertical position of the cell's center of mass and diminish with the distance from the electrodes. Vertical cell displacements as small as 0.1 to 0.25 μm can be registered, permitting determination of the extent of actuation that occurs between sites D1 and D2 by simply comparing P_1 and P_2.

The DEP force is proportional to cell polarizability, α, and considered attractive (pDEP), for $\alpha > 0$, and repulsive (nDEP) for $\alpha < 0$; point $\alpha = 0$ is called the "crossover." Simulations estimate the crossover frequency (when $\alpha = 0$) for viable cells at about 0.5 MHz. Therefore, AC DEP signals above 1 MHz can distinguish between the healthy viable and early apoptotic cells, as the difference in polarizability will produce DEP forces of opposite sign. This provides information of the dielectric properties of individual cells in a population as opposed to the bulk average dielectric properties obtained with an online capacitance probe.

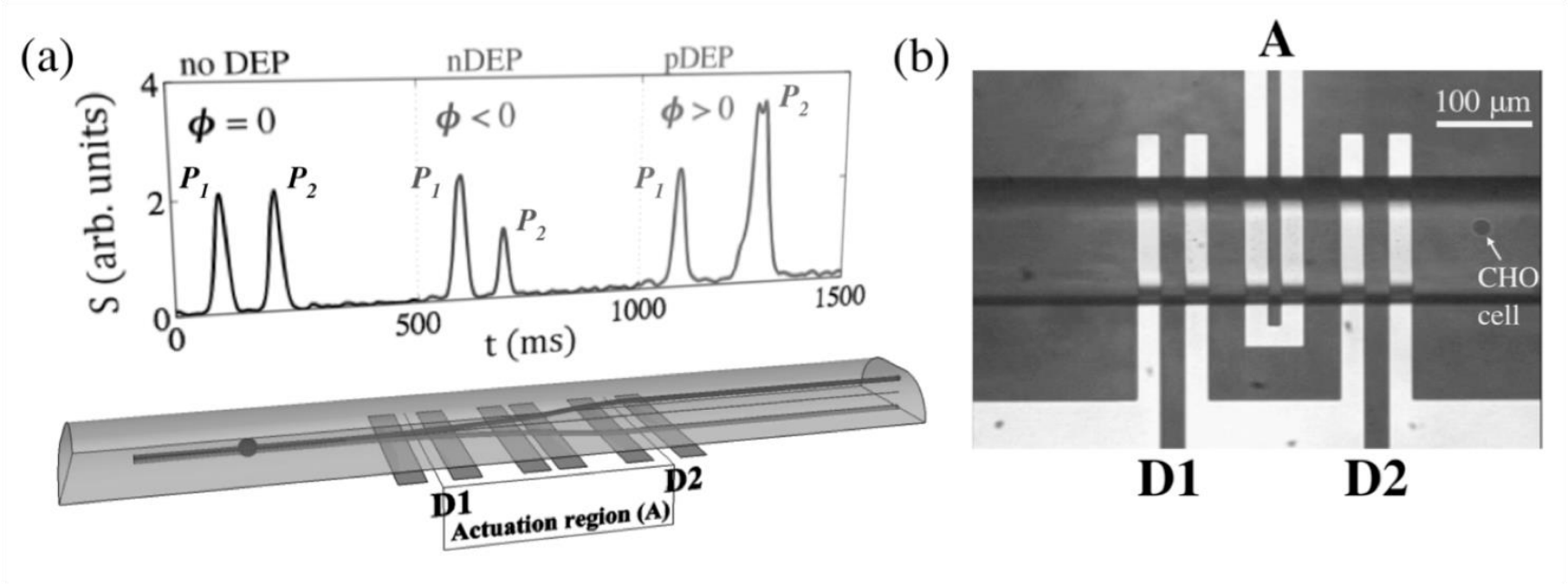

Figure 1.5: (a) Schematic representation of the microfluidic channel. A cell (modeled to scale as a small sphere) is flowing through the analysis volume above the differential electrode array. Three possible cell trajectories are shown: pDEP-actuated cells are attracted to the electrodes, nDEP-actuated cells are repelled, and unactuated cells continue along a straight line. Corresponding signatures (in the vertical plane) are the true signatures produced by CHO cells of similar sizes captured at different times during the experiment. Similarly sized entrance peak, indicates that they were initially flowing at approximately the same elevation. The change in amplitude resulted from about 4µm vertical deflection in both the pDEP and nDEP examples. **(b)** Micrograph of the differential electrodes, showing detection and actuation region, with a CHO cell on the exit from the analysis volume. (taken from Braasch et al., 2013; p. 5)

1.5.5 Adenylate energy charge

Nucleotides including adenosine 5'-triphosphate (ATP), guanosine 5'-triphosphate (GTP), uridine 5'-triphosphate (UTP) and cytidine 5'-triphosphate (CTP) play central roles in metabolism. They serve as sources of energy, participate in cellular signaling and provide information about the physiological state of the cell (Kochanowski et al., 2006). The state of phosphorylation of these nucleotides within the cell can vary typically between tri, di- and mono-phosphate forms. This can be used to monitor the metabolic status of the cell (Atkinson, 1968), particularly through phosphorylation indices such as the adenylate energy charge (AEC) (Barnabe and Butler, 2000). The AEC is an index calculated based on the concentration of the intracellular nucleotides ATP, ADP and AMP.

$$\mathrm{AEC} = \frac{[\mathrm{ATP}] + 0.5[\mathrm{ADP}]}{[\mathrm{ATP}] + [\mathrm{ADP}] + [\mathrm{AMP}]}$$

ATP is a high energy compound needed for many functions within the cell and hence a good indicator for overall cell fitness. For healthy cells AEC values of 0.85 – 0.95 would be expected (Atkinson, 1968). A decrease in the AEC is a good indicator for the demise of cells in culture.

The concentration of ATP, ADP, and AMP can be determined using either chromatography (HPLC) or a luminescence luciferin-luciferase assay (Tomiya et al., 2001; Holm-Hansen and Karl, 1978; Lundin et al., 1986).

1.6 Intracellular nucleotide and nucleotide sugars

Intracellular nucleotides such as ATP, CTP, GTP, and UTP are not only an important part of the cells energy metabolism but also an important part of the intracellular nucleotide sugar activation needed for the glycosylation process. Many factors such as the cell line (Nakajima et al., 2010), culture conditions, media composition and the physiological status of the cells (Ritter et al., 2008) can influence the metabolite concentrations. This emphasizes the value of accurately measuring these metabolites to study their connection and impact on the energy metabolism and the glycosylation process during biopharmaceutical production.

1.6.1 Monosaccharide Metabolism

Glucose and fructose are the main carbon and energy source for mammalian cells. All monosaccharides needed for energy and glycosylation processes can be derived from those two sources (Figure 1.6) and through the interconversion or salvage of already existing glycans. In addition, other monosaccharides can be added to the culture medium to improve the intracellular pool of certain nucleotides / nucleotide sugars. This addition of precursors has shown to influence these pools for some cell lines and the glycan addition in the respective recombinant proteins produced (Gawlitzek et al., 1998; Grammatikos et al., 1998).

The monosaccharides are synthesized mainly in the cytoplasm, with the exception of sialic acid, which is created in the nucleus. Once the monosaccharides are synthesized they must be activated prior to being able to be used in the glycosylation process. To activate the monosaccharides nucleoside triphosphates are needed. When activated all monosaccharides, but the sialic acids, are di-nucleotides.

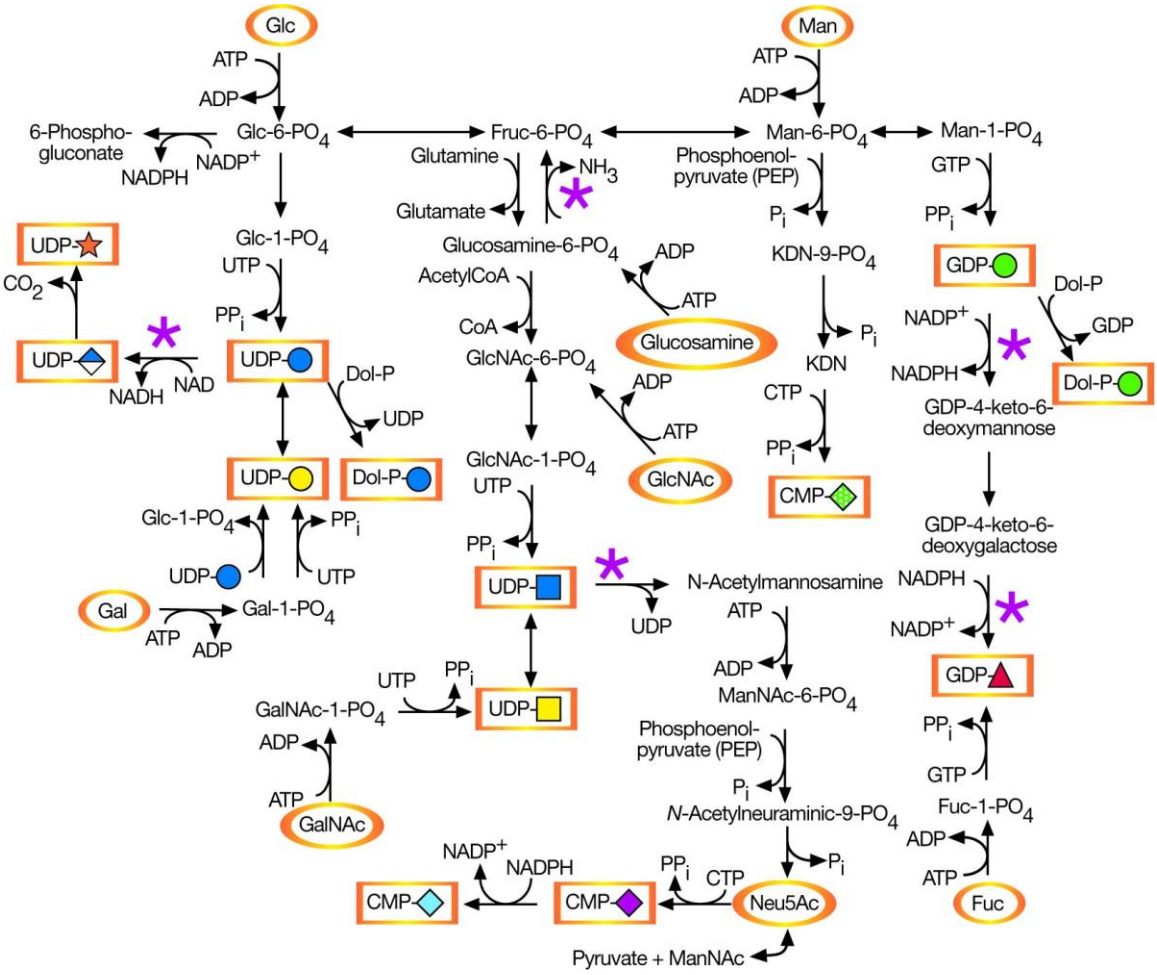

Figure 1.6: Overview of the monosaccharide metabolism. (Freeze and Elbein, 2009; p. 6)

The nucleotide sugars used as precursors for glycosylation must then be localized to the ER and Golgi where glycosylation occurs. This localization occurs via anti-porters, which allow activated nucleotide sugars into the ER and Golgi while removing nucleoside monophosphates into the cytoplasm where they will be restored (Hirschberg et al., 1998).

1.6.2 Building blocks for glycosylation

˜Intracellular concentrations of nucleotides and nucleotide sugars are essential during the

biosynthesis of glycoproteins (Tomiya et al., 2001) as they make up the building blocks for glycosylation (Figure 1.6). Activated nucleotide sugars, such as UDP-*N*-acetylglucosamine (UDP-GlcNAc), UDP-*N*-acetylgalactosamine (UDP-*N*-GalNAc)), UDP-glucose (UDP-Glc), UDP-galactose (UDP-Gal), GDP-mannose (GDP-Man) and GDP-fucose (GDP-Fuc) act as donor substrates of glycosyltransferases. Therefore, the abundance of these nucleotide sugars can regulate the flux of glycosyltransferase reactions in the cell and hence N-glycan synthesis (Varki et al., 2008; Nakajima et al., 2010; Rijcken et al., 1995; Rabina et al., 2001).

Several factors such as nutrient availability, waste accumulation, pH and dissolved oxygen (dO_2) can influence the intracellular metabolism of cells in a culture. Since the glycosylation of proteins in a culture is dependent on the intracellular pools of activated nucleotide sugars it is important to monitor these during the synthesis of glycoproteins. This will give a better insight on how external changes can influence the internal metabolism and subsequently the product quality.

1.6.3 Nucleotide / Nucleotide Sugar Analysis

˜Nucleotide sugars are the donor substrates of glycosyltransferases and their availability is known to have an impact on the glycosylation of recombinant proteins including monoclonal antibodies (Varki et al., 2008; Nakajima et al., 2010; Rijcken et al., 1995; Räbinä et al., 2001). In addition, the intracellular concentration levels of these metabolites can provide information about the physiological / energetic state of the cell (Kochanowski et al., 2006; Atkinson, 1968; Barnabé and Butler, 2000). Therefore, the ability to qualitatively and quantitatively determine the intracellular nucleotides and nucleotide sugars can give valuable insight into the metabolism associated with the glycosylation processes in cells. However, in order to be able to perform a

consistent and reliable time specific analysis of these metabolites during a cell culture the metabolism of the cell needs to be stopped immediately at the point of sampling and an efficient extraction needs to be performed. Once the nucleotides and nucleotide sugars are extracted from the cell sample an efficient HPLC method is needed to separate all or most of the metabolites of interest to allow for their identification and quantification.

For the work in this thesis, an optimized method for the analysis of the intracellular nucleotide / nucleotide sugar pool in CHO suspension cells was established (Appendix A). The method includes protocols for quenching, extraction and HPLC analysis. To quench the cell sample the quenching method by Sellick et al. (2009) was the most effective in the recovery of ATP from the cell samples. In addition, this quenching method minimized ATP conversion and stabilized cell samples resulting in higher and expected AEC values compared to the alternative methods even after a 1-week storage period at -70°C. Therefore the "Methanol/Ammonium bicarbonate (AMBIC)" method was chosen as the preferred quenching protocol (Braasch et al., 2015). For nucleotide / nucleotide sugar extraction the "Envi^{TM}-Carb column" protocol is the most suitable for the experiments related to this thesis. This method was chosen because it provides high recovery of nucleotides and nucleotide sugars with low variability. In addition, the column extraction allows for easier adaptation for the analysis of multiple samples (Braasch et al., 2015). Lastly, the HPLC method used for the qualitative and quantitative analysis of nucleotides extracted from cells is based on a previously published HPAEC method by Tomiya et al. (2001).

1.7 Glycosylation

Many factors can influence the addition and distribution of glycans in secreted proteins including cell line, culture method and extracellular environment (Butler, 2009). In glycoproteins two types of glycans can be found: N-glycans and O-glycans. IgG type antibodies have a fairly simple glycosylation and exhibit one N-glycan in the CH2 domain of the Fc region.

1.7.1 N-linked glycans

N-linked glycosylation is a co-translational modification of proteins in eukaryotic cells such as mammalian cells. The process starts in the ER where a dolichol-oligosaccharide precursor containing 14 sugars is assembled (Figure 1.7). The oligosaccharide portion of this dolichol structure is then transferred by the oligosaccharyltransferase to the appropriate asparagine-X-serine sequon onto a nascent protein (Stanley et al., 2009). Since not all sequons in a particular protein will be glycosylated, glycoproteins will exhibit macroheterogeneity between the glycoproteins in a production process (Spearman et al., 2010). Once the oligosaccharide is transferred to the nascent protein the first steps in the process are the sequential removal of the three terminal glucose residues. The final glucose residue in the added glycan structure is an important part of the folding quality control in glycoproteins (Hammond et al., 1994). After the glycoproteins are properly folded and the final glucose residue and one mannose residue are cleaved off, the protein is moved to the Golgi for further glycosylation processing.

Once the glycoprotein moves into the Golgi the glycan precursor structure is further modified by the addition of other sugars. An array of glycosyltranferases is using the pool of nucleotide sugars available as substrates to add other sugars to the glycan core structure. These

enzymes and precursors are spread throughout the Golgi causing variability in the final addition of glycans among proteins going through the process (Schachter et al., 1986). This means that

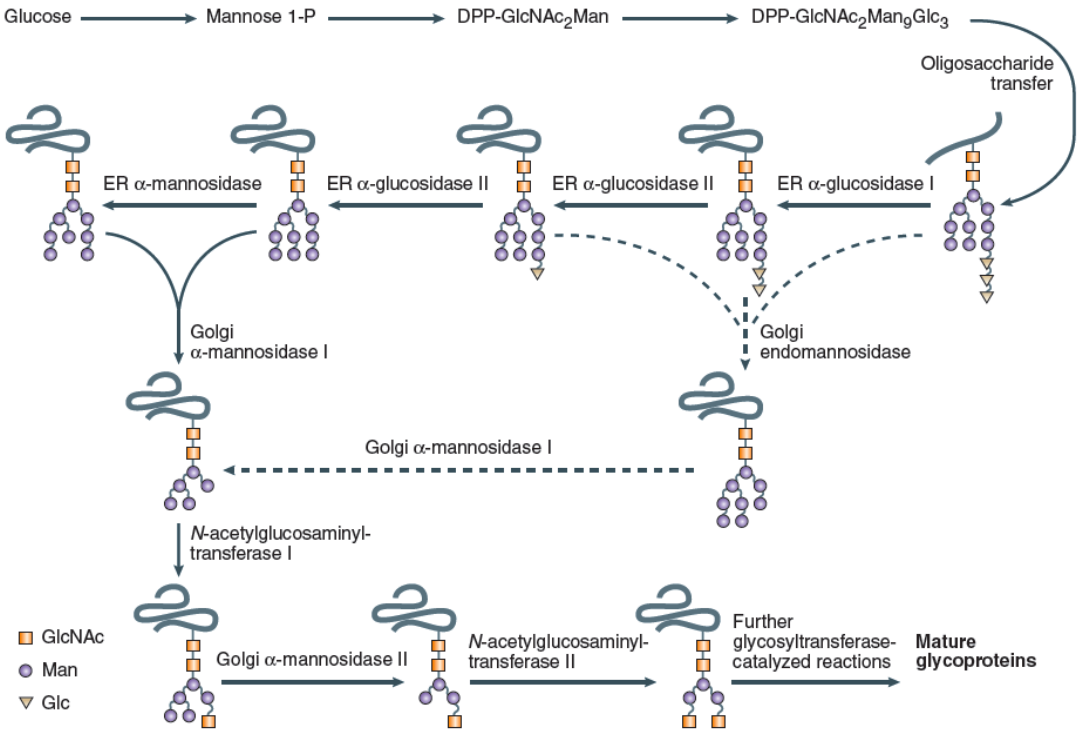

Figure 1.7: Overview of the N-glycosylation process in mammalian cells. (Dwek et al., 2002; p. 66)

not all glycan structures will be the same. Hence, microheterogeneity among the glycoproteins within the culture will be observed. Other culture parameters that have been shown to influence the microheterogeneity are the pH (Borys et al., 1993), temperature (Nabi and Dennis, 1998) and dissolved oxygen content (Kunkel et al., 1998).

In antibodies the typical glycan structures observed are complex biantennary glycans with either zero, one or two galactose molecules added to the glycan structure. While most antibody glycan structures have a fucose residue attached to their core structure, the majority of glycans will not be sialylated.

1.7.2 Importance of glycans

The glycans in glycoproteins such as antibodies have shown to have a great impact on the protein's stability, solubility (Ghirlando, 1999), transport, clearance (Gala and Morrison, 2002), and functionality (Shields et al., 2002; Siberil et al., 2006; Scallon et al., 2007; Wright and Morrison, 1998). These qualities of the biopharmaceuticals are so important because they will dictate how well the biopharmaceutical will work and for how long it is able to stay in the body before being excreted. If biopharmaceuticals are able to stay in the body for longer periods of time, a less frequent administration of that medicine is needed.

In the glycan structure specifically fucosylation, sialylation, and galactosylation can impact the functionality, stability and solubility (Ghirlando et al., 1999), and cellular transport and clearance (Gala and Morrison, 2002). It has been shown for erythropoietin that the loss of sialylation reduced the half-life in the blood stream by 50% (Erbayraktar et al., 2003).

While antibodies such as IgG have a fairly simple glycosylation pattern in the Fc region it has a great impact on the effector function. Antibodies are an important part of our immune system and as such are important biopharmaceuticals that can take advantage of our own immune system to help them in their therapeutic application. When an antibody binds to its intended antigen, the Fc region is undergoing a conformational change activating the complement-dependent cytotoxicity (CDC) or the antibody-dependent cell mediated cytotoxicity (ADCC) pathway. Non-glycosylated IgG have a reduced affinity to the Fc gamma receptor III hindering the CDC pathway (Sarmay 1992, Tao and Morrison 1989). However, a lack of fucose has shown to lead to a 50-fold increase in the ADCC activation (Shields et al., 2002). An increase in the bisecting GlcNAc has also shown to increase the ADCC activity (Shinkawa 2003, Umana 1999) – most likely due to the reduction in fucosylation (Schachter 1986, Takahashi

2009, Umana 1999). Based on the known influence of the glycosylation on the biopharmaceutical effector function, biopharmaceuticals with improved and desired functions can be determined.

1.7.3 Biomanufacturing

In biopharmaceutical production it is very important to consistently produce the same high quality product. These products are administered to patients and therefore need to have the same qualities from batch to batch to be reliable. Because glycosylation has such an impact on the functionality of recombinant proteins, such as antibodies, it is especially important to produce the desired glycan profile in a consistent manner (Restelli and Butler, 2002). Hence a better understanding of the glycosylation process will allow for an improvement to shift and/or maintain the glycan profile for glycoprotein of interest. However, it is also important to monitor the viability of a bioprocess. A decline in viability could mean that cells will soon lyse and release proteases and exoglycosidases, which can destroy or alter the already produced glycoprotein of interest (Winchester, 2005). In addition, a decline in viability might be associated with a lack of nutrients, which are needed to prepare the building blocks for the glycosylation process. Therefore, understanding the methods available for viability monitoring and being able to detect cell demise early is also necessary to ensure a consistent glycan profile.

1.8 Aims of PhD

The aim of this thesis is to study two important aspects in the monitoring of biopharmaceutical production in mammalian cells. In the first part of this thesis the monitoring of cell viability during the production processes will be explored. The second part will look at

the effects of precursor feeding on the cell growth, viability, productivity and the glycosylation process. The two CHO cell lines used for this study produce two types of antibodies making them good representatives of current biopharmaceutical processes. The cell lines were chosen specifically for the precursor experiments due to their distinct differences in the regular glycan structure.

A) Monitoring cell viability using image, flow cytometer and dielectric analysis.

1) To compare common viability assays for cell culture with dielectric measurements (Chapter 3)

The monitoring of viable cell density is an integral part in the overall monitoring of a bioprocess and the early detection of cell demise is of interest. Several direct methods are available including microscopic counting, electronic particle counting, image analysis, and fluorescent cytometry. These more established methods were compared to the dielectric analysis done with the in situ capacitance probe and the DEP prototype developed at the University of Manitoba. The aim of this study was to determine if dielectric measurements can be used to monitor cell health and viability in batch processes using CHO cells. An important aspect was to determine whether dielectric measurements could be used to detect the onset of cell demise early.

2) To evaluate the use of dielectric measurements to monitor artificially induced apoptosis in bioprocesses (Chapter 4).

The dielectric properties of mammalian cells have been linked to cell health. Since early detection of apoptosis induction is of interest the dielectric measurements will be explored more in depth. In order to follow apoptotic induction through different pathways, apoptosis was

induced artificially for these experiments. This allowed to further evaluate the possibilities of using dielectric measurements in the monitoring of cell culture viability. The goal of this study was to correlate the measurements of the dielectric properties of cells to stages of apoptosis. A special interest was the identification of rare events and sub-populations of CHO cells, which are established during the progression of apoptosis, using the dielectric data from the capacitance probe and the DEP cytometer.

B) Nucleotide sugar precursor feeding for the manipulation of glycosylation.

1) To study the effect of the nucleotide sugar precursor feedings on the growth, viability and recombinant protein production for EG2, and DP12 in CHO cells (Chapter 5).

In this experiment nucleotide / nucleotide sugar precursors (e.g. galactose, uridine, manganese) were added to the medium alone and in combination to observe their effect on the nucleotide / nucleotide sugar pool and the antibody glycan profiles in those cultures. However, changes made to the culture media can also affect the cell growth, viability and productivity in a bioprocess, which are important aspects to consider in any bioprocess. Hence, it was important to also monitor these parameters in addition to the expected changes (i.e. nucleotide / nucleotide sugar pool and product glycosylation) to determine the overall effectiveness of the precursor additions to the medium.

2) To study the effect of the nucleotide sugar precursor feedings on the nucleotide / nucleotide sugar pool in CHO-EG2, and CHO-DP12 (Chapter 6).

The addition of nucleotide sugar precursors has been shown to have an effect on the nucleotide / nucleotide sugar pool. However, the effect is cell line dependent and in the past

only specific nucleotide sugars were monitored. Here a set of 18 nucleotide / nucleotide sugars was monitored to get a more global picture of the impact of the precursor feeding using galactose, uridine, and manganese in different combinations. By using two different cell lines the aim of this experiment was to monitor how the precursor feeding affects the nucleotide / nucleotide sugar pool in each cell line and to determine the similarities and differences.

3) To study the effect of the nucleotide sugar precursor feedings and the nucleotide / nucleotide sugar pool on the recombinant protein glycosylation in CHO-EG2, and CHO-DP12 (Chapter 7).

The nucleotide / nucleotide sugar pool contains all of the precursors needed for glycosylation and their availability has been shown to influence the glycosylation profiles of recombinant proteins. Since the two CHO cell lines used produce two different types of antibodies with very different starting glycosylation profiles it was of interest to see how the profiles changed with the addition of precursors. The goal of this study was to relate the changes in the glycosylation profile to the precursor feedings and to the related changes in the nucleotide / nucleotide sugar pool as discussed in Chapter 6. Again, the similarities and differences between the two cell lines and antibodies were of great interest to further elucidate the glycosylation process in CHO cells.

Chapter 2

Materials and Methods*

2.1 Chemicals and reagents

All chemicals and reagents used were of the highest purity available and purchased from either Sigma (St. Louis, MO, USA) or Fisher Scientific (NJ, USA) unless otherwise indicated. Solutions were prepared using Milli-Q grade water and filtered using a 0.2 μm filter if needed.

2.2 Cell culture

2.2.1 Cell line

Two different Chinese Hamster Ovary (CHO) cell lines were used for this work. The main cell line (CHODG44-EG2-hFc/clone 1A7; BRI, Montreal) used expresses a human-llama chimeric antibody (EG2) for the epidermal growth factor receptor and was provided to the Butler lab by Yves Durocher of the NRC, Canada (Bell et al., 2010). The second cell line (CHOK1-Anti-IL8) used expresses an antibody against interleukin 8 (IL8) and was purchased from the American Type Culture Collection (ATCC, CRL-12445).

* Partial content of this chapter was included in several papers:
Butler, M., Spearman, M. and Braasch, K. (2014), Monitoring cell growth, viability and apoptosis: in Animal Cell Biotechnology – Methods and Protocols (ed. Ralf Poertner), 1104: 169-192. Methods in Molecular Biology. Humana Press.
Braasch, K., Villacres, C., and Butler, M. (2015), Evaluation of quenching and extraction methods for nucleotide / nucleotide sugar analysis: in Glyco-Engineering: Methods and Protocols (ed. Alexandra Castilho), Methods in Molecular Biology. Humana Press.

2.2.2 Culture medium

All cells were cultured in BioGro-CHO serum-free medium (BioGro Technologies, Winnipeg, MB). Unless otherwise indicated the medium was supplemented with 0.5 g/L yeast extract (BD, Sparks, MD), 1 mM glutamine, and 4 mM GlutaMax I (Invitrogen, Grand Island, NY).

2.2.3 Culture Maintenance

Both cell lines were maintained in 125 mL or 250 mL baffled shaker flasks (vented caps) (VWR International, Mississauga, Canada) with culture volumes of 30 mL and 80 mL, respectively. Every 3 to 4 days cells were passaged at a seeding density of $2x10^5$ cells/mL. The cultures were grown on a shaker platform (120 rpm) in an incubator with a 10% CO_2 overlay at 37°C.

2.2.3.1 Viable cell determination

For the culture maintenance cell viability determination was performed by trypan blue exclusion. In this procedure equal parts of the cell sample and 0.4% (w/v) trypan blue (Gibco) were mixed prior to applying the mixture to the Cedex slides (Roche). The slides were then entered into the Cedex (Innovatis AG, Bielefeld, Germany) for automatic image analysis. The program is able to determine cell density and viability since viable cells do not take up the blue dye. In addition, the image analysis program can determine cell diameter and cell aggregation.

2.2.4 Experimental Cultures and Sampling

2.2.4.1 Viability assay comparison in a batch culture*

For this experiment CHO-EG2 cells were grown in a 3 L glass bench-top bioreactor (Applikon, Foster City, CA). Throughout the run the culture was kept at 37°C, 30% dO_2, pH 7.2 and a stirrer speed of 200 rpm. During the batch culture two 10 mL samples were taken at the designated sampling points to determine the cell density and viability of the culture. Each 10 mL sample was analyzed twice using the Cedex, Coulter Counter, and Guava Assays (described below) giving a total of four technical replicates at each sampling point for these offline measurements. The capacitance probe (Aber, Aberystwyth, UK) was a continuous online measurement and two technical replicate measurements were performed at each sampling point using the DEP Cytometer (University of Manitoba). The remainder of the 10 mL samples was spun down at 352xg for 1 min to collect the supernatant which was then filtered through a 0.2 μm filter before being stored at -20°C for later media component, productivity and glycan analysis.

For some experimental runs an additional cell sample ($1x10^7$ cells) was taken as described in the "Nucleotide and Nucleotide Sugar Analysis" section (Chapter 2.7).

2.2.4.2 Apoptosis induction experiments

CHO-EG2 cells were cultured in 250 mL flat-bottom shaker flasks (VWR International) with a culture volume of 200 mL and a seeding density of $7x10^5$ cells/mL. In between measurements cultures were kept on a shaker platform (160 rpm) in the incubator at 37°C with a 10% CO_2 overlay. Each experimental set consisted of three cultures – one control culture and

two cultures in which apoptosis had been induced. To ensure identical time measurements the cultures were each seeded 1 hour apart (Fig. 2.1).

The inducers used for this experiment were starvation, 8 µg/mL oligomycin and 50 nM staurosporine. For the induction by starvation the BioGro-CHO medium was prepared without glucose and glutamine. For the induction by oligomycin a stock solution of 2 mg/mL was prepared with dimethyl sulfoxide (DMSO). In addition, a stock solution of staurosporine at 0.05 mg/mL was prepared in DMSO. The volume of DMSO used in the oligomycin and staurosporine induction experiment was also added to the 'Control' and 'Starvation' culture to ensure that differences seen in the culture were based on inducers and not DMSO.

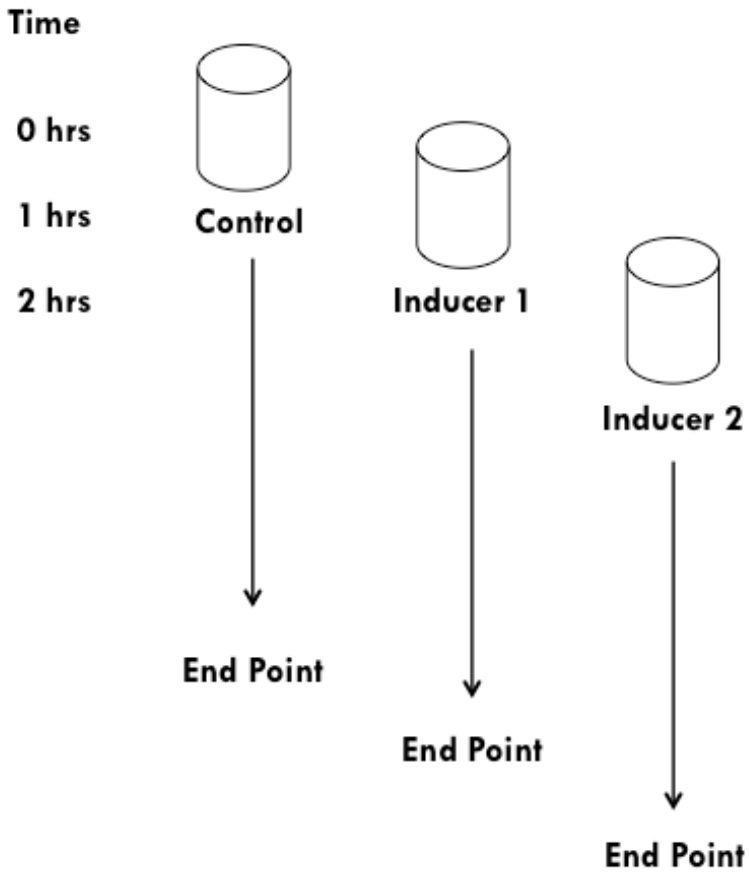

Figure 2.1: Experimental set-up for the apoptosis induction experiment.

A 1 mL preliminary sample was taken from each culture every 12 hours to determine the cultures cell density and viability using trypan blue exclusion. Based on those preliminary results the proper dilutions for the Guava flow cytometer and the DEP cytometer were determined. For the actual culture analysis two small samples (less than 0.5 mL) were taken from each shaker flask and centrifuged at 352xg for 1 min. After removing the supernatant and filtering it through a 0.2 μm filter for later media analysis the cell pellet was re-suspended in 750 – 1000 μL fresh medium to reach a final cell density of $5x10^5$ cells/mL. The re-suspended cell samples were then used for trypan blue and Guava flow cytometer assay analysis in duplicate, resulting in four technical replicates at each time point. An additional cell sample was taken for the DEP Cytometer analysis. The sample was also centrifuged at 352xg for 1 min to remove the supernatant. The cell pellet was then re-suspended in a mixture of low conductivity medium and regular BioGro-CHO medium (15:1) to reach a cell density of about $2x10^5$ cells/mL and a conductivity of (0.17 S/m).

2.2.4.3 Precursor feeding experiments

CHO-EG2 and CHO-DP12 cells were cultured in 250 mL baffled shaker flasks with a working volume of 80 mL. Cultures were seeded at $2x10^5$ cells/mL and incubated on a shaker platform (120 rpm) at 37°C with a 10% CO_2 overlay for the duration of the experiment. For each condition tested seven shaker flasks were run in parallel. The culture and feed media used for each precursor experiment were as follows:

<u>Batch – 'Batch':</u>

Basal medium – BioGro

Feed medium – no feed

Non-precursor Supplemented Fed-batch – 'NS':

Basal medium – BioGro

Feed medium – BioGro

Galactose – 'Galactose':

Basal medium – BioGro + 10 mM Galactose

Feed medium – BioGro + 25 mM Galactose

Galactose + Uridine – 'UG':

Basal medium – BioGro + 20 mM Galactose + 1 mM Uridine

Feed medium – BioGro + 25 mM Galactose + 25 mM Uridine

Galactose + Uridine + Manganese – 'UMG':

Basal medium – BioGro + 20 mM Galactose + 1 mM Uridine + 8 μM $MnCl_2$

Feed medium – BioGro + 25 mM Galactose + 25 mM Uridine + 25 μM $MnCl_2$

All cultures were run for 7 days without feeding for the batch culture and daily feeding starting on day 3 for the all other cultures. The volume of feed solution was calculated based on the culture volume after sampling that day to reach 1 mM glucose in the culture volume by feeding.

A 1 mL sample volume was taken at every sampling point for cell density and viability from all seven shakers. The media component and productivity were determined for two shakers per time point. The shakers used for sampling were alternated every day. In addition, starting on day 3 for CHO-EG2 and day 4 for CHO-DP12 two cell samples ($1x10^7$ cells each) for nucleotide / nucleotide sugar analysis and two 10 mL supernatant samples for glycan analysis were taken.

These samples were taken from the two shakers used for the media component and productivity analysis that day.

2.2.5 Specific growth rate and integral viable cell density

The specific growth rate is defined as the rate of cell growth over a given time and calculated as follows:

$$\mu(h^{-1}) = \frac{lnN - lnN_0}{\Delta t}$$

In which N is the cell density at time t and N_0 is the cell concentration at time t_0.

The integral viable cell density (IVCD) is defined as the integration of the viable cell density over time and calculated as follows:

$$IVCD\ \left(10^6 \frac{cells - days}{mL}\right) = \int_{t_v}^{t} X_v dt$$

Where X_V is the viable cell density at time t.

2.3 Analysis of media components

The analysis of the media components glucose and glutamine and their metabolic products lactose and glutamate was done using the YSI2700 Biochemistry Analyzer. The YSI is based on an immobilized enzyme sensor technology. The enzymes bound on the membranes

convert the substrate of interest to produce hydrogen peroxide. A probe signal is produced when the produced hydrogen peroxide is electrochemically oxidized at the platinum anode of the probe. This signal is then converted into a concentration.

2.3.1 Glucose consumption and lactate production

Glucose and lactate concentration in the culture supernatant were determined simultaneously. For the analysis the glucose and lactate membranes (YSI 2365 and 2329) were installed in the YSI and the appropriate buffer (YSI 2357) was prepared. Once installed the YSI automatically flushes buffer over the membranes until the baseline current stabilized. After a stable baseline current was detected an automatic internal calibration was performed with a YSI standard (2.5 g/L glucose, 0.50 g/L lactate). Once the YSI was set up and calibrated, supernatant samples were taken up for analysis. After every 5 samples the machine automatically re-calibrated.

The specific glucose consumption (q_G) and lactate production (q_L) was calculated using the following equation:

$$q_G \; or \; q_L = \frac{[\Delta C/\Delta t]}{[(N - N_0)/(lnN - lnN_0)]}$$

Where ΔC is the change in concentration over the time period t and N and N_0 are the cell concentrations at the beginning and the end of the time period, respectively.

2.3.3 Glutamine consumption and glutamate production

The YSI was also used to simultaneously determine the glutamine and glutamate concentration in the culture supernatant. For the analysis the glutamine and glutamate membranes (YSI 2735 and 2754) were installed in the YSI and the appropriate buffer (YSI 2357) was prepared. Once installed the YSI automatically flushes buffer over the membranes until the baseline current stabilized. After a stable baseline current was detected an automatic internal calibration was performed with a YSI standard (0.75 g/L glutamine, 0.731 g/L glutamate). Once the YSI was set up and calibrated supernatant samples were taken up for analysis. Every 5 samples the machine automatically re-calibrated.

The specific glutamine consumption and glutamate production was calculated using the same equation as above.

2.4 Cell Density and Viability Determination

2.4.1 Coulter Counter

Cell samples were diluted 1:125 with PBS (Invitrogen) containing 1 mM EDTA (Fisher, Fair Lawn, NJ) and analyzed using a Coulter Counter (Coulter Electronics, Inc., Hialeah, FL). The electronic particle count was then converted to a cell density count using the following equation:

$$cell\ density\ (cells/mL) = \frac{(particle\ count * dilution\ factor)}{(volume\ measured * 1.0E6)}$$

$$cell\ density\ (cells/mL) = \frac{(particle\ count * 125)}{(0.5\ mL * 1.0E6)}$$

2.4.2 Image Analysis

A Cedex Image Analyzer (Innovatis AG, Bielefeld, Germany) was used to analyze cell samples diluted 1:2 with 0.4% (w/v) trypan blue (Invitrogen) to determine the cell density and viability. The Cedex was calibrated using polystyrene balls similar in size to CHO cells (standard calibration method). In addition, a light calibration (to correct for exposure) was performed every 3-4 months. A comparison of viable cell counts by Cedex and a Haemocytometer method using trypan blue exclusion gave values within 5%.

2.4.3 Flow Cytometry Analysis

Three different assays were performed using the Guava 8HT system and easyCyte software (EMD Millipore, Danvers, MA). Initially, a ViaCount (Catalog No. 4000-0040, EMD Millipore) assay was performed to determine the viability and cell density during the bioprocess. The ViaCount assay consists of two DNA binding dyes – one that enters all cells and the second that only stains cells with a compromised membrane. The assay was performed based on the supplier's protocol with an incubation time of 10 min. To achieve an in-depth analysis of the culture Nexin, Caspase 8, and MultiCaspase (EMD Millipore) assays were also performed. The Nexin assay (Catalog No. 4500-0450) is based on the detection of phosphatidylserine on the outer leaflet of the plasma membrane of cells, a characteristic of early apoptosis. The assay was performed using the supplier's protocol with 200 μL of Guava Nexin Reagent (EMD Millipore) and an incubation time of 20 min. The Caspase 8 assay (Catalog No. 4500-0550) is based on the detection of the active caspase 8 enzymes while the MultiCaspase assay (Catalog No. 4500-0530) detected any activated caspase enzymes. Both assays were performed according to the supplier's protocol. The 7-Amino-actinomycin D (7-AAD) stain was incorporated with the

Nexin and both Caspase assays to determine cells in late stage apoptosis. The cells detected in the late stages of apoptosis were designated as "dead". The designation of sub-populations of cells following the Nexin and Caspase-8 assays was based on the acquisition of 2000 data points per sample from the flow cytometer. The quadrant markers were positioned manually following the supplier's protocol.

2.4.4 Dielectric Measurements

2.4.4.1 Capacitance Probe

For the on-line capacitance measurement a capacitance probe (Aber Instruments, Aberystwyth, UK) was incorporated aseptically into the bioreactor. The probe was connected via an amplifier to a 220 Model detector and set to measure ΔC throughout the bioprocess. The probe was set to perform a frequency sweep from 0.1 – 20 MHz every minute.

The measurements were later saved as a .csv file for further analysis by plotting in Excel.

2.4.4.2 Dielectrophoretic Cytometer

For the offline measurement a sample (5-10 mL) was taken from the bioreactor at timed intervals, centrifuged (377xg) and the cell pellet was then reconstituted in a mix of fresh growth medium (37°C) and a low conductivity (~ 0.067 S/m) medium (37°C) [22.9 mM sucrose (Sigma), 16 mM glucose (Fisher), 1 mM $CaCl_2$ (Fisher), 16 mM Na_2HPO_4 (Fisher)] (Polevaya et al., 1999). The cell pellet was reconstituted to $2x10^5$ cells/mL using a ratio of 2:30 (fresh : low conductivity medium) and to reach a conductivity of ~ 0.17 S/m as measured by a conductivity meter (Orion 3-Star Plus, Thermo Scientific). An initial time course experiment showed that the

cell viability and the cell size were stable (within 5% of the original sample) for at least an hour – the time needed for the DEP measurement during the experiment.

For the analysis only single cell signatures were considered. All other signatures indicating aggregated cells were dismissed.

2.5 Protein quantification

The volumetric productivity was determined by the overall production of EG2 and DP12 for each culture volume using an ELISA while the specific productivity for each culture was calculated based on the product concentration over the integral viable cell density (IVCD). For the EG2 ELISA assay the standard used was provided by Yves Durocher (NRC) and the standard for the DP12 assay was an IgG calibrator taken from a commercial kit (Immunology Consultants Laboratory (E-80G); 7.35 mg/mL). Each standard was prepared as outlined below.

2.5.1 ELISA for EG2

All supernatants were analyzed using an ELISA method developed in the Butler lab. The anti-human IgG (Fc specific) primary (1°) antibody (Sigma I2136) and the anti-human IgG (Fc-specfic)-Peroxidase secondary (2°) antibody (Sigma A0170), both produced in goat, and the detection solutions were purchased from Sigma.

For each ELISA analysis the buffers were prepared fresh and brought to room temperature prior to starting. The plates were coated with 100 µL/well of 1° antibody at a 1/3000 dilution in 1X PBS (coating buffer) overnight at 4°C. The coating buffer was then removed from the plate by forcefully dumping it out and blotting the plate several times on a stack of paper towels. After each step in the ELISA procedure the plates were washed 3 times

with 300 μL/well wash buffer (1X PBS with 0.04% Tween). After washing the plate it was blocked by adding 275 μL/well blocking buffer (1X PBS with 3% BSA and 0.04% Tween) and incubated covered for 1 h at room temperature. During the blocking process the supernatant samples were diluted to 1/1,000 or 1/5,000 in dilution buffer (1X PBS with 0.5% BSA and 0.04% Tween) depending on the expected concentration of antibody. The EG2 standard provided by Yves Durocher (3.34 mg/mL) was diluted to 0.1 μg/mL. Before adding the samples and standards to the plate 120 μL of dilution buffer were added to the wells needed for the serial dilution of the samples and standards. 240 μL of the prepared samples and standards were then added to the appropriate wells in the 96-well plate and serially diluted before incubating the plate for 1 h at room temperature. Next 100 μL/well of the secondary antibody were added to the plate at a 1/60,000 dilution for 1 h at room temperature. While the plates were incubating the developing solution was prepared by dissolving two 3,3',5,5'-Tetramethylbenzidinedihydrochloride (TMB) tablets in 20 mL of 0.05 M Phosphate-Citrate buffer (pH 5). This substrate is light sensitive and must be protected by tinfoil while dissolving and until used. Just prior to adding the developing solution to the plates 4 μL of 30% hydrogen peroxide per 20 mL solution were added to the developing solution. 200 μL of this solution were then added to each well before incubating the plate at room temperature for 30 min. During the incubation period the plates were wrapped in tin foil. Before reading the plates at 450 nm 50 μL of 2 M H_2SO_4 was to be added to each well to stop the developing process.

2.5.2 ELISA for DP12

The procedure was as outlined in the ELISA for EG2 except for the use of a different standard. In the case of the DP12 ELISA analysis a human IgG calibrator from a human IgG

ELISA Kit (Immunology Consultants Laboratory (E-80G); 7.35 mg/mL) was used as the standard.

2.6 Glycan Analysis

For the glycan analysis the glycan structures were removed from the protein and fluorescently labeled before being analyzed via a hydrophilic interaction liquid chromatography (HILIC) method. The glycan analysis was performed as described in Tayi and Butler (2015).

2.6.1 Glycan release

The glycans from the EG2 and DP12 antibodies were released while being captured on a Protein A column (GE Healthcare). The Protein A columns were prepared by washing the column twice with 400 µL of 20 mM phosphate wash buffer (80% 20 mM Na_2HPO_4, 20% of 20 mM NaH_2PO_4), forcing the wash buffer through by spinning the Protein A column at 172xg for 1 min after each wash step. Next 400 µL of the concentrated culture supernatant (containing at least 50 ng antibody) were applied to the capped column and left to incubate at room temperature for 10 min on a shaking platform. After the incubation period the supernatant was spun out (172xg for 1 min) of the column. Washing the column three times with phosphate wash buffer washed through any leftover un-bound antibodies. To remove the glycans from the bound antibodies 200 µL of phosphate wash buffer and 1 µL of Peptide-N-Glycosidase F (PNGaseF) (10 units) (Promega) were added to the capped Protein A column. The column was then incubated overnight at 37°C on a shaking platform.

After the incubation the released glycans were extracted by spinning down the supernatant in the column at 172xg for 1 min. To remove any further glycans released 400 µL of

water was added to the column and also spun down. The extracted glycans were then filtered using a NanoSep 10K column to remove the PNGaseF enzyme from the sample. Next the pure glycan sample was dried down in the SpeedVac.

After the extraction the Protein A column was washed with glycine-Cl to remove any bound antibodies. The column was then rinsed twice with phosphate wash buffer before being stored in 20% ethanol. The columns were reused up to 5 times.

2.6.2 Glycan labeling and clean up

The glycan labeling solution was prepared by mixing 350 µL DMSO with 150 µL glacial acetic acid in a 1.5 mL microcentrifuge tube. Next 10 mg 2-aminobenzamide (2-AB) were weighed into a fresh microcentrifuge tube and dissolved in 200 µL of the DMSO and glacial acetic acid mixture. 100 µL of the dissolved 2-AB mixture were then added to 6.2 mg sodium cyanoborohydride ($NaBH_3(CN)$) and mixed well.

The completely dried glycans were incubated with 5 µL of 2-AB labeling solution for 2 hours at 65°C. After the incubation period the unbound 2-AB was removed using the HypoSep Diol column (Thermo Scientific). Before retrieving the 2-AB labeled sample for cleanup 45 µL of acetonitrile (ACN) was added to it. The column was prepared by washing with 1 mL Milli-Q water and 4 x 1 mL ACN before the labeled glycan sample was applied. After each mL of liquid was applied it was forced through the column at 2 mL/min using air flow applied to the top of the column. Next the sample was applied to the top of the column and left at room temperature to incubate for 15 minutes. After the incubation period the extra 2-AB labeling was removed by washing the column 5 x 1 mL ACN before eluding the labeled glycan sample with 3 x 400 µL

Milli-Q water. The eluted glycan sample was then dried down in the SpeedVac. Prior to the HPLC analysis the dried down glycan sample was re-suspended in 40 µL Milli-Q water.

2.6.3 HPLC using HILIC

The glycan sample was analyzed using an XBridge™ Amide column (4.6 x 250 mm, 3.5 µm – Waters). The HPLC system used consisted of a Waters 1525µ binary HPLC pump, a Waters 2475 multi λ fluorescence detector, a Waters 2707 autosampler, a Waters in-line degasser AF, and an Eppendorf CH-30 column heater. The HPLC system was controlled using the Waters Empower Pro Software. The same software was used for data analysis.

The buffers used were 50 mM ammonium formate (pH 4.4) [Buffer A] and Acetonitrile [Buffer B]. Both buffers were HPLC grade and buffer A was also filtered using a 0.2 µm filter. The buffer solutions were not degassed as an in-line degasser was used with the HPLC system.

The glycan elution was monitored using the fluorescent detector with the excitation set at 330 nm and the emission set at 420 nm with the following settings: 10000 euf, gain 1, and data rate 1 pts/sec. For the run the column heater was set to 30°C.

The elution program was as follows:

Table 2.1: Elution program for glycan analysis.

Time	Flow	Buffer A	Buffer B	Curve
0 min	0.86 mL/min	20	80	6
48 min	0.86 mL/min	50	50	6
49 min	0.86 mL/min	100	0	6
53 min	0.86 mL/min	100	0	6
55 min	0.86 mL/min	20	80	6
63 min	0.86 mL/min	20	80	6
64 min	0.00 mL/min	20	80	6

The samples were prepared for HPLC analysis by adding 6 μL of the re-suspended unknown sample to a 20:80 mixture of sample and buffer B to give 30 μL. The injection volume for each standard or extraction sample was 25 μL.

2.6.4 Glycan analysis

A dextran ladder was run with the regular glycan samples to determine a standard curve for the glucose unit (GU) values. This standard curve correlated the elution time with the GU value. This was then used to determine the GU values of the peaks found in the unknown glycan samples. The GU values in turn were used to determine the structures associated with those peaks found in the glycan sample by referring to the Oxford GU database and by comparing former exoglycosidase digest results.

2.6.5 Index calculations

Index calculations were performed as described below to better compare the identified glycan distribution among precursor feeding experiments. Indices were calculated based on the percentage of the different galactosylated, fucosylated and sialylated glycoforms present in each sample.

2.6.5.1 Galactosylation Index (GI)

The three main glycan structures found on antibodies are G0, G1, and G2, which are structures containing none, one or two galactose residues, respectively. The Galactosylation Index (GI) was calculated based on the percentage of these glycoforms as follows:

$$GI = \frac{(G1 * 0.5) + (G2 * 1)}{G0 + G1 + G2}$$

2.6.5.2 Fucosylation Index (FI)

Each glycan can potentially have a fucose molecule attached to its core structure. To compare the overall fucosylation among glycan samples the Fucosylation Index (FI) was calculated based on the percentage of these glycoforms as follows:

$$FI = \frac{F1}{F0 + F1}$$

2.6.5.3 Sialylation Index

The Sialylation Index (SI) is an indication on how many sialic acid molecules are attached to the glycans in a sample. In antibodies the majority of samples have a maximum of two sialic acid molecules attached. Based on the presence of sialic acid the SI was calculated based on the percentage of these glycoforms as follows:

$$SI = \frac{(S1 * 0.5) + (S2 * 1)}{S0 + S1 + S2}$$

2.7 Nucleotide and Nucleotide Sugar Analysis

The protocol was developed for the extraction and analysis of intracellular nucleotide and nucleotide sugar pools in CHO cells cultured in suspension. This protocol was chosen based on

the comparison of two quenching protocols and a control (no quenching) in combination with four extraction protocols found in the literature. Special attention was paid to the recovery of ATP, the overall extraction of the metabolites of interest and the methods overall reproducibility. It was determined that the "Methanol/AMBIC" quenching with the "Envi^{TM}-Carb column" extraction is the best combination for an efficient and reproducible nucleotide / nucleotide sugar analysis (see Appendix A). An overview of the entire method is shown in Figure 2.2.

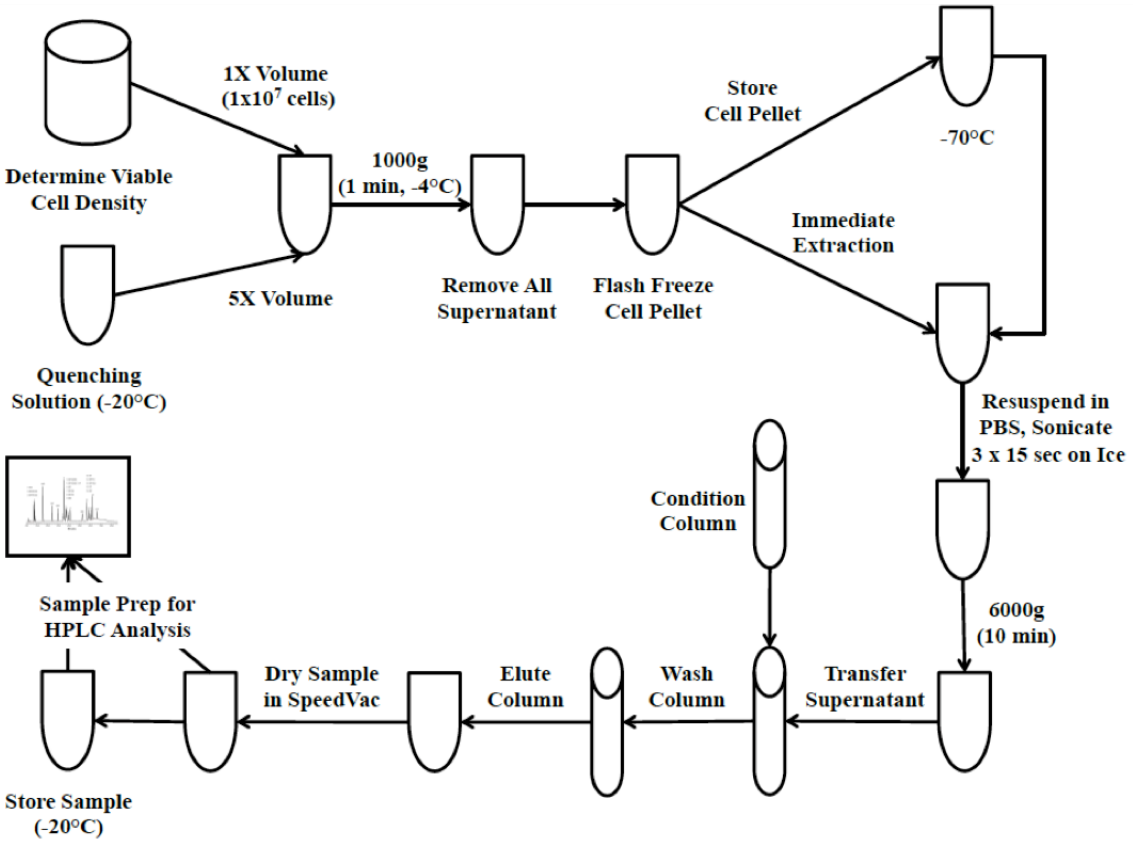

Figure 2.2: The workflow for the quenching, extraction and HPLC analysis of cell samples to determine the intracellular nucleotide / nucleotide sugar pool (taken from Braasch et al., 2015).

2.7.1 Quenching

The quenching solution used was 60% methanol / 0.85% ammonium bicarbonate (pH 7.4) based on Sellick et al. (2009). The first step in preparing to quench a cell sample was to pre-

cool the quenching solution to -20°C. Next a supernatant sample containing $1x10^7$ viable cells was taken and added to 5 times the sample volume of quenching solution (-20°C). The sample tube was then inverted gently twice before the cells were spun down at 1000xg for 1 min at -4°C. Afterwards the supernatant was decanted and the residual liquid was removed using a Pasteur pipette and vacuum. The cell pellet was then flash frozen in liquid nitrogen. Once the cells were flash frozen the extraction was performed immediately or the cell pellet was stored at -70°C for up to 1 week.

2.7.2 Extraction

For the extraction procedure the following solutions were prepared and stored ice-cold prior and during use:

1. Phosphate buffered saline (PBS) (Invitrogen)
2. 10 mM NH_4HCO_3 (pH 7.0)
3. Condition solution 1: 80% (v/v) acetonitrile in 0.1% (v/v) trifluoroacetic acid (TFAA)
4. Condition solution 2: Milli-Q water
5. Wash solution 1: Milli-Q water
6. Wash solution 2: 25% (v/v) acetonitrile
7. Wash solution 3: 50 mM triethylammonium acetate (TEAA) buffer (pH 7.0) (Fluka)
8. Elution solution: 25% (v/v) acetonitrile in 50 mM TEAA buffer (pH 7.0)

Prior to the extraction methanol treated 1.5 mL samples tubes were prepared by rinsing the tubes with methanol. Two 1.5 mL tubes per sample were needed. The Envi^{TM}-Carb column

was then put into a 15 mL sample tube in a stand or Styrofoam box. To condition the column 3 mL of 'condition solution 1' were applied. Each solution added to the column was left to elute completely by gravity flow before proceeding to the next step. Next 3 mL of 'condition solution 2' were applied to the column.

While the 'condition solution 2' was eluting through the column the cell samples were prepared. The cell pellet was re-suspended in 0.5 mL PBS in a 50 mL sample tube. The cell mixture was then sonicated for 3 x 15 sec on ice at level 7 with a narrow probe sonicator (Qsonica XL-2000 Series) with the sonicator tip at the top of the liquid level. The sonicated sample was then transferred into a 1.5 mL sample tube before it was centrifuged at 6000xg for 10 min. Next the supernatant was transferred into new 1.5 mL sample tube and topped up to 1 mL with 10 mM NH_4HCO_3 (pH 7.0). Until the column was ready the samples were kept on ice.

After the column 'condition solution 2' completely eluted the diluted extract was applied onto the column. The Envi^{TM}-Carb column was then washed with 3 mL of 'wash solution 1'. Next the Envi^{TM}-Carb column was washed with 3 mL of 'wash solution 2' and 3 mL of 'wash solution 3'. Lastly the bound nucleotide / nucleotide sugars were eluted from the Envi^{TM}-Carb column with 2 mL of 'elution solution' into two 1.5 mL methanol treated tubes.

The samples from both tubes were then combined and dried to complete dryness in the SpeedVac. Once the samples were completely dry they were re-suspended in 40 µL Milli-Q water each and stored at -20°C until HPLC analysis.

2.7.3 HPLC

2.7.3.1 HPLC Program and Set-Up

The nucleotide / nucleotide sugar samples were analyzed using a CarboPac^{Tm} PA1 column (4 x 250 mm). The HPLC system used consisted of a Waters 1525 binary HPLC pump, a Linear UV/Vis 200 detector, a Waters 717plus autosampler, and a Transgenomic column heater. The HPLC system was controlled using the Waters Empower Pro Software. The same software was used for data analysis.

The buffers used were 1 mM NaOH (Acros) [Buffer A] and 1 M NaAc (J.T Baker) in 1 mM NaOH [Buffer B]. Both buffers were HPLC grade and filtered using a 0.2 μm filter. Prior to use the buffer solutions were degassed.

The nucleotide / nucleotide sugar elution was monitored using the UV detector at 260 nm with the following settings: column temperature at 27°C, UV detector at 260 nm with a range of 0.2 AUFS and a rise time of 0.1 sec.

The elution program was as follows:

Table 2.2: Elution program for nucleotide / nucleotide sugar analysis.

Time	Flow	Buffer A	Buffer B
0 min	0.8 mL/min	80	20
10 min	0.8 mL/min	70	30
20 min	0.8 mL/min	60	40
30 min	0.8 mL/min	45	55
45 min	0.8 mL/min	45	55
55 min	0.8 mL/min	20	80
60 min	0.8 mL/min	0	100
70 min	0.8 mL/min	0	100
80 min	0.8 mL/min	80	20
85 min	0.8 mL/min	80	20
86 min	0.0 mL/min	80	20

2.7.3.2 Nucleotide / Nucleotide Sugar Standards

5 mM stock solutions of all standards of interest were prepared in 1.5 mL sample tubes using HPLC grade chemicals and Milli-Q water. A mix of all standards was prepared by adding equal volumes of individual standards to a 1.5 mL sample tube. The individual standards and the mixed solutions were then stored at -20°C until use in HPLC analysis.

2.7.3.3 HPLC Sample Preparation

The samples were prepared for HPLC analysis by adding 15 μL of the re-suspended unknown sample to an 80:20 mixture of buffers A and B to give 60 μL. The injection volume for each standard or extraction sample was 30 μL.

2.7.3.4 Data Analysis

To identify the nucleotide / nucleotide sugars in the unknown samples all standards were run alone and in a mix to determine their elution time (Figure 2.3). To allow for quantitative analysis a mix of 19 standards was run at three different concentrations to calculate individual standard molar responses.

$$molar\ response = \frac{moles\ (std)}{area\ (std)}$$

This information was used to identify and quantify the peaks in each elution profile determined for the extracted samples. After determining the moles of each nucleotide / nucleotide sugar per cell this value is converted to a concentration (mM) per cell as follows:

$$mM/cell = \frac{fmol/cell}{(^4/_3 * \pi * r^3)}$$

where r, in dm, is the average radius of the cells sampled as determined using the Cedex.

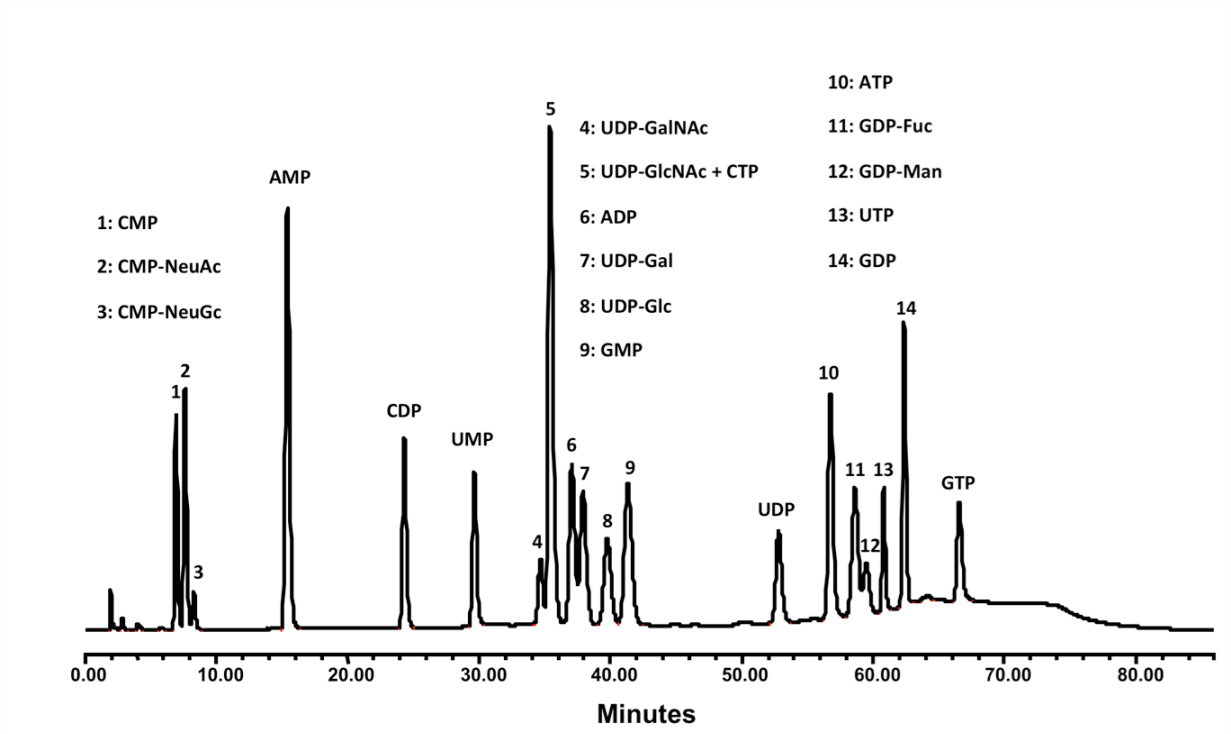

Figure 2.3: HPLC elution profile of a mixture of 20 nucleotide / nucleotide sugar standards. The chromatogram was produced by injecting 30 µL of a mixture of 19 standards at 27°C using a CarboPac^{TM} PA-1 column. Each component was at a concentration of 0.0375 mM in the mixture. The elution protocol was based on the method developed by Tomiya *et al.*, 2001 with the UV detector set at 260 nm. The elution gradient was as follows: T_0= 20% (v/v) E2; T_{10} = 30% (v/v) E2; T_{20}= 40% (v/v) E2; T_{30} = 55% (v/v) E2; T_{45}= 55% (v/v) E2; T_{55} = 80% (v/v) E2; T_{60}= 100% (v/v) E2; T_{70} = 100% (v/v) E2; T_{80} = 20% (v/v) E2; T_{85} = 20% (v/v) E2 (taken from Braasch et al., 2015).

2.8 Statistical Analysis

Differences between measurements were assessed by un-paired two-tailed Student's *t*-test. A *P*-value of <0.02 was considered as statistically significant.

In part A all data points are based on four technical replicates with the exception of the DEP measurements, which were based on two technical replicates, and the capacitance probe, which is a contiuous measurement.

In part B all data points for the cell density and viability measurements are based on seven biological replicates. The media component, productivity, glycan, and nucleotide / nucleotide sugar analysis are all based on two biological replicates.

Section A

Monitoring cell viability using image, flow cytometer and dielectric analysis

Introduction

Monitoring the cell density and viability is an integral part in the cell culture process. The cell density and viability measurements can be used to determine the initiation of a feeding strategy in a batch culture or the termination of a culture. The monitoring of viable cells in a culture process is also important because those cells are considered the metabolically active producer cells needed for biopharmaceutical production.

However, the definition of viability is very complex and depends very much on the characteristics used to define it (Browne and Al-Rubeai, 2011). Because of this complexity it is important to understand viability and the process of cell demise (apoptosis) in a cell culture. In addition, it is important to understand what different cell density and viability assays measure to better understand their capability and applicability.

For this study image analysis (trypan blue exclusion), coulter counter, flow cytometer assays, and two dielectric measurements (bulk and single) were compared in regular batch cultures and cultures in which apoptosis was artificially induced by starvation, oligomycin, and staurosporine. These experiments were used to measure and further understand the progression of apoptosis during cell demise.

Chapter 3

The comparison of different cell density and viability assays for cell culture*

3.1 Introduction

To ensure maximum productivity of recombinant proteins it is desirable to prolong cell viability during a mammalian cell bioprocess, and therefore important to carefully monitor cell density and viability. An important aspect is the early detection of the onset of cell demise. The early detection is of importance since it will allow for measures to be taken to either extend cell culture viability with nutrient feeding or to terminate the process when very sensitive proteins are produced.

One of the most commonly used assays is the trypan blue exclusion method in combination with an image analyzer. Trypan blue is a high molecular weight dye that will only be taken up by cells when the cell membrane is compromised (Strober, 2001). However, the loss of the cell membrane integrity exclusion method marks the end point in apoptosis. When and while cells go through apoptosis specific changes associated with apoptosis can be detected by fluorescent markers (Vermes, 2000). While flow cytometer assays can be very specific they are fairly costly and take more time than simple staining procedures, which can lead to artificially decreased cell viability.

* Partial content of this chapter was included in a paper:
Braasch, K., Nikolic-Jaric, M., Cabel, T., Salimi, E., Bridges, G.E., Thomson, D.J., and Butler, M. (2013), The changing dielectric properties of CHO cells can be used to determine early apoptotic events in a bioprocess. Biotechnology and Bioengineering. 110 (11): 2902-2914.

In addition to changes that can be observed with fluorescent assays cells exhibit changes in the dielectric properties when entering apoptosis (Demierre et al., 2008; Duncan et al., 2008; Flanagan et al., 2008; Gagnon, 2011; Huang et al., 1992; Pethig et al., 2010). Those changes in cell membrane capacitance and within the ionic content of the cytoplasm can be detected using dielectric measurements. In the past dielectric measurements have become of interest because currently available probes allow on-line measurements, which would allow a constant monitoring of the cell culture. In previous studies the *in situ* bulk capacitance probe was used to measure cell density in cell culture processes (Ansorge et al., 2010; Ducommun et al., 2002; Knabben et al., 2010; Opel et al., 2010; Tibayrenc et al., 2011). The measurements were compared to the more common trypan blue exclusion method. During the regular growth phase the measurements in previous studies aligned very well but during the decline phase the capacitance data exhibited either higher or lower cell densities than the trypan blue method. However, no further examination of this difference was done. Some further research went into developing algorithms to adjust the capacitance data to fit the trypan blue data (Opel et al., 2010). This makes sense in already existing industrial processes in which certain key elements of the process (feeding, harvest) are linked to a certain cell density and / or viability. However, in new processes or process development a better understanding of the data sets will be helpful in the overall process engineering.

In this study, six different and independent methods of monitoring were applied to Chinese hamster ovary (CHO) cells grown in a batch culture in a controlled bioreactor to determine cell density and/or cell viability. They included: a particle counter, trypan blue exclusion (Cedex), an *in situ* bulk capacitance probe, an off-line fluorescent flow cytometer with various assays, a prototype dielectrophoretic (DEP) cytometer, and the adenylate energy charge.

The measurements of these methods were compared with each other to show and explain differences in the detection of the onset of cell demise.

3.2 Results

3.2.1 Cell culture profiles

The results of the comparative measurements of cell density and viability for two separate batch cultures (A inoculated from passage 25, B inoculated from passage 35) are shown in Figs. 3.1 and 3.2. Profiles in panel A of both Figs. 3.1 and 3.2 were based on samples taken every 24 h from inoculation up to 170 h. In a second culture (panel B) samples were analyzed every 6 h from 96 h – 130 h in order to monitor the viable to non-viable transition of the cells more closely. Total and viable cell densities (Fig. 3.1) were determined using four different methods: Coulter counter, Cedex, ViaCount and *in situ* capacitance probe. The data in Fig. 3.1 show that during the exponential growth phase each set of measurements gave similar values. However, divergence in measurements occurred beyond the point of maximum cell density at 90 h – 100 h, which coincided with a decline in cell viability as seen in Fig. 3.2. The Coulter counter provides an electronic measure of presence of particles and does not distinguish between viable and non-viable cells; consequently, high cell density values were observed up to the end of the cultures. The other three measurements showed an apparent decline in cell density beyond the point of maximum cell density. However, there was a statistically significant difference ($P < 0.02$) between the Cedex measurements and the measurements by the capacitance probe (Fig. 3.1A after 120 h, Fig. 3.1B after 100 h) and the ViaCount assay (Fig. 3.1A after 120 h, Fig. 3.1B after 100 h). The cell density determined by the capacitance probe was comparable to measurements made using the ViaCount assay. The consistently higher values determined from

the Cedex can be explained by the mechanism of trypan dye exclusion, which depends upon cell membrane damage – a late event in apoptosis (Hughes et al., 1997). Although the ViaCount assay is based on the same principle of dye exclusion it appears to be able to detect an earlier stage of membrane damage and hence registers lower viabilities compared to trypan blue exclusion (Millipore Technical Publication: MK80000410).

Figure 3.2 shows data from the same two bioreactor cultures monitored for the percentage viability of the cell population. As in the previous data this showed a decline in viability beyond the maximum cell density at 90 h – 100 h. Divergence can be observed for the rate of loss of viability as determined using the Cedex (trypan blue), ViaCount assay, Nexin assay, and DEP cytometer. Statistical analysis showed that the Cedex viability determination were significantly different ($P < 0.02$) from measurements made by the ViaCount assay (Fig. 3.2A after 70 h, Fig. 3.2B after 75 h), the Nexin assay (Fig. 3.2A after 70 h, Fig. 3.2B after 90 h), and the DEP cytometer measurements (Fig. 3.2A after 100 h, Fig. 3.2B after 100 h). In addition measurements by the ViaCount assay were significantly different ($P < 0.02$) from measurements made by the Nexin assay (Fig. 3.2A between 100 –145 h, Fig. 3.2B after 90 h) and the DEP cytometer measurements (Fig. 3.2A between 100 – 145 h, Fig. 3.2B after 105 h). The measurements by the Nexin assay and the DEP cytometer were not significantly different before 118 h of culture. However, there was a significant difference ($P < 0.02$) between the measurements after that time for both runs. These profiles are consistent between the two cultures shown in Fig. 3.2 and other repeated runs (not shown).

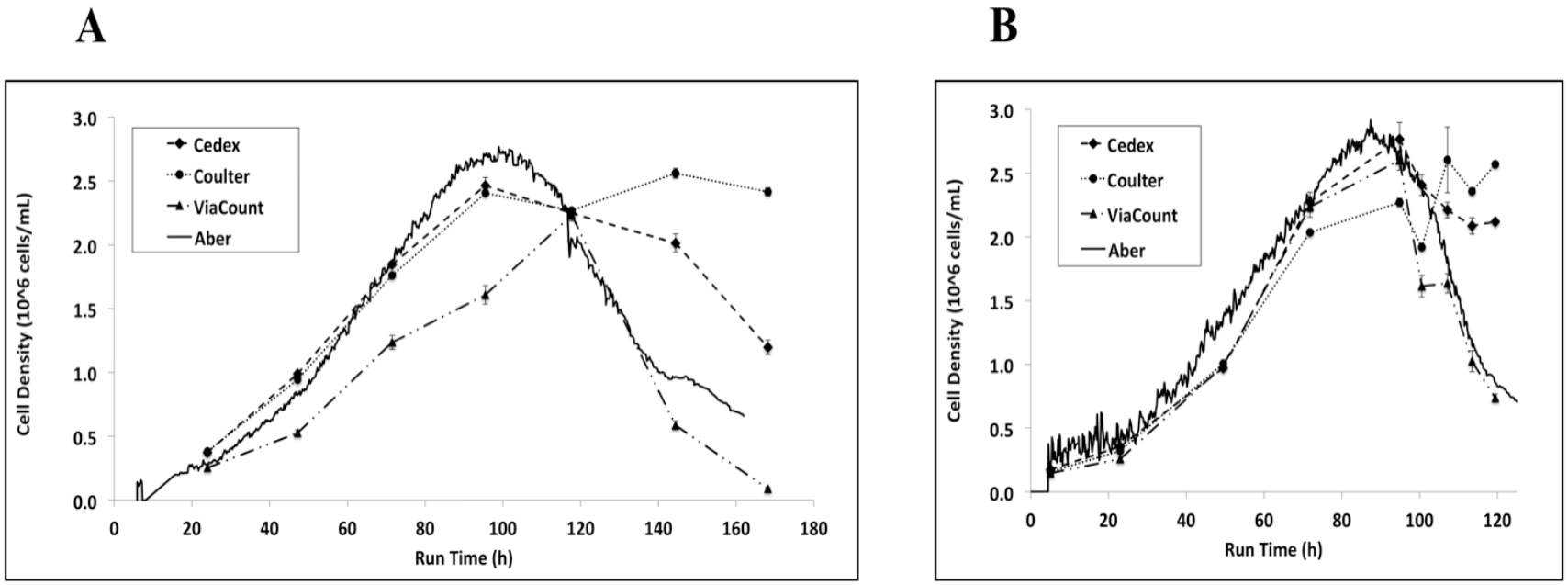

Figure 3.1: Comparison of cell density and capacitance determined for two representative CHO EG2 batch cultures using Trypan blue (Cedex), Coulter Counter, Guava flow cytometer (ViaCount) and Capacitance probe (Aber). The culture (3L) was sampled every 24 h from 0 h to 168 h **(A)**. The culture (3L) was sampled every 24 h from 0 h to 95 h and then every 6 h from 95 h to 119 h **(B)**. The continuous ΔC measurement taken from the probe was adjusted to align with cell density at 72 h determined by Cedex. The values graphed for the off-line measurements are the average of four technical replicates for each sampling point with error bars representing the standard error of the mean. (taken from Braasch et al., 2013)

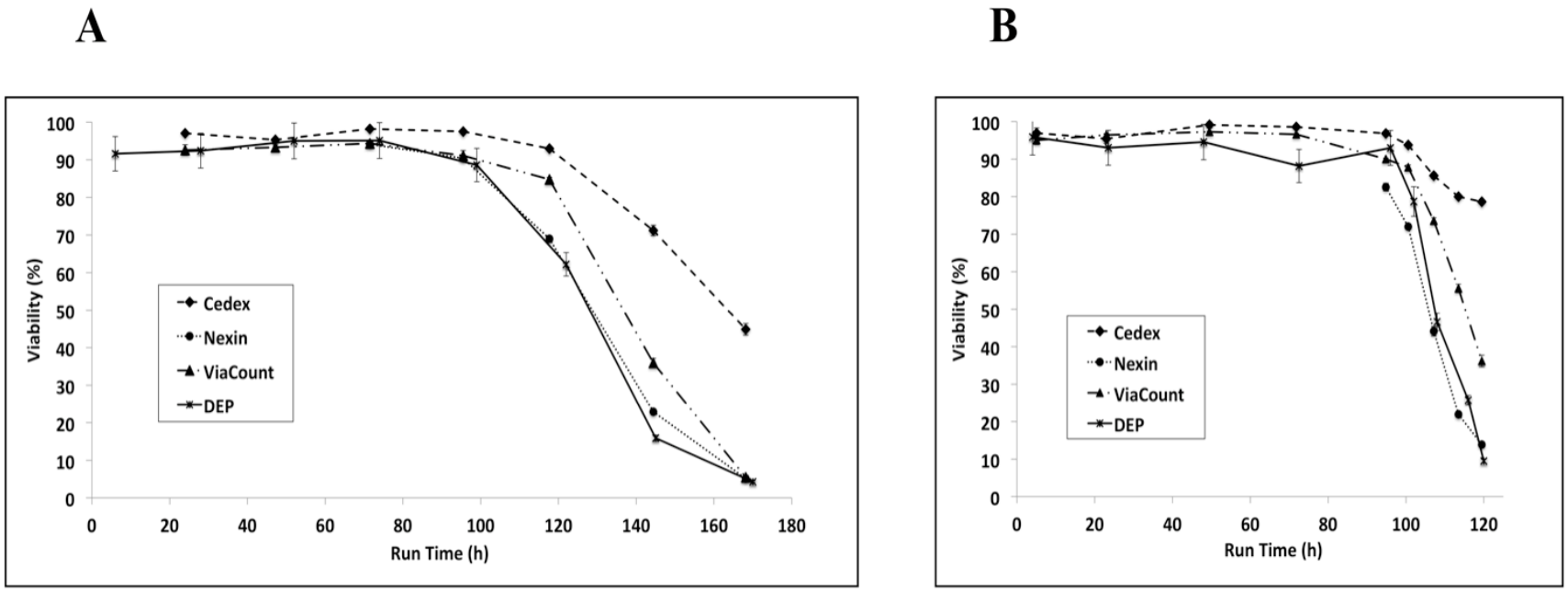

Figure 3.2: Comparison of cell viability determined for CHO EG2 batch cultures using trypan blue (Cedex), ViaCount and Nexin (Guava flow cytometer) and DEP cytometer. The culture (3L) was sampled every 24 h from 0 h to 168 h **(A)**. The culture (3L) was sampled every 24 h from 0 h to 95 h and then every 6 h from 95 h to 119 h **(B)**. The values graphed are the average of four technical replicates for each sampling point with error bars representing the standard error of the mean. Each DEP value is based on 2 determinations from >200 cells per sample (error bars represent 5% - error of method). (taken from Braasch et al., 2013)

In addition to the above measurements the glucose and lactate concentrations were also monitored for bioreactor runs A (passage 25) and B (passage 35) (Fig. 3.3A). The data in Fig. 3.3A show that for both runs the start of the decline phase in Fig. 3.2A and B correlated with the glucose concentration in the medium decreasing below 1 mM (run A at ~ 100 h and run B at ~ 90 h). Furthermore in run B between 50 – 95 h glucose was consumed slightly faster and lactate accumulated more than in run A. This difference in lactate production during the run in combination with a difference in glucose consumption manifested in a significantly higher yield of lactate per glucose in the exponential growth phase of run B (Fig. 3.3B) ($P < 0.02$).

Overall, the profiles of the two bioreactor runs were similar although the time difference in the onset of apoptosis in run A (~ 100 h) and B (~ 90 h) (Fig. 3.1/3.2) may be attributed to the difference in the metabolic state of their respective inoculum and the subsequent difference in metabolism during the run (Fig. 3.3).

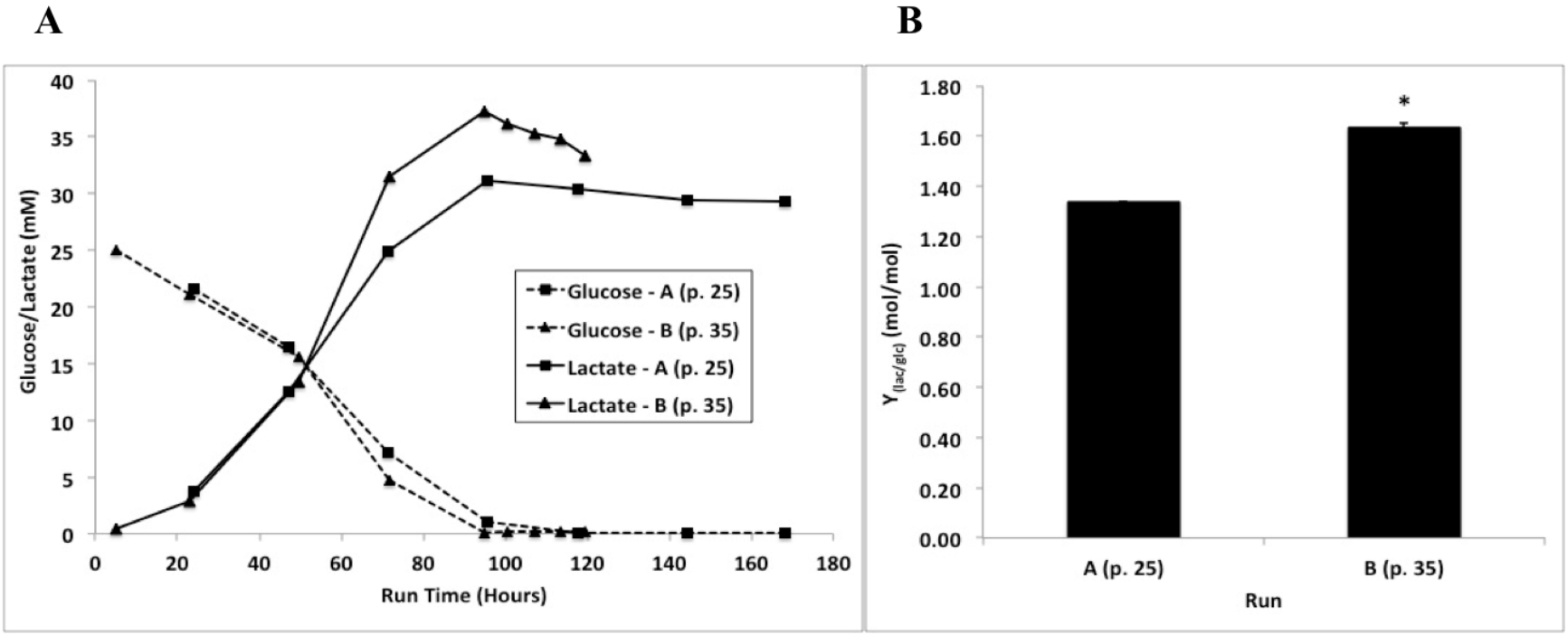

Figure 3.3: (a) Comparison of glucose consumption and lactate accumulation for run A (passage 25) (■) and run B (passage 35) (▲). Concentrations of glucose (- - -) and lactate (———) were plotted against days in culture. Each point represents the average of two technical replicates with error bars representing the standard error of the mean. (b) Comparison of the average yield lactate/glucose ($Y_{lac/glc}$) for run A (passage 25) and run B (passage 35) during the exponential growth phase. Each bar represents the average of two technical replicates with error bars representing the standard error of the mean. (* $P < 0.02$). (taken from Braasch et al., 2013)

3.2.2 Measurements and modeling with the capacitance probe

Figure 3.1 shows that the profile of the bulk capacitance measurement from the online probe in the cultures followed the ViaCount measurements fairly closely during the exponential phase and indicated the decline of the viable cell population. Some divergence was detected at the point in which non-viable cells predominate as shown at 140 h in Fig. 3.1A. Closer examination of the profile from the capacitance probe showed a distinct inflexion at 140 h for culture A and 120 h in culture B (Fig. 3.4).

The divergence of these profiles was examined. The experimental observations showed that during the growth phase the mean cell radius, R, remains at a constant value, R_v, of 13.2 μm as measured by Cedex. During the exponential phase $\Delta\varepsilon$ increased proportionally to the increase in the N, reaching the value of $\Delta\varepsilon_{max} = NR_v^4$ at ~100 h for run A, and ~90 h for run B (Fig. 3.1). At $\Delta\varepsilon_{max}$, a total of N cells were assumed to be healthy (non-apoptotic), with an average radius R_v. Beyond $\Delta\varepsilon_{max}$, as was evident from the Coulter counter measurements (Fig. 3.1), N remained consistently high even as the bioprocess population underwent apoptosis and $\Delta\varepsilon$ steadily declined. With $N \approx constant$, it followed that the decrease in $\Delta\varepsilon$ can only be due to changes in the average cell radius. Even though the trypan blue viability estimates began to decline after $\Delta\varepsilon_{max}$, they remained above 70% until ~145 h (run A) and above 80% until ~120 h (run B), the times when the DEP cytometer and the Nexin assay both indicated that the predominant cell subpopulation is apoptotic. It was assumed that the average radius of the viable cells remained at R_v while the radius of apoptotic cells changed to rR_v. From the data on the average decrease in size of all cells with intact membranes obtained by Cedex Image analysis (not shown) the average decrease in size of apoptotic cells was estimated as $r \sim 0.87$. For example, data from culture A indicated that the mean cell diameter changed from 13.2 μm at

24 h to 11.5 μm at 168 h when most cells were apoptotic. The DEP cytometer identified two subpopulations, viable and apoptotic, contributing in fractions v and $(1-v)$, respectively. These data was used to model the expected drop in permittivity:

$$\Delta\varepsilon = [\mathrm{v} + (1-\mathrm{v})\ \mathrm{r}^4]\ \Delta\varepsilon_{\max}$$

The bulk capacitance measurements and the model are both represented in Fig. 3.4. The divergence between the theoretical and observed $\Delta\varepsilon$ increased progressively over time, resulting in a considerable discrepancy towards the end of the culture. Even if the average radius of *all* cells were to decrease to $0.87\ R_v$, $\Delta\varepsilon$ would not be expected to decrease below $0.57\Delta\varepsilon_{max}$. However, the value of run A measurements at 145 h and $v = 0.16$ is $\Delta\varepsilon = 0.454\ \Delta\varepsilon_{max}$, and the value of run B measurements at 120 h and $v = 0.09$ is $\Delta\varepsilon = 0.415\ \Delta\varepsilon_{max}$, both well below the theoretically predicted values. Thus, we concluded that the decrease in $\Delta\varepsilon$ during the decline phase cannot be explained only by the decrease in average cell radius, but should instead be attributed to the decrease in both the cell radius and the cell polarizability of dielectrically diverse subpopulations of cells. The decrease in polarizability could be due to changes in cell metabolism, membrane surface capacitance and conductance, possibly by thickening of cell membrane or changed cytoplasmic conductivity.

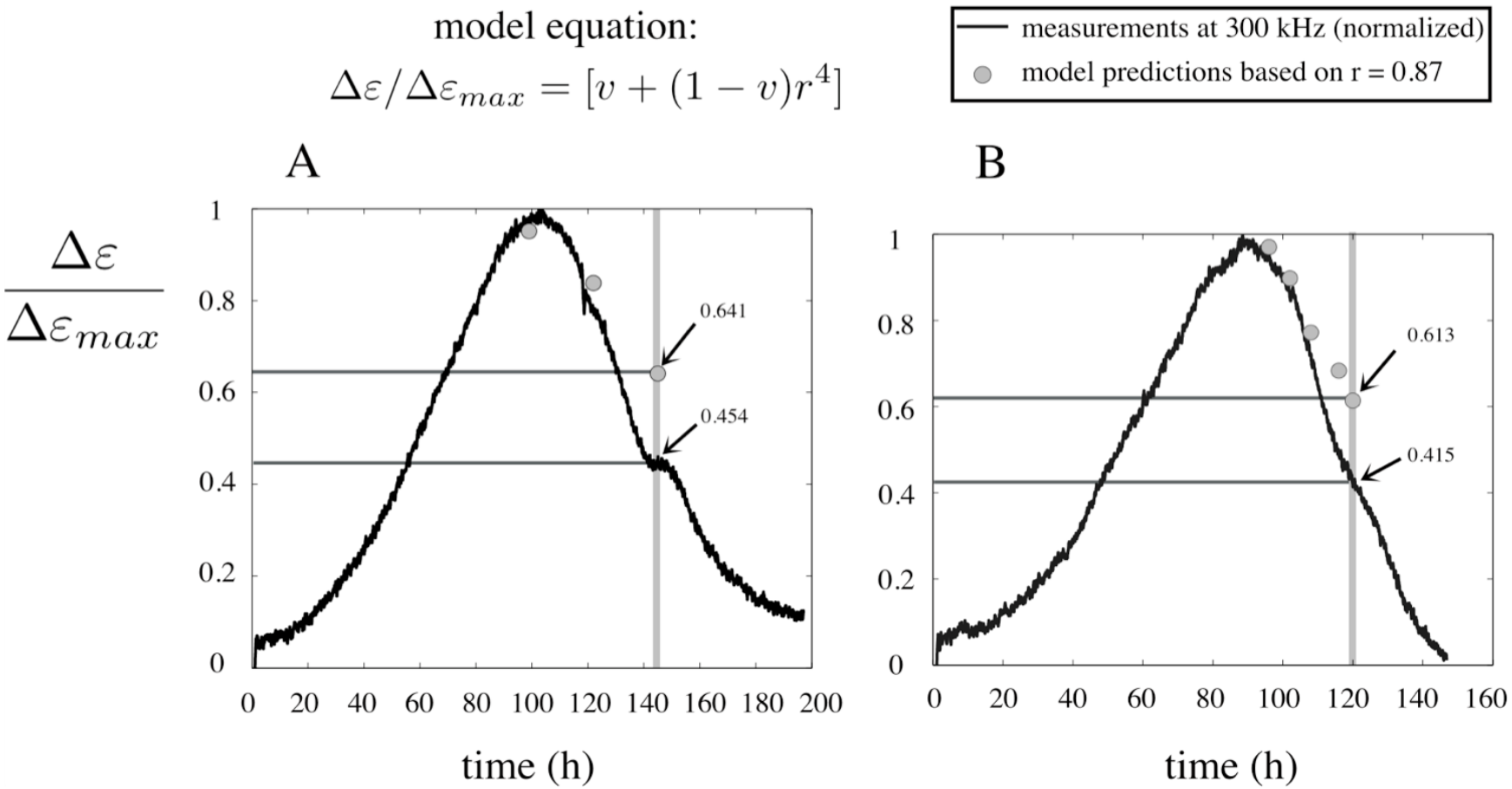

Figure 3.4: Bulk capacitance probe profiles compared to values predicted by cell volume changes. The continuous lines represent experimentally determined profiles from the two cultures described in Fig 4. Individual points (O) represent the model predictions for a decrease in $\Delta\varepsilon$ if two subpopulations are present as determined by DEP cytometer. For the model, the assumed change in radius of the apoptotic cells was 13% ($R \rightarrow 0.87Rv$) based on CEDEX measurement. It is assumed that the radius of viable cells does not change. (taken from Braasch et al., 2013)

3.2.3 Subpopulations of cells analyzed by flow cytometry

Figure 3.5 shows the cell subpopulations found in samples from the two separate bioreactor cultures as measured by the flow cytometer. Up to 70 h only the ViaCount assay was used to differentiate between the viable and non-viable cells. After 70 h a more in-depth analysis of the cell populations in the bioreactor cultures is shown by identifying and quantifying the non-apoptotic, early-apoptotic, caspase 8 positive, and dead subpopulations (Fig. 3.5) using the Nexin and Caspase 8 assay. The bar graphs in Fig. 3.5 clearly show that the cell population in the bioreactor was not homogeneous and that not all cells progressed through apoptosis at the same time. In addition, Fig. 3.5 shows the increase in size of the early apoptotic sub-population over time, with eventual transition to late apoptotic stage. Fig. 3.5 also shows a consistently low fraction of Caspase-8 (+) and 7-AAD (-) cells after 70 h for culture A and B. Over the course of the bioprocess the total fraction of cells staining Caspase-8 (+) increased steadily until most cells stained Caspase-8 (+) at the end of the run. The majority of these cells were late stage apoptotic and dying/dead cells staining Caspase-8 (+) and 7-AAD (+).

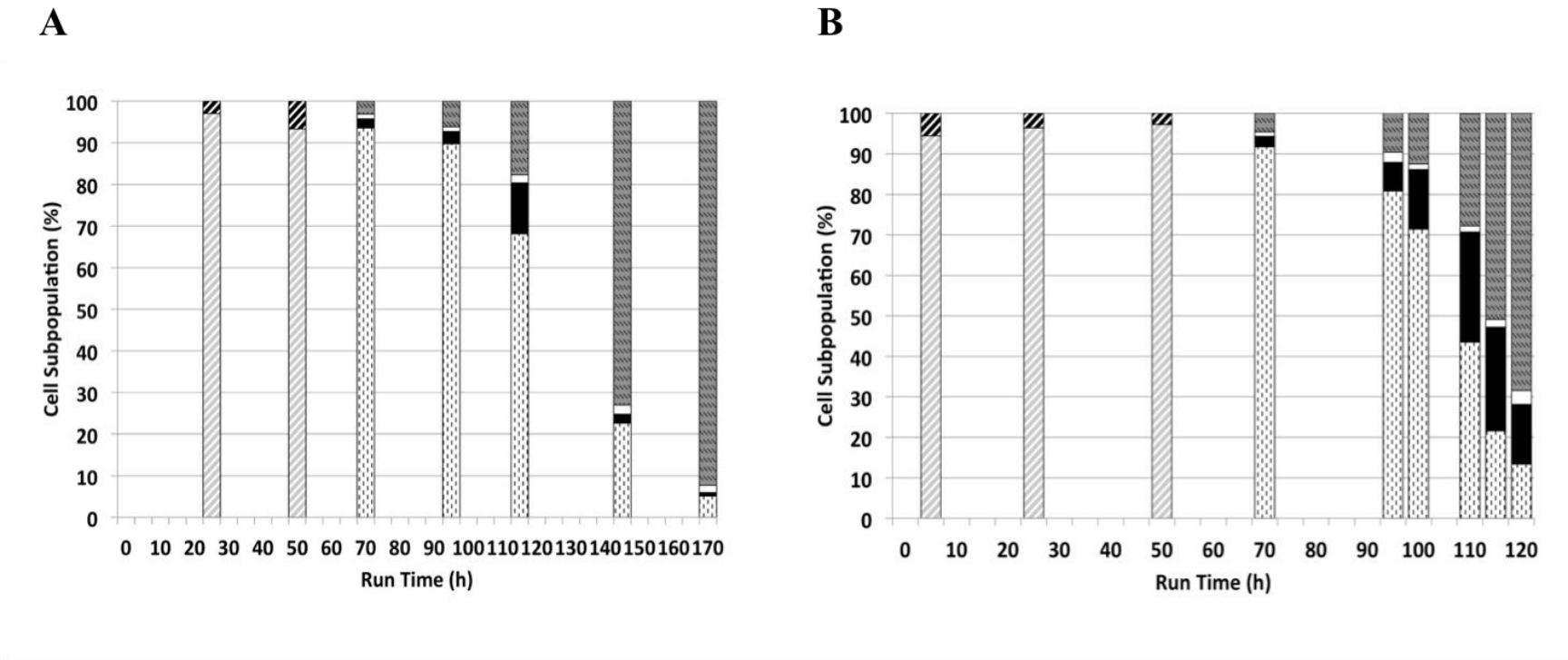

Figure 3.5: Overview of subpopulations determined during the bioprocess using three flow cytometer assays (ViaCount, Nexin, Caspase 8). The culture (3L) was sampled every 24 h from 0 h to 168 h (A). The culture (3L) was sampled every 24 h from 0 h to 95 h and then every 6 h from 95 h to 119 h (B). During exponential growth cells were distinguished as viable (▨) or dead (▨) based on the ViaCount assay. During the late exponential and the decline phase (>70 h) the cell subpopulations were distinguished as non-apoptotic (Annexin V (-) & 7-AAD (-)) (▯), early apoptotic (Annexin V (+) & 7-AAD (-)) (■), Caspase 8 (Caspase 8 (+) & 7-AAD (-)) (▯), or dead (7-AAD (+)) (▨). The values graphed are the average of mostly four technical replicates for each sampling point. The proportion of dead cells determined by the ViaCount assay was within <10% of the value determined by the Nexin and Caspase 8 assays. (taken from Braasch et al., 2013)

3.2.4 DEP cytometer measurements

Examples of experimental DEP signatures produced by individual CHO cells are shown in Fig. 1.5(a) (see Chapter 1). In a suspension with a conductivity of $\sigma_{sm} \approx 0.17$ S/m, the crossover frequency was identified experimentally as ~ 0.5 MHz above which viable cells produced pDEP signatures and non-viable cells nDEP signatures. The force index was measured for CHO cells in nine discrete frequency steps, from 0.1 to 6 MHz as identified in Fig. 3.6. Experimental signatures from these samples were collected for 200-400 cells (~5 minutes) at each frequency and each control set. Figure 3.6 (b) represents stacked distributions of force index values for each of the nine discrete steps during the frequency sweep. These distributions were obtained from two samples taken early in the culture, and after the decline phase. Viability was defined as the fraction of pDEP signatures in the total number of cell signatures captured. DEP cytometer viability counts for these samples were 93% and 9%, respectively. During repeated runs we were able to show that the percent viability determined by the DEP Cytometer was consistent with the data from the Nexin assay (Fig. 3.2).

A detailed analysis of the data from the DEP cytometer during the critical time in which cells display a rapid loss in viability shows the changes in force index distribution for the cell population (Fig. 3.7). Within this time interval (96 h – 120 h from inoculation in culture B), signatures from 300 – 400 cells actuated with 6 MHz DEP signals were collected every six hours (only data at 12 hour intervals are shown). Each of the resulting histograms shows a sharply bimodal distribution, with a clear shift over time from

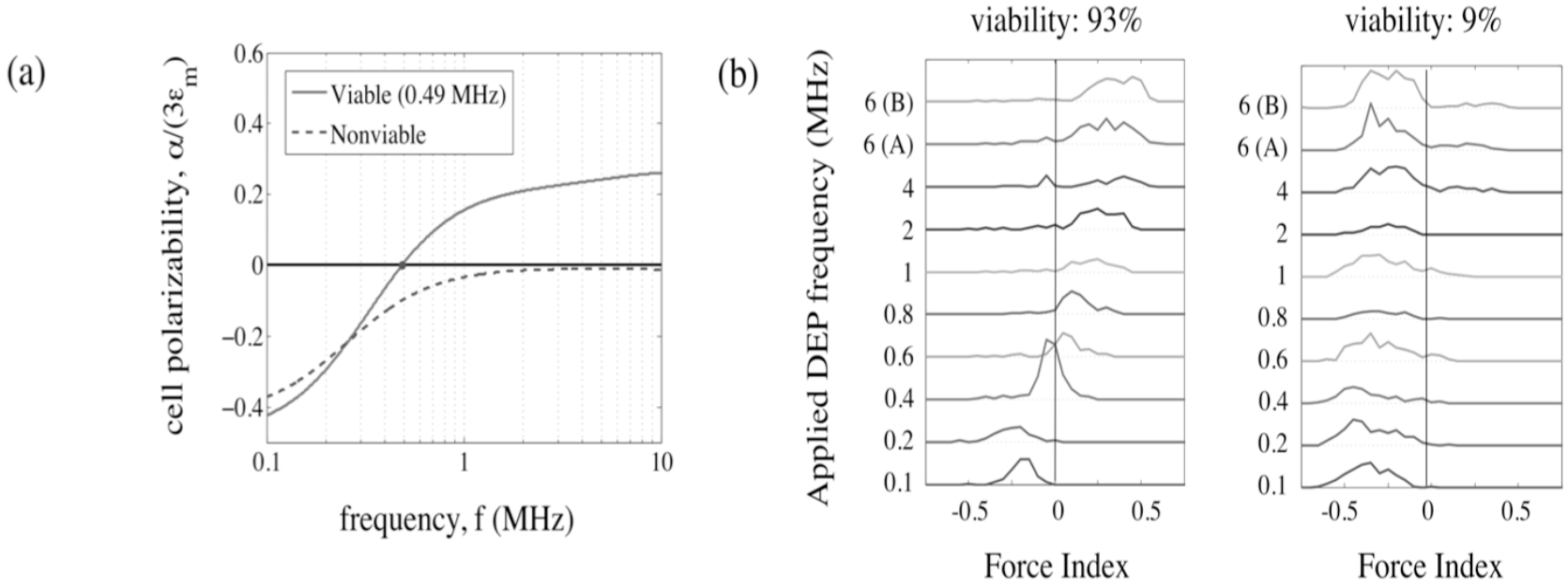

Figure 3.6: (a) Numerical simulation of the polarizability, produced for a double-shell model (Jones, 1995) and based on the assumption that cell volume shrinks and the conductivity of the cytoplasm drops as the cell undergoes the apoptotic process; parameters used in this simulation were obtained from previously published work (Asami et al., 1989; Cemazar et al., 2011) as given in Table 1 (ref 2 and 1, respectively). This simulation was used as an aid in choosing 6 MHz as the frequency at which to perform the viability measurements. **(b)** Stacked distributions of force index, ϕ, for the collection of signatures captured early and late in a previous experiment (Days 1 and 10, respectively). Signatures were collected at nine discrete steps in frequency. Two collections were made at the 6 MHz frequency at the beginning and at the end (6B and 6A standing for "before" and "after") of the time interval to do the full frequency sweep and to ensure that the viability of cells was not changed during the course of the experiment. (taken from Braasch et al., 2013)

predominantly positive to predominantly negative force index values. These results were consistent with the data from the Nexin assay, illustrated in Figs. 3.2 and 3.5. The table in Fig. 3.7 shows that the nDEP measurements determined over the period of changing cell viability have a closer correlation to the Nexin assay than the other colorimetric or fluorescent assays used. This suggests that the DEP measurements are indicative of changes related to the early stages of the apoptotic process.

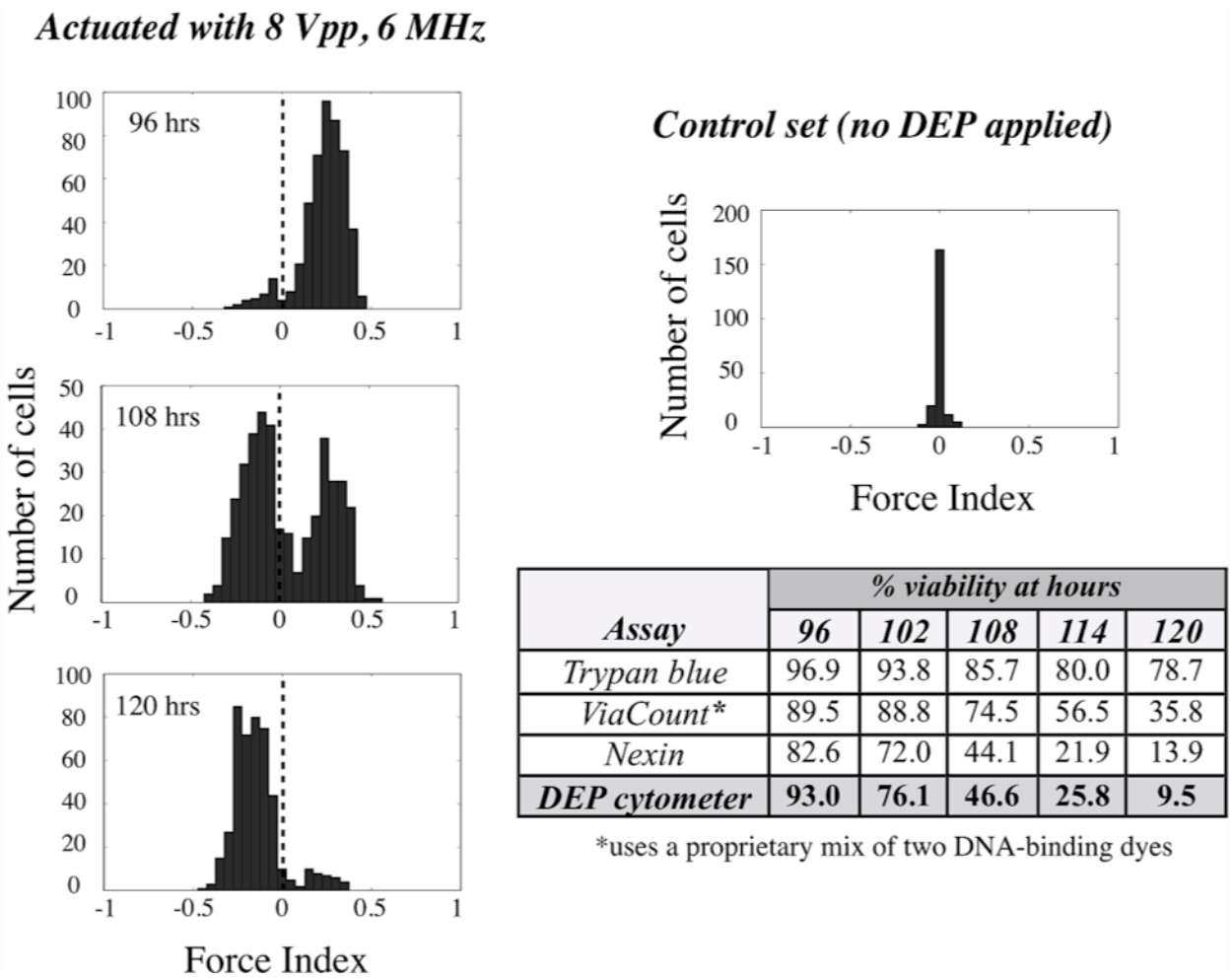

Assay	% viability at hours				
	96	102	108	114	120
Trypan blue	96.9	93.8	85.7	80.0	78.7
*ViaCount**	89.5	88.8	74.5	56.5	35.8
Nexin	82.6	72.0	44.1	21.9	13.9
DEP cytometer	**93.0**	**76.1**	**46.6**	**25.8**	**9.5**

*uses a proprietary mix of two DNA-binding dyes

Figure 3.7: Time-lapse histograms showing a binary population of cells with rapidly changing dielectric properties (~ 96 h – 120 h from bioreactor seeding) accompanied by a comparison table of viability assessments for different cell monitoring techniques. (taken from Braasch et al., 2013)

3.2.5 Adenylate energy charge

The results of the comparative measurements of cell viability and the adenylate energy charge (AEC) for one representative batch is shown in Fig. 3.8. The profile was based on samples taken every 24 h from inoculation up to 83 h and from 107 h to 120 h and every 6 h from 83 h – 107 h in order to monitor the viable to non-viable transition. As observed in Fig. 3.2 a divergence between the Cedex (trypan blue), ViaCount assay, Nexin assay, and the DEP cytometer can be seen. In addition to the just mentioned measurements the AEC was determined for this run by taking a cell sample for nucleotide sugar analysis for the sampling points between 73 h to 107 h. The data in Fig. 3.8 shows a higher AEC (>0.9) for the analysis at 73 h and 83 h

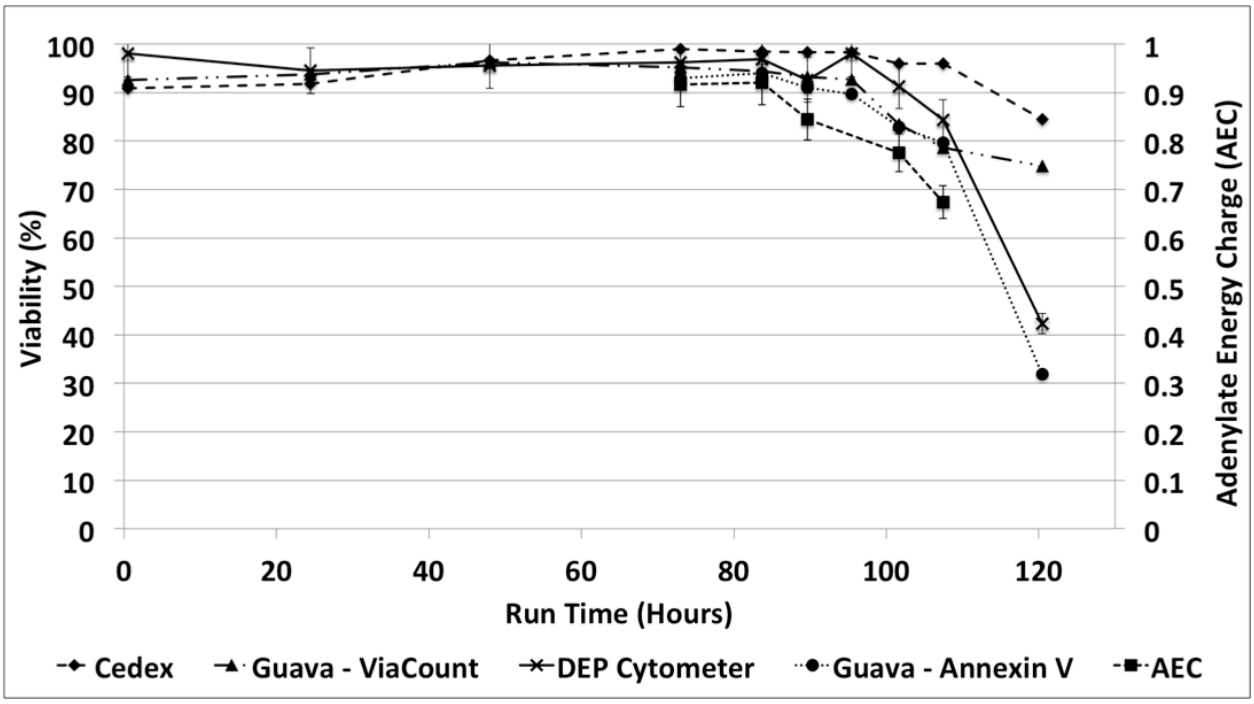

Figure 3.8: Comparison of cell viability determined for CHO EG2 batch cultures using trypan blue (Cedex), ViaCount and Nexin (Guava flow cytometer), DEP cytometer and adenylate energy charge (AEC). The culture (3L) was sampled every 24 h from 0 h to 73 h and then every 6 h from 73 h to 120 h. The values graphed are the average of four technical replicates for each sampling point with error bars representing the standard error of the mean. The DEP value is based on 2 determinations from >200 cells per sample and the AEC value is based on the analysis of 1 cell pellet sample (error bars represent 5%, which represents the measurement uncertainty).

that indicates that the cells were healthy. After 83 h a steady decline in the AEC was determined, which is indicative of a decline in the overall health of the culture and individual cells. At 83 h an extracellular glucose concentration of 2 mM was measured. It is of interest that the drop in AEC was observed prior to seeing a substantial decline in the viability of the culture determined with any of the other methods used.

Overall, the viability profile of the bioreactor run was similar to the runs shown in Fig. 3.2. In addition to the previously observed trend it was shown that the AEC drops prior to monitoring a drop in the other methods used.

3.3 Discussion

The ability to prolong the viability of cells at high density is a key factor in enhancing the productivity of a mammalian cell bioprocess (Wurm, 2004). This requires an understanding and monitoring of the events that take place during the decline phase and loss of cell viability, which is usually associated with apoptosis. Viability has often been defined by the loss of integrity of the cell membrane which allows the entry of high molecular weight dyes like trypan blue (Strober, 2001). However, this is likely to be a late stage event in the demise of CHO cells in a bioreactor that undergo programmed cell death (Browne and Al-Rubeai, 2011). During apoptosis the membrane can remain intact during events of cell shrinkage, chromatin condensation and caspase activation (Hughes et al., 1997). An early molecular change during apoptosis is the translocation of the phosphatidylserine to the outer leaflet of the plasma membrane and the activation of a series of caspases (Budihardjo et al., 1999; Martin et al., 1995). These can be labeled by fluorescent stains and monitored in a cell population via flow cytometry. This brings into question the most appropriate measure of viability, as a population of cells

undergoing apoptosis may indicate significantly different values of percentage of viability depending on the assay used.

The profiles of the two initial bioreactor runs in this study were similar with the second run showing faster growth, increased glucose uptake and lactate accumulation during the exponential growth phase. This in turn led to an earlier glucose depletion and subsequent earlier onset of apoptosis attributed to nutrient depletion in the culture. The difference in the observed metabolism may be attributed to the use of cells from different passage numbers used for inoculation. This finding agrees with observations made by Beckmann et al. (2012) for cells of higher passage numbers. However, overall trends between methods used and the onset of apoptosis in accordance to nutrient (i.e. glucose) depletion are the same for all three runs.

This study compared 5 different methods to monitor and evaluate the changes in viable cell densities and cell viability that occur to CHO cells at the later stages of a culture. The electronic counter (Coulter) is a rapid method of determining cell density but does not distinguish between viable and non-viable cells. Trypan blue exclusion is a widely used colorimetric method that is usually combined with haemocytometer counting or image analysis and distinguishes the colour of non-viable cells (blue) and viable cells (non-coloured). However, as we and others have shown this overestimates viability by not recognizing apoptotic cells with an intact membrane (Altman et al., 1993; Browne and Al-Rubeai, 2011) but is rather dependent on gross membrane damage, which occurs at a later stage of apoptosis (Koopman et al., 1994).

The flow cytometer analysis can be combined with a range of florescent dyes to determine different stages of apoptosis including phosphatidyl serine translocation (Nexin), cell membrane permeability (ViaCount) and caspase activation (e.g. Caspase 8). The Nexin assay recognizes an early event in apoptosis and so it is not surprising that our results indicate that

among the fluorescence assays it produces the lowest estimates of viability. The Caspase-8 assay was used to recognize cells positive for Caspase-8 activation indicating cells going through the extrinsic cell surface death receptor apoptotic pathway (Budihardjo et al., 1999). While only a small fraction of cells was determined to be Caspase-8 (+) and 7-AAD (-) at each sampling point, the overall fraction of Caspase-8 (+) and 7-AAD (+) cells increased over the time of the bioprocess. This suggests that in most cells the Caspase-8 initiator caspase was activated but that the transition from Caspase-8 (+) and 7-AAD (-) to Caspase-8 (+) and 7-AAD (+) was too rapid to be detected. With the Caspase-8 assay used we observed up to 15% of the cells in the bioprocess to be necrotic for some sampling points. To determine whether this percentage was an artifact of the staining procedure a visual assessment of the Nexin assay would have to be performed to determine if phosphatidyl serine was found on the inside of Annexin V (+) and 7-AAD (+) cells (Wlodkowic et al., 2011). This would be indicative of a necrotic cell.

For future experiments it would be interesting to use the Caspase-3/7 assay to monitor the activation of the key effector caspase 3 during the bioprocess (Vermes et al., 2000), which is activated by both caspase 8 and 9 during the next stage in the apoptosis pathway. Furthermore, as a key effector caspase, caspase 3 is activated in the intrinsic and extrinsic apoptotis pathway (Scoltock and Cidlowski, 2004). However, it was interesting to note a steady increase of Caspase 8 (+) staining cells during the cultures as this agrees with findings that a depletion in glucose is a potential cause for caspase 8 activation (Yun et al., 2007; Muñoz-Pinedo et al., 2003).

The capacitance probe has been widely accepted in the biotechnology industry as a sterilizable probe that can be inserted *in situ* in a bioreactor for continuous monitoring of viable cell densities (Carvell and Dowd, 2006). Previous reports have confirmed our conclusion that

on-line measurements for biomass by capacitance correlate well with the trypan blue assay of viable cell concentration (VCC) in the exponential phase of cell growth but deviate in either direction in the stationary and the decline phases (Ducommun et al., 2002; Opel et al., 2010).

The changing capacitance measurements are based on the total biovolume as well as the membrane charge on each cell. These parameters are likely to be constant during exponential growth of cells. However, interpretation of the data becomes more difficult during the stationary and decline phases for which our data indicates a non-homogeneous culture in which reduction in both the cell size and surface charge occur at varying degrees. The data we measured using the change of $\Delta\varepsilon$ and the software interpretation from the capacitance probe correlates well with the ViaCount fluorescent assay analyzed using the Guava flow cytometer and provides a more realistic measure of viable cell density in the final stages of culture compared to trypan blue exclusion. However, deviations from the simple model of a direct relationship between capacitance and biovolume during the decline phase could be attributed to a decrease in both the cell size and polarizability as cells become apoptotic. This observation is compatible with previously reported changes due to altered metabolism in the decline phase (Opel et al., 2010).

In this study a novel DEP cytometer that enhances the analysis of cells during the critical stage of culture as cell viability decreases is described. The DEP-derived data are based on individual cells flowing over a detector and therefore differs from the averaged bulk dielectric measurements made with the capacitance probe. The DEP cytometer measures the dielectric properties of individual cells and was able to identify at least two populations of cells, each with a distinct polarizability as distinguished by the measured force index. One population was associated with viable cells and the other with apoptotic cells. From the end of the exponential through the stationary and decline stages there was a gradual shift of cell count from the viable

into the apoptotic population; however, the two populations always maintained their individual dielectric properties throughout this shift.

In addition to all the direct methods used an indirect method for cell viability determination was used. By determining the intracellular levels of ATP, ADP, and AMP the AEC index can be calculated which has been shown to correlate with cell health (Atkinson, 1968).

The observed substrate (i.e. glucose) deprivation during the later stages of a culture leads to the observed declining intracellular concentrations of ATP (Burgener et al., 2006) that would in turn lead to perturbations in the membrane-bound Na^+/K^+ ATPase essential for maintaining resting electrical potential of cells (Jaitovich and Bertorello, 2006). As it takes some time to perturb the potential to a point where it can be detected a drop in the viability determined with the DEP cytometer is seen only 6 – 12 h after a drop in AEC. The appearance of subpopulations of cells, which results in the changes in dielectric properties as analyzed by the DEP cytometer, can be attributable to the rapid change in cell conductivities, resulting from ionic efflux or influx that may act as an "on" switch for apoptosis, as suggested by earlier literature (Bortner and Cidlowski, 2003; Bortner and Cidlowski, 2002).

3.4 Conclusion

In this batch study the different methods used for cell density and viability determination were compared and correlated with changes within the cells going through apoptosis due to nutrient depletion (Figure 3.9).

In healthy cells several ion pumps, including the Ca^{2+} and N^+/K^+ ATP-dependent pumps, balance the ionic content in the cytoplasm and the cell membrane capacitance. Furthermore

healthy cells characteristically present phosphatidylserine on the inner leaflet of the plasma membrane. Once the cells experience a low glucose concentration less ATP is produced via glycolysis. After some time the existing ATP in the cells will be used up and at the same time the AEC will continually drop. The low levels of ATP present in the cells will then have an impact on all operations inside the cell that are ATP-dependent. Since some of the ion pumps are ATP-dependent, this loss will make those pumps less efficient and subsequently cause a shift in the ionic make-up of the cell. This in turn can cause the electric potential in the cytoplasm to shift, which can be detected using the DEP cytometer. One of the ATP dependent pumps is responsible for the transport of Ca^{2+} out of the cell. This is particularly important, as Ca^{2+} is a signaling molecule that can induce apoptosis intrinsically.

In addition to the change of the electric potential in the cytoplasm the decrease in ATP causes the phosphatidylserine to stay on the outer leaflet as it takes ATP to flip them back to the inner leaflet. The phosphatidylserine presented on the outer leaflet can then be detected using the Annexin V assay and the flow cytometer.

The above-mentioned increase in cytosolic Ca^{2+} concentration will eventually initiate the intrinsic apoptosis pathway. The pathway will lead to the activation of the caspase proteins that can be detected using the Caspase assays and the flow cytometer.

The capacitance probe is providing a bulk measurement of the cells in the electric field of the probe. While cells with compromised membranes are not able to act as a capacitor all other cells are. However, depending on the physiological state of the cell the capacitor strength will vary from healthy cells with the highest capacitor strength to cells going through early and mid

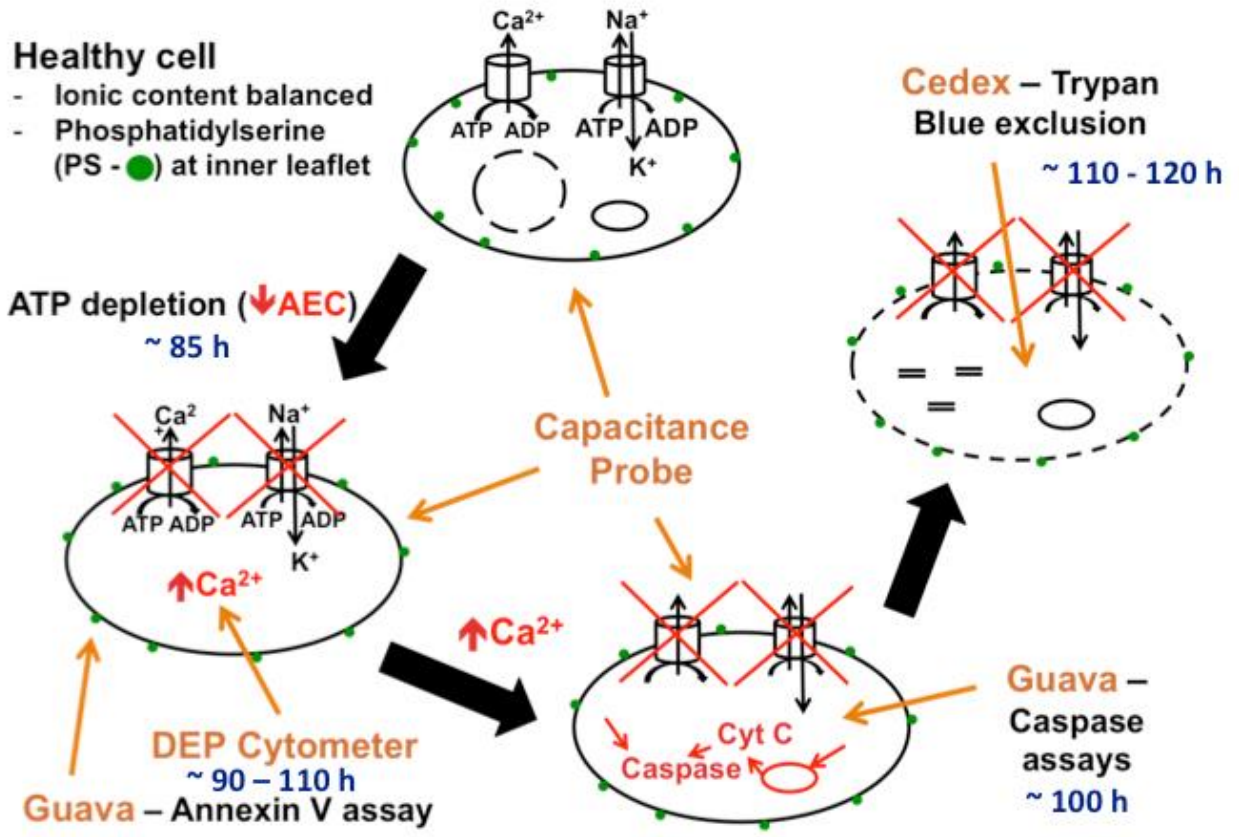

Figure 3.9: Schematic overview of detected changes in batch CHO-EG2 cultures using a variety of cell density / cell viability detection methods. The overview contains the plasma membrane (---) with the position of the phosphatidylserine (●), the Ca^{2+} and N^{+}/K^{+} ATP-dependent pumps, the mitochondria (⬭), the nucleus (◌), and fragmented DNA (⁼₌⁼). The times at each stage indicate the approximate time of detection for that specific assay based on the run shown in Fig. 3.8.

apoptotic stages with declining capacitor strength. Hence, a summation of the capacitor strength of all cells in the electric field will be measured.

The end stage of apoptosis in a bioprocess is the loss of the cell membrane integrity. By loosing its integrity the cell membrane becomes leaky, which allows molecules to freely enter or exit the cell cytoplasm. This characteristic is the basis for dye exclusion assys in which dyes such as trypan blue are only able to enter the cell once it becomes leaky, indicating the final

stage of apoptosis in a bioprocess. At this stage the cells will now be considered non-viable by this type of assay.

The comparison of a variety of viability measurements done here supports the notion by Browne and Al-Rubeai (2011) that a "true" value for viability does not exist but rather that "viability" is a user-defined concept. Each method used in this experiment gave a value for "viability" that differed from other methods because each method is looking for different indicators to determine whether a cell is viable. Hence, it is important to not only state the method of viability detection used when stating viability values but also to understand the concept of the method used.

The objective was to find a method that can detect the early onset of cell decline. The AEC determination, the Annexin V assay and the DEP cytometer offer this advantage over the other methods used for the observation of a batch culture. The advantage of the DEP cytometry is that it can be used as a non-invasive diagnostic and research tool that does not require any specific markers or dyes. The DEP cytometer used in this work is a prototype with a promise to become an electronic monitor of physiological changes in the cell. Furthermore, the all-electronic operation principle makes this instrument particularly suitable for miniaturization and fully automated analysis.

Chapter 4

Induction of apoptosis in bioprocesses

4.1 Introduction

Previously it was shown that dielectric measurements can be used to detect the changes in the dielectric properties of mammalian cells during the course of a batch culture (Chapter 3). However, apoptosis is defined by a complex network of pathways, which are induced by a variety of triggers. Hence the progression of a cell through apoptosis is dependent on the specific trigger. Nutrient limitations and a variety of antibiotics can artificially induce apoptosis in cells and cell cultures. This allows for a more in depth study of the onset and progression of apoptosis. Some of the inducers that can be used are glucose and glutamine starvation, oligomycin, and staurosporine.

Glucose and glutamine starvation causes the induction of apoptosis in cells due to a loss in nutrients. Starving the cells artificially simulates the end of a regular batch process when nutrients run out. By removing the two main carbon sources for the cells, the main source for ATP production is absent. ATP is the energy molecule needed in the cell for many vital functions. Hence, a lack of ATP is expected to cause distress in the cells eventually resulting in the induction of apoptosis. In addition, glutamine is a source for amine groups needed for purine and pyrimidine synthesis (Curi et al., 2005) and therefore, essential for cell survival.

Oligomycin is an ATP-Synthase inhibitor, which blocks the ATP-Synthase and prevents the protons from traveling through the channel necessary for ATP production. This causes a change in the mitochondrial membrane potential and the activation of apoptosis through the intrinsic pathway (Matsuyama et al., 1998).

Staurosporine is a non-specific inhibitor of protein kinase C and induces apoptosis by translocating the pro-apoptotic Bax protein onto the mitochondrial matrix resulting in cytochrome c release (Zwelling et al., 1991; Qiao et al., 1996; Scarlett et al., 2000). As described in the intrinsic pathway the release of cytochrome c causes the subsequent assembly of the apoptosome complex and executioner caspase activation.

For this study apoptosis was artificially induced in mid-exponential phase CHO cultures using starvation (lack of glucose and glutamine in medium), 8 μg/mL oligomycin, and 50 nM staurosporine. The inducers and their specific concentrations were chosen to induce apoptosis gradually for best observation opportunities. The onset and progression of apoptosis were then analyzed using a bulk and a single cell dielectric measurement, trypan blue exclusion and several fluorescent apoptosis assays. For each inducer the results of the individual methods were compared amongst each other and to a healthy control culture. Of particular interest was the analysis of the dielectric measurements and their correlation to the fluorescent methods for each trigger to further evaluate their use in cell culture viability monitoring.

4.2 Results

4.2.1 Growth

The effects of apoptosis induction to the cell growth in CHO cell cultures are shown in Figure 4.1. While the cells in the 'Control' were grown in BioGro CHO medium, the cells in the 'Starvation' culture were starved in BioGro CHO medium without glucose and glutamine. When apoptosis was induced using an antibiotic, the inducer was added to the regular BioGro CHO medium. Each culture – other than the oligomycin-treated culture – was inoculated at $7x10^5$ cells/mL in a 250 mL shaker flask without baffles using a working volume of 200 mL. The

oligomycin-treated culture was inoculated at $2x10^5$ cells/mL at the same volume as all other cultures. During the experiment the cultures were incubated at 37°C with a 10% CO_2 overlay on a shaker platform (160 rpm). At the times of sampling the viable cell density was determined by trypan blue exclusion and the fluorescent ViaCount assay.

The growth of all cells is shown in Figure 4.1. For the control (Fig. 4.1 A) the cell density increased exponentially until 48 h to approximately $4x10^6$ cells/mL after which the cell growth was stagnant. While the trypan blue exclusion method and the ViaCount assay showed similar results during the exponential phase, the trypan blue exclusion method gave a lower viable cell density than the ViaCount assay at 60 h.

Both methods used showed that the growth in the starvation culture was arrested from the beginning and that the viable cell density declined slightly over the course of 48 h (Fig. 4.1 B). The decrease in viable cell density observed was greatest with the ViaCount assay when compared to the trypan blue exclusion method. At 48 h the difference between the two methods was significant ($P < 0.02$).

In Figure 4.1 C it can be seen that when apoptosis was induced using 8 µg/mL oligomycin the cell growth was arrested over the course of the experiment (48 h) with no significant loss in viable cell density. For all time points both the trypan blue and ViaCount measurements gave similar results.

While oligomycin arrested the cell growth completely the induction with 50 nM staurosporine only caused growth inhibition (Fig. 4.1 D). Compared to the control culture cells treated with staurosporine reached 50% of the maximum viable cell density seen in the control - roughly $2x10^6$ cells/mL. This maximum viable cell density was reached only after 60 h. During

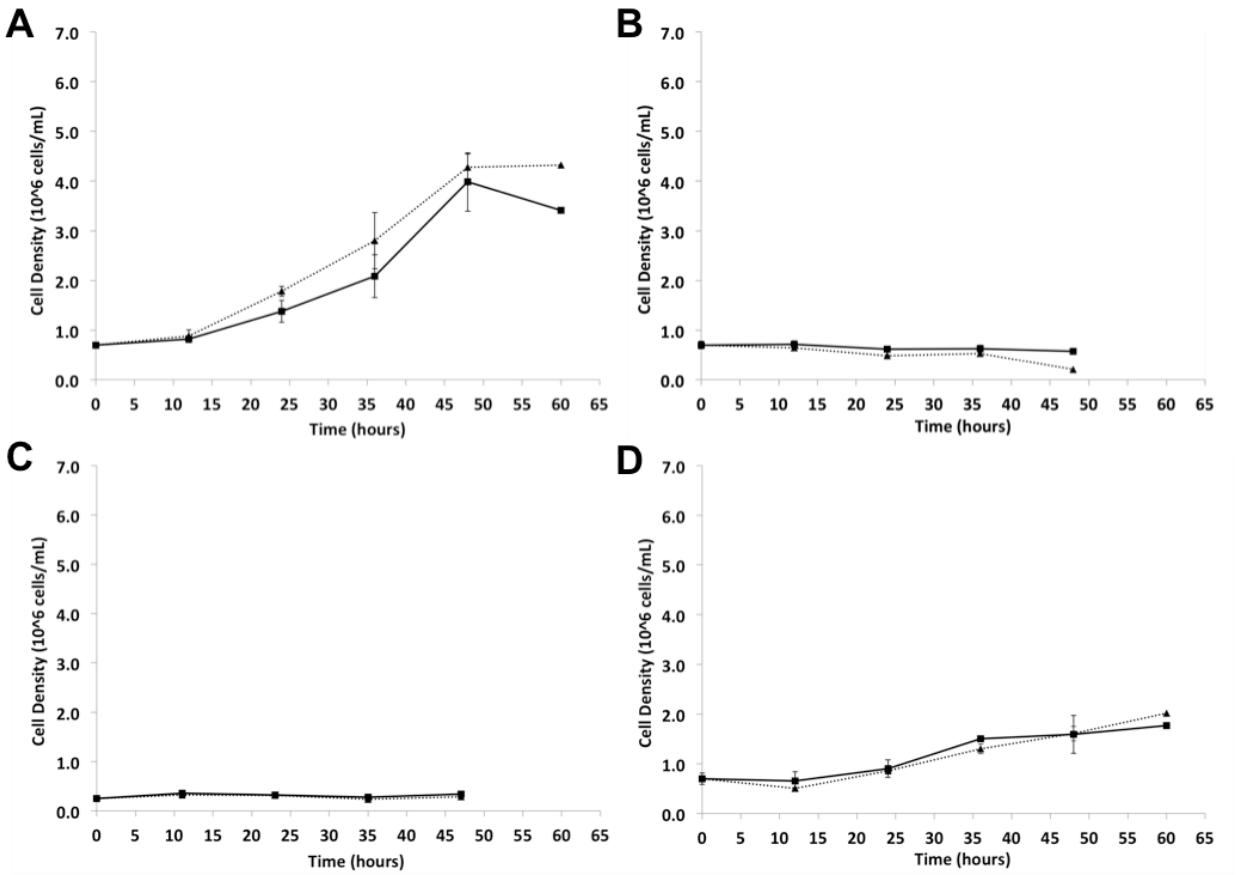

Figure 4.1: Representative cell growth during apoptosis induction A) Control, B) Starvation, C) Oligomycin, and D) Staurosporine measured using trypan blue exclusion (—■—) and ViaCount (···▲···). The values graphed are the average of four technical replicates for each sampling point with error bars representing the standard error of the mean. For the DEP cytometer only one measurement was performed.

the first 12 h of the experiment the growth was stagnant. After the first 12 h an increase in growth of the culture was observed which again flattens 36 h after induction.

Overall, the induction of apoptosis via starvation and oligomycin caused a complete growth arrest while the addition of staurosporine only inhibited the cell growth by 50%. In addition, the starvation treatment was the only treatment in which a significant loss in viable cell density was observed with the ViaCount assay compared to the trypan blue exclusion assay used.

4.2.2 Viability

The apparent viability of any cell population is dependent upon the assay used, as each measures a distinct parameter related to the metabolic status of the cell. The viability measurements using the Cedex (trypan blue exclusion), ViaCount, Annexin V, Caspase 8, MultiCaspase assays, and the DEP cytometer are shown in Figure 4.2. For the control culture (Figure 4.2 A) all methods used showed viabilities above 90% for the entire experimental run (63 h).

In the representative starvation culture an initial drop in viability was observed at 12 h post induction (Figure 4.2 B). At this time point the Caspase 8, MultiCaspase, and Annexin V assays showed viabilities below 90% while the remainder of the assays still gave viabilities above 90%. Over the course of the experiment the viability determined by all assays declined. At 48 h the lowest viabilities of 5% and 7 % were determined using the DEP cytometer and the Annexin V assays, respectively. Significantly higher viabilities ($P < 0.02$) were observed with the Caspase 8 (33%), MultiCaspase (25%), and ViaCount assay (24%). However, an even higher viability was observed with the trypan blue exclusion assay (77%), which was significantly higher than all other measurement methods ($P < 0.02$)

In Figure 4.2 C the cell viabilities in the 8 μg/mL oligomycin-induced culture determined by the different methods can be seen. At 12 h post induction viabilities below 80% were determined by the Annexin V (79%), Caspase 8 (79%), and the MultiCaspase assay (74%). These viabilities were significantly lower than what was observed with the trypan blue exclusion and ViaCount assay ($P < 0.02$). After 12 h the decline in viability was moderate. At 48 h the lowest viabilities were determined with the Annexin V (60%), Caspase 8 (57%), and the MultiCaspase assay (57%). Significantly higher viabilities ($P < 0.02$) were determined with the

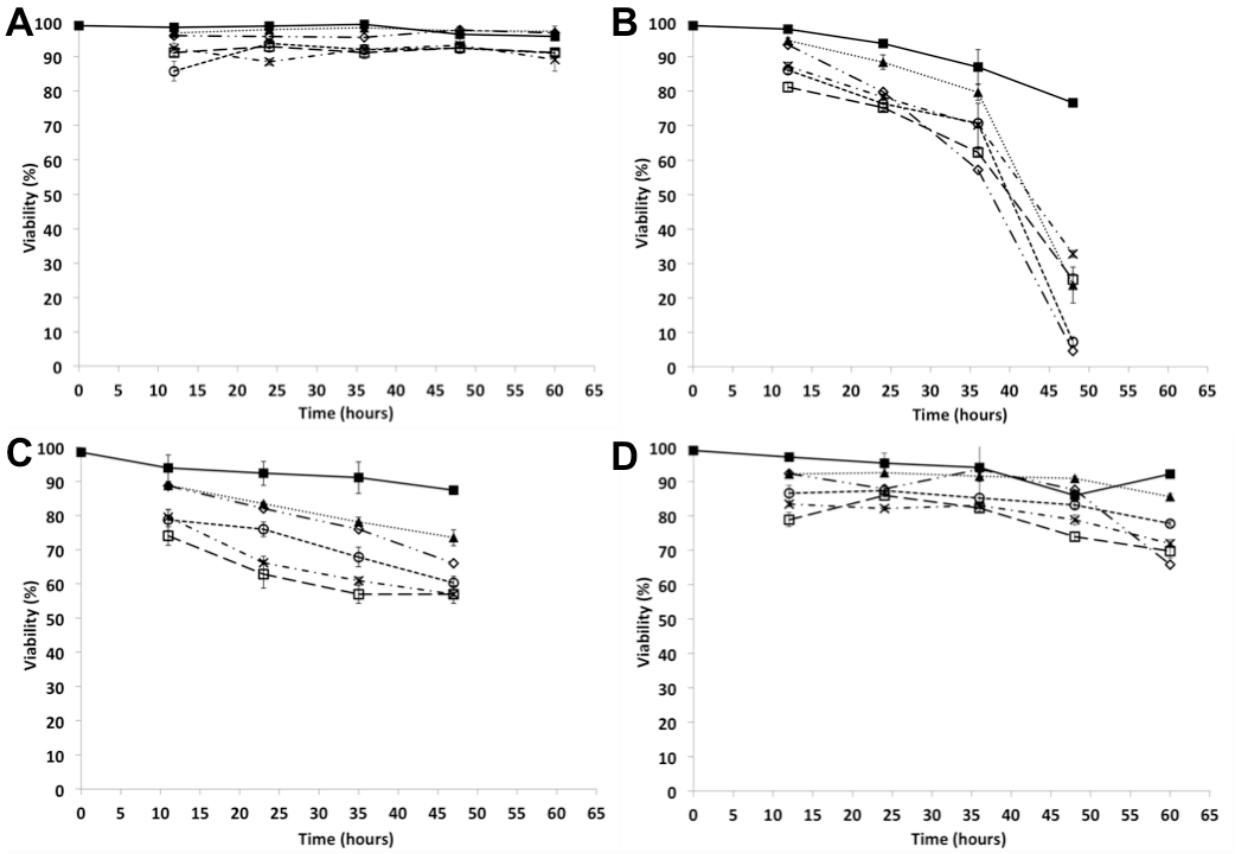

Figure 4.2: Representative cell viability during apoptosis induction. A) Control, B) Starvation, C) Oligomycin, D) Staurosporine using trypan blue exclusion (—■—), ViaCount (···▲··), Annexin V (-⊖·), Caspase 8 (-✕-), MultiCaspase (-⊟-) assays, and the DEP cytometer (—◈·). The values graphed are the average of four technical replicates for each sampling point with error bars representing the standard error of the mean. For the DEP cytometer only one measurement was performed.

DEP cytometer (66%) and the ViaCount assay (73%). As in the starvation culture a significantly higher viability than all other measurements ($P < 0.02$) was observed with the trypan blue exclusion assay (87%).

The changes in the viabilities for the 50 nM staurosporine-induced culture determined by the different methods can be seen in Figure 4.2 D. In this culture, viabilities below 90% were observed in the Annexin V (87%), Caspase 8 (83%), and MultiCaspase assay (79%) 12 h after apoptosis induction. At that time significantly higher viabilities ($P < 0.02$) above 90% were

determined with the trypan blue exclusion (97%) and the ViaCount assay (92%) as well as the DEP cytometer (92%; not significantly higher compared to Annexin V). During the course of the experiment the viabilities determined seem fairly constant for the initial 36 h after which a slight decline in the viability was observed. The lowest viability was measured 63 h post induction with the DEP cytometer at 66%. Slightly higher viabilities were determined using the Caspase 8 (72%) and MultiCaspase assay (70%). The Annexin V and ViaCount assay gave significantly higher viabilities than all of these three methods ($P < 0.02$) at 78% and 86%, respectively. The significantly highest viability at 92% ($P < 0.02$) was determined with the trypan blue exclusion method.

Generally, using a range of viability assays allowed for the detection of differences in the onset and progression between different apoptosis inducers. The onset in the starvation culture was similar to what was observed in the staurosporine culture and modest compared to the initial decrease seen in the culture induced by oligomycin. While the oligomycin caused the largest initial decrease in viability, it declined slowly over the rest of the experiment. A slow and gradual decline in viability was also observed in the staurosporine culture. The steepest decline in viability was observed in the starvation culture. In all apoptotic cultures the trypan blue exclusion method gave the highest viability for the entirety of the cell culture. The order of assays and their respective viabilities (lowest to highest) in each culture varied based on the inducer used.

4.2.3 Aber

For the control and starvation culture samples were taken at all time points to perform frequency sweep measurements. During the sweeps the cell sample was exposed to a range of

frequencies (0.1 – 20 MHz) to measure its respective response i.e. measured capacitance. Those raw measurements were then normalized and graphed versus their respective frequency (Figure 4.3). The data points were connected by a trendline based on the moving average (period = 3). By graphing these data points a β-dispersion was developed, which can be compared amongst the different time points for each culture and between different cultures. The inflection point of the trendline was defined as the critical frequency (f_c).

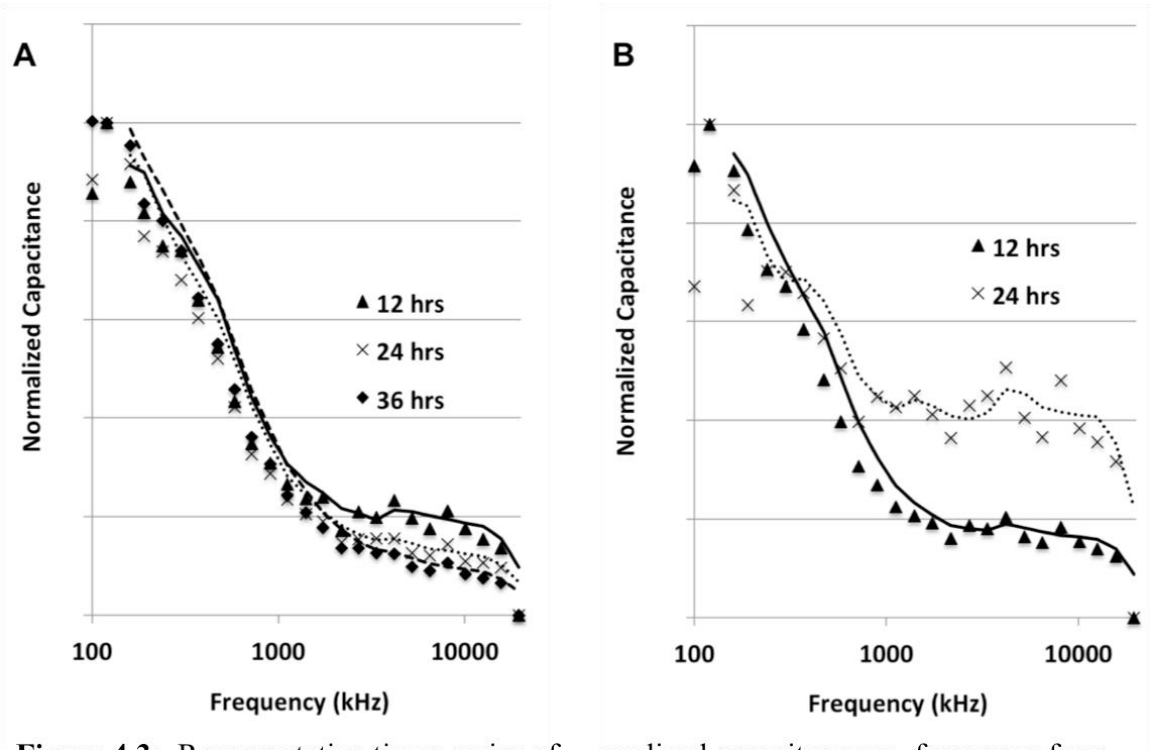

Figure 4.3: Representative times-series of normalized capacitance vs. frequency for a A) Control and B) Starvation culture showing change in β-dispersion over time after apoptosis induction.

In the control culture a very typical β-dispersion graph was observed (Figure 4.3 A). At low frequencies high capacitance readings were detected, which were then followed by a steep decline in the capacitance as frequencies increased. Eventually at even higher frequencies the

capacitance readings plateaued out at low levels. It was also noticeable that the overall β-dispersion did not change over time. The f_c for the 12, 24, and 36 h sampling points were 620, 574, and 561 kHz, respectively. Both observations would indicate that the cells dielectric properties remained constant throughout the experiment.

A typical β-dispersion graph was also produced for the starvation culture 12 h post induction (Figure 4.3 B). However, 24 h after starvation induction the shape of the β-dispersion changed displaying an increased capacitance reading of some cells at higher frequencies. This indicated the presence of a second cell population at this point of apoptosis induction through starvation. This sub-population of cells presented a higher capacitance reading at higher frequencies compared to cells in the control culture, indicating a change in the dielectric properties of these cells. This was also supported by the increase in f_c associated with the change in the capacitance readings. During starvation the f_c increased from 553 kHz at 12 h to 905 kHz at 24 hours.

4.2.4 DEP

At each sampling point approximately 600 cells per treatment were analyzed using the DEP cytometer. For each measurement the overall viability of the sample was determined based on the percentage of pDEP signals. In addition, the force index (FI) for each cell was determined based on the amplitude and the sign of polarizability of the cell. The force indices were then grouped and graphed to show how their distribution changes over time and between different apoptosis inducers (Figure 4.4).

The FI distribution of the control culture is shown in Figure 4.4 A. While only a single population of cells with a high viability was detected, the figure shows that the cell population

detected actually showed a Gaussian (bell-shaped) distribution of the FI. For the normal distribution of this population the average FI was stable for the first three measurements (0.15 – 0.14) and then slightly decreased to 0.09. Over the same time the DEP viability was stable at 96-97%.

For the starvation culture the initial measurement at 12 h gave an average FI of 0.15 (Figure 4.4 B) with a normal population distribution. While this was the same average FI as observed in the control culture, the DEP viability determined for the control was higher than in the starvation culture. The average FI in the starvation was the same because the small sub-population of cells with an nDEP was balanced out with the cells that exhibited a large positive FI. Over the course of the experiment the subpopulation of cells with an nDEP increased until a predominant second population was observed at 36 h after induction. At this point two main peaks were observed, of which one matched the main peak found in the control culture. 12 h later the majority of the cells exhibited an nDEP. As the cells progressed to a lower DEP and eventually became negative the DEP-measured viability and average FI decreased from 93.45 to 4.66% and 0.15 to -0.06, respectively.

The distribution graphed for the oligomycin culture exhibited a lower FI than observed in the control culture (Figure 4.4 C) and showed two subpopulations in the culture from the first measurement on. Interesting for this culture was that the normal pDEP population dispersion had a peak population at a higher FI (0.23) than the control culture (0.15) and a larger nDEP population than found in the starvation culture. This was also indicated in the lower DEP viability in the oligomycin culture at 12 h after induction. During the next three measurements the sup-population of cells with an nDEP only slightly increased, decreasing the DEP viability

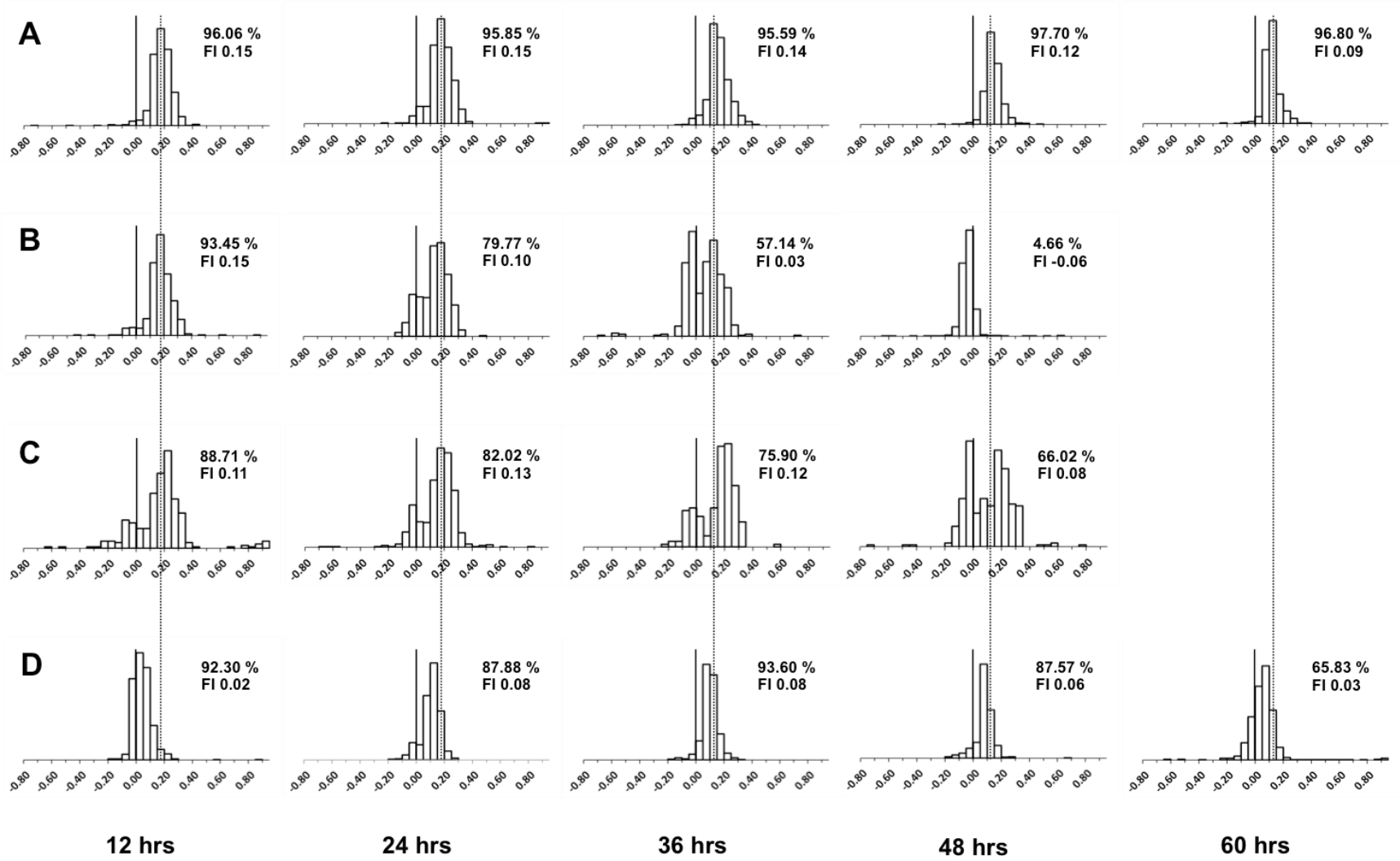

Figure 4.4: Representative force index distribution during apoptosis induction over time in a A) Control, B) Starvation, C) Oligomycin, and D) Staurosporine culture.

from 89% at 12 h to 76% at 36 h after induction. However, even though the DEP viability decreased the average FI remained constant due to the higher FI seen in some pDEP cells. 48 h after apoptosis induction the subpopulation of nDEP cells continually increased while a large population still exhibited a higher FI than observed in the control.

Figure 4.4 D shows the distribution observed in the staurosporine-induced culture. Throughout the experiment the peak FI determined for this culture was lower than what was observed in the control. At 12 h post apoptosis induction a very low average FI of 0.02 was determined. However, the DEP viability was still determined to be 92% since most of the cells exhibited a pDEP. The FI then increased to 0.08 at 24 h post induction as cells shifted to a higher pDEP. At the same time the DEP viability decreased to 88% as more nDEP cells were present. The average FI then remained stable until it decreased again at the 60 h measurement. While the cultures average FI and DEP viability decreased it looked like the heterogeneous population of cells moved as one single population as the emergence of a subpopulation was not observed.

In summary, the induction of apoptosis for each inducer caused a unique response, which could be detected with the DEP cytometer. This allowed for the observation of detailed differences in the onset and progression in each apoptosis induction. The onset in the starvation culture was slow in the first 24 h but then progressed very fast for the rest of the experiment. This was seen by the establishment and increase of a second population of cells in the bioprocess. On the other hand, the oligomycin induced culture immediately (12 h post induction) showed the presence of a larger subpopulation of cells. This subpopulation of cells then only marginally increased during the rest of the experiment with the largest increase from 36 to 48 h post induction. In addition, the viable cell population (pDEP) showed a higher peak

force index than observed in the control. Besides the control the staurosporine culture was the only culture with only one distinguishable cell population. For that population of cells the initial force index was very low (0.02) at 12 h post induction and was increased in the 24 h measurement (0.08). At 24 h post induction the force index stayed fairly constant before again decreasing at the 60 h post induction measurement.

4.3 Discussion

Understanding the onset and progression of apoptosis in mammalian cells is an important contribution to better understand the overall bioprocess. In addition, it is important to understand the basis and limitations of the individual methods used for cell culture viability monitoring. By understanding these two aspects we can understand the metabolic changes associated with the different ways of inducing apoptosis and how they are manifested through specific cellular changes that can be detected. This will improve the monitoring of the bioprocess by making it more efficient thereby allowing for an improvement of the overall bioprocess.

In the previous study (Chapter 3) a variety of different viable cell density and viability assays including a bulk capacitance and a single cell dielectric measurement were compared over the course of a batch culture. This study concluded that dielectric, especially single cell dielectric measurements were able to detect apoptosis in the early stages (Braasch et al., 2013). It was reasoned that this was possible because of the progression of apoptosis in a batch culture. In a batch culture cells are entering apoptosis most often due to nutrient limitations, which arise at the end of a batch run. The lack of nutrients, especially glucose, will then reduce the energy content in the cell (Burgener et al., 2006). This in turn will perturb the ATP-dependent pumps in the membrane that are maintaining the balanced ionic content (Jaitovich and Bertorello, 2006).

The change in the ionic content of the cell then causes the cell cytoplasm conductivity to change, which results in a different response of the cells to dielectric measurements. However, apoptosis is a very complex system, which can be induced in a variety of ways and from there, progresses down different pathways. Hence the monitoring of apoptosis induced using a variety of inducers is a critical aspect to further the understanding of the apoptotic processes possible in bioprocesses. By using starvation, 8 μg/mL oligomycin, and 50 nM staurosporine as inducers both the intrinsic and the extrinsic pathway can be explored. This will allow determining whether the dielectric measurements can also detect the onset of apoptosis under other induction circumstances. In this study, trypan blue exclusion, the flow cytometer, a bulk capacitance and a single cell dielectric measurements were used to detect the onset and progression through apoptosis. For each induction experiment viabilities were compared amongst the different methods and to the control culture.

The growth profiles showed that when apoptosis was induced, the cell culture growth was partially inhibited in the staurosporine culture and completely in the starvation and oligomycin culture. These findings agree with previous studies by (Godard et al., 1999), Caro-Maldonado (2011), and Breen and Scheffler (1980), respectively. In both the starvation and oligomycin-induced cultures the ATP content within each cell was disturbed resulting in a drop of the ATP concentration within the cell. In turn this increases the overall AMP concentration, which activates the SNF1/AMP-activated protein kinase (AMPK) (Hardie, 2007). This protein complex subsequently causes the inhibition of cell proliferation (Jones and Thompson, 2009) to reduce the energy and carbon requirement of the cell.

As expected, the control culture showed high viabilities with all assays used. The bulk dielectric measurements performed with the capacitance probe resulted in a constant β-dispersion

graph and f_c over the course of the experiment. This is comparable to the results seen during the exponential growth phase in the batch bioreactor (Chapter 3) when culture conditions are optimal. The viability analysis using the DEP cytometer also resulted in a stable viability measurement throughout the control run. However, when graphing the force index (FI) distribution of a healthy cell sample for each time point it was interesting to see that the cells' FI were following a normal distribution. This supports the general knowledge that cells in a bioprocess are not identical but rather exhibit diversity in certain characteristics (biological noise) (Niepel et al., 2009; Pilbrough et al., 2009).

The starvation culture was an artificial replication of the previous batch culture experiments. While cells were running slowly of out glucose in the batch culture, in this experiment the loss was intensified by removing cells from an environment containing glucose and glutamine and transferring them into a medium missing both of these sugars. Even though the cell demise progressed faster than in the batch culture the overall progression is identical to what was observed previously (Chapter 3). In Figure 4.5 the progression of the different stages of apoptosis in the starvation culture and their respective detection assays are shown. As discussed in chapter 3 the loss of glucose and glutamine results in the cells inability to produce ATP via glycolysis (Burgener et al., 2006). Eventually the drop in ATP will cause a decrease in the adenylate energy charge (AEC). The low ATP level will then have an impact on processes including ATP- dependent ion pumps and flippases (Jaitovich and Bertorello, 2006; Fadok et al., 1992). The hindrance of the following ATP-dependent membrane-bound Na^+/K^+ and the Ca^{2+} pumps will cause a change in the ionic content of the cell that is also reflected in the change of the cytoplasm conductivity (Jaitovich and Bertorello, 2006). This change can be detected using

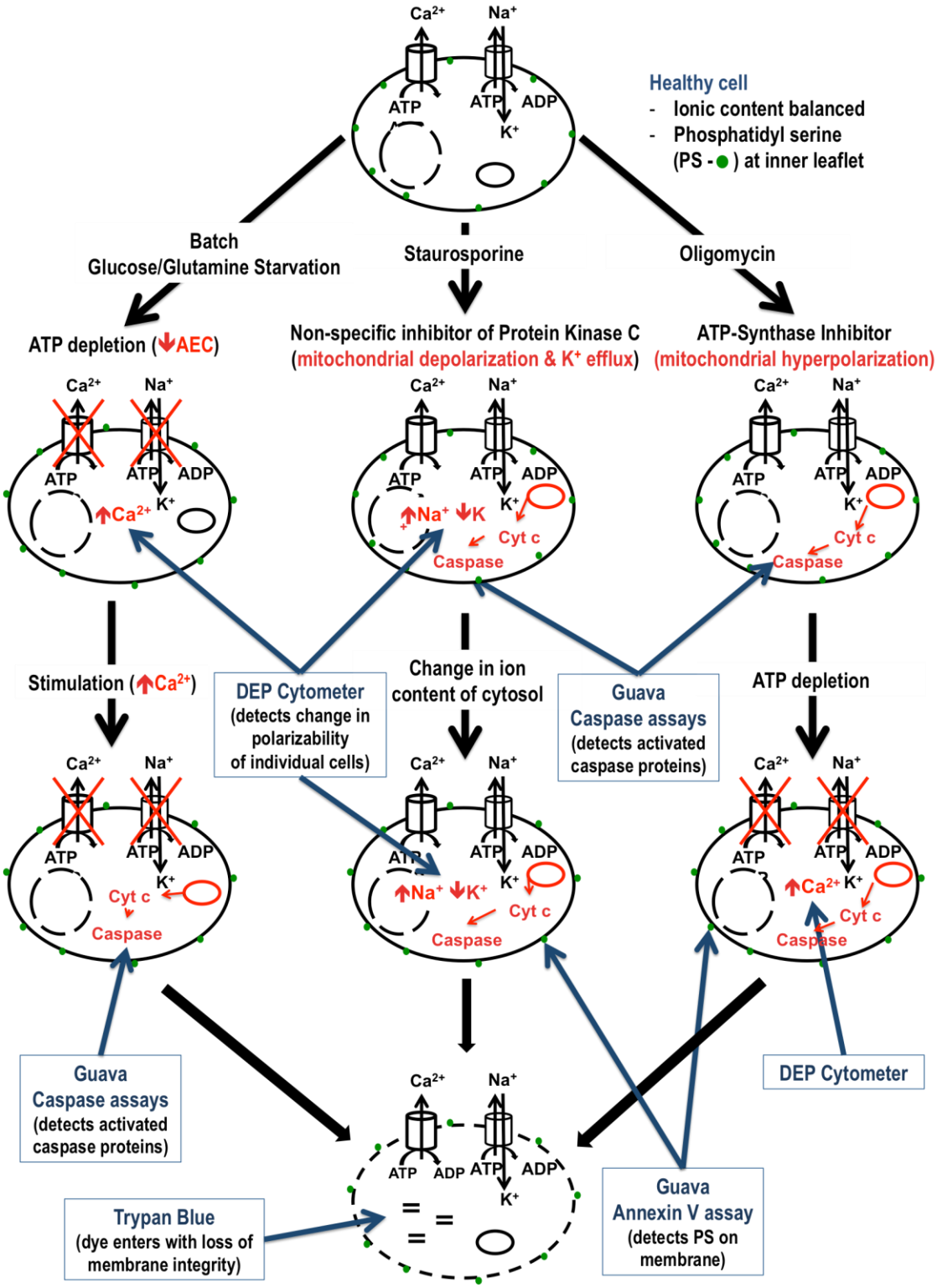

Figure 4.5: Overview of the apoptosis progression using different inducers and the methods used for detecting the respective changes. The overview contains the plasma membrane (---) with the position of the phosphatidylserine (●), the Ca^{2+} and N^{+}/K^{+} ATP-dependent pumps, the mitochondria (⬭), the nucleus (◌), and fragmented DNA (⁼₌⁼).

dielectric measurements such as the capacitance probe and the DEP cytometer. In addition, the flippases involved in keeping the phosphatidyl serine (PS) facing the cytosolic side of the membrane are hindered by the lack of ATP (Bitbol et al., 1987). This will result in the appearance of phosphatidylserine facing the outer side of membrane. Using the Annexin V assay the presence of these PS molecules can be detected. Because these are the first events to occur after ATP is depleted both the DEP cytometer and the Annexin V assay give the lowest viability throughout the starvation culture. With the change in the ionic content within the cell, an increase in Ca^{2+} is possible since the excretion pump is hindered. In the cell Ca^{2+} acts as a signaling molecule, which can activate the release of cytochrome c from the mitochondria (Hajnoczky et al., 2003). This will eventually lead to the activation of caspase molecules, which are then detected using the caspase assays (Hajnoczky et al., 2003). Since this is happening after the initial change in the ionic content of the cell the viability determined with the caspase assays is higher than the DEP cytometer and Annexin V assay. Only at the end of the apoptosis pathway will the membrane integrity of the cells fail, allowing for trypan blue to determine the cell as dead.

In the bulk dielectric measurement of the starvation culture a subpopulation was identified that showed a higher capacitance reading at higher frequencies 24 h after induction by starvation. This indicates that the change in the ionic content has an impact on the cytoplasm conductivity and the membrane capacitance. In addition to the decrease in the cytoplasm conductivity in dying cells (Asami et al., 1989), the decrease in the cell diameter of those cells allows them to polarize even at higher frequencies (Ansorge et al., 2010) hence contributing to the higher capacitance reading at higher frequencies.

For the DEP cytometer force index analysis the formation of a sub-population was observed early on. The cells in this sub-population were characterized by a lower force index when compared to the main population, which resembled the population in the control culture. Over the course of the starvation experiment this subpopulation became more and more established as cells from the viable population experience a decline in their force index shifting towards the non-viable population. As the cytoplasmic conductivity decreases in dying cells (Asami et al., 1989), they progress from a pDEP to an nDEP signal. Eventually all cells in the bioprocess will experience a shift in their force index to nDEP. As seen in the batch culture (Chapter 3) – over the course of the experiment the specific dielectric properties of both populations, which are visualized through the force index, remain constant.

Oligomycin acts as an ATP-Synthase inhibitor in cells. When oligomycin binds to the ATP-Synthase reversibly the production of ATP in the mitochondria is hindered (Huijing and Slater, 1961; Cho et al., 1997). Since ATP is not produced, a build up of H^+ ions in the mitochondria causes a mitochondrial hyperpolarization, as these H^+ ions would normally be used to create the force needed to produce ATP (Shchepina et al., 2002). This change in the mitochondrial potential will eventually cause the release of cytochrome c from the mitochondria thereby initiating the caspase cascade (Zou et al., 1999). The initiation of the caspase cascade can be monitored with fluorescent probes (Figure 4.5). As mentioned earlier the cells in the oligomycin-treated culture did not double. This is an indication that although glucose is present in the medium, not enough ATP can be produced to support growth. This lack of ATP in the cells can also have an impact on the ATP-dependent pumps discussed in the course of the starvation culture. Hence, the cell does not maintain its proper ionic balance and keep the

phosphatidylserine on the cytoplasmic site (Figure 4.5). As apoptosis progresses further trypan blue can enter the cells, identifying the cells as dead.

When looking at the DEP cytometer data for the oligomycin-induced culture two populations of cells can be distinguished one with an average force index higher than the control and one with an average force index lower than the control. The shift in the viable population could be a sign of the mitochondrial hyperpolarization of those cells. The non-viable population shows similar force indices as observed in the starvation non-viable population. Only after 36 h the cells in the viable hyperpolarized population slowly shift over to the non-viable population.

The use of staurosporine results in the inhibition of the protein kinase C. This in turn initiates the release of cytochrome c from the mitochondria and subsequent caspase cascade activation (Jing et al., 2011). In addition, the induction with staurosporine is associated with the efflux of K^+ causes (Trimarchi et al., 2000), which leads to a shift in the cell cytoplasm conductivity. The initial induction of the caspase cascade is the reason for the early detection of a cell demise using the fluorescent caspase assays. The third lowest viability is detected with the Annexin V assay indicating that the exposure of phosphatidylserine is one of the earlier events happening during apoptosis induced with staurosporine. This finding agrees with observations made by Godard et al. (1999). During these early stages the DEP cytometer does not show a loss in cell viability. All these changes precede the loss of cell membrane integrity. Hence, the trypan blue exclusion method gives a higher viability for all time point except for at 48 h.

The DEP cytometer is only identifying a decline in cell viability 63 h after apoptosis induction. This result is most likely based on the subtle changes in the dielectric properties observed using staurosporine. While the use of staurosporine induces the efflux of K^+ from the cell it is expected that the cell is still able to control and stabilize the cytoplasm conductivity

because only a small unanimous decrease in the average force index can be observed. Hence, this drop in the force index later stabilizes until the last measurement when a drop in the force index is seen again. Overall, the peak and average force index at every time point for the staurosporine induction is lower than observed in the control indicating a mitochondrial depolarization representative for staurosporine induction (Scarlett et al., 2000). It is also interesting to note that during the entire experiment only one population of cells can be observed as opposed to the two populations during the other induction experiments.

4.4 Conclusion

In this study the onset and progression of apoptosis induced by starvation, 8 μg/mL oligomycin, and 50 nM staurosporine was monitored with a bulk and a single cell dielectric measurement, as well as some common fluorescent methods. By comparing and correlating the dielectric measurements to the fluorescent measurements a better understanding of the dielectric measurements was reached. It was shown that changes in the dielectric properties of CHO cells could be used to monitor changes in cell health and metabolism during cell culture processes that are linked to changes in the cytoplasm conductivity and cell membrane conductivity. These changes can be monitored using either an online bulk capacitance probe or a single cell analysis DEP cytometer prototype. While both methods can detect early emerging apoptotic sub-populations single cell analysis allows for a faster, more distinct and sensitive monitoring of changes and rare events in the polarizability of individual cells in a label-free, non-invasive and all electronic manner. Recent work has shown that the sensitivity of the DEP cytometer can be further improved by using a low conductivity measurement medium that resembles the

cytoplasm conductivity of a healthy cell. This allows for even small changes in the cytoplasm conductivity to be detected (Saboktakin Rizi et al., 2014).

Overall, the results and knowledge gained by this study about the use of dielectric – specifically single cell dielectric – measurements will further support the use of dielectric measurements as stand alone or complementary method to monitor cell health and viability in bioprocesses.

Section A

Summary

The continuous monitoring of cell growth and viability represents an important part of bioprocess control in the manufacture of biopharmaceuticals. An optimal method for monitoring would be simple and fast but also detect the onset of apoptosis early. While a variety of methods are available methods based on dielectric measurements are particularly promising for identifying emerging subpopulations of apoptotic cells. Bulk average capacitance measurements of a cell population in a bioreactor have been made possible by commercially available sterilizable probes. However, the analysis of single cells allows a unique insight into the metabolism and energy flow within cells. By using single cell analysis discoveries of rare events and subpopulations can be made that might otherwise be masked by the overall response of a cell population.

In the initial experiments the dielectric measurements were done for regular batch cultures to monitor the cell culture during the growth and death phase. By comparing the dielectric measurements to more commonly used methods such as trypan blue exclusion and a variety of apoptosis detecting fluorescent assays a better understanding and interpretation of the data collected with the DEP cytometer and the bulk capacitance probe was reached. In a batch culture when cells usually die due to glucose starvation an early detection of the onset of cell demise was possible. This early detection was linked to the prominent changes within the cells ionic content during this starvation mode. Because the cells response to the non-uniform electric field produced by the DEP cytometer and the capacitance probe is based on their ionic

composition i.e. cytoplasm conductivity as well as their cell membrane capacitance these changes can be easily monitored.

Since apoptosis is not always induced in the same manner in a bioprocess it was important to monitor several mechanisms of induction. This allowed monitoring if the capacitance probe and DEP cytometer are also sensitive to changes observed during the onset and progression of apoptosis induction by starvation, oligomycin, and staurosporine. The bulk capacitance probe was able to show the onset apoptosis in the starvation culture due to a change in the β-dispersion plot that can be associated with a secondary population apoptotic population. However, the bulk capacitance probe does not allow for a real quantification of this subpopulation. It was also shown that when the onset and progression through apoptosis is not directly affecting the cytoplasm conductivity less prominent changes are seen in the DEP cytometer viability analysis. However, the single cell force index analysis using the DEP cytometer allowed seeing even rare events and small changes in the overall FI distribution associated with apoptosis that are not necessarily reflected in the DEP viability.

Section B

The effects of nucleotide sugar precursor feedings on the nucleotide / nucleotide sugar pool and glycosylation

Introduction

For antibodies and other glycoproteins a relationship between the glycan profile and the functionality has been reported (Ghirlando, 1999). This means that biopharmaceuticals – specifically their functionality – could be optimized by reaching a specific glycan profile that is correlated to a desired function. Thus, the glycosylation of therapeutic and diagnostic proteins such as antibodies is an important aspect in biomanufacturing. However, the overall glycosylation process is very complex and still not completely understood (Hossler et al., 2009).

Nucleotide and nucleotide sugars are important precursors in the glycosylation process, as they provide the necessary building blocks for the glycan structure. The nucleotide sugars needed for the glycan assembly are all assembled and activated in the cytoplasm with the exception of CMP-NeuAc, which originates in the nucleus (Freeze and Elbein, 2009). To assemble the final glycan structure these building blocks are then transported to the Golgi (Freeze and Elbein, 2009). Once in the Golgi the nucleotide sugars are transferred to the existing glycan core structure via specific glycosyltransferases. This process does not resemble a linear assembly line but rather depends on the availability of the glycosyltransferases and the nucleotide sugars (Spearman and Butler, 2015). Hence, not all glycans will have the same sugars attached to the core structure resulting in a microheterogeneity observed in the final product. However, an increase in the building blocks due to precursor feeding has shown an effect on the

final glycosylation product (Fan et al., 2015). It was also shown that this effect is cell line and product dependent.

Precursors that lead to an increase in the final galactosylation are galactose, uridine, and manganese as well as combinations of these precursors (Gramer et al., 2011; Grainger and James, 2013). Galactose is a direct precursor for UDP-Gal, which is added to the core structure glycan to yield the galactosylated glycan structure. The addition of galactose has shown to increase the intracellular UDP-Gal pool in some cells and consequently increase galactosylation (Amand et al., 2014; Hills et al., 2001). Uridine is added to the medium as a precursor for UTP needed for galactose activation (Freeze and Elbein, 2009). It is also suggested that the addition of manganese can further increase the galactosylation as it acts as an enzyme cofactor for the galactosyltransferase (Witsell et al., 1990).

In this study the addition of 10 mM galactose (Hills et al., 2001; Wong et al., 2010) ['Galactose'], 20 mM galactose + 1 mM uridine (adapted from Gramer et al., 2011) ['UG'] and 20 mM galactose + 1 mM uridine + 8 μM manganese (adapted from Gramer et al., 2011) ['UMG'] as precursor feedings was investigated in two independent CHO cell lines (CHO-DG44 and CHO-K1), producing two different antibodies (EG2 and DP12). Fed-batch processes as outlined in Chapter 2.2.4.3 were used to observe the impact of the precursor feeding regimes on the cells' metabolism, the nucleotide / nucleotide sugar pool and subsequently the glycosylation profile in those two independent cell lines. These results were then compared to a batch ['Batch'] and a non-precursor supplemented fed-batch ['NS'] process performed in medium without precursor additions. Because this precursor addition study was performed as fed-batch and not in batch culture like other studies with these precursors, the concentration of the initial

uridine concentration added was decreased to 1 mM and the manganese concentration for the feed-medium was decreased to 1 μM.

The objective of this study was to determine whether the addition of these specific nucleotide sugar precursors to the culture medium would increase the intracellular UDP-Gal concentration and respectively increase the galactosylation of the two antibodies used. In addition, it was of interest to see if the continuous feeding of these precursors would result in a stable glycosylation profile throughout the culture. While these objectives were directly related to the precursor addition it was also important to assess their general impact on the bioprocess performance (i.e. growth, viability, metabolism, productivity).

Chapter 5

The effects of nucleotide sugar precursor feedings on the growth, metabolism and recombinant protein production of EG2, and DP12 in CHO cells

5.1 Introduction

In biopharmaceutical production a high viable cell density in combination with consistent productivity and product quality is of importance. However, the addition of any media additives to the regular medium can have an influence on these process attributes. The effects additives have are still not completely understood and considered cell line dependent (Butler, 2006; Hossler et al., 2009).

The use of different precursor feeding strategies has had an impact on the intracellular nucleotide / nucleotide sugar pool and / or the glycosylation profile in various cell lines (Hills et al., 2001; Crowell et al., 2007). In addition to having an impact on these culture parameters some precursor feeding strategies containing uridine or glucosamine have shown an impact on the culture growth, viability and / or productivity in different cell lines (Hills et al., 2001; Wong et al., 2010; Grainger and James, 2013). Hence, the additions of any precursors to the medium need to be tested not only on their effect on the intracellular nucleotide / nucleotide sugar pool and the final glycosylation but also on the general performance of the cell culture. Only when taking all these results into consideration a reasonable decision can be made regarding the process development.

Here two independent CHO cell lines producing two different antibodies were used to test the effects of the addition of 10 mM galactose (Hills et al., 2001; Wong et al., 2010) [‘Galactose’], 20 mM galactose + 1 mM uridine (adapted from Gramer et al., 2011) [‘UG’] and

20 mM galactose + 1 mM uridine + 8 μM manganese (adapted from Gramer et al., 2011) ['UMG'] as nucleotide sugar precursors to improve galactosylation. While the main reason for the addition of these precursors is galactosylation, the study of their impact on the cell growth, viability, productivity and basic metabolism during cell culture is just as important. Considering the effect these precursor feeding strategies have on the cell culture will improve the understanding of the overall bioprocess and allow for educated decisions to be made in regards to the process development.

5.2 Results

5.2.1 Effect of precursor feeding in EG2 cultures on growth and viability

Monitoring the growth and viability in a bioprocess is an important aspect in biopharmaceutical production. In this study the monitoring was important to detect any effects on the cell culture caused by the addition of the galactosylation precursors studied. The effects of added precursors on the growth and viability profiles of CHO EG2 fed-batch cultures were compared to the 'Batch' and the fed-batch 'NS' culture (Figure 5.1). The cultures were grown in BioGro CHO medium alone or supplemented with the appropriate precursor feed as outlined in Chapter 2.4.4.3. Each culture was inoculated at $2x10^5$ cells/mL in a 250 mL shaker flask (n=7) using a working volume of 80 mL. During the experiment the cultures were incubated at 37°C with a 10% CO_2 overlay on a shaker platform (120 rpm). At the times of sampling the viable cell density was determined by trypan blue exclusion.

As shown in Figure 5.1 (A) the exponential phase for all cultures lasted until day 3. After the exponential phase cultures entered the stationary phase, which lasted from day 3 to day 5 for all cultures except 'UG' and 'UMG' in which it lasted until day 6. For the 'Batch', 'NS' and

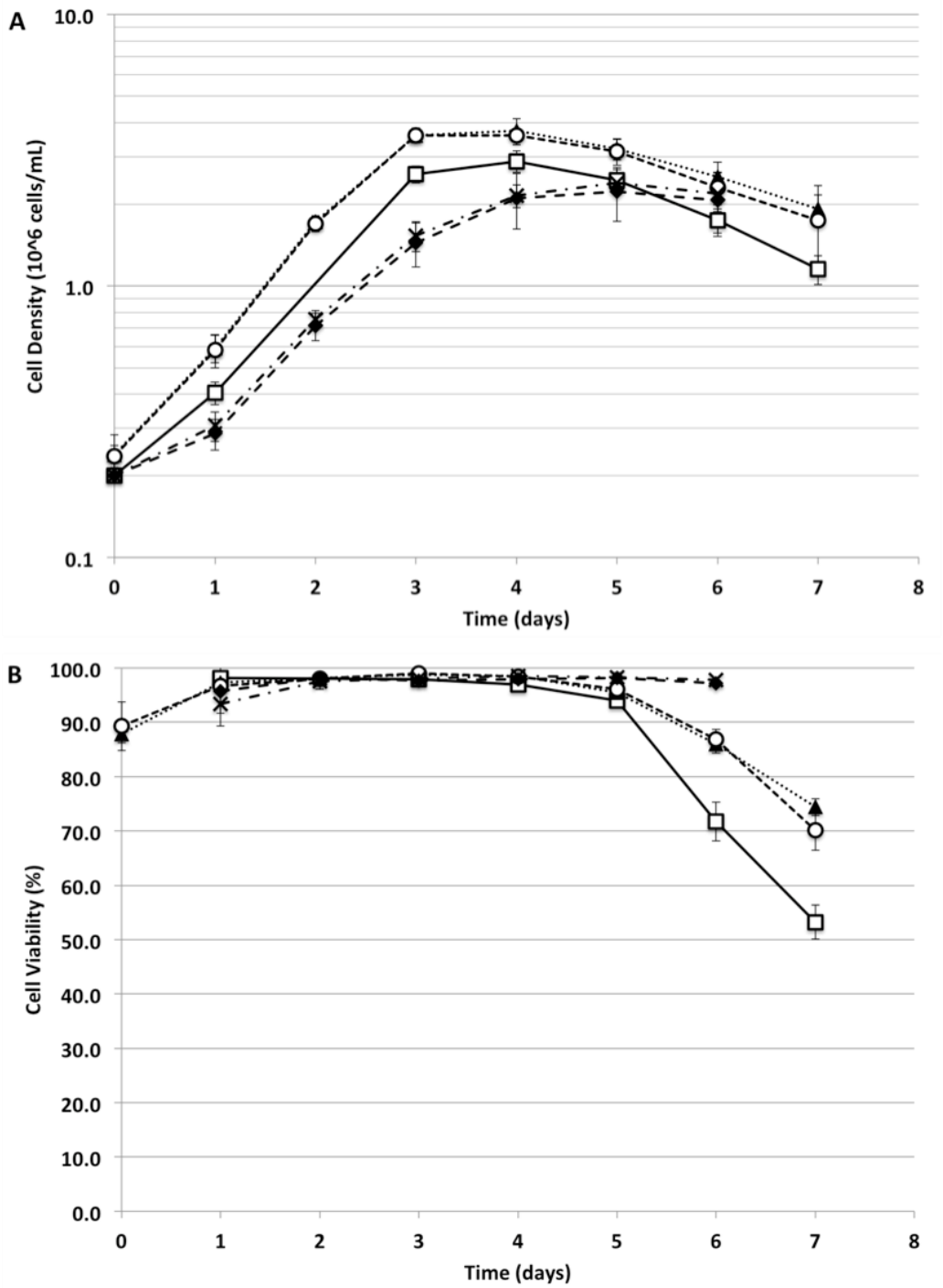

Figure 5.1: The effect on the growth and viability profiles for EG2 producing CHO cells using different precursor feeding strategies. Cells were inoculated at $2x10^5$ cells/mL into 80 mL culture medium in the appropriate precursor feeding strategy basal medium. The 'Batch' (—□—) and fed-batch 'NS' culture (···▲···) were used as controls. The precursor feeding strategies compared to the controls were 10 mM galactose ('Galactose';-○-·), 1 mM uridine + 20 mM galactose ('UG'; —◆—), and 1 mM uridine + 8 μM $MnCl_2$ + 20 mM galactose ('UMG'; —×-). (n = 7; error bars indicate the standard deviation)

'Galactose' culture the maximum cell density was reached on day 4 whereas the 'UG' and 'UMG' cultures reached the maximum cell density on day 5. The highest overall cell density was reached with the 'NS' and 'Galactose' cultures at $3.6x10^6$ cells/mL while the 'Batch'culture yielded a significantly lower ($P < 0.02$) maximum cell density of $2.9x10^6$ cells/mL. The lowest maximum cell density was reached in the 'UG' and 'UMG' culture with 2.2 -2.4 x 10^6 cells/mL, respectively. On day 6 when the 'UG' and 'UMG' cultures reached the stationary phase the viable cell density was not significantly different compared to all other cultures ($P > 0.02$) on that day.

Table 5.1 shows the comparison of the specific growth rate during the exponential phase for each treatment. While the specific growth rates for the 'Batch', 'NS' and 'Galactose' cultures were not significantly different ($P > 0.02$), the specific growth rates for the 'UG' and 'UMG' were significantly lower compared to both the 'Batch' and 'NS' culture ($P < 0.02$).

Table 5.1: Comparison of the specific growth rate for EG2 producing CHO cells using different precursor feeding strategies. Cells were inoculated at $2x10^5$ cells/mL into 80 mL culture medium in the appropriate precursor feeding strategy basal medium. The 'Batch' and fed-batch 'NS' culture were used as controls and compared with the 'Galactose', 'UG', and 'UMG' precursor feeding strategies (n = 7).

	Batch	**NS**	**Galactose**	**UG**	**UMG**
$\mu^{\sim}$	0.035 ± 0.001 h^{-1}	0.038 ± 0.003 h^{-1}	0.038 ± 0.002 h^{-1}	0.027 ± 0.003 h^{-1} *	0.028 ± 0.002 h^{-1} *

~ The specific growth rate and standard deviation were determined using linear regression analysis.

* ($P < 0.02$) compared to 'Batch' and 'NS'

The viability profiles for all cultures are shown in Figure 5.1 (B). All cultures showed viabilities of over 90% until day 5. After day 5 a steep decline in the cell viability was observed

in the ‘Batch’ culture, which was decreasing from 94% on day 5 to 71% on day 6 and eventually to 53% on day 7. A more moderate decline in the cell viability was observed for the ‘NS’ and ‘Galactose’ cultures, which fell to 87% on day 6 and 71% and 74% on day 7, respectively. In comparison the ‘UG’ and ‘UMG’ cultures were at 98% even on day 6. Prior to day 6 the viabilities observed among all cultures were not significantly different. However, on day 6 the significantly highest viabilities ($P < 0.02$) were determined for the ‘UG’ and ‘UMG’ cultures. The ‘NS’ and ‘Galactose’ cultures had a significantly lower viability ($P < 0.02$) than the ‘UG’ and ‘UMG’ culture but a significantly higher viability ($P < 0.02$) than the ‘Batch’ culture. The same trend was observed on day 7.

In summary, the change from a ‘Batch’ to a fed-batch ‘NS’ system increased the total cell yield. In addition, this total cell yield was not further increased by the addition of galactose to the medium. While, the addition of uridine to the medium resulted in a lower total cell yield it also allowed the ‘UG’ and ‘UMG’ cell cultures to remain at higher viabilities throughout the bioprocess.

5.2.2 Effect of precursor feeding in EG2 cultures on protein productivity

The production of EG2 was determined by ELISA to determine if the addition of any of the galactosylation precursors influenced the cell lines productivity. Figure 5.2 shows the accumulation of produced EG2 against the integral viable cell density (IVCD) for the different cultures. The secretion of EG2 commenced with the start of the culture and continued through the exponential and stationary phase. The significantly highest volumetric production ($P < 0.02$) was observed in the ‘NS’ culture with 27 µg/mL on day 6. In the ‘Galactose’ culture the second highest volumetric productivity was observed with 21 µg/mL on day 5. However, a decline in

product quantity was observed for day 6 and 7, which fell into the decline phase of the culture. While the 'Batch' culture showed a maximum volumetric productivity of 12 µg/mL on day 6 the 'UG' and 'UMG' cultures showed the highest yield at 9 and 9.7 µg/mL on day 6 and 7, respectively.

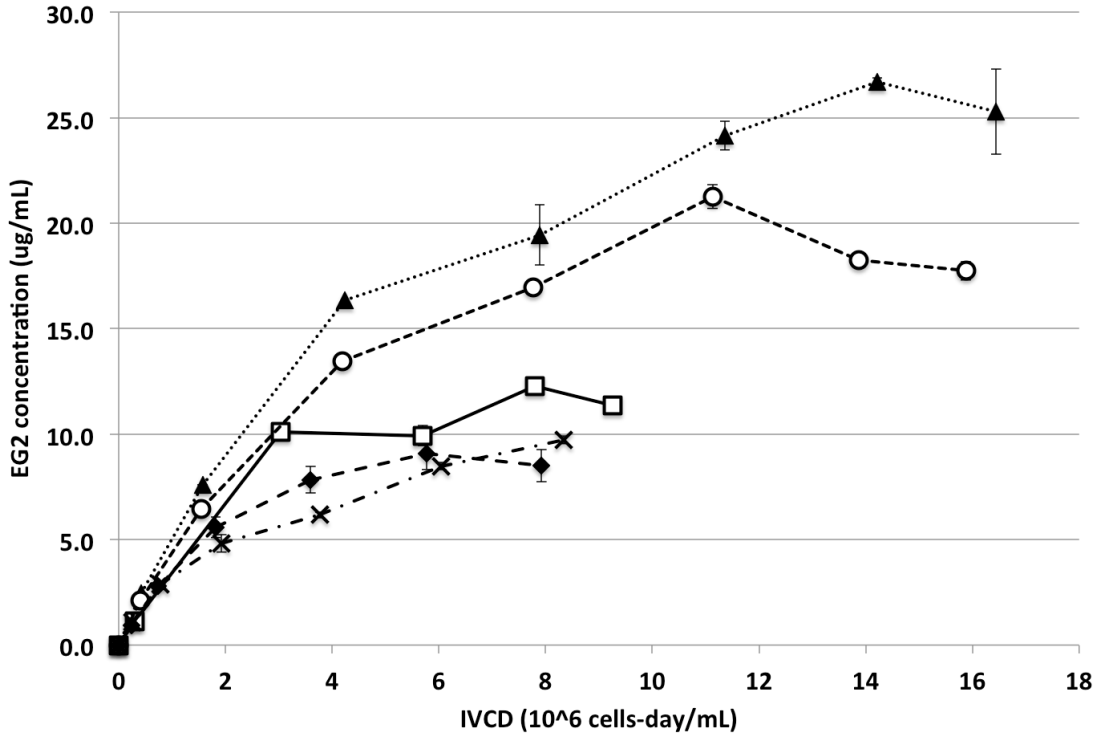

Figure 5.2: The effect on the EG2 production for CHO EG2 cells using different precursor feeding strategies. Cells were inoculated at $2x10^5$ cells/mL into 80 mL culture medium in the appropriate precursor feeding strategy basal medium. The 'Batch' (—□—) and fed-batch 'NS' culture (···▲···) were used as controls. The precursor feeding strategies compared to the controls were 10 mM galactose ('Galactose';-○-), 1 mM uridine + 20 mM galactose ('UG'; —◆—), and 1 mM uridine + 8 µM $MnCl_2$ + 20 mM galactose ('UMG'; —×—). (n = 2; error bars indicate the standard deviation)

For better comparison of the EG2 productivity in each culture the specific productivity for the exponential and stationary phase in each culture was determined using linear regression analysis. Table 5.2 shows a comparison of the determined values. During the exponential phase the highest specific productivity was found in the 'Batch' (3.7 ± 0.0 pg/cell-day) and 'NS'

culture (4.0 ± 0.2 pg/cell-day), whereas the lowest specific productivity was observed in the 'UMG' culture (2.7 ± 0.3 pg/cell-day). In the stationary phase the 'Batch' culture then showed no further production but rather a loss of product. Meanwhile the 'NS' (1.1 ± 0.1 pg/cell-day) and 'Galactose' cultures (1.1 ± 0.1 pg/cell-day) showed the highest specific productivity with the lowest specific productivity in the 'UG' culture at 0.5 ± 0.2 pg/cell-day.

Table 5.2: Comparison of the specific productivity for EG2 producing CHO cells using different precursor feeding strategies during the exponential (exp) and stationary phase (stat). Cells were inoculated at $2x10^5$ cells/mL into 80 mL culture medium in the appropriate precursor feeding strategy basal medium. The'Batch' and fed-batch 'NS' culture were used as controls and compared with the 'Galactose', 'UG', and 'UMG' precursor feeding (n=2).

	Batch	**NS**	**Galactose**	**UG**	**UMG**
q_{Mab}~ **(exp)**	3.7 ± 0.0 pg/cell-day	4.0 ± 0.2 pg/cell-day	3.3 ± 0.2 pg/cell-day	3.2 ± 0.1 pg/cell-day*	2.7 ± 0.2 pg/cell-day*
q_{Mab}~ **(stat)**	- 0.1 ± 0.0 pg/cell-day	1.1 ± 0.1 pg/cell-day*	1.1 ± 0.1 pg/cell-day*	0.5 ± 0.2 pg/cell-day	0.8 ± 0.1 pg/cell-day*

~ The specific productivity and standard deviation were determined using linear regression analysis. exp – exponential phase; stat – stationary phase

* ($P < 0.02$) compared to 'Batch' culture

Overall, it can be seen that the switch from a regular 'Batch' to a fed-batch 'NS' system increased the volumetric productivity by extending the stationary phase and hence the duration of EG2 production in the culture. It was also observed that the addition of galactose as a precursor did not negatively impact the volumetric productivity of the culture. However, the addition of uridine decreased the specific productivity in both the exponential and stationary phase leading to an overall decreased product yield.

5.2.3 Effect of precursor feeding in EG2 cultures on glucose, lactate, glutamine, glutamate

The concentration of glucose, lactate, glutamine and glutamate in cell culture supernatants was determined using YSI analysis to analyze the impact the precursor feeding regimes have. The consumption of glucose for EG2 producing CHO cell cultures against the IVCD is shown in Figure 5.3 (A). During the exponential phase all cultures showed a high consumption of glucose, which then tapered off in the stationary phase. When comparing the specific glucose consumption for each culture in the exponential and stationary phase as determined by linear regression analysis it was observed that the rates of consumption were similar among the different treated cultures (Figure 5.4 (A)).

Figure 5.3 (B) shows the overall lactate production throughout the culture time in each experiment against the IVCD. Similar to what was observed with the glucose consumption a steep incline in lactate was observed in the exponential phase, while the lactate level in the stationary phase remained constant. For the cultures entering the decline phase towards the end of the experiment ('Batch', 'NS', 'Galactose') an increase in the lactate concentration was measured. The specific lactate production during the exponential and stationary phase for each culture was determined by linear regression analysis and is shown in Figure 5.4 (B). The comparison showed higher specific lactate production in the exponential phase of the 'UG' and 'UMG' cultures compared to the 'Batch', 'NS' and 'Galactose' culture.

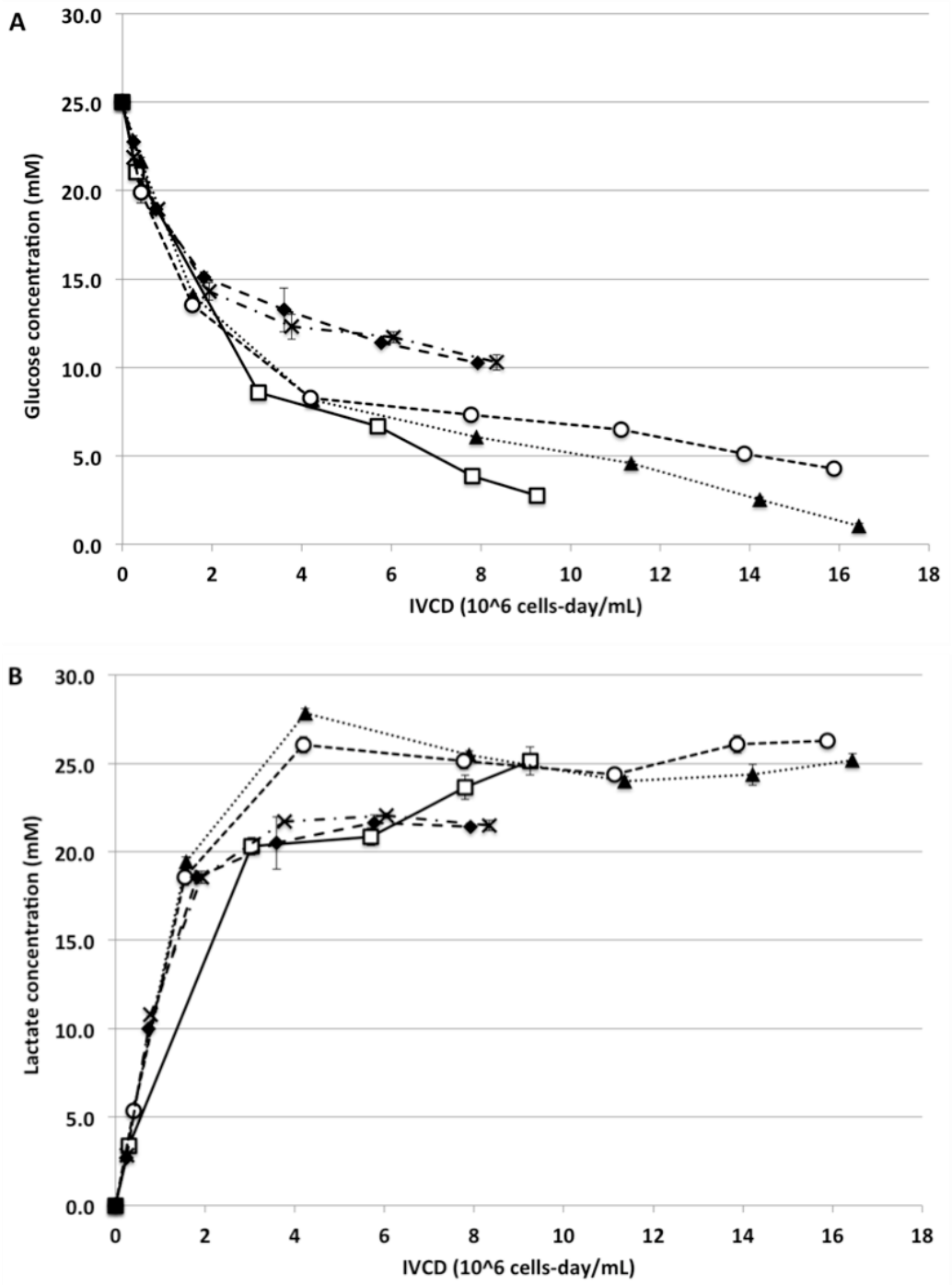

Figure 5.3: The effect on the glucose consumption and lactate production profiles for EG2 producing CHO cells using different precursor feeding strategies. Cells were inoculated at $2x10^5$ cells/mL into 80 mL culture medium in the appropriate precursor feeding strategy basal medium. The 'Batch' (−□−) and fed-batch 'NS' culture (···▲···) were used as controls. The precursor feeding strategies compared to the controls were 10 mM galactose ('Galactose';-○-), 1 mM uridine + 20 mM galactose ('UG'; −◆−), and 1 mM uridine + 8 μM $MnCl_2$ + 20 mM galactose ('UMG';−×-) cultures. (n = 2; error bars indicate the standard deviation)

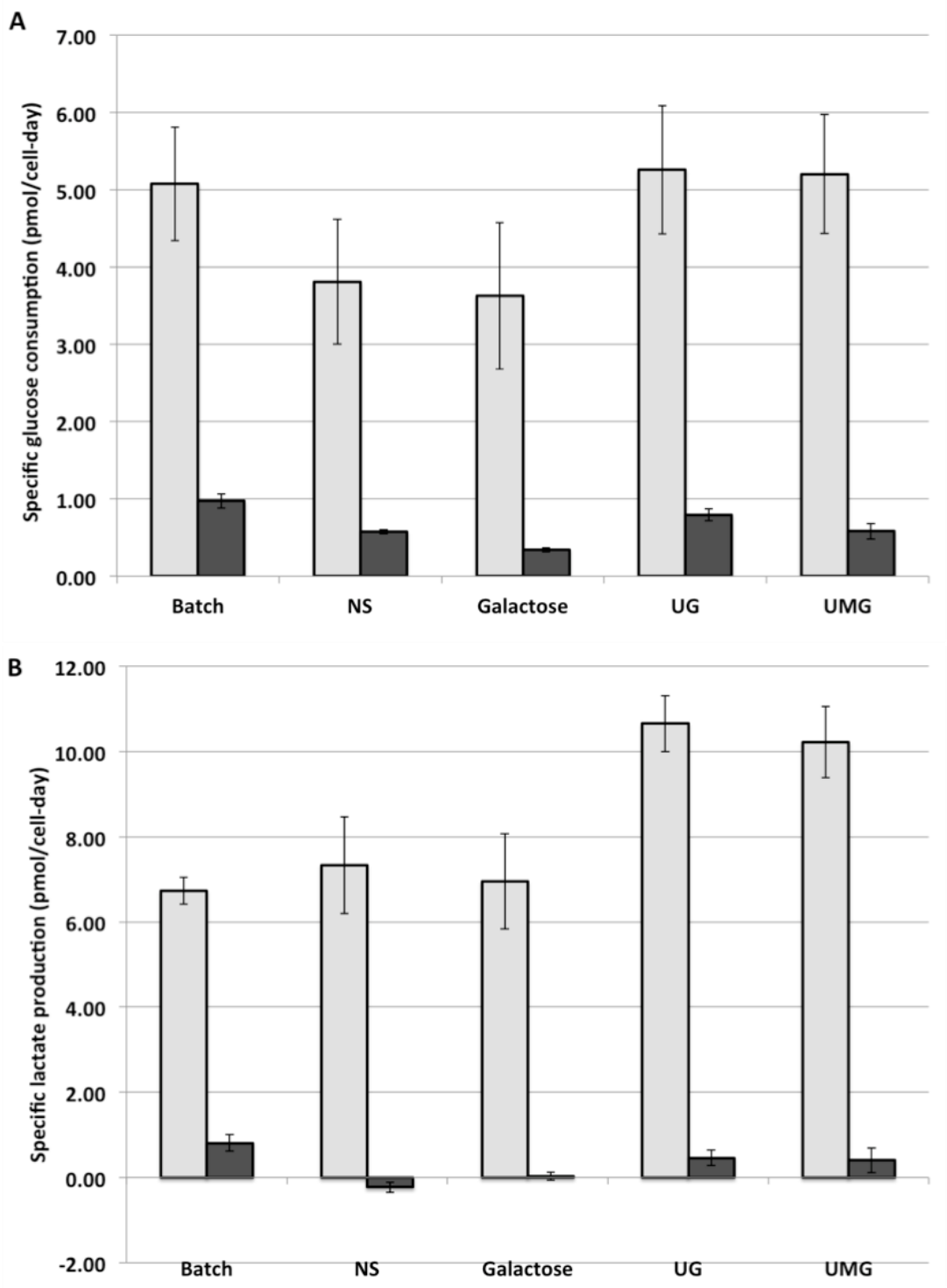

Figure 5.4: The effect on the specific glucose consumption and lactate production for EG2 producing CHO cells using different precursor feeding strategies during the exponential ( ) and stationary phase ( ). Cells were inoculated at $2x10^5$ cells/mL into 80 mL culture medium in the appropriate precursor feeding strategy basal medium. The 'Batch' and fed-batch 'NS' culture were used as controls and compared with the 'Galactose', 'UG', and 'UMG precursor feeding strategies. (n = 2; error bars indicate the standard deviation)

When comparing the overall yield of lactose from the glucose utilized in the exponential phase it was seen that the highest yield was found for the 'UG' and 'UMG' culture with 2.03 and 1.96, respectively (Table 5.3). The 'NS' and 'Galactose' culture showed a lower yield with 1.92 each, while the 'Batch' culture had the lowest yield at 1.33. Per molecule of glucose two molecules of lactate can be produced. This means that in the 'UG' and 'UMG' culture theoretically 100% and 98%, respectively, of the glucose taken up by the cell was converted to lactate. In the 'NS' and 'Galactose' cultures these number decreased down to 96%, while in the 'Batch' culture only 66.5% of the glucose taken up was converted to lactate. In the stationary phase these numbers changed considerably showing that the majority of the glucose was not converted to lactate anymore.

Table 5.3: Comparison of the yield of lactate molecule produced per glucose molecule consumed for the different culture conditions in CHO EG2 cultures during the exponential (exp) and the stationary (stat) phase.

	Batch	**NS**	**Galactose**	**UG**	**UMG**
$Y_{Lac/Glc}$ (exp)	1.33	1.92	1.92	2.03	1.96
$Y_{Lac/Glc}$ (stat)	0.83	NA	0.10	0.58	0.70

The glutamine and glutamate concentration against the IVCD for each culture is shown in Figure 5.5. An accumulation of glutamine starting between IVCD values of 2 and 4 was observed in the 'Batch', 'UG' and 'UMG' culture. In the 'NS' and 'Galactose' culture an increase in the glutamine content was not observed until an IVCD of 8. The highest glutamine accumulation over the entire culture period was seen in the 'Batch' and 'UG' culture at max

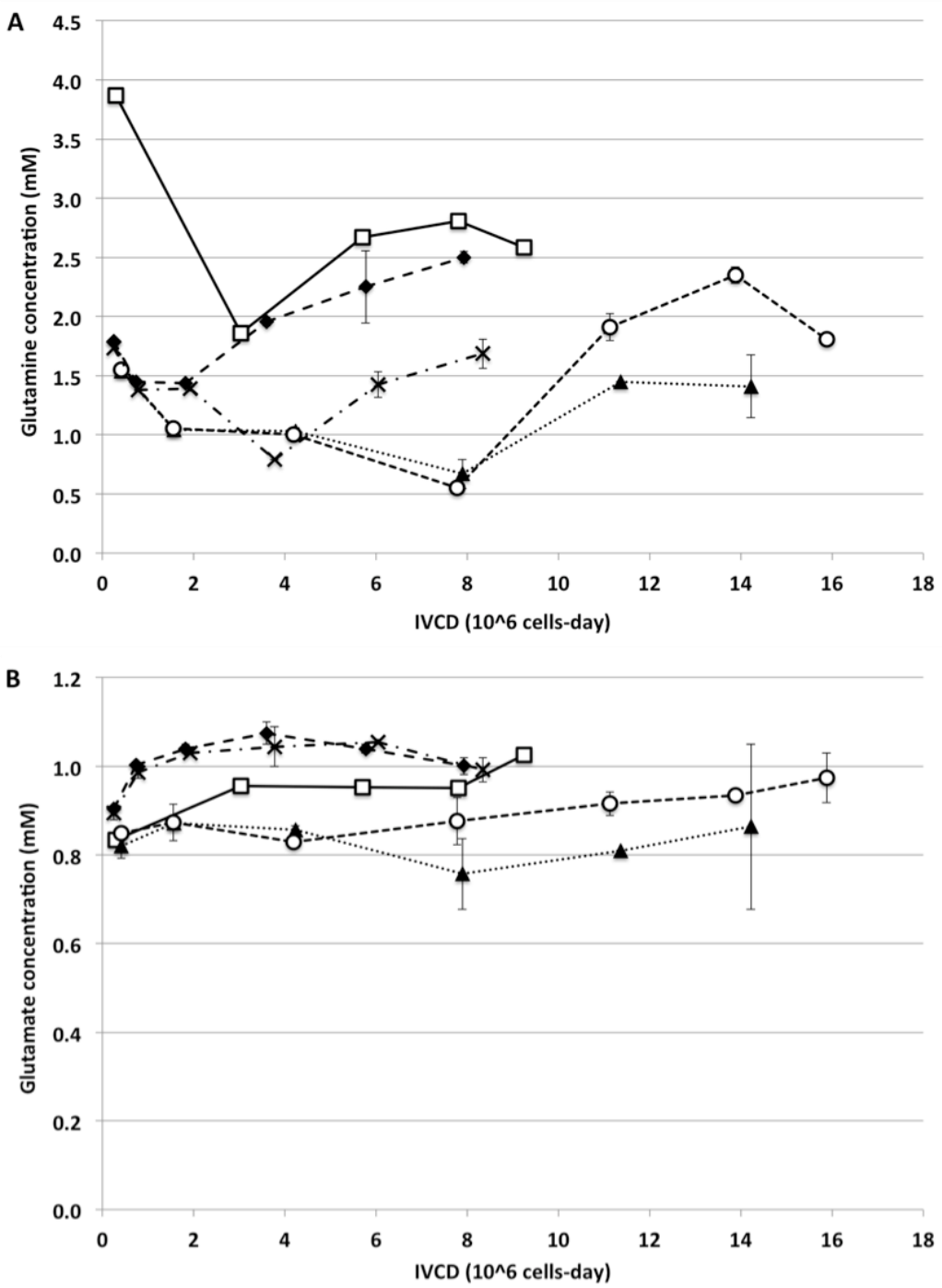

Figure 5.5: The effect on the glutamine consumption and glutamate production profiles for EG2 producing CHO cells using different precursor feeding strategies. Cells were inoculated at $2x10^5$ cells/mL into 80 mL culture medium in the appropriate precursor feeding strategy basal medium. The 'Batch' (—□—) and the fed-batch 'NS' culture (···▲···) were used as controls. The precursor feeding strategies compared to the controls were 10 mM galactose (-○-), 1 mM uridine + 20 mM galactose (UG; —◆—), and 1 mM uridine + 8 μM $MnCl_2$ + 20 mM galactose (UMG; —×—) cultures. (n = 2; error bars indicate the standard deviation)

values of 2.8 and 2.5 mM, respectively. In the 'Galactose' culture the highest accumulation was determined to be 2.35 mM. The 'NS' and 'UMG' culture exhibited the lowest glutamine accumulation at 1.45 and 1.69 mM, respectively. On the other hand, the glutamate concentration in all cultures was fairly stable and reached values of 0.8 to 1.05 mM (Figure 5.5 (B)).

In total, it was seen that while the specific glucose consumption rate was similar in all cultures, the specific lactate production was not. The specific lactate production in the 'Batch', 'NS' and 'Galactose' cultures were similar resulting in comparable $Y_{lac/glc}$ values. The higher specific lactate production in the 'UG' and 'UMG' indicated a change in the metabolism induced by the addition of uridine leading to higher $Y_{lac/glc}$ values. As seen in the glucose consumption the glutamate production was fairly stable between 0.85 to 1.05 mM and not affected by the precursor feedings.

5.2.4 Effect of precursor feeding in DP12 cultures on growth and viability

In this study the monitoring was important to detect any effects on the cell culture growth and viability caused by the addition of the galactosylation precursors, which were studied regarding galactosylation improvement. The effects of added precursors on the growth and viability profiles of CHO DP12 fed-batch cultures were compared to the 'Batch' and the non-precursor supplemented 'NS' fed-batch culture (Figure 5.6). The cultures were grown in BioGro CHO medium alone or supplemented with the appropriate precursor feed as outlined in Chapter 2.4.4.3. Cultures were inoculated at $2x10^5$ cells/mL in a 250 mL shaker flask (n=7) using a working volume of 80 mL. During the experiment the cultures were incubated at 37°C with a 10% CO_2 overlay on a shaker platform (120 rpm). At the times of sampling the viable cell density was determined by trypan blue exclusion.

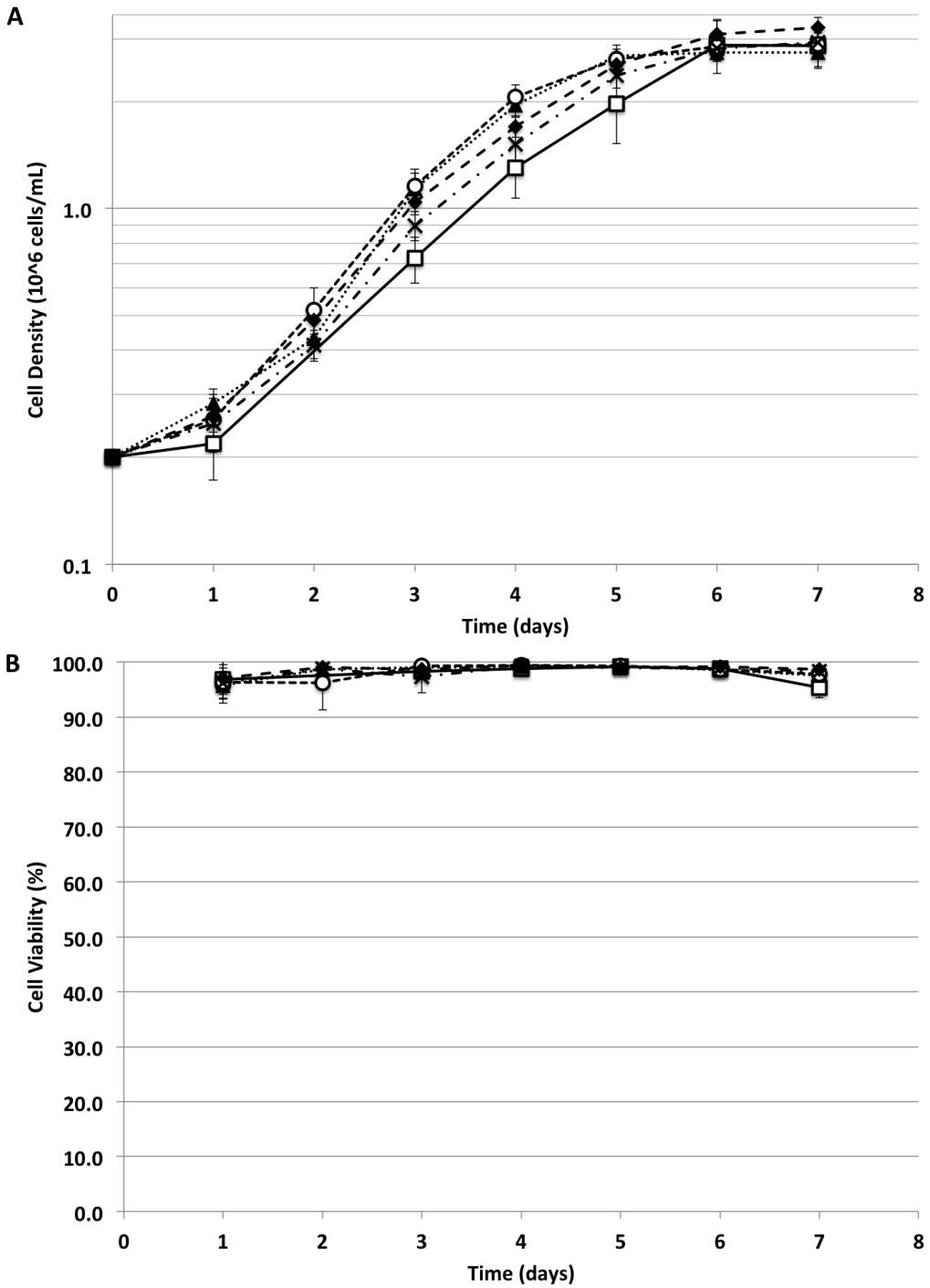

Figure 5.6: The effect on the growth and viability profiles for DP12 producing CHO cells using different precursor feeding strategies. Cells were inoculated at $2x10^5$ cells/mL into 80 mL culture medium in the appropriate precursor feeding strategy basal medium. The 'Batch' (—□—) and the 'NS' fed-batch culture (···▲···) were used as controls. The precursor feeding strategies compared to the controls were 10 mM galactose ('Galactose';-○-), 1 mM uridine + 20 mM galactose ('UG'; —◆—), and 1 mM uridine + 8 μM $MnCl_2$ + 20 mM galactose ('UMG'; —×—). (n = 7; errors bars indicate the standard deviation)

As shown in Figure 5.6 (A) the exponential phase for all cultures lasted until day 4. After the exponential phase cultures entered the stationary phase, which lasted from day 4 to day 7 for all cultures. On the last day of the experiment all cultures reached their maximum cell density, which was between 2.7 – 3.2 x 10^6 cells/mL. The specific growth rate for each culture is shown in Table 5.4. The specific growth was very similar in the 'NS' and 'Galactose' cultures and both cultures had a significantly higher growth rate ($P < 0.02$) than what was observed for all other cultures ('Batch', 'UG', 'UMG). It was also determined that the specific growth rate of the 'UG' culture was significantly higher ($P < 0.02$) than what was observed in the 'Batch' culture.

The viability profiles for all cultures are shown in Figure 5.6 (B). All cultures showed similar viabilities of over 95% from day 1 to day 7 with no apparent decrease in viability even on day 7.

Table 5.4: Comparison of the specific growth rate for DP12 producing CHO cells using different precursor feeding strategies. Cells were inoculated at $2x10^5$ cells/mL into 80 mL culture medium in the appropriate precursor feeding strategy basal medium. The 'Batch' and 'NS' fed-batch culture were used as controls and compared with the 'Galactose', 'UG', and 'UMG' precursor feeding strategies. (n=7)

	Batch	**NS**	**Galactose**	**UG**	**UMG**
$\mu^{\sim}$	0.019 ± 0.002 h^{-1}	0.024 ± 0.001 h^{-1} *	0.024 ± 0.001 h^{-1} *	0.022 ± 0.001 h^{-1} #	0.021 ± 0.001 h^{-1}

~ The specific growth rate and standard deviation were determined using linear regression analysis.

* ($P < 0.02$) compared to all other cultures in the experiment

($P < 0.02$) compared to 'Batch' culture

For the DP12 culture experiment the change from a 'Batch' to a 'NS' fed-batch system did not result in an increase of the total cell yield as expected. While the specific growth rate

was higher in the 'NS' and 'Galactose' culture the same overall total viable cell density was reached as these cultures entered into stationary phase earlier than others. In addition, the nucleotide precursors added to the different cultures did not affect the total viable cell density or viability in the DP12 cultures.

5.2.5 Effect of precursor feeding in DP12 cultures on protein productivity

While the precursor feedings are likely to have a positive impact on the overall galactosylation, it was important to determine whether they also have an impact on the productivity in each culture. The DP12 concentration in the cell culture supernatants was determined by ELISA. Figure 5.7 shows the DP12 concentration against the IVCD of the different cultures. The secretion of DP12 commenced with the start of the culture and continued throughout the exponential and stationary phase. The highest volumetric production was observed in the 'Galactose' culture with 29.7 μg/mL on day 6. All other cultures showed the highest yield on day 7 - with the second highest volumetric productivity observed in the 'NS' treatment with 27.4 μg/mL. Similar volumetric productivity values are seen in the 'UG' and 'UMG' culture with 25.6 and 26.2 μg/mL. While the 'Batch' culture has the lowest volumetric productivity with 21.9 μg/mL it also has the lowest IVCD over the time of the culture with only 8.2×10^6 cells-day/mL compared to $9.8 - 11 \times 10^6$ cells-day/mL. However, no significant difference was observed between the maximum volumetric productivity in each culture.

The specific productivity for each culture during the exponential and stationary phase as determined by linear regression analysis is shown in Table 5.5. During the exponential phase the highest specific productivity was found in the 'Batch' (7.4 ± 0.5). The second highest specific productivity was seen for the 'Galactose' culture (6.0 ± 0.7). Similar specific productivities were

determined for the 'NS' (5.2 ± 0.7) and the 'UMG' culture (4.9 ± 0.2). The lowest specific productivity was found in the 'UG' culture (3.1 ± 0.1), which is significantly lower than in the 'Batch' culture ($P < 0.02$). The specific productivity in both the 'UG' and 'UMG' culture was

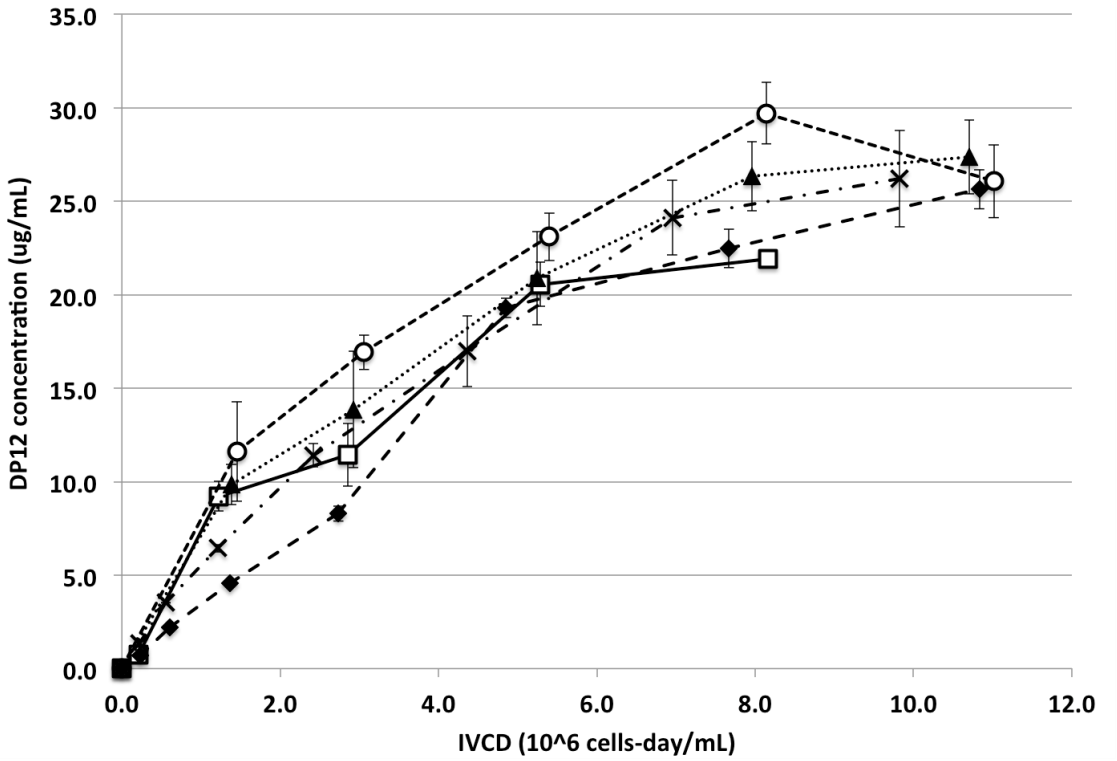

Figure 5.7: The effect on the DP12 production for CHO DP12 cells using different precursor feeding strategies. Cells were inoculated at $2x10^5$ cells/mL into 80 mL culture medium in the appropriate precursor feeding strategy basal medium. The 'Batch' (—□—) and fed-batch 'NS' culture (···▲···) were used as controls. The precursor feeding strategies compared the controls were 10 mM galactose ('Galactose';-○-), 1 mM uridine + 20 mM galactose (UG; —◆—), and 1 mM uridine + 8 μM $MnCl_2$ + 20 mM galactose (UMG; —×—) cultures. (n = 2; error bars indicate the standard deviation).

lower than what was observed in the 'Batch' culture. In the stationary phase all cultures showed a similar specific productivity.

The switch from a regular 'Batch' to a fed-batch 'NS' system increased the volumetric productivity by increasing IVCD. For the DP12 cultures the addition of nucleotide sugar precursors also did not seem to affect the volumetric productivity significantly. However, the

addition of only uridine decreased the specific productivity in the exponential phase. The addition of uridine and manganese in combination, on the other hand, resulted in a specific productivity similar to what is observed in the 'NS' culture but still lower than what was observed in the 'Batch' culture.

Table 5.5: Comparison of the specific productivity for DP12 producing CHO cells using different precursor feeding strategies during the exponential (exp) and the stationary (stat) phase. Cells were inoculated at $2x10^5$ cells/mL into 80 mL culture medium in the appropriate precursor feeding strategy basal medium. The 'Batch' and fed-batch 'NS' culture were used as controls and compared to the 'Galactose', 'UG', and 'UMG' precursor feeding (n=2).

	Batch	**NS**	**Galactose**	**UG**	**UMG**
q_{Mab} **(exp)~**	7.4 ± 0.5 pg/cell-day	5.2 ± 0.7 pg/cell-day	6.0 ± 0.7 pg/cell-day	3.1 ± 0.1 pg/cell-day*	4.9 ± 0.2 pg/cell-day
q_{Mab} **(stat)~**	2.0 ± 0.5 pg/cell-day	1.7 ± 0.4 pg/cell-day	1.2 ± 0.7 pg/cell-day	2.0 ± 0.6 pg/cell-day	2.0 ± 0.4 pg/cell-day

~ The specific productivity and standard deviation were determined using linear regression analysis. exp – exponential phase, stat – stationary phase.
* ($P < 0.02$) compared to the 'Batch' culture

5.2.6 Effect of precursor feeding in DP12 cultures on glucose, lactate, glutamine, glutamate concentration

The concentration of glucose, lactate, glutamine and glutamate in cell culture supernatants was determined using YSI analysis. The consumption of glucose for DP12 producing CHO cell cultures against their IVCD is shown in Figure 5.8 (A). During the exponential phase all cultures show a high consumption of glucose, which then decreased in the stationary phase. The remaining glucose concentration in almost all cultures leveled out around

7 mM. The exception was the 'NS' culture in which the residual glucose concentration in the medium decreased below 5 mM on day 7. When comparing the specific glucose consumption for each culture in the exponential phase it was observed that the 'Batch' culture had a higher specific glucose consumption compared to the rest of the cultures. In the stationary phase the rates of consumption were fairly similar among the different treated cultures (Figure 5.9 (A)).

Figure 5.8 (B) shows the overall lactate production against the IVCD throughout the culture time in each experiment. In the exponential phase a steep increase in lactate was observed, while the lactate level in the stationary phase remained constant. The highest lactate accumulation was observed in the 'NS' and 'Galactose' culture at 25 mM while the 'UG' and 'UMG' culture reached max values of 22.2 and 21.9 mM, respectively. The specific lactate production for each culture shown in Figure 5.9 (B) was similar in all cultures except for the 'Batch' culture, which showed a higher specific glucose consumption and lactate production.

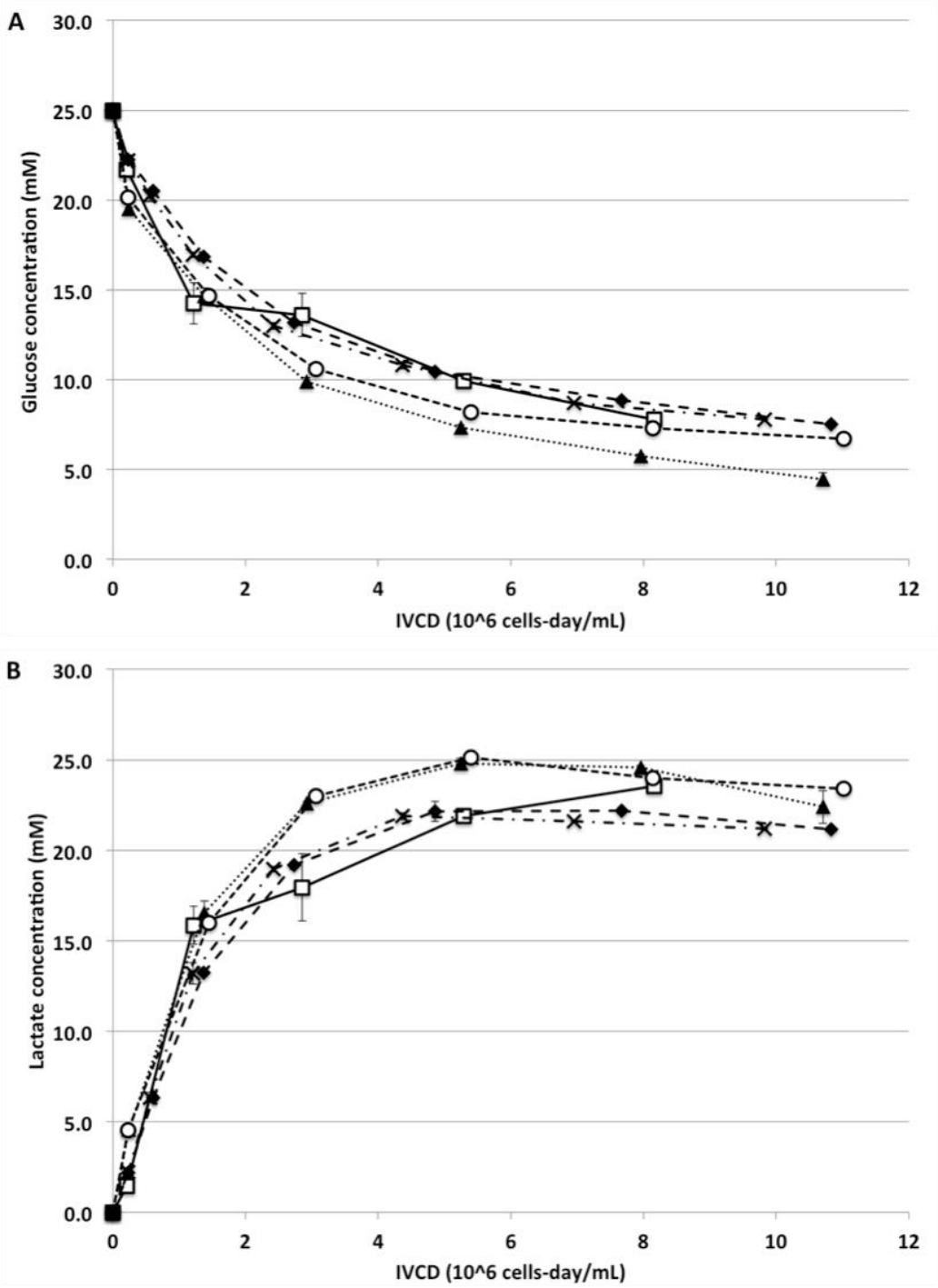

Figure 5.8: The effect on the glucose consumption and lactate production for DP12 producing CHO cells using different precursor feeding strategies. Cells were inoculated at $2x10^5$ cells/mL into 80 mL culture medium in the appropriate precursor feeding strategy basal medium. The 'Batch' (−□−) and fed-batch 'NS' culture (···▲···) were used as controls. The precursor feeding strategies compared to the controls were 10 mM galactose ('Galactose';-○-), 1 mM uridine + 20 mM galactose ('UG'; −◆−), and 1 mM uridine + 8 μM $MnCl_2$ + 20 mM galactose ('UMG'; −×-) cultures. (n = 2; errors bars indicate the standard deviation)

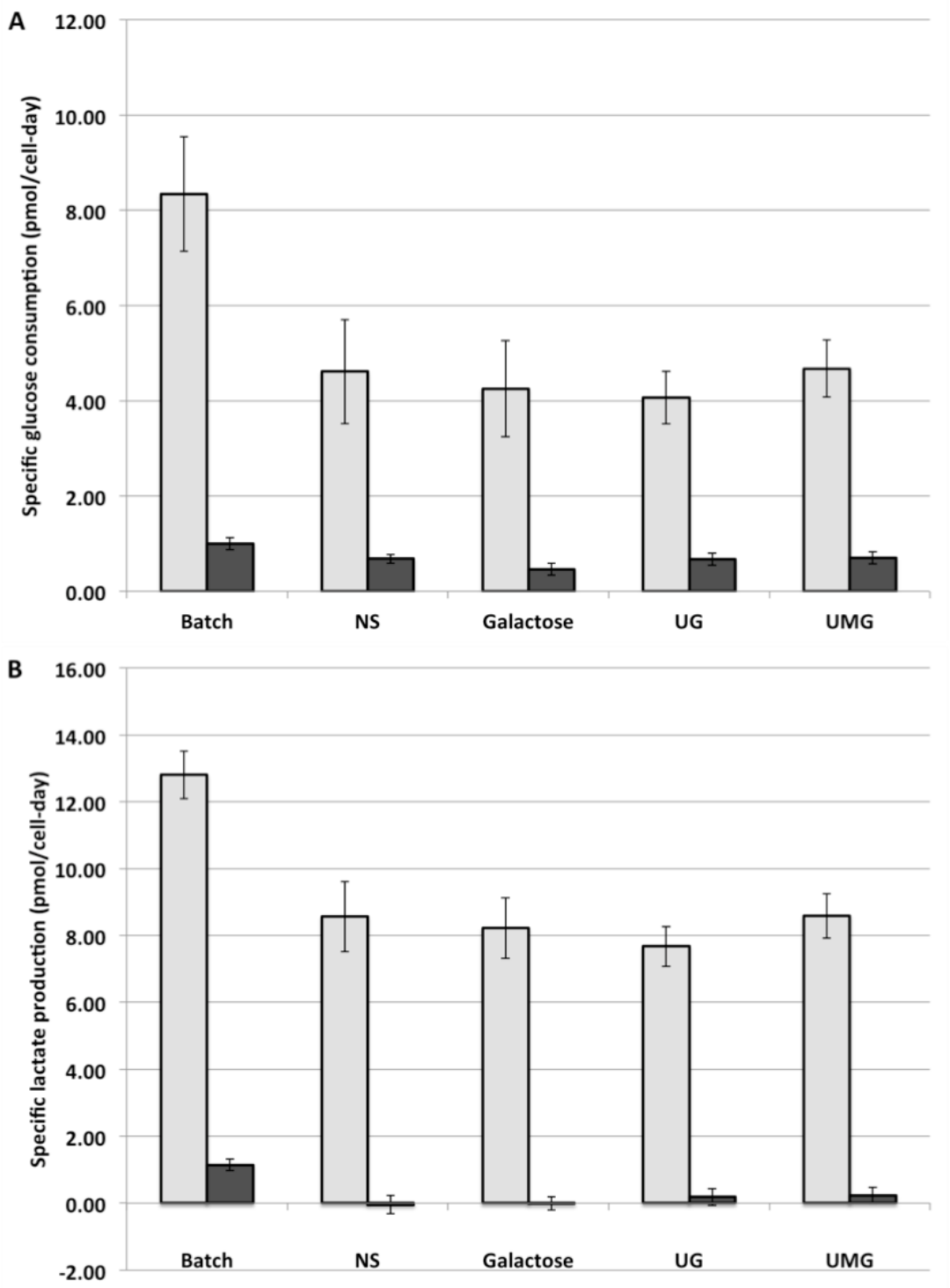

Figure 5.9: Comparison of the specific glucose consumption and lactate production for DP12 producing CHO cells using different precursor feeding strategies during the exponential ( ) and stationary phase ( ). Cells were inoculated at $2x10^5$ cells/mL into 80 mL culture medium in the appropriate precursor feeding strategy basal medium. The 'Batch' and fed-batch 'NS' culture were used as controls and compared with the 'Galactose', 'UG', and 'UMG' precursor feeding. (n = 2; error bars indicate the standard deviation)

Table 5.6: Comparison of the yield of lactate molecules produced from each glucose molecule consumed for the different culture conditions in CHO DP12 cultures during the exponential (exp) and the stationary (stat) phase. (n = 2)

	Batch	**NS**	**Galactose**	**UG**	**UMG**
$Y_{Lac/Glc}$ (exp)	1.53	1.86	1.93	1.89	1.84
$Y_{Lac/Glc}$ (stat)	1.14	NA	NA	0.28	0.33

When comparing the overall yield of lactose from the glucose utilized shown in Table 5.6 it can be seen that the highest yield was found for the 'Galactose', 'UG', 'NS' and 'UMG' culture with values of 1.93, 1.89, 1.86 and 1.84, respectively. The 'Batch' culture showed a lower yield at 1.53. This means that in the 'Batch' culture theoretically 76.5% of the glucose taken up by the cell was converted to lactate. In the 'UMG', 'NS', 'UG' and 'Galactose' cultures these number went up to 92%, 93%, 94.5%, and 96.5%, respectively. In the stationary phase these number changed considerably showing that the majority of the glucose was not converted to lactate anymore.

Figure 5.10 shows the glutamine and glutamate concentration against the IVCD in the respective cultures at each time point. Figure 5.10 (A) showed a significantly ($P < 0.02$) higher accumulation of glutamine in the 'Batch' culture (above 4 mM) over the entire culture period. The glutamine concentration in the 'NS' and 'Galactose' culture increased for the first 3 days (up to 3 mM) before declining again down to almost 2 mM. However, in the 'UG' and 'UMG' culture the glutamine level was consistently low and only increased marginally over the course of the culture (max 2.5 mM). The glutamate concentration in all cultures was increasing over time with the highest concentration reached in the 'Batch' culture at 1.8 mM (Figure 5.10 (B)).

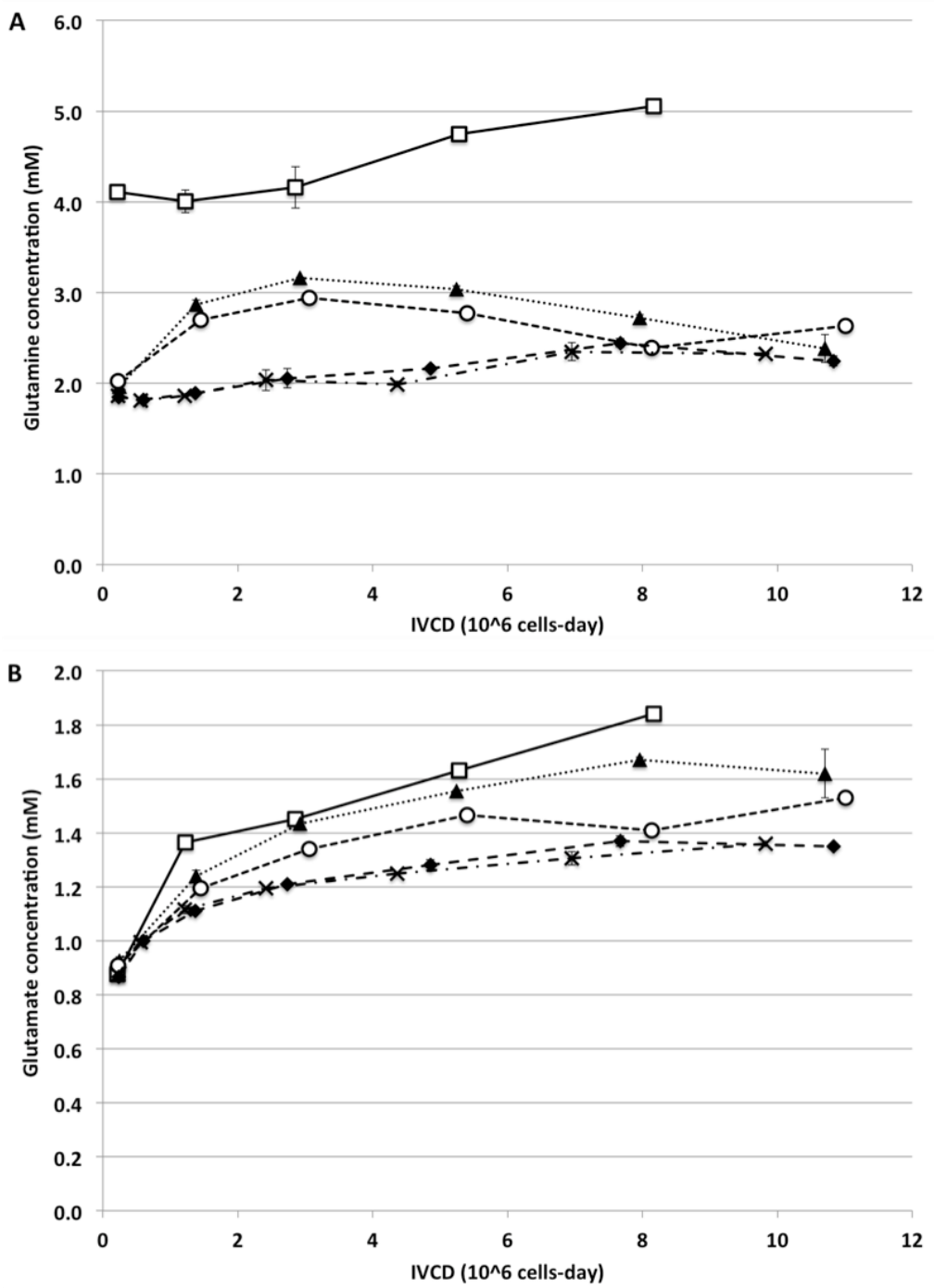

Figure 5.10: Glutamine consumption and glutamate production profiles for DP12 producing CHO cells using different precursor feeding strategies. Cells were inoculated at $2x10^5$ cells/mL into 80 mL culture medium in the appropriate precursor feeding strategy basal medium. The 'Batch' (—□—) and fed-batch 'NS' culture (···▲···) were used as controls. The precursor feeding strategies compared to the controls were 10 mM galactose ('Galactose';-○-), 1 mM uridine + 20 mM galactose ('UG'; —◆—), and 1 mM uridine + 8 μM $MnCl_2$ + 20 mM galactose ('UMG'; —×—) cultures. (n = 2; error bars indicate the standard deviation)

The lowest concentrations were reached in the 'UG' and 'UMG' culture with 1.35 and 1.36 mM, respectively.

In summary, it was seen that all DP12 fed-batch cultures exhibited similar glucose consumption and lactate production rates while the 'Batch' culture exhibited a higher glucose consumption and lactate production rate. This resulted in similar $Y_{lac/glc}$ values for all fed-batch cultures (1.84 – 1.93). On the other hand, the 'Batch' culture showed a lower $Y_{lac/glc}$ value of 1.53 meaning that less glucose was converted to lactate. However, a larger accumulation of glutamine and glutamate was seen in the 'Batch' culture. Over the course of the culture the glutamine accumulation in the fed-batch cultures was at only 50% of the value seen in the 'Batch' culture.

5.2.7 Comparison of effect on EG2 and DP12

When comparing the effect of precursor feeding on the specific growth rate of CHO-EG2 and CHO-DP12 cells it was observed that the addition of uridine had a negative impact on the growth rate of CHO-EG2 cells but not CHO-DP12 cells (Figure 5.11). It was also noted that the general growth rate of CHO-DP12 cells was lower than the growth rate observed in CHO-EG2 cells. This lower initial growth rate was slightly increased with the introduction of the fed-batch culture mode in the 'NS' and 'Galactose' culture. The increase in the 'UG' and 'UMG' fed-batch culture was lower and possibly indicated a small inhibition effect by uridine observed mainly in the CHO-EG2 cultures.

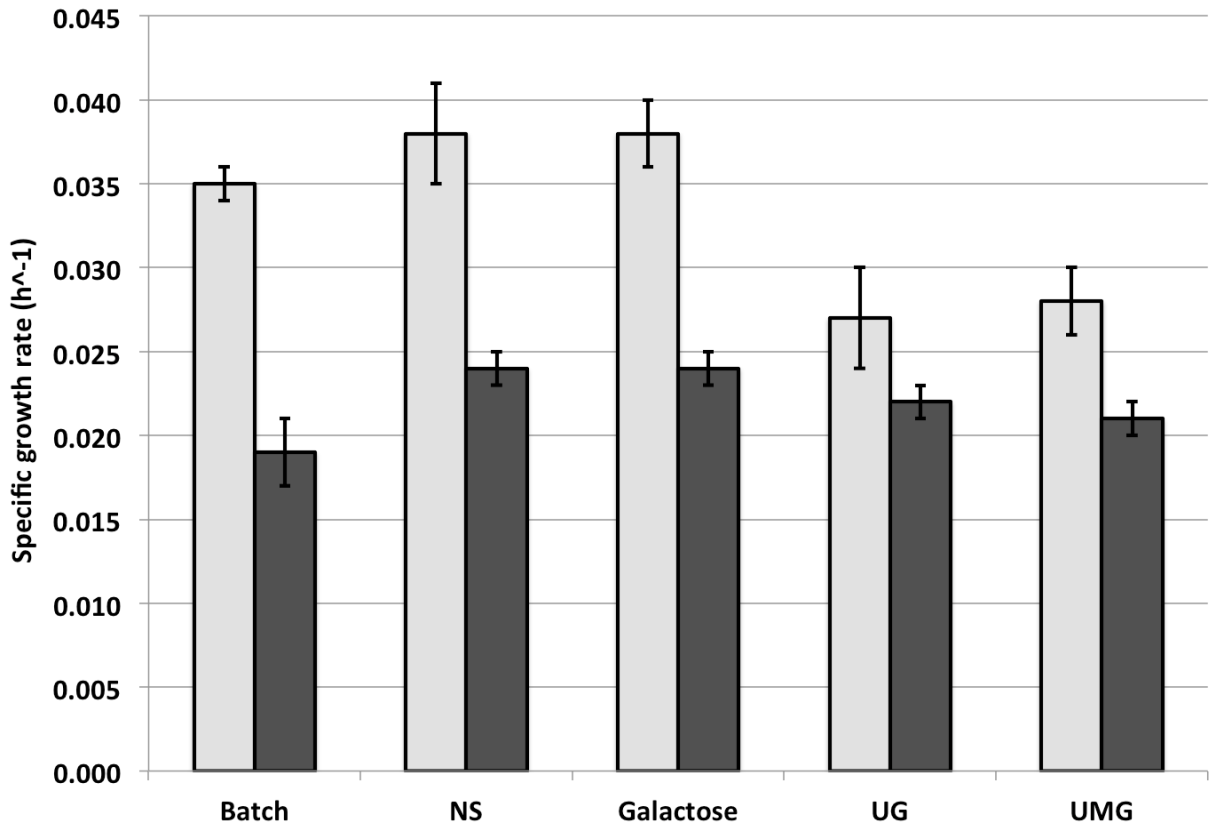

Figure 5.11: Comparison of the specific growth rate for EG2 ( ) and DP12 ( ) producing CHO cells using different precursor feeding strategies during the exponential phase. Cells were inoculated at $2x10^5$ cells/mL into 80 mL culture medium in the appropriate precursor feeding strategy basal medium. The 'Batch' and fed-batch 'NS' culture were used as controls and compared with the 'Galactose', 'UG', and 'UMG' precursor feeding (n = 7; error bars indicate the standard deviation).

Figure 5.12 shows the comparison of the specific productivity during the exponential and stationary phase in the CHO-EG2 and CHO-DP12 cell cultures. The specific productivity in the CHO-DP12 cell cultures was always higher compared to the CHO-EG2 cell cultures except for the respective 'UG' treatment during the exponential phase. It also determined that the addition of galactose in combination with uridine had a negative effect on the specific productivity in both CHO-EG2 and DP12 cultures during the exponential growth phase. However, by adding

manganese chloride the specific productivity in CHO-DP12 cultures seemed rescued whereas in CHO-EG2 cultures the specific productivity stayed low.

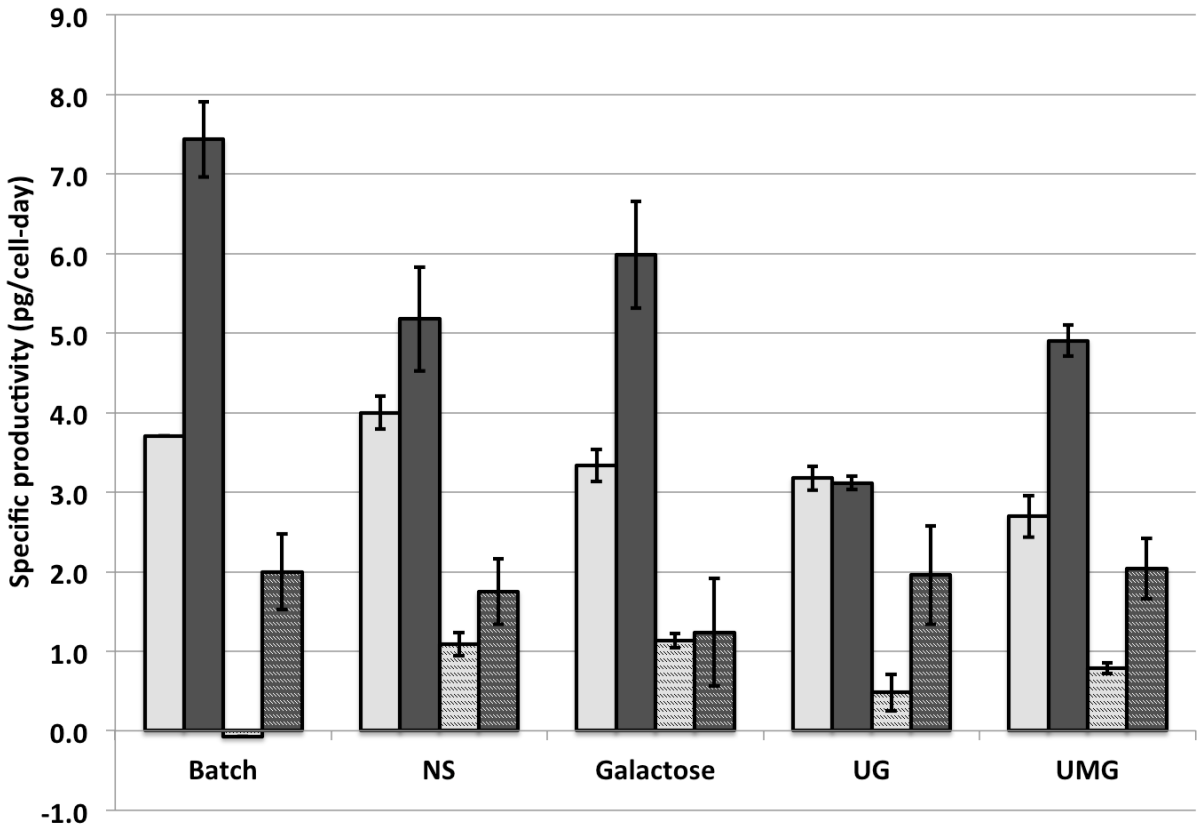

Figure 5.12: Comparison of the specific productivity in CHO -EG2 (exponential: , stationary:) and DP12 (exponential: , stationary:) cultures with different precursor treatments. (n = 2; error bars indicate the standard deviation).

The specific glucose consumption rate was highest in the CHO-DP12 'Batch' culture during the exponential phase (Figure 5.13 (A)). The figure also shows that in all other cultures the specific glucose consumption rates were similar. In the stationary phase the specific glucose consumption for all cultures was significantly lower ($P < 0.02$) compared to the exponential phase. While the specific glucose consumption between the same CHO-EG2 and DP12 cultures was similar the lowest rate was seen in the 'Galactose' culture. Similar to the glucose

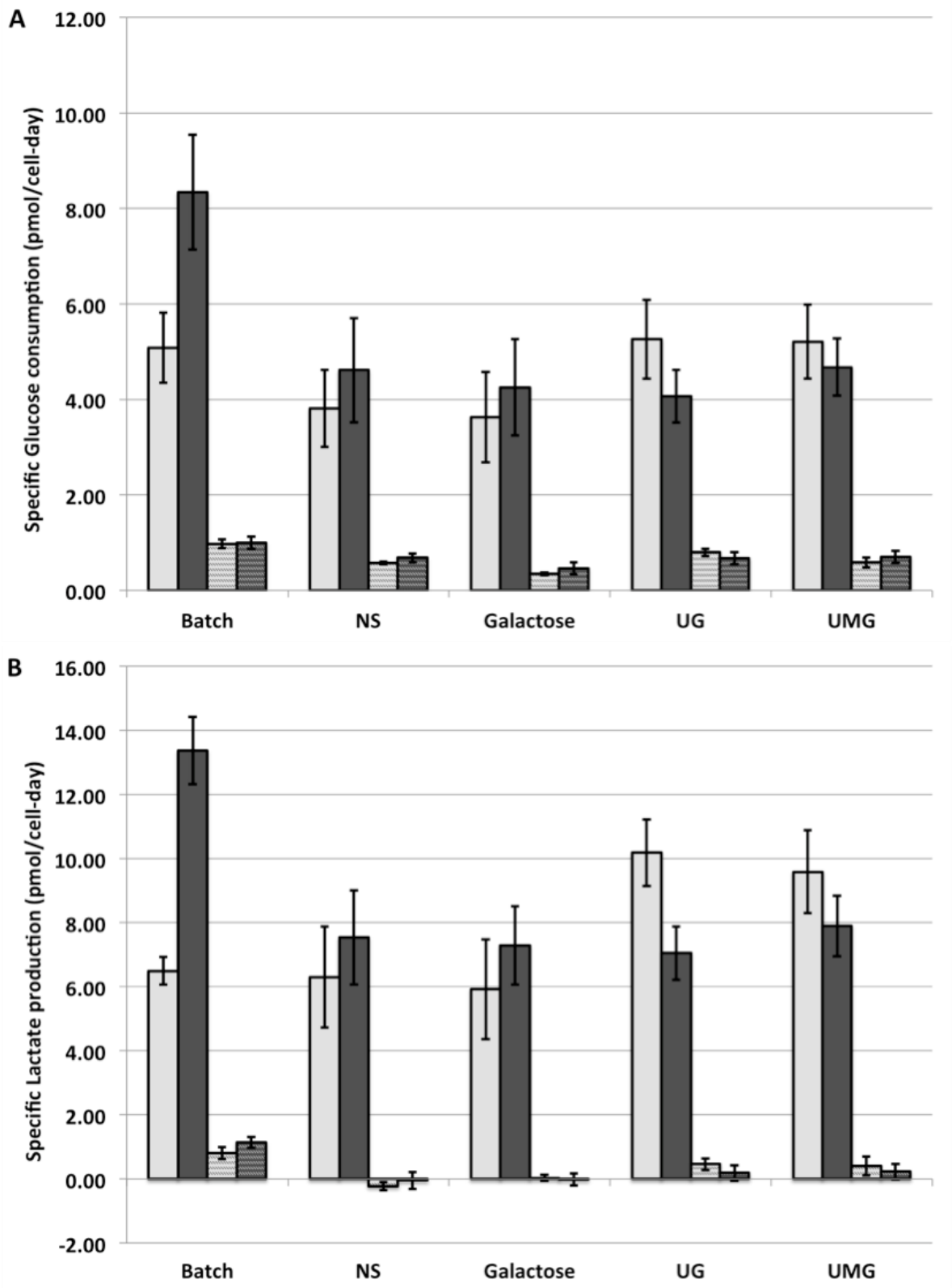

Figure 5.13: Comparison of the specific glucose consumption and lactate production rate in CHO -EG2 (exponential: , stationary:) and DP12 (exponential: , stationary:) cultures with different precursor treatments. (n = 2; error bars indicate the standard deviation).

consumption the highest specific lactate production was seen in the 'Batch' DP12 culture. However, the lactate production rate in the 'UG' and 'UMG' culture was higher for the CHO-EG2 cultures in the exponential phase compared to the respective DP12 'UG' and 'UMG' cultures.

The comparison of the final yield (lac/glc) in each culture and culture stage can be seen in Figure 5.14. The lowest yield for both the CHO-EG2 and DP12 culture was seen in 'Batch' culture with the lowest value in the CHO-EG2 'Batch' culture. However, the stationary phase in the 'Batch' culture exhibited higher yields compared to any other culture in the stationary phase. For the other cultures the values were consistently high in both the CHO-EG2 and CHO-DP12 cultures. While the 'NS' and 'Galactose' cultures showed higher yields in the exponential phase they had the lowest values in the stationary phase. In the exponential and stationary phase of the 'UG' and 'UMG' culture the CHO-EG2 yield values were higher than in the respective CHO-DP12 cultures indicating a less efficient metabolism with the addition of uridine.

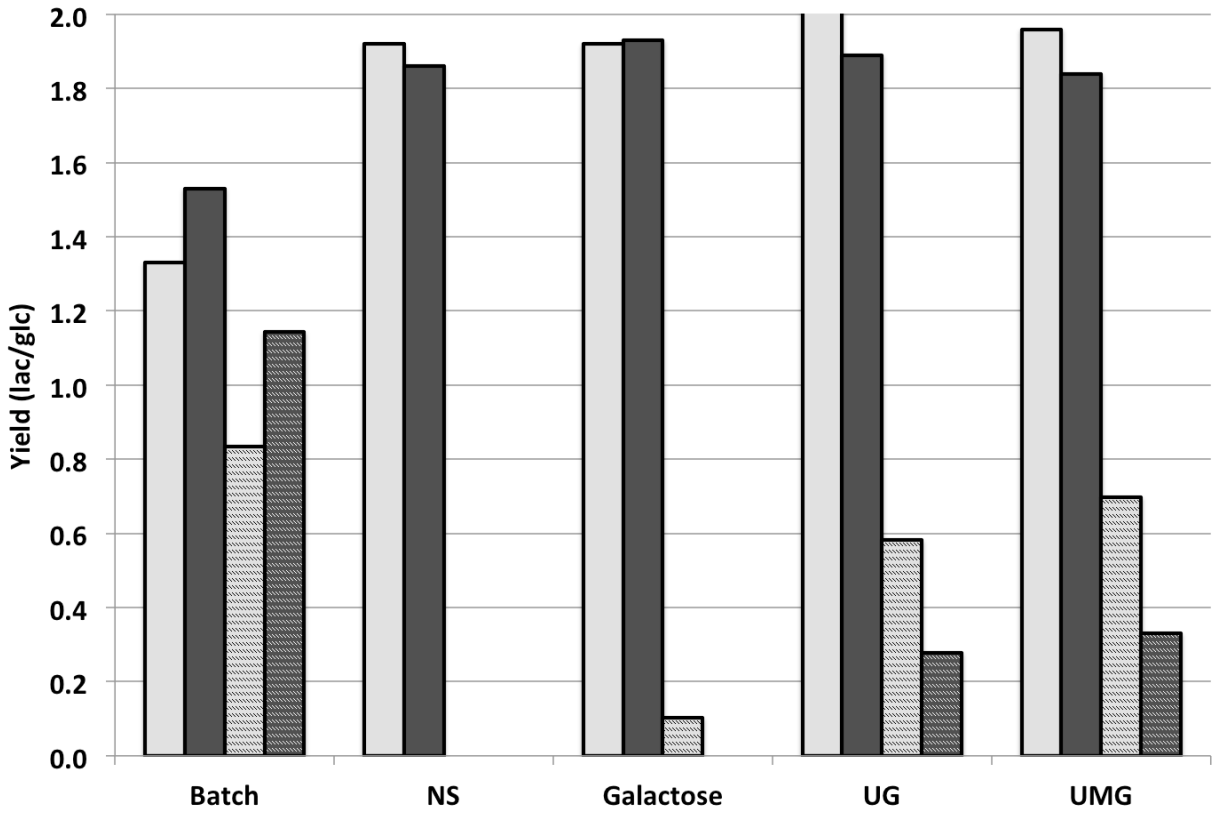

Figure 5.14: Comparison of the yield of lactate from glucose in CHO-EG2 (exponential: , stationary:) and DP12 (exponential: , stationary:) cultures with different precursor treatments (n = 2).

5.3 Discussion

In biopharmaceutical production the effect any media additives have on the cell growth, viability, productivity, metabolism and product quality are important. An improved understanding of these effects will allow for better media development resulting in optimized production of glycoproteins in mammalian cells. Here I described the effects of precursor feedings using 10 mM galactose, 20 mM galactose + 1 mM uridine, and 20 mM galactose + 1 mM uridine + 8 μM $MnCl_2$ on the growth, viability, metabolism and protein production compared to a 'Batch' and 'NS' fed-batch control culture.

In previous research by other groups the sole addition of galactose at concentrations of up to 20 mM in the basal medium (Wong et al., 2010; Clark et al., 2005) or up to 111 mM in the feed medium (Schilling et al., 2008) had shown no impact on the cell culture performance. The use of 60 mM galactose in combination with 12 mM uridine and 0.024 mM $MnCl_2$ (12x UMG) as a daily feed starting on day 3 had also shown no effects on the cell culture performance in CHO fed-batch cultures (Gramer et al., 2011). However, Gramer et al. (2011) did show suppression in the glucose and lactate metabolism at 16x and 20x UMG and an additional slight drop in the product titer at 20x UMG. They thought that this impact on the process was caused by higher Mn^{++} concentrations in the medium, which had shown an impact in studies by Crowell et al. (2007).

The effects of the nucleotide sugar precursors on cell growth in the CHO-DP12 cultures reported here are similar to results shown in another cell line treated with UMG and UG (Gramer et al., 2011; Wong et al., 2010). While the CHO-DP12 growth and viability was not impacted by the nucleotide sugar precursor addition an effect was observed in the CHO-EG2 cell cultures. As seen in previous research by Wong et al. (2010), Clark et al. (2005) and Schilling et al. (2008) no impact was observed in the 'Galactose' cultures. However, the addition of galactose in combination with uridine as well as uridine + $MnCl_2$ resulted in a decreased growth rate while extending the viability compared to the 'Batch', 'NS' and 'Galactose' fed-batch cultures. Considering that in this experiment the final concentrations in the culture medium after adding the feed are lower than the ones reported by Gramer et al. (2011) the effect observed might be related to cell specific differences. The cell line used by Gramer et al. (2011) was a CHO-K1SV (glutamine synthase (GS) expression system) and the cell line used by Wong et al. (2010) was a CHO Dukx (dihydrofolate reductase (DHFR) expression system). In both cell lines the DHFR

gene is functional during the bioprocess. The CHO-DP12 cell line is a CHO-K1 cell line with a restored DHFR while the CHO-EG2 is a CHO-DG44 cell line in which the DHFR gene was not restored during the cell line engineering. Due to this deficiency the CHO-EG2 cell line needs the addition of thymine, hypoxanthine (HT supplement) and glycine to the basal medium. The lack of this gene has reportedly shown poor growth and lower peak cell densities in fed-batch cultures of some DHFR-/- CHO cell lines even when using the HT supplement (Florin et al., 2011). However, in this experiment this poor growth and low peak cell density was only observed in the 'UG' and 'UMG' fed-batch cultures but not the 'NS' and 'Galactose' fed-batch cultures. DHFR is an important part in the production of deoxy thymidine monophosphate (dTMP), which is needed for DNA synthesis (thymine production) (Schnell et al., 2004). In addition the lack of DHFR blocks all other tetrahydrofolate (THF) dependent pathways. In the case of the CHO-EG2 cell line the added HT supplement and glycine contained in the basal medium and feed seems to allow for regular growth as observed in the 'Batch', 'NS' and 'Galactose' fed-batch cultures. However, the addition of uridine in the fed-batch regime then has an inhibitory effect on cell growth. A possible explanation for this is that the addition of uridine leads to an excessive intracellular increase in the intermediates of reactions related to the DHFR pathway (i.e. deoxy uridine monophosphate (dUMP)). Excess in dUMP can result in an increased level of dUTP after the sequential phosphorylation of dUMP (Caradonna et al., 1980). This in turn can lead to an increase in uracil incorporation into the DNA needing to be repaired (Grafstrom et al., 1978). While pyrophosphatase dUTP nucleotidohydrolase (dUTPase) degrades dUTP to dUMP limiting the intracellular accumulation of this nucleotide (Webley et al., 2001), the addition of uridine to the culture medium might increase the levels of dUTP to cell growth inhibitory concentrations.

The specific productivity in CHO-EG2 was reduced with the addition of any nucleotide sugar precursor or combination thereof whereas the specific productivity in CHO-DP12 cells was reduced in all fed-batch cultures compared to the 'Batch' culture. However, a significant loss in specific productivity was observed in the 'UG' culture. This loss seems to be rescued in the 'UMG' culture. Although Gramer et al. (2011) observed a small loss in production it was reported at higher UMG concentrations.

Glucose and glutamine are the main carbon sources used by the mammalian cells in culture as a carbon and energy source (Butler and Jenkins, 1989). In the exponential phase the primarily aerobic glycolysis leads to a high conversion of glucose to lactate (Cruz et al., 2000, Lao and Toth, 1997). This flux will decrease in the stationary phase (Cruz et al., 2000, Lao and Toth, 1997). The glutamine in the culture will be shuffled through the tricarboxylic acid (TCA) cycle for energy production while also contributing to the synthesis of nucleotides (Engstrom and Zetterberg, 1984). During those pathways ammonium ions are released as by-products. The overall accumulation of lactate and ammonium as by-products of these pathways (Quek et al., 2010) can be detrimental to the cell culture (Ahn et al., 2008; Dorai, 2009, Hassell et al., 1991, Li et al., 2012).

In the CHO-DP12 culture a difference was only seen between the 'Batch' and all of the fed-batch cultures. In this case the CHO-DP12 cells showed higher specific glucose consumption and lactate production. The specific rates for the fed-batch cultures showed no difference. However, the addition of nucleotide sugar precursors 'UG' and 'UMG' showed an effect on the cells energy metabolism in CHO-EG2 cultures. While the specific glucose consumption was similar in all cultures including the precursor fed-batch cultures, the specific lactate production in the 'UG' and 'UMG' culture was increased. This increase in lactate

production resulted in a higher yield of lactate per molecule of glucose consumed by the cells in culture. Gramer et al. (2011) reported a mildly suppressed glucose and lactate metabolism in their cell line at 16x and 20x UMG. As this effect is not seen in the CHO-DP12 culture and present only in the cultures affected by the uridine addition I am suspecting that the lack of the DHFR gene plays a role in the change of metabolism.

Glutamine is not only a carbon source for mammalian cells but also contributes its energy via the TCA cycle (Lanks and Li, 1988) and plays an essential role in the synthesis of nucleotides (Engstrom and Zetterberg, 1984). However, it is also the main contributor to the increasing ammonia concentration throughout the cell culture, which can inhibit growth (Doyle and Butler, 1990). To avoid an excess of ammonia accumulation the glutamine concentration in the culture should be low during the experiment. Hence, the media contain GlutaMaxI, which is a dipeptide with L-alanyl-L-glutamine that the cells can split to slowly release glutamine over time. To avoid a longer lag phase in the beginning of the cell culture the media is also supplemented with 1 mM glutamine. The glutamine concentration was fairly constant in the DP12 culture indicating a constant uptake and use by the cells. On the other hand, the increase in the glutamine towards the end of the EG2 culture indicated an initial use of glutamine after which a possible change in the culture metabolism reduced the glutamine uptake. A difference was also observed in the glutamate concentration, which was fairly stable over time in the EG2 culture while it consistently increased over time in the DP12 culture as part of the TCA cycle process.

5.4 Conclusion

In this study the effects of the nucleotide sugar precursors galactose, uridine, and $MnCl_2$ on the glycosylation were not of interest. Rather their effect on the growth and productivity in CHO-EG2 and DP12 fed-batch cultures was assessed. It was determined that the effect is cell line dependent showing minimal impacts on the CHO-DP12 culture but significant effects in CHO-EG2 culture growth, viability and lactate production. In the CHO-EG2 culture the addition of uridine causes inhibitory effects due to the lack of the enzyme DHFR. The lack of this enzyme is proposed to cause the accumulation of an intermediate molecule, dUMP, whose concentration would increase even more in the presence of uridine in the medium. Because dUMP cannot be degraded as fast as it is produced some of it is phosphorylated to dUTP, which results in an increased uracil incorporation into the DNA. Since uracil is wrongly incorporated the DNA needs to be repaired resulting in cell growth inhibition. In addition, the supplementation with uridine increased the specific lactate production in the CHO-EG2 cell line.

Overall, the results showed that the addition of precursors can also have an effect on the general bioprocess (i.e growth) other than on the final glycosylation profile. In the case of the CHO-EG2 cell line the reduced growth but extended viability with uridine exposure also needs to be taken into consideration when making the final choices for optimal basal and feed medium development.

Chapter 6

The effects of nucleotide sugar precursor feedings on the nucleotide / nucleotide sugar pool in CHO EG2, and CHO DP12

6.1 Introduction

Protein glycosylation is dependent on several different factors including the availability of nucleotide sugars for the actual glycosylation process (Freeze and Elbein, 2009). These sugars are formed from precursors such as galactose, mannose, and fucose. In addition nucleosides triphosphates are needed to activate these sugars so that they can be transported into the Golgi. Once in the Golgi the activated sugars can be attached to the glycan core structure by glycosyltransferases. Some of these enzymes need co-factors to function efficiently. Considering that the glycosyltranferases are membrane-bound a high abundance of nucleotide sugars will positively affect the chance of their addition to the glycan. Hence the addition of nucleotide and nucleotide sugar precursors – to increase the intracellular pool – and glycosyltransferase co-factors is a great option to influence the glycosylation profile outcome.

For the improvement of the galactosylation in an antibody the addition of galactose, uridine, and manganese are good candidates. Both galactose and uridine added in various combinations to cell culture medium act as direct sources for the production of UDP-Gal and UDP-GalNAc. The addition of manganese is important, as it is a co-factor for the galactosyltransferase (Witsell et al., 1990). Previous studies have shown that addition of galactose, uridine, and manganese have potential to increase the intracellular UDP-Gal pool and the galactosylation in some cell lines and glycoproteins (Gramer et al., 2011; Grainger and James, 2013).

In this study, a closer look is taken at the overall intracellular nucleotide sugar pool to determine the correlations between the addition of galactose by itself or in combination with uridine or uridine and manganese. This was done to see especially the impact of the precursor feedings on the UDP-Gal content necessary for galactosylation but also to monitor the overall nucleotide sugar pool regarding the energetic and metabolic state of the cells.

6.2 Results

6.2.1 The effects of precursor feedings in EG2 cultures on the nucleotide / nucleotide sugar pool

To study the effects of nucleotide sugar precursor feedings the intracellular nucleotide / nucleotide sugar pool was determined from samples taken throughout the cell culture. At each sampling point $1x10^7$ cells were collected from the culture and quenched to stop the metabolism in the cell. After the quenching procedure the cell samples were stored at -70°C for a maximum of 1 week before extraction. Both quenching and extraction procedures were performed as outlined in the methods section (see Section 2.7.1 and 2.7.2). The intracellular pool was then compared between the 'Batch', 'NS' and the cultures with precursor feedings (n = 2).

Figure 6.1 shows the intracellular concentrations of UDP-GalNAc, UDP-GlcNAc + CTP, UDP-Gal, and UDP-Glc for each culture during the bioprocess. The UDP-GalNAc and UDP-GlcNAc + CTP increased in all cultures over time (Figuure 6.1 A/B). In the 'Batch' and 'NS' culture UDP-Gal was barely detected throughout the culture (Figure 6.1 C). Over the same time an increased UDP-Gal was detected in the 'Galactose', 'UG', and 'UMG' cultures. While the 'Galactose' culture exhibited a fluctuating UDP-Gal concentration, both the 'UG' and 'UMG' displayed a steady increase in the intracellular UDP-Gal concentration from day 3 at ~0.9 mM to day 5 at ~1.4 mM. These concentrations were significantly higher ($P < 0.02$) than what was

observed in the ‘Batch’ and ‘NS’ culture. The ‘Galactose’ culture showed significantly higher UDP-Gal concentrations ($P < 0.02$) compared to the ‘Batch’ and ‘NS’ culture on day 2, 4, and 7. In Figure 6.1 (C) the UDP-Glc concentration for each culture is shown. The highest intracellular concentrations were observed for the ‘UG’ and ‘UMG’ culture on day 5 at 1.1 and 1.0 mM, respectively.

The adenylate energy charge (AEC) determined at each sampling point is shown in Figure 6.2. In the ‘Batch’, ‘UG’, and ‘UMG’ cultures consistently high values between 0.7 – 0.8 were observed until day 6. On day 7 the AEC value for the ‘Batch’ culture decreased to 0.48. On the other hand, for the ‘NS’ and ‘Galactose culture high fluctuations between AEC values of 0.3 – 0.75 were observed.

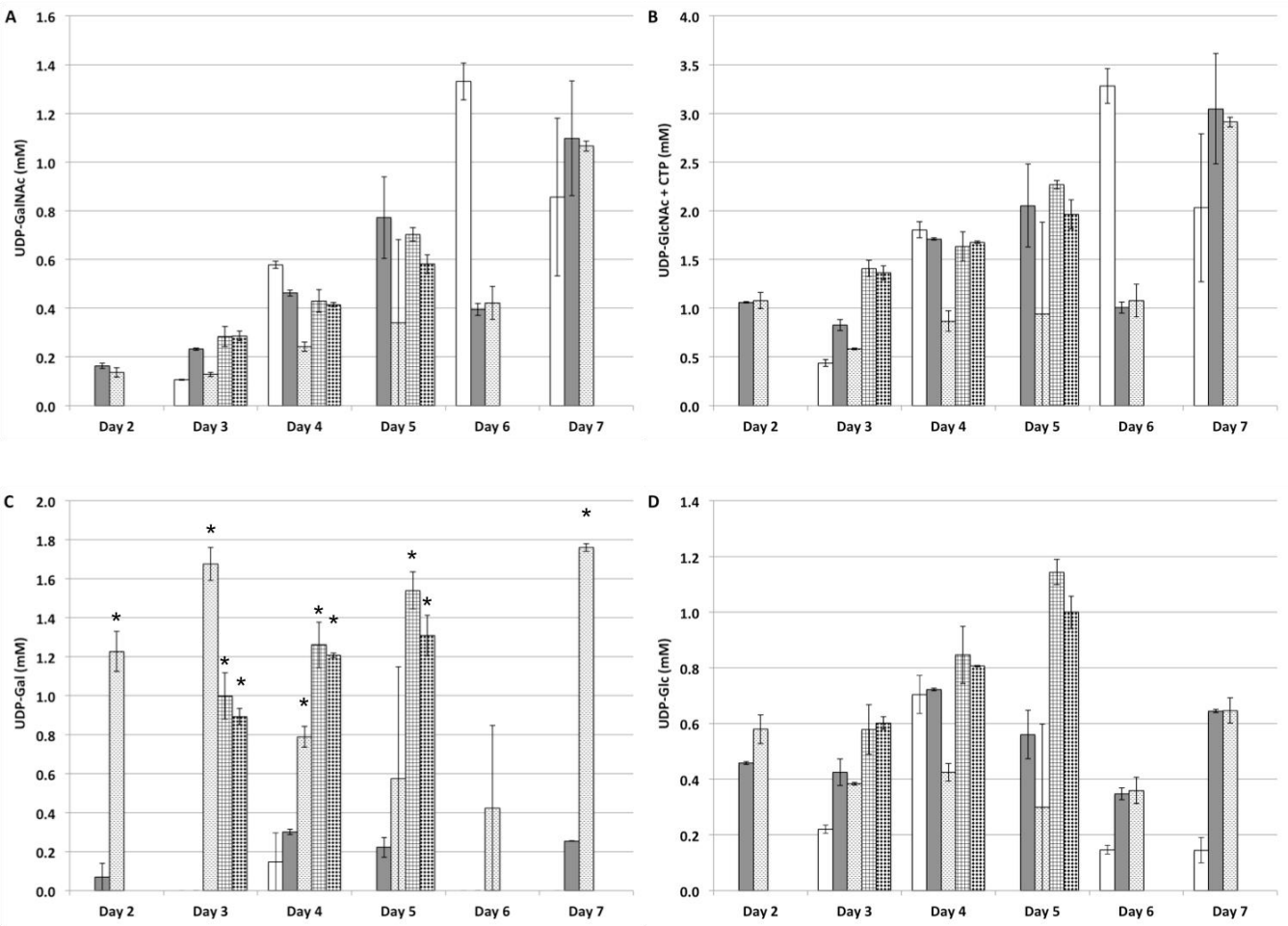

Figure 6.1: The intracellular concentrations of A) UDP-GalNAc, B) UDP-GlcNAc + CTP, C) UDP-Gal, and D) UDP-Glc during a 'Batch' (▭), 'NS' (▬), 'Galactose' (▤), 'UG' (▦), and 'UMG' (▩) in cells of fed-batch EG2 cultures. (n = 2; error bars indicate the standard deviation)

* ($P < 0.02$) compared to 'Batch' and 'NS' on that day

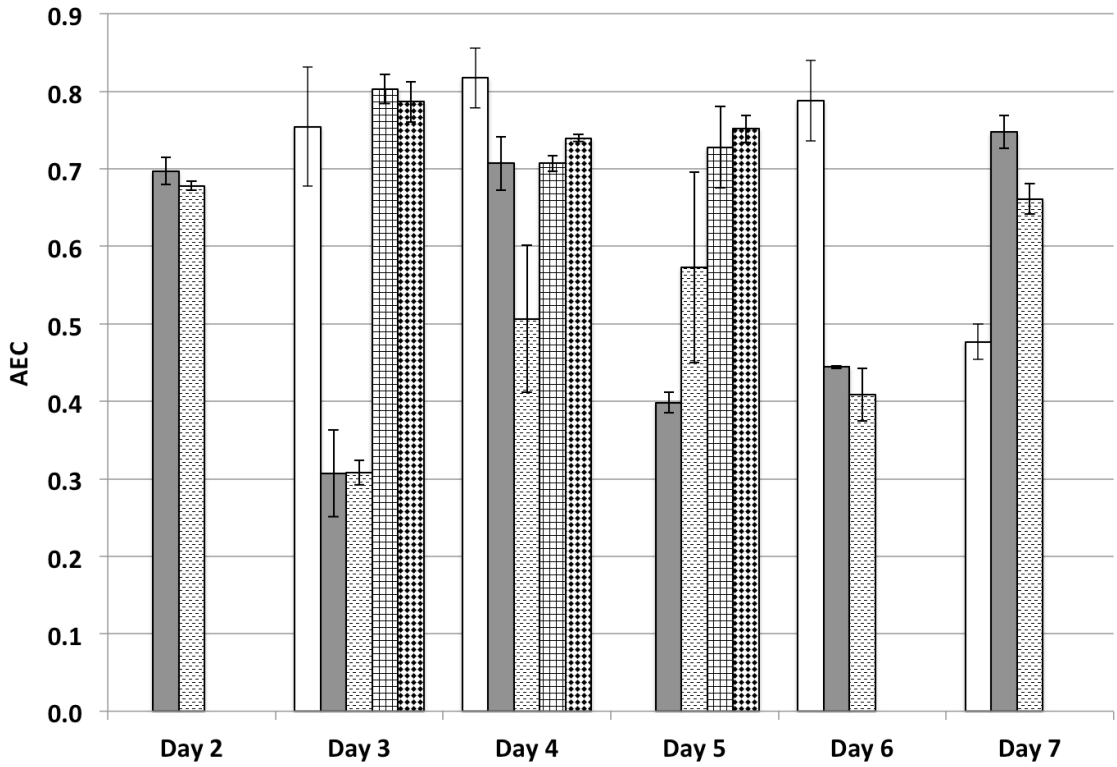

Figure 6.2: The adenylate energy charge (AEC) value determined at each sampling point during a 'Batch' (▭), 'NS' (▭), 'Galactose' (▭), 'UG' (▭), and 'UMG' (▭) fed-batch EG2 cultures. (n = 2; error bars indicate the standard deviation)

The overall uridine fraction concentration during the precursor feeding experiments is shown in Figure 6.3 (A). For the 'Batch' culture an increase in the intracellular uridine fraction from 1.16 to 5.04 mM was observed until day 6 after which the concentration decreased to 3.37 mM. A level from 2.31 to 4.51 mM was determined in the 'NS' culture until day 6 after which the concentration of the intracellular uridine fraction increased to 5.92 mM. A similar observation was made for the 'Galactose' culture in which the intracellular uridine fraction decreased from 4.29 to 2.92 mM on day 6. On day 7 an increase to 7.22 mM in the concentration per cell was measured. Meanwhile a steady increase in the uridine fraction was determined for the 'UG' and 'UMG' cultures from 4.82 to 7.9 mM in the cell and from 4.68 to 6.72 mM, respectively.

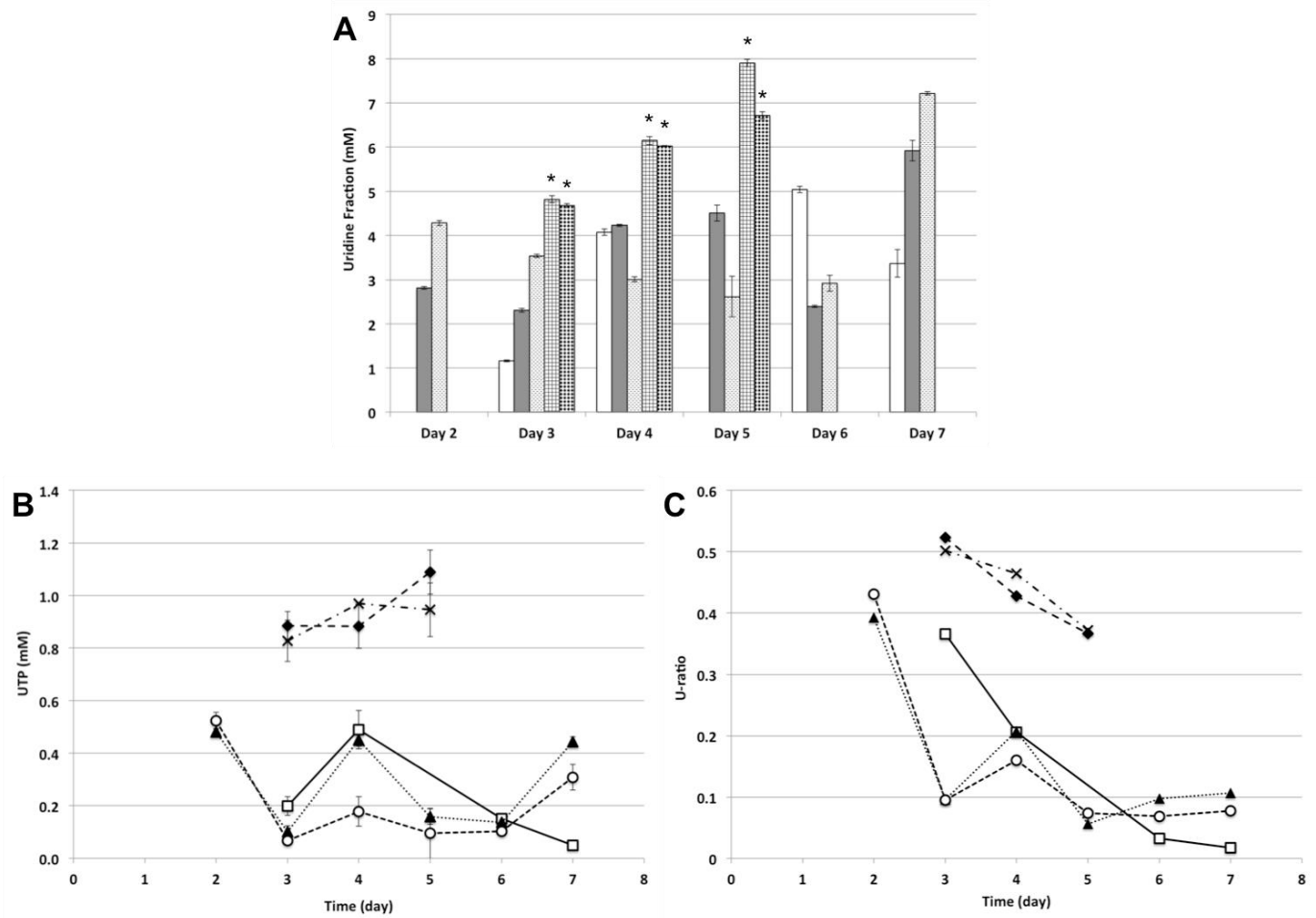

Figure 6.3: The intracellular concentrations of the A) uridine fraction, B) UTP, and the C) U-ratio determined for a 'Batch' (□;—□—), 'NS' (■;···▲···), 'Galactose' (▨;–○–), 'UG' (▦;—◆—), and 'UMG' (▩;—×–) in cells of fed-batch EG2 cultures. (n = 2; error bar indicates the standard deviation)

* ($P < 0.02$) compared to all other cultures that day

The concentration on all three days was significantly higher ($P < 0.02$) than what was observed in the other cultures. A closer look at the UTP concentrations is shown in Figure 6.3 (B). The concentration in the 'Batch', 'NS', and 'Galactose' cultures showed a similar behavior fluctuating between 0.05 and 0.5 mM. However, in the 'UG' and 'UMG' cultures the UTP concentrations were significantly higher ($P < 0.02$) compared to all other cultures on day 3 and 5. In addition, an increase in the intracellular UTP concentration from 0.9 to 1.09 mM in the 'UG' culture and from 0.8 to 0.9 mM in the 'UMG' culture was seen. The U-ratio shown in Figure 6.3 (C) gives the fraction of UTP/UDP-GNAc for each culture over time. A decline in the ratio during the experiment was seen for all cultures but an overall higher ratio was identified in the 'UG' and 'UMG' culture.

The NTP-ratio and NTP/U-ratio for all cultures are shown in Figure 6.4. The NTP-ratio is shown in Figure 6.4 (A) and showed a decrease for all cultures over time. The NTP/U-ratio displayed in Figure 6.3 (B) was stable for the 'UG' and 'UMG' culture. For the 'Batch', 'NS', and 'Galactose' culture the ratio decreased from day 3 to day 4 after which an increase was observed. The 'Batch' culture showed the overall highest increase and with a decrease on the last day of culture. The 'Galactose' culture decreased for the last two days of culture. The lowest increase was seen in the 'NS' culture until day 6 after which the ratio decreased again.

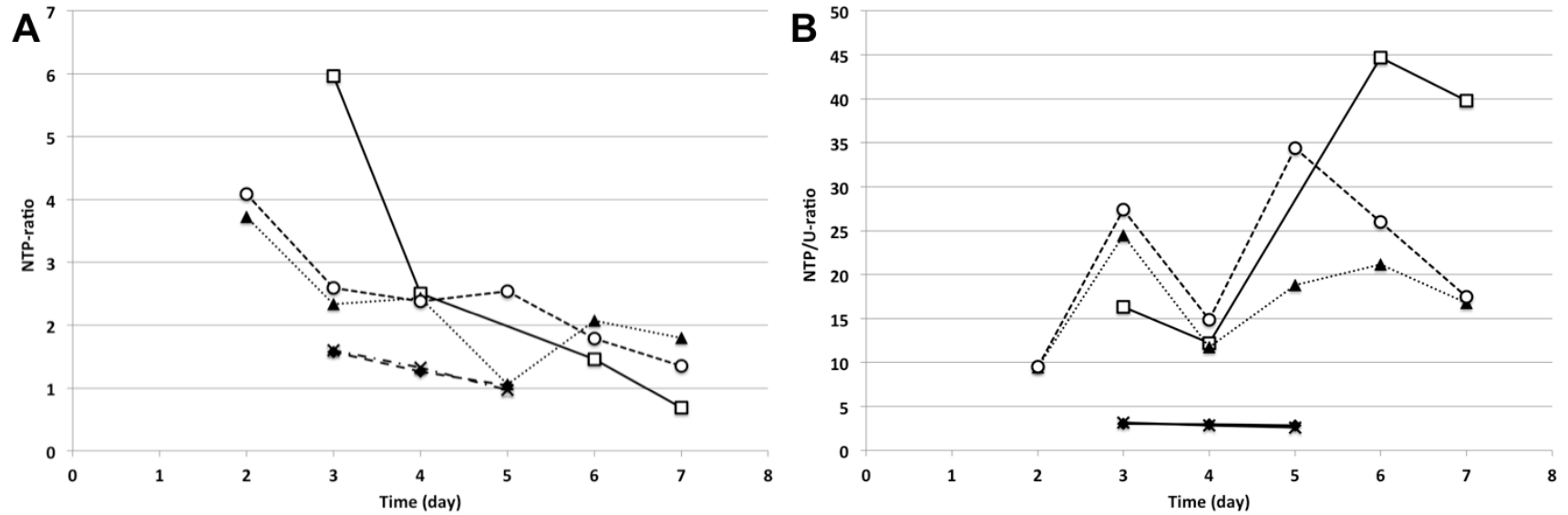

Figure 6.4: The A) NTP-ratio and B) NTP/U-ratio determined at the sampling points during a 'Batch' (—□—), 'NS' (···▲···), 'Galactose' (-○-·), 'UG' (—◆—), and 'UMG' (—×—) fed-batch EG2 cultures. (n = 2)

Figure 6.5 shows the ATP/GTP ratio calculated for all cultures. A constant decline was observed in the 'Batch', 'UG', and 'UMG' culture. The lowest average ratios were observed in the 'UG' and 'UMG' culture. In the 'NS' and 'Galactose' culture the ratio increased after day 3 and 4, respectively, before it again decreased after day 5.

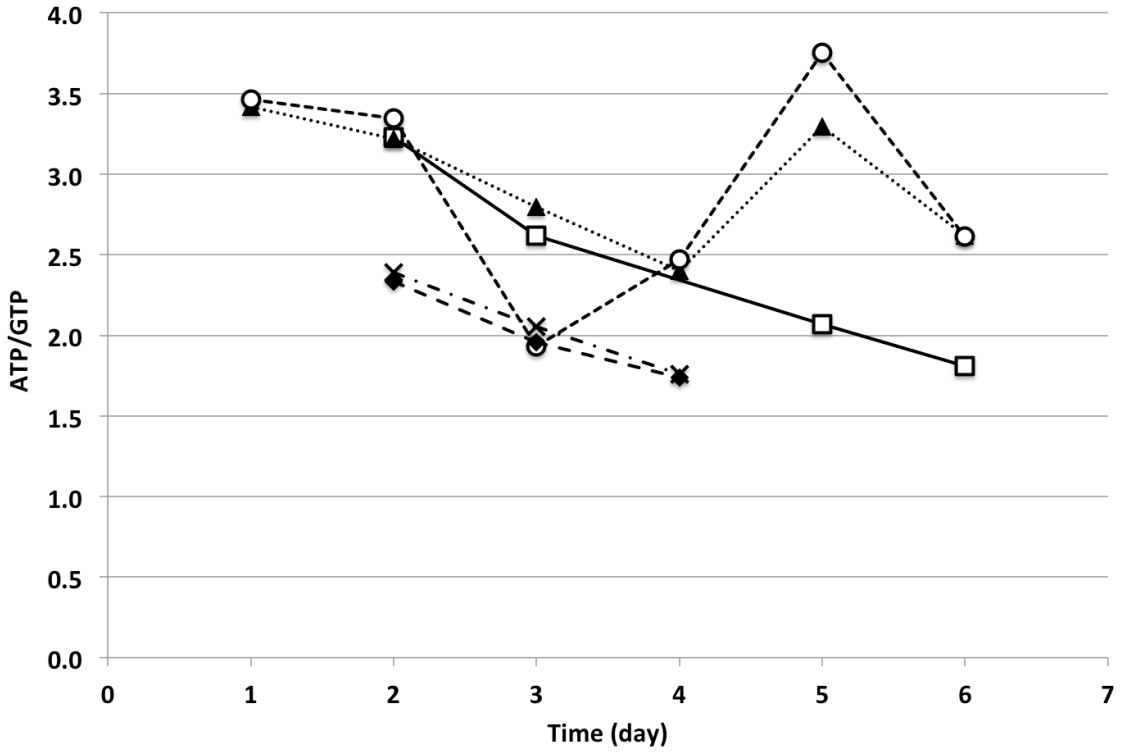

Figure 6.5: The ATP/GTP ratios during a 'Batch' (—□—), 'NS' (···▲···), 'Galactose' (-○-), 'UG' (—◆—), and 'UMG' (—× -) fed-batch EG2 cultures. (n = 2)

6.2.2 The effects of precursor feedings in DP12 cultures on the nucleotide / nucleotide sugar pool

To study the effects of nucleotide sugar precursor feedings the intracellular nucleotide / nucleotide sugar pool was determined from samples taken throughout cell culture. At each sampling point $1x10^7$ cells were collected from the culture and quenched to stop the metabolism in the cell. After the quenching procedure the cell samples were stored at -70°C for a maximum of 1 week before extraction. Both quenching and extraction procedures were performed as outlined in the methods section (see Sections 2.7.1 and 2.7.2). The intracellular pool was then compared between the 'Batch', 'NS' and the cultures with precursor feedings.

Figure 6.6 shows the intracellular concentrations of UDP-GalNAc, UDP-GlcNAc + CTP, UDP-Gal, and UDP-Glc for each culture during the bioprocess. The UDP-GalNAc and UDP-GlcNAc + CTP in all cultures was slightly increasing over time. In the 'Batch' and 'NS' culture UDP-Gal was not detected throughout the culture – except for in the 'NS' culture on day 7 (Figure 6.1 (C)). Over the same time an increased UDP-Gal was detected in the 'Galactose', 'UG', and 'UMG' cultures. While the 'Galactose' culture exhibited a stable intracellular concentration around 0.57 mM, both the 'UG' and 'UMG' cultures displayed a steady increase in the UDP-Gal concentration from day 4 at ~0.7 mM to day 7 at ~1.1 mM. These concentrations were significantly higher ($P < 0.02$) than what was observed in the 'Batch' and 'NS' culture on day 4, 5, and 7. In Figure 6.1 (C) the UDP-Glc concentration for each culture is shown. The

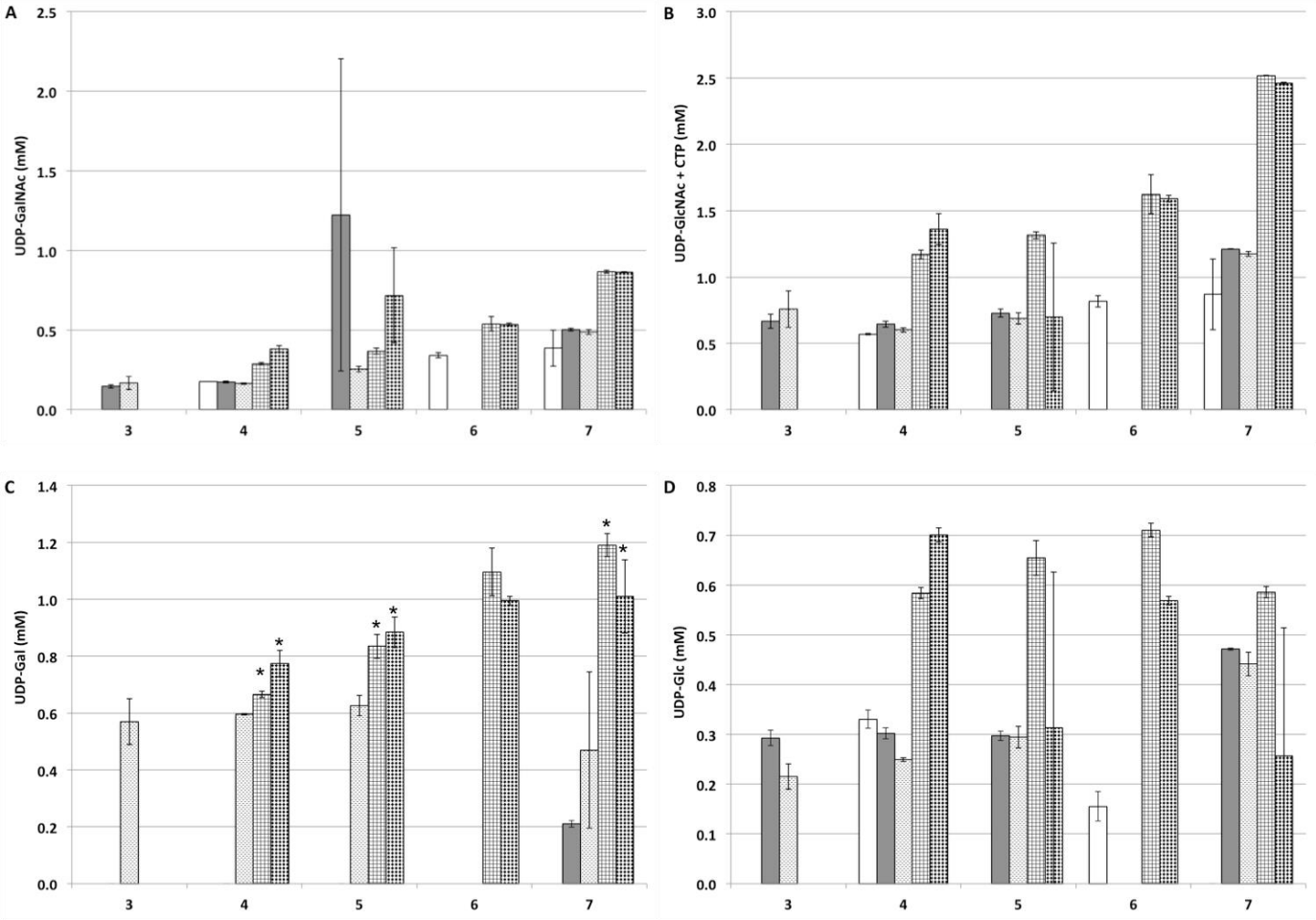

Figure 6.6: The intracellular concentrations of A) UDP-GalNAc, B) UDP-GlcNAc + CTP, C) UDP-Gal, and D) UDP-Glc during a 'Batch' (▭), 'NS' (▬), 'Galactose' (▤), 'UG' (▦), and 'UMG' (▩) in cells of fed-batch DP12 cultures. (n = 2; error bars indicate the standard deviation)

* ($P < 0.02$) compared to all other cultures that day

highest average concentrations in each cell were observed for the 'UG' and 'UMG' cultures on day 4, 5, and 6 at 0.65 and 1.0 mM, respectively. While the 'Batch' culture UDP-Glc concentration decreased during the bioprocess, the intracellular concentration in the 'NS' and 'Galactose' cultures stayed stable around 0.25 – 0.3 mM for the first 5 days and then increased to 0.45 mM.

The adenylate energy charge (AEC) determined at each sampling point is shown in Figure 6.7. A similar trend was observed for all cultures as the AEC decreased steadily over the course of the experiment with AEC values being similar among the cultures on each day.

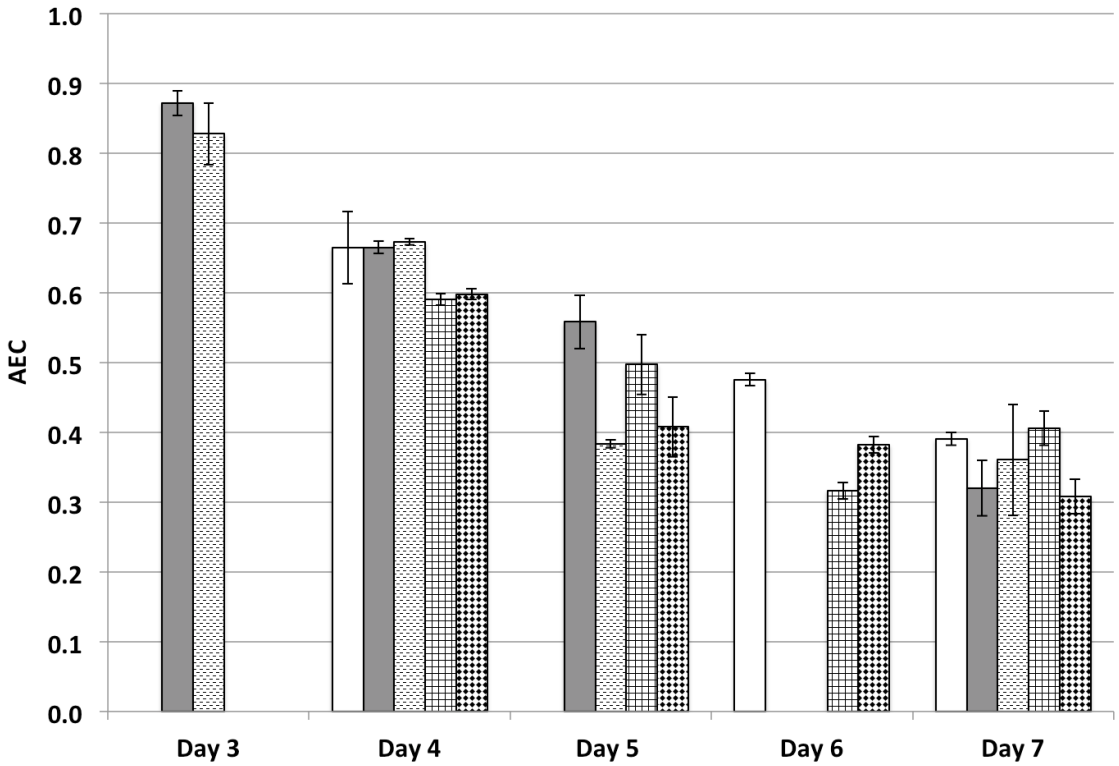

Figure 6.7: The adenylate energy charge (AEC) value determined at each sampling point during a 'Batch' (▭), 'NS' (▭), 'Galactose' (▭), 'UG' (▭), and 'UMG' (▭) fed-batch DP12 cultures. (n = 2; error bars indicate the standard deviation)

The overall uridine fraction concentration during the precursor feeding experiments is shown in Figure 6.8 A. For the 'Batch' culture a stable uridine fraction around 1.7 mM was

observed in each cell. A steady increase in the intracellular concentration from 1.8 mM on day 3 to 3.0 mM on day 7 was determined in the 'NS' culture. A similar observation was made for the 'Galactose' culture in which the uridine fraction in each cell remained stable from day 3 to day 5 (2.3 mM) and then increased to 3.1 mM on day 7. Meanwhile a steady increase in the uridine fraction in the cell was determined for the 'UG' and 'UMG' cultures from 5.1 to 6.4 mM and from 5.0 to 5.8 mM, respectively. The concentration on all four days was significantly higher ($P < 0.02$) than what was observed in the other cultures – with the exception of 'UMG' versus 'NS' on day 5. A closer look at the UTP concentration is shown in Figure 6.8 B. The concentration in all cultures showed a steady decrease over time. The 'Batch', 'NS', and 'Galactose' cultures showed a similar behavior decreasing in the concentration from 0.45 to 0.09 mM in each cell. While the UTP concentrations in the 'UG' and 'UMG' culture were also decreasing they initially started at a higher concentration – two times higher than observed in the other cultures on that day. Over the course of the experiment the UTP concentration per cell then decreased to 0.1 mM. The U-ratio shown in Figure 6.8 (C) gives the fraction of UTP/UDP-GNAc for each culture over time. A similar decline in the ratio during the experiment was seen for all cultures.

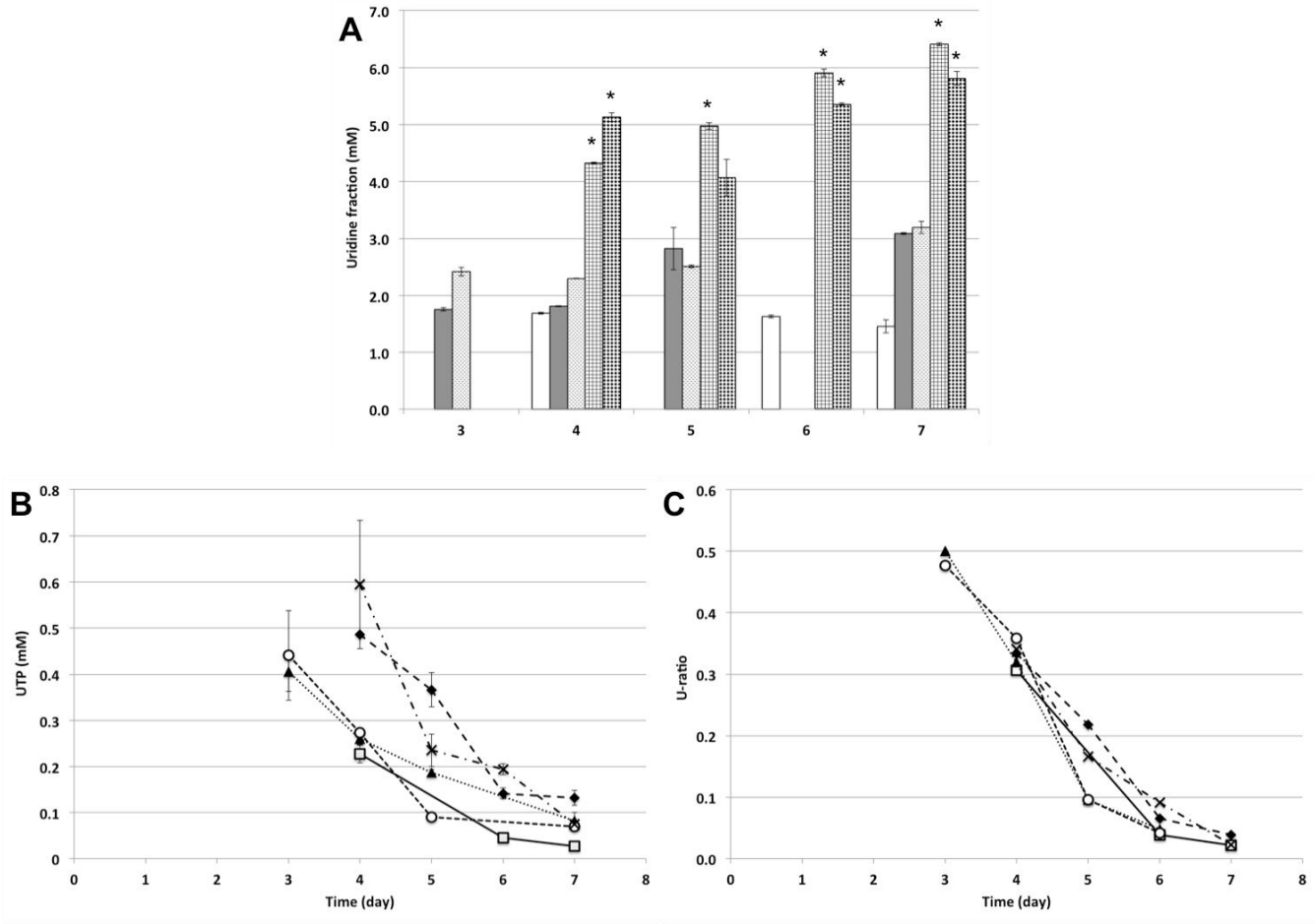

Figure 6.8: The intracellular concentrations of the A) uridine fraction, B) UTP, and the C) U-ratio determined for a 'Batch' (□;—□—), 'NS' (■;···▲···), 'Galactose' (▨;-○-), 'UG' (▦;—◆—), and 'UMG' (▩;—×-) fed-batch DP12 cultures. (n = 2; error bars indicate the standard deviation)

* ($P < 0.02$) compared to all other cultures that day

The NTP-ratio and NTP/U-ratio for all cultures are shown in Figure 6.9. The NTP-ratio is shown in Figure 6.9 (A) and revealed a decrease for all cultures over time. On day 4 the ratio for the 'UG' and 'UMG' cultures is 50% of the ratio determined for the rest of the cultures. After day 4 the ratio in the 'UG' and 'UMG' culture decreased less drastically resulting in all cultures ending with a similar NTP-ratio on day 7. The NTP/U-ratio displayed in Figure 6.8 (B) increased for the 'Galactose', 'UG', and 'UMG' cultures throughout the culture. In the 'Batch' and 'NS' culture an increase was observed from day 3 to day 6 and day 5, respectively, after which the NTP/U-ratio decreased.

Figure 6.10 shows the ATP/GTP ratio calculated for all cultures. The ratio observed was stable for all cultures. However, a difference was observed between the average ratio in the 'UG' and 'UMG' cultures compared to all other cultures. In the 'UG' and 'UMG' culture the lowest average ratios were observed at 1. In the 'Batch', 'NS', and 'Galactose' cultures the average ratio was at 3.8.

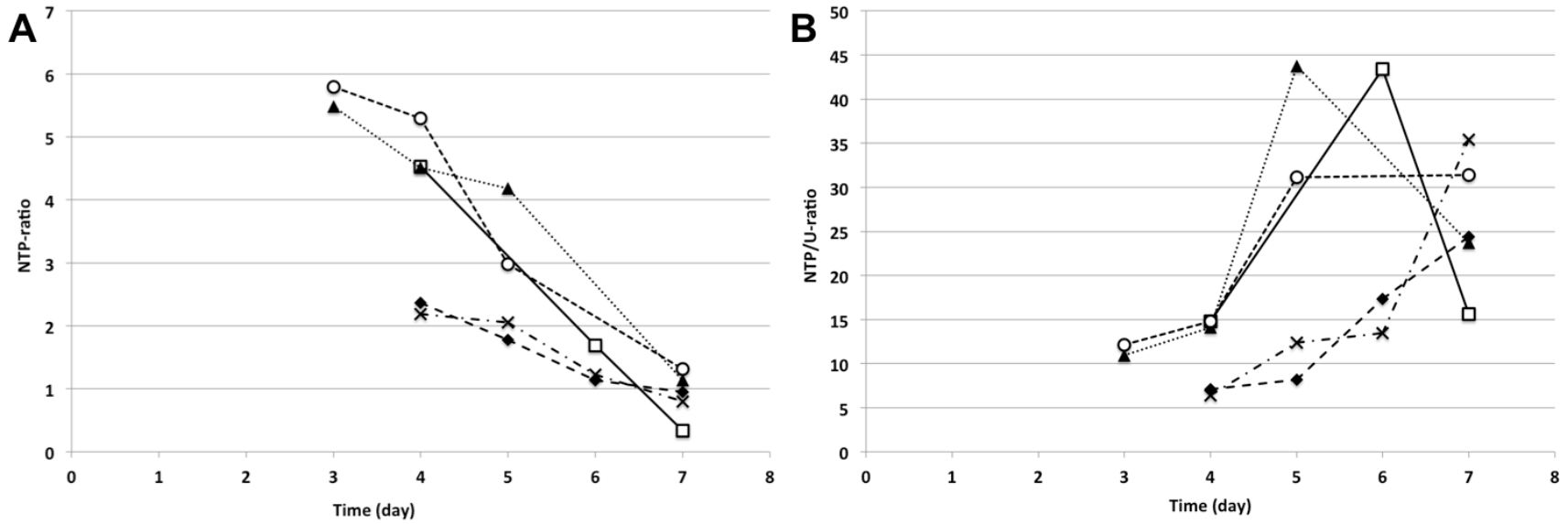

Figure 6.9: The A) NTP-ratio and B) NTP/U-ratio determined at the sampling points during a 'Batch' (−□−), 'NS' (···▲···), 'Galactose' (-○-·), 'UG' (−◆), and 'UMG' (−× -) fed-batch DP12 cultures. (n = 2)

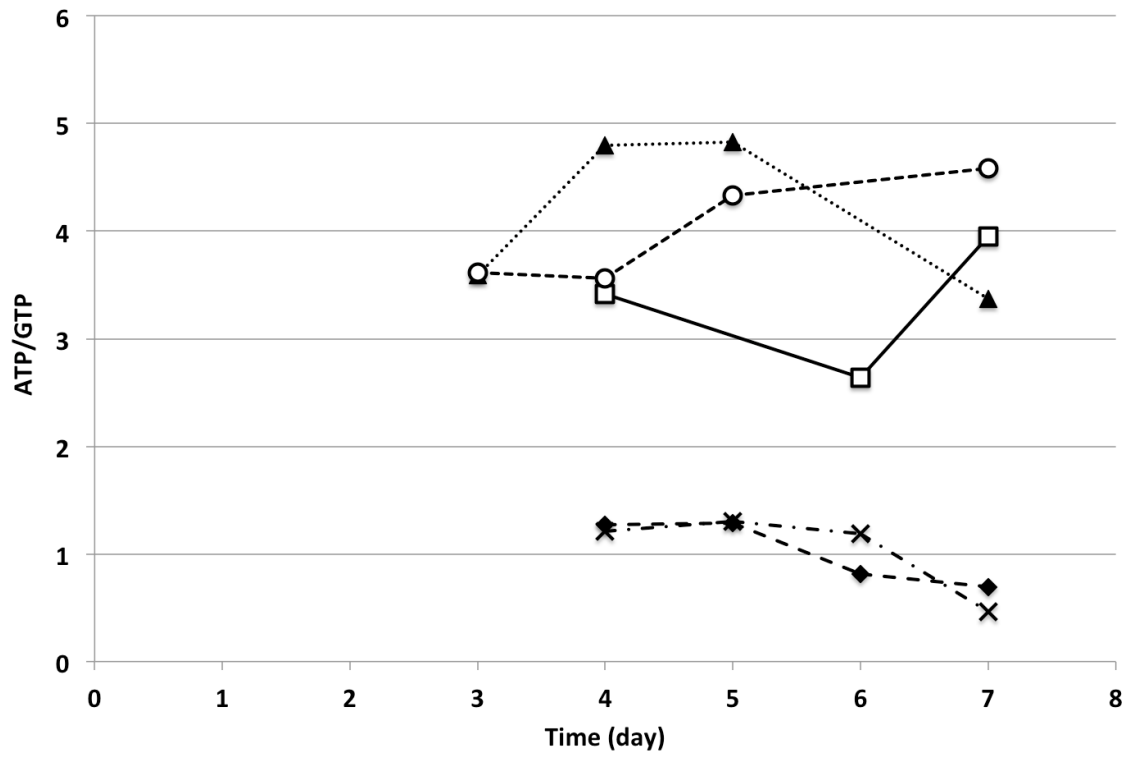

Figure 6.10: The ATP/GTP ratio during the 'Batch' ( ), 'NS' ( ), 'Galactose' ( ), 'UG' ( ), and 'UMG' ( ) fed-batch DP12 cultures. (n = 2)

6.2.3 Comparison of effects in the EG2 and DP12 cultures.

The overviews of the precursor feeding effects on the intracellular nucleotide / nucleotide sugars, which provide the glycosylation building blocks, are summarized in Tables 6.1-5.

In Table 6.1 the impact of the precursors feedings on the UDP-Gal concentration in both cell lines is shown. It is notable that UDP-Gal was barely detected in both cell lines in the 'Batch' culture. In the 'NS' culture a low but stable concentration was observed in the EG2 cell lines, whereas the DP12 cell line still only had a very low concentration present. In the 'Galactose', 'UG' and 'UMG' cultures of EG2 and DP12 cell lines similar observations were made. In the 'Galactose' a stable intracellular UDP-Gal concentration of roughly 0.57 mM was determined for the DP12 culture. However, in the EG2 culture supplemented with galactose, the

UDP-Gal concentration declined from day 3 to day 6 before again increasing on day 7. In the 'UG' and 'UMG' cultures the UDP-Gal concentration in both cell lines increased over time. On day 4 of both cultures the concentration in the EG2 cell line was significantly greater ($P < 0.02$) than what was seen in the DP12 culture. However, on day 5 a significantly higher UDP-Gal concentration ($P < 0.02$) for the EG2 cell line was only observed in the 'UG' culture.

Table 6.1: Comparison of the effect of the nucleotide sugar precursor feedings on the intracellular UDP-Gal concentration in CHO-EG2 and DP12 cultures.

	EG2 culture	**DP12 culture**
Batch	• Only detection on day 4: 0.15 mM	• No detection
NS	• Low detection • Average: 0.21 mM	• Only detection on day 7: 0.21 mM
Galactose	• ↓ from day 3 to 6 (1.68 – 0.42 mM) • ↑ on day 7 to 1.76 mM	• Stable over bioprocess • Average: 0.57 mM
UG	• ↑ from day 3 to 5 (1.0 – 1.54 mM)	• ↑ from day 4 to 7 (0.67 – 1.19 mM
UMG	• ↑ from day 3 to 5 (0.89 – 1.31 mM)	• ↑ from day 4 to 7 (0.77 – 1.01 mM)

Table 6.2 shows the effect the precursor feedings had on the adenylate energy charge (AEC) in both cell lines. In the DP12 cell line the AEC decreased in a similar manner in all cultures over time. On the other hand, the AEC determined in the 'Batch', 'NS', and 'Galactose' EG2 cultures was fluctuating over time between high and low AEC values without an apparent trend over the course of the experiments. In the 'UG' and 'UMG' cultures the AECs were stable above 0.75.

Table 6.2: Comparison of the effect of the nucleotide sugar precursor feedings on the adenylate energy charge in CHO-EG2 and DP12 cultures.

	EG2 culture	DP12 culture
Batch	• Stable between day 3 and day 6 (~ 0.79) • ↓ on day 4 to 0.48	• ↓ from day 4 to day 7 • 0.67 → 0.39
NS	• High on day 2, 4, 7: ~ 0.72 • Low on day 3, 5, 6: ~ 0.38	• ↓ from day 3 to day 7 • 0.87 → 0.32
Galactose	• High on day 2, 5, 7: ~ 0.64 • Low on day 3, 4, 6: ~ 0.41	• ↓ from day 3 to day 7 • 0.82 → 0.36
UG	• Stable: ~ 0.75	• ↓ from day 4 to day 7 • 0.59 → 0.31
UMG	• Stable: ~ 0.76	• ↓ from day 4 to day 7 • 0.60 → 0.31

The comparison of the UTP concentration and the U-ratio in the two cell lines for this study is shown in Table 6.3. While the UTP concentration in the 'UG' and 'UMG' DP12 cultures was slightly higher than in the other DP12 cultures these concentrations were all declining during the bioprocess. On the other hand, the 'Batch', 'NS' and 'Galactose' cultures had stable UTP concentrations. In the 'UG' and 'UMG' culture the UTP content even increased during the bioprocess. For both cell lines an overall decline of the U-ratio was observed over time. While this decline was comparable for most of the cultures, the 'UG' and 'UMG' culture in the EG2 cell line showed a smaller decline due to the higher UTP content in those cells.

Table 6.3: Comparison of the effect of the nucleotide sugar precursor feedings on the UTP concentration and U-ratio (UTP/UDP-GNac) in CHO-EG2 and DP12 cultures.

	EG2 culture	**DP12 culture**
Batch	• Stable UTP: ~ 0.22 mM	• ↓ in UTP • 0.23 → 0.03 mM
	• ↓ in U-ratio • 0.37 → 0.02	• ↓ in U-ratio • 0.31 → 0.02
NS	• Stable UTP: ~ 0.29 mM	• ↓ in UTP • 0.41 → 0.08 mM
	• ↓ in U-ratio • 0.39 → 0.11	• ↓ in U-ratio • 0.50 → 0.05
Galactose	• Stable UTP: ~ 0.21 mM	• ↓ in UTP • 0.44 → 0.08 mM
	• ↓ in U-ratio • 0.43 → 0.08	• ↓ in U-ratio • 0.48 → 0.04
UG	• ↑ in UTP • 0.88 → 1.09 mM	• ↓ in UTP • 0.49 → 0.13 mM
	• ↓ in U-ratio • 0.52 → 0.37	• ↓ in U-ratio • 0.33 → 0.04
UMG	• ↑ in UTP • 0.83 → 0.95 mM	• ↓ in UTP • 0.59 → 0.08 mM
	• ↓ in U-ratio • 0.50 → 0.37	• ↓ in U-ratio • 0.34 → 0.02

The trends in the NTP ratio and the NTP/U-ratio for both cell lines are shown in Table 6.4. It is noteworthy that in both cell lines the NTP ratio was decreasing over time. The NTP/U-ratios in all DP12 cultures are high and mostly increasing throughout the bioprocess with the exception of a drop towards the end of the 'Batch' and 'NS' culture. A similar observation was

made for the EG2 'Batch', 'NS', and 'Galactose' cultures. However, in the EG2 'UG' and 'UMG' cultures the NTP/U-ratio is low and stable due to only a small decrease in both the NTP and U-ratio over time.

Table 6.4: Comparison of the effect of nucleotide sugar precursor feedings on the NTP ([ATP + GTP]/[UTP]) and the NTP/U-ratio in CHO-EG2 and DP12 cultures.

	EG2 culture	**DP12 culture**

Batch	• ↓ in NTP
	  • 5.96 → 0.68
		• ↓ in NTP
		  • 4.53 → 0.34

	• ↑ in NTP/U-ratio from ~ 14.26 (day 3/4) to ~ 42.25 (day 6/7)	• ↑ in NTP/U-ratio from 14.79 → 43.59 • ↓ from 43.59 → 15.60

NS	• ↓ in NTP
	  • 3.72 → 1.79
		• ↓ in NTP
		  • 5.48 → 0.95

	• Fluctuating NTP/U-ratio • ~17.07	• ↑ in NTP/U-ratio from 10.95 → 43.7 • ↓ from 43.7 → 23.7

Galactose	• ↓ in NTP
	  • 4.09 → 1.35
		• ↓ in NTP
		  • 5.79 → 1.31

	• Fluctuating NTP/U-ratio
	  • ~ 21.59
		• ↑ in NTP/U-ratio
		  • 12.1 → 31.4

UG	• ↓ in NTP
	  • 1.57 → 1.04
		• ↓ in NTP
		  • 2.36 → 0.80

	• Stable NTP/U-ratio
	  • ~ 2.93
		• ↑ in NTP/U-ratio
		  • 7.1 → 24.4

UMG	• ↓ in NTP
	  • 1.57 → 1.04
		• ↓ in NTP
		  • 2.19 → 0.80

	• Stable NTP/U-ratio
	  • ~ 2.88
		• ↑ in NTP/U-ratio
		  • 6.4 → 35.4

Table 6.5 shows the trends in the ATP/GTP ratio for the EG2 and DP12 cell lines during this experiment. While a consistent decrease over time was observed for all EG2 cultures, a decrease in the DP12 culture was only observed in the 'UG' and 'UMG' cultures. For the DP12 cell line a stable ratio was observed for the 'Batch' and 'NS' cultures, while the 'Galactose' culture showed an increasing trend.

Table 6.5: Comparison of the effect of the nucleotide sugar precursor feedings on the ATP/GTP ratio in CHO EG2 and DP12 cultures.

	EG2 culture	**DP12 culture**
Batch	• ↓ in ATP/GTP ratio • 3.2 → 1.8	• Stable ATP/GTP ratio: ~ 3.33
NS	• ↓ in ATP/GTP ratio • 3.4 → 2.6	• Stable ATP/GTP ratio: ~ 4.15
Galactose	• ↓ in ATP/GTP ratio • 3.5 → 2.6	• ↑ in ATP/GTP ratio • 3.6 → 4.6
UG	• ↓ in ATP/GTP ratio • 2.3 → 1.7	• ↓ in ATP/GTP ratio • 1.2 → 0.7
UMG	• ↓ in ATP/GTP ratio • 2.4 → 1.8	• ↓ in ATP/GTP ratio • 1.2 → 0.5

6.3 Discussion

The objective of this study was to determine the effects the media additives galactose, uridine, and manganese have on the intracellular nucleotide / nucleotide sugar pool. Since the nucleotide sugars are the building blocks needed for the glycosylation process their availability is important (Fan et al., 2015). Here the availability of the nucleotide / nucleotide sugars were

assessed in an attempt to better understand their impact on the galactosylation and the cell's overall energy metabolism.

Previous research has shown that nutrient levels have an effect on the intracellular nucleotide / nucleotide sugar pool (Nyberg et al., 1999). This is the basis for research into the addition of nucleotide sugar precursor feedings to increase the pool of specific glycosylation building blocks. The most common media additivies used to increase galactosylation are galactose, uridine, and manganese.

In both cell lines UDP-GNAc (UDP-GlcNAc and UDP-GalNAc) was accumulating over time as previously observed by Kochanowski et al. (2008). UDP-GlcNAc and UDP-GalNAc are isomers and can be converted from one another. At a closer look at the UDP-GlcNAc/UDP-GalNAc ratio higher values than reported by Span et al. (2001) were determined. However, these higher ratios are most likely due to the fact that in our nucleotide sugar analysis UDP-GlcNAc eluted with CTP increasing the combined concentration.

Over time the UDP-Gal concentration in both cell lines remained at very low and mostly undetectable levels in the 'Batch' and 'NS' cultures. In the 'Galactose' culture of the EG2 cell line the UDP-Gal fluctuated throughout the experiments while in the DP12 cell line the concentration remained stable. Only in 'UG' and 'UMG' cultures did the UDP-Gal concentration steadily increase. However, in the EG2 cell line the UDP-Glc concentrations increased steadily during the 'UG' and 'UMG' cultures while the remainder of the cultures showed a more consistent concentration over time. In the DP12 culture the UDP-Glc concentration remained stable in all cultures with the exception of a small increase seen in the 'NS' and 'Galactose' cultures. This increase coincided with the initial measurement of UDP-Gal in those cultures. This correlation is not surprising as UDP-Gal and UDP-Glc can be converted

into each other. The relative ratio for these two nucleotide sugars (UDP-Gal/UDP-Glc) for the 'Batch' and 'NS' culture in both cell lines was similar to what was observed by Kochanowski et al. (2008) at the end of culture (1:2). When UDP-Gal was detected in the cells the ratio found was between 1:2 to 1:3 without a detectable change over time as observed by Kochanoswki et al. (2008). However, this trend was not observed during the precursor feeding experiments. In the 'Galactose', 'UG', and 'UMG' experiments the UDP-Hex concentration (UDP-Gal + UDP-Glc) in both cell lines increased compared to the 'NS' culture more than 2 – 3 times in the EG2 and 2 – 4 times in the DP12 cell line, which agreed with findings by Wong et al. (2010). Of the two UDP-Hex sugars the UDP-Gal concentration increased to be higher than the UDP-Glc concentration. Over time the EG2 cell lines exhibited a relative ratio (UDP-Gal/UDP-Glc) from (1.6 : 1) to (1.3 : 1) in the 'UG' and 'UMG' cultures indicating a slight favor for the conversion of UDP-Gal into UDP-Glc. In the DP12 cell line the opposite trend was observed when the same ratio shifted from (1.1 : 1) to (2.0 : 1) (not taking into account the days when the UDP-Glc had a very high standard deviation). This showed favoritism for UDP-Gal but still resulted in generally lower UDP-Gal concentrations than seen in the EG2 cell line. The increase in UDP-Gal when adding galactose (10 mM) alone was also observed by Amand et al. (2014) and Hills et al. (2001). A further increase was achieved by adding galactose (20 mM) in combination with uridine (1 mM). As expected, the addition of manganese in combination with galactose and uridine did not further increase the UDP-Gal concentration.

The adenylate energy charge is a good indication of cell health. In a healthy cell an AEC value between 0.85 to 0.95 is normal (Atkinson, 1968). In the EG2 cell culture a fluctuation in the AEC was observed with no apparent trend. Considering that ATP is very unstable and has a high turnover rate (Weibl et al., 1974) the variation in the AEC could be due to a longer wait

until the cell sample was flash frozen or an inconsistency in the stopping of the metabolism. However, on average a high AEC value can be observed with an obvious decline in the 'Batch' culture consistent with the drop in viability (see Chapter 5). A stable AEC was only determined for the 'UG' and 'UMG' EG2 cultures, which was consistent with their high viability (above 90%) even after a decline in viability was observed in all other cultures. On the other hand the DP12 cell cultures experienced a consistent decline in the AEC over time while the viability determined with the trypan blue exclusion remained very high (see Chapter 5). Even though the DP12 cell line is DHFR+ the medium used for culture contained hypoxanthine, thymine, and glycine. In cell culture hypoxanthine is a precursor for ATP and uric acid (Harmsen et al., 1984). Since the overall adenosine fraction did not increase during the bioprocess it can be assumed that the hypoxanthine was converted mainly to uric acid during the bioprocess. This could lead to an accumulation of uric acid in the cell culture. Sanchez-Lozada et al. (2012) found that the accumulation of uric acid in human aortic endothelial cells caused alterations in the mitochondria in combination with decreased ATP levels.

When adding uridine as precursor for glycosylation (Ryll et al., 1991) the uridine fraction in both the EG2 and DP12 cell line increases. A higher increase was seen in the EG2 cell line, which was accompanied by a higher UTP concentration. This difference could be explained by the possible difference in the uptake of uridine. It has been shown that hypoxanthine can inhibit the uridine transport in CHO cells (Plagemann and Wohlhueter, 1984). However, it also seemed that there was a generally lower uridine fraction in the DP12 cultures. This could mean that the uridine that was taken up then gets converted to UTP and redistributed to activate the nucleotide sugars. Hence, the UTP would not accumulate in the cells.

The NTP and NTP/U-ratio have been associated with the physiological states of cells in culture (Ryll and Wagner, 1992). For this study the NTP-ratio was calculated as [(ATP + GTP)/(UTP + (UDP-GlcNAc + CTP)]. During HPLC analysis CTP was co-eluted with UDP-GlcNAc and hence the combined concentration value is used for this calculation. For both cell lines a decrease in the NTP-ratio was observed while the NTP/U-ratio increased over the course of the experiment. The trend seen for the NTP/U-ratio is consistent with the trend observed by Ryll and Wagner (1992) and Barnabe and Butler (1994) as cell go through the stages of culture. However, the trend in the NTP-ratio is opposite to what was observed by Ryll and Wagner (1992) and Barnabe and Butler (1994). Since the UDP-GlcNAc concentration is known to increase over time it will contribute significantly to the increase of the denominator. This would most likely explain the overall decrease in the ratio as opposed to the increase observed by Ryll and Wagner (1992). While, the NTP/U-ratio is similar between both cell lines the EG2 'UG' and 'UMG' culture showed a stable ratio during the experiment. Although the NTP-ratio for those cultures was similar to the remaining EG2 cultures the U-ratio was significantly higher – due to the uridine feeding – resulting in this lower and stable NTP/U-ratio.

An indication for the division in the purine nucleotide pathway is given by the ATP/GTP ratio (Barnabe and Butler, 1994). While in both cell lines a lower ratio is observed in the 'UG' and 'UMG' cultures, the ratio in the DP12 cell line is around 1 indicating a 50:50 division of the pathway products. For all other cultures a higher and stable ratio is determined for the DP12 cell line and a higher and declining ratio in EG2 'Batch' culture, while the ratio is stable in the 'NS' and 'Galactose' culture.

6.4 Conclusion

This study showed that the addition of the precursors galactose alone or in combination with uridine as media supplements was able to increase the UDP-Gal concentration in both cell lines. This provided conditions that were anticipated to maximize galactosylation. While the addition of galactose and uridine had an impact on the nucleotide / nucleotide sugar pool, the addition of manganese did not. The indicators of the physiological states for the cell lines used followed similar trends. Overall, the uridine feeding had a larger impact on the EG2 culture resulting in a higher uridine fraction compared to the DP12 culture. The DP12 culture also showed a consistent decrease in the AEC, which was most likely caused by alterations in the mitochondria due to the addition of hypoxanthine in the culture medium. This supports the fact that the media composition is not only important in regards to the changes in glycosylation precursors but also in regards to the nucleotides / nucleotide sugars that play an important part in the cells energetics.

Chapter 7

The effects of nucleotide sugar precursor feedings and the intracellular nucleotide sugar pool on recombinant protein glycosylation

7.1 Introduction

Glycosylation is a very important aspect of the post-secondary modification in proteins. In antibodies the glycosylation has an important impact on their stability and overall functionality (Ghirlando, 1999). While there are many factors that have shown to influence the glycosylation in a bioprocess, the availability of the building blocks for the glycosylation is a very important one (Varki et al., 2008).

It was shown that the addition of precursors is able to increase the nucleotide sugar building blocks needed for glycosylation and specifically galactosylation (Chapter 6) in two different cell lines. Previous studies have also looked at the particular addition of galactose, urdine, and manganese. These studies showed varied results within different cell lines and for a variety of glycoproteins. Hence, it was of interest to see if the increase observed in the UDP-Gal pool would translate into an increase in the GI in the antibodies produced by the two cell lines tested.

For this part of the study the glycosylation of two different antibodies in two different CHO cell lines was tested after the addition of 10 mM galactose (galactose), 20 mM galactose + 1 mM urdine (UG), and 20 mM galactose + 1 mM uridine + 8 μM manganese (UMG). The change in glycosylation was furthermore correlated to the changes in the intracellular nucleotide / nucleotide sugar pool to determine the correlations and advantages but also the limitations of the simple precursor addition.

7.2 Results

7.2.1 Effects of the precursor feeding on the glycosylation of EG2

The effects of the nucleotide sugar precursor feedings in CHO-EG2 fed-batch cultures on the galactosylation of the antibodies produced are shown in Figure 7.1. The galactosylation observed in the precursor experiments was compared to the galactosylation in a 'Batch' and a regular fed-batch 'NS' culture. Each culture was inoculated at $2x10^5$ cells/mL in 250 mL shaker flasks at a final working volume of 80 mL. During the experiment the cultures were incubated at 37°C with a 10% CO_2 overlay on a shaker platform (120 rpm). At each sampling point 10 mL of supernatant were collected and filtered through a 0.2 μm filter to remove the cells. The glycosylation of the antibody present in the supernatant was then analyzed as described in the methods (n = 2) (see Section 2.6).

Figure 7.1 shows the galactosylation index (GI) (see Section 2.6.5.1) for each culture during the experiment. In the 'Batch' culture a decrease in the GI from 0.8 to 0.56 (-30%) was observed during the experiment. A slight decrease from 0.79 to 0.64 (-19%) and from 0.85 to 0.68 (-20%) was also seen in the 'NS' and 'Galactose' culture, respectively. On the other hand, in the 'UG' and 'UMG' culture the decrease in the GI observed was minimal and the value appeared stable at 0.88 and 0.89, respectively. These values were significantly higher ($P < 0.02$) on day 4 compared to the 'Batch' and 'NS' culture. On day 5 the GI calculated for the 'UG' and 'UMG' culture was significantly higher ($P < 0.02$) than the GI in all other cultures. However, the largest decrease in the 'Batch', 'NS', and 'Galactose' culture was after day 5 for which no glycan analysis was performed in the 'UG' and 'UMG' culture.

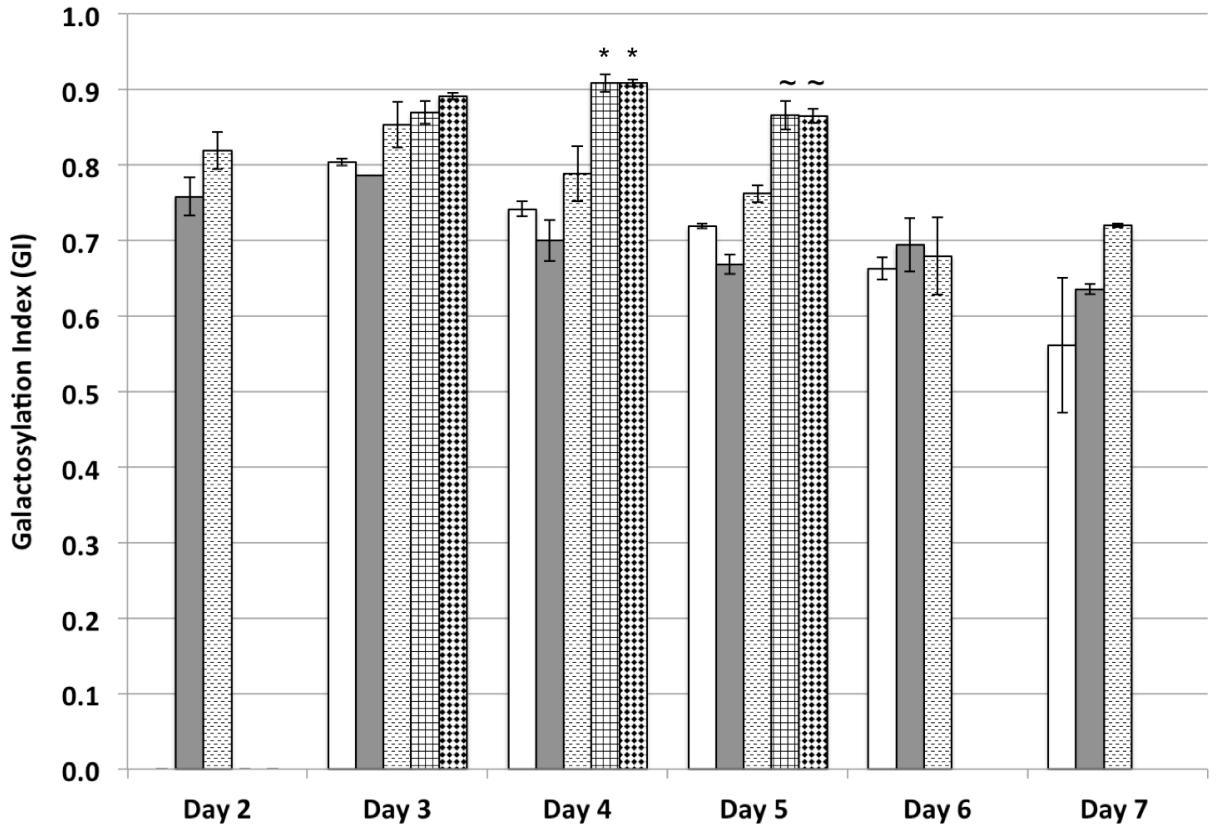

Figure 7.1: The galactosylation indices (GI) during a 'Batch' (▭), 'NS' (▬), 'Galactose' (▨), 'UG' (▦), and 'UMG' (▩) fed-batch EG2 cultures. (n = 2; error bars indicate the standard deviation)

* ($P < 0.02$) compared to 'Batch' and 'NS' cultures that day

~ ($P < 0.02$) compared to all other cultures that day

Figure 7.2 shows the distribution and percentage of the different galactosylated glycan forms (i.e. G0, G1, G2, and G3) that were used to determine the overall GI during the bioprocess. The percentage of G0 in each culture during the bioprocess is shown in Figure 7.2 (A). An increase in the percentage of G0 was observed in the 'Batch' (7 → 26%), 'NS' (8 → 20%), and 'Galactose' (4 → 17%) culture after day 3. For the 'UG' (4 → 6%) and 'UMG' (4 → 7%) culture the increase in the G0 content was less prominent. For day 4 and 5 the G0 content in the 'UG' and 'UMG' precursor experiments was significantly lower ($P < 0.02$) than in the 'Batch' and 'NS' culture. On day 5 the G0 content was also determined to be significantly lower

than the GI calculated for the 'Batch' and 'NS' cultures. In the 'Batch' and 'Galactose' culture an increase in the G1 content was also observed over time (Fig. 7.2 B). During the 'Batch' and 'Galactose' bioprocess the G1 content increased from 27 to 37% and 23 to 31%, respectively. However, for the 'NS', 'UG', 'UMG' culture the G1 content remained stable around 30, 19, and 18%, respectively. On day 4 and 5 the G1 content of the 'UG' and 'UMG' culture was significantly lower ($P < 0.02$) than in the 'Batch' and 'NS' cultures. Figure 7.2 (C) shows the percentage of the G2 glycans present in each culture during the bioprocess. From day 3 a decrease in the G2 content was observed for the 'Batch' (63 → 35%), the 'NS' (64 → 48%), and the 'Galactose' (72 → 57%) cultures. Meanwhile the G2 content in the 'UG' and 'UMG' remained stable around 70%. For day 4 and 5 the G2 percentage in the 'UG' and 'UMG' fed cultures was significantly higher ($P < 0.02$) than in the 'Batch' culture. In addition, the 'UG' and 'UMG' cultures showed a significantly higher ($P < 0.02$) G2 content than what was observed in the 'NS' culture on day 5. The G3 content of all cultures is shown in Figure 7.2 (D). For the 'NS' culture no G3 content was observed throughout the experiment. For the 'Batch' culture a low but stable G3 content around 2% was observed. For the 'Galactose' culture the G3 content was highest on day 3 at 7 % after which it decreased to 4%. The highest content for the 'UG' and 'UMG' was observed on day 4 at 6 and 7%, respectively. After day 4 the G3 content decreased to 5% in both cultures. On day 3 and 5 the G3 content in the 'UG' and 'UMG' cultures were significantly higher ($P < 0.02$) than what was observed in the 'Batch' cultures.

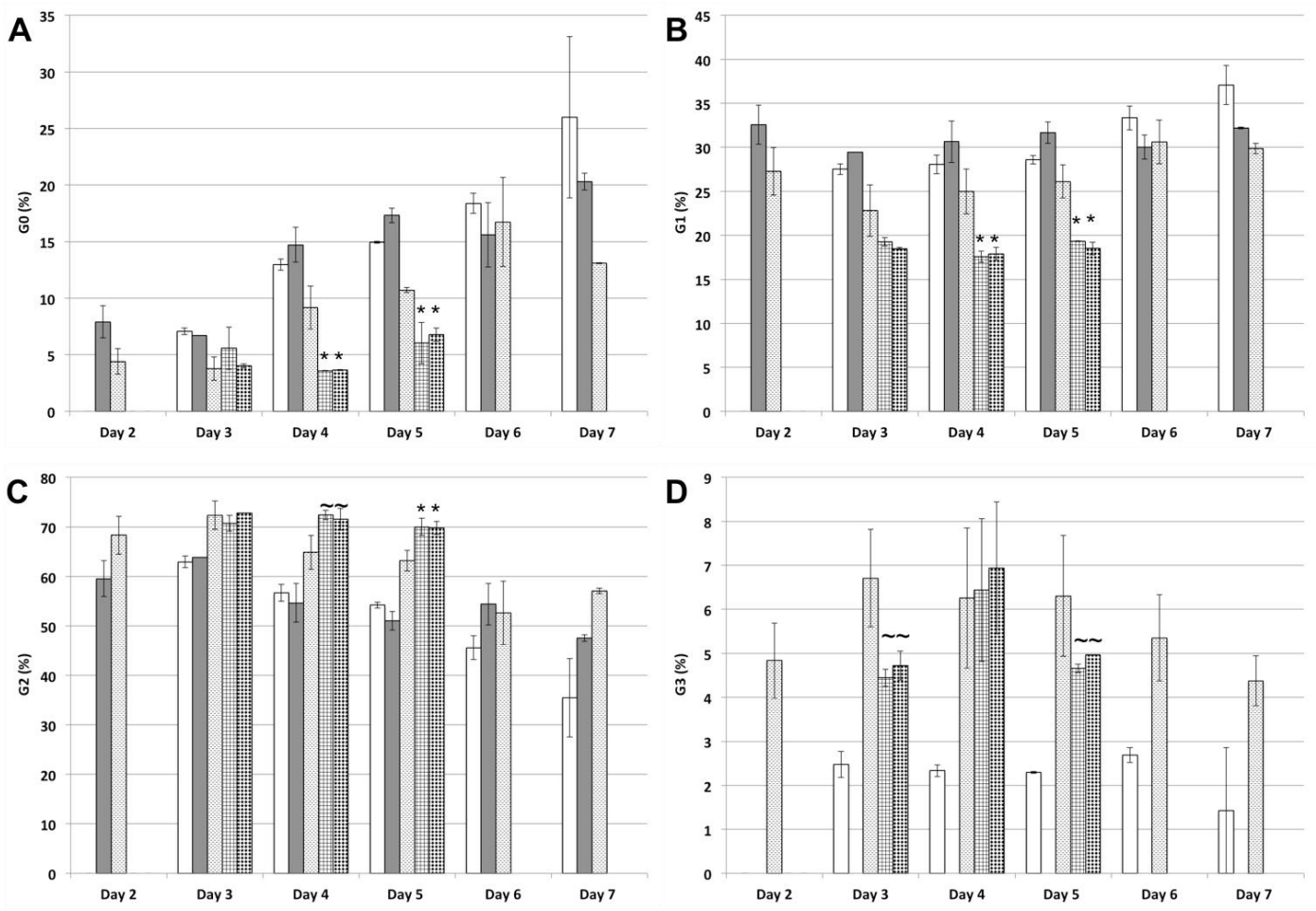

Figure 7.2: The distribution of galactosylation forms present during the 'Batch' (▭) and 'NS' (▬), 'Galactose' (▤), 'UG' (▦), and 'UMG' (▩) fed-batch EG2 cultures. (n = 2; error bars indicate the standard deviation)

* ($P < 0.02$) compared to the 'Batch' and 'NS' culture that day

~ ($P < 0.02$) compared to the 'Batch' culture that day

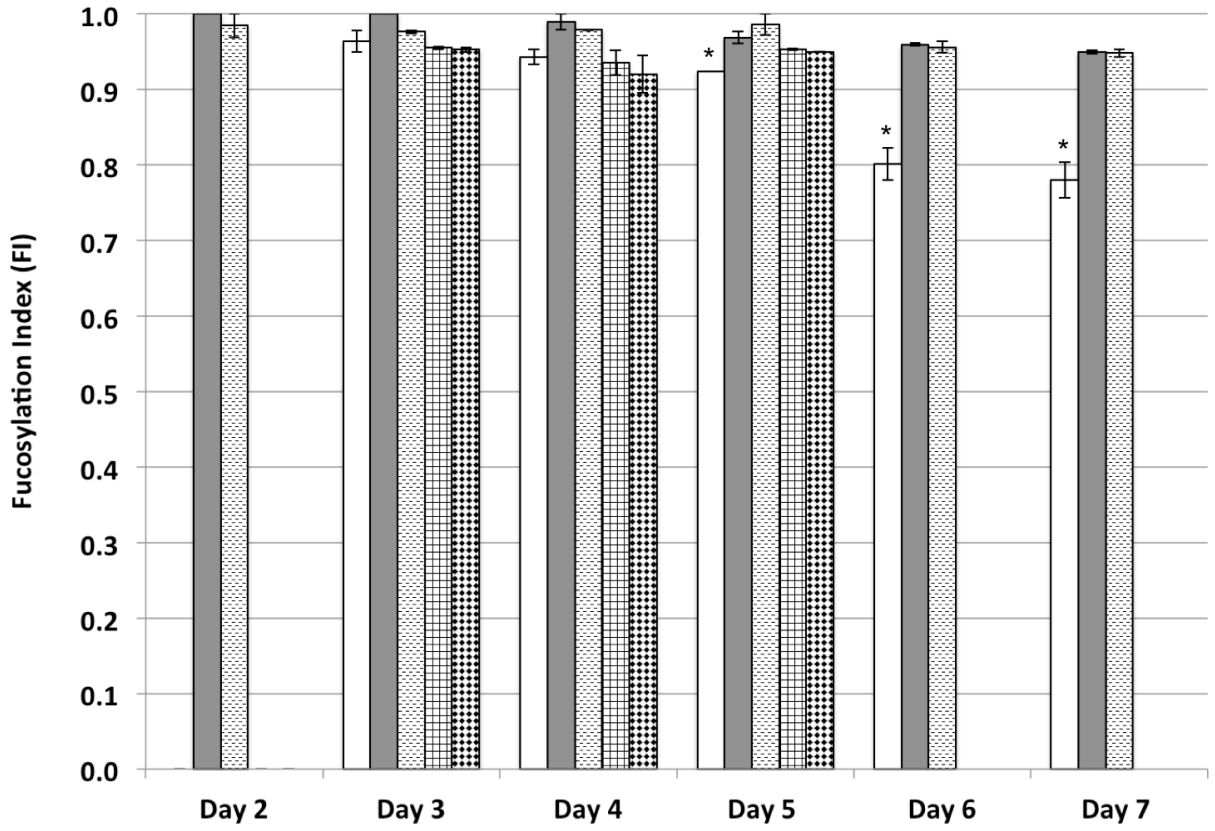

Figure 7.3: The fucosylation indices during the 'Batch' (▭), 'NS' (▬), 'Galactose' (▨), 'UG' (▦), and 'UMG' (▩) fed-batch EG2 cultures. (n = 2; error bars indicate the standard deviation)
* ($P < 0.02$) compared to all other cultures that day

Figure 7.3 shows the fucosylation index (FI) (see Chapter 2.6.5.2) for each culture throughout the bioprocess. While the FI decreased in the 'Batch' culture over time from 0.96 to 0.78, the FI remained fairly stable around 0.98, 0.97, 0.95, and 0.94 in the 'NS', 'Galactose', 'UG', and 'UMG' cultures, respectively. Starting at day 5 the FI determined for the 'Batch' culture was significantly lower ($P < 0.02$) than the FI in the all other cultures.

The change in the sialylation index (SI) (see Chapter 2.6.5.3) over time for each culture is shown in Figure 7.4. The 'Batch' culture showed a decrease in the SI from 0.13 to 0.06 over time. A similar decrease from 0.12 to 0.09 and from 0.14 to 0.10 in the SI was observed in the

'NS' and 'Galactose' cultures, respectively. In the 'UG' and 'UMG' cultures the SI was lower throughout the culture but remained constant at 0.10 and 0.09, respectively.

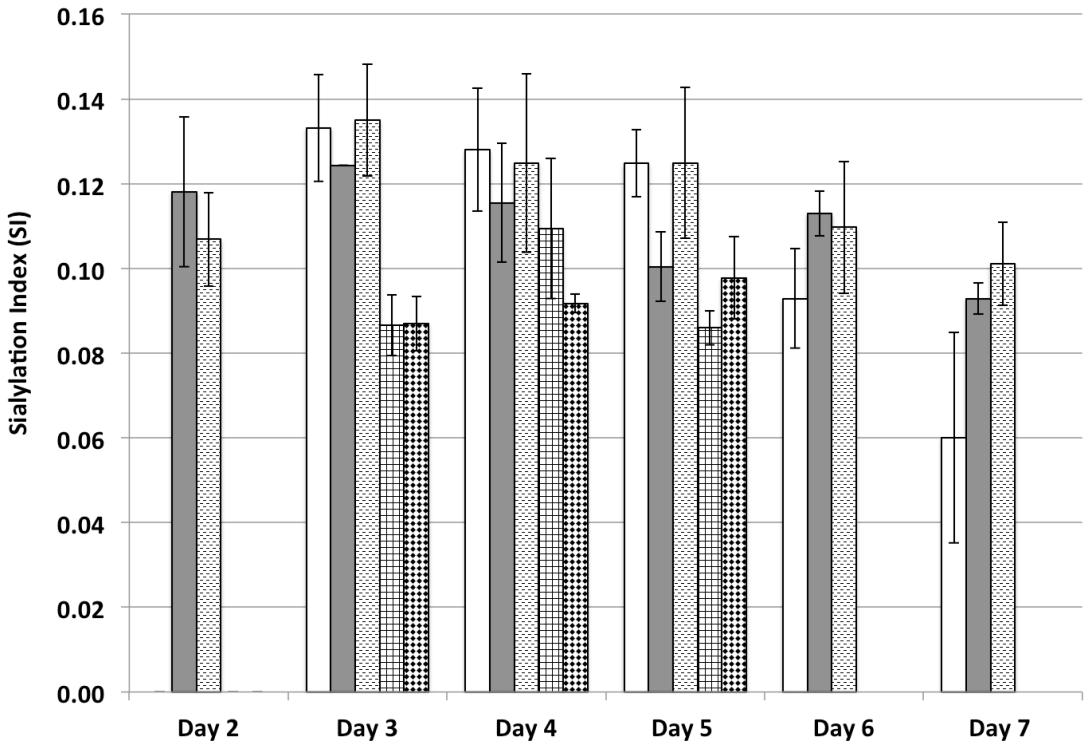

Figure 7.4: The sialylation indices during the 'Batch' ( ), 'NS' ( ), 'Galactose' ( ), 'UG' ( ), and 'UMG' ( ) fed-batch EG2 cultures. (n = 2; error bars indicate the standard deviation)

Overall, the addition of 'UG' and 'UMG' precursor combinations to the CHO EG2 culture was able to increase and maintain the GI over the time observed. This decrease was mainly observed due to the increase in G2 and G3 glycoforms. In addition, the 'UG' and 'UMG' cultures showed a stable FI and SI for the days observed. While, the 'Galactose' addition by itself was able to slightly increase the GI of the EG2 sample, the feeding was not able to maintain the GI over time. Although a higher SI was observed for the 'Galactose' culture, the feeding again was not able to maintain the SI over time. In the 'Batch' and 'NS' culture both the

GI and the FI decreased over time. The 'Batch' culture was also the only culture that showed a decrease in the FI over time.

7.2.2 The correlation of the intracellular UDP-Gal pool on the protein galactosylation in EG2 cultures.

The UDP-Gal concentration versus the GI for each experimental run is graphed in Figure 7.5. In the 'Batch' culture the intracellular UDP-Gal was low and an actual presence was only detected on one day. Even at this low level UDP-Gal detection the GI was detected to vary between 0.8 on day 3 and 0.56 on day 7. In the 'NS' culture a slightly higher level of UDP-Gal was detected throughout the culture. However, this did not reflect in a higher GI – only a slightly higher maintenance from 0.79 on day 3 and 0.64 on day 7. Compared to the 'Batch' and 'NS' culture a significantly ($P < 0.02$) higher UDP-Gal concentration was seen in the 'Galactose' culture (Figure 6.1). This higher UDP-Gal concentration resulted in a higher GI (0.85). However, this high GI was not maintained and decreased to about 0.7 on day 6 and 7. In the 'UG' and 'UMG' culture similar UDP-Gal levels were detected as seen in the 'Galactose' culture. Yet, with similar levels of UDP-found the GI was further increased than what was observed in the 'Galactose' culture. As previously observed this led to significantly higher GI values on day 4 and 5 for the 'UG' and 'UMG' cultures compared to the 'Batch' and 'NS' cultures.

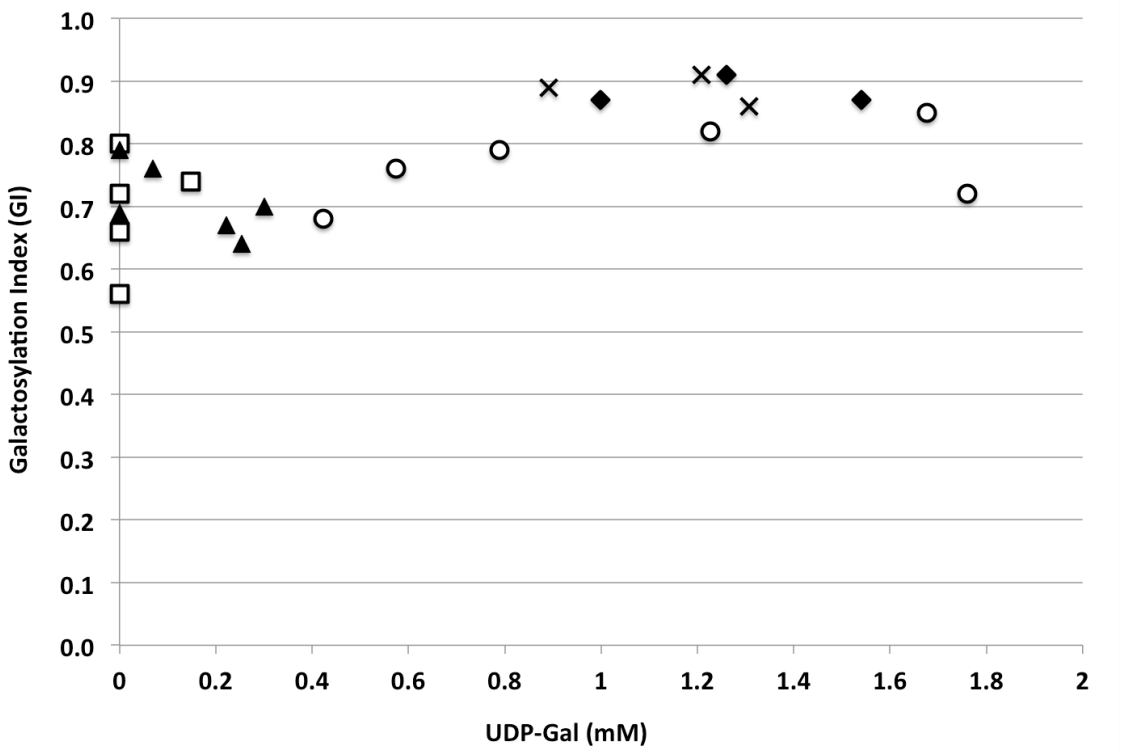

Figure 7.5: The UDP-Gal concentration versus the galactosylation index (GI) during the 'Batch' (□), 'NS' (▲), 'Galactose' (○), 'UG' (◆), and 'UMG' (×) fed-batch EG2 cultures.

7.2.3 Effects of the precursor feeding on the glycosylation of DP12

The effects of the nucleotide sugar precursors feeding in CHO-DP12 fed-batch cultures on the galactosylation of the antibodies produced are shown in Figure 7.6. The galactosylation observed in the precursor experiments was compared to the galactosylation observed in a 'Batch' and a regular fed-batch 'NS' culture. Each culture was inoculated at $2x10^5$ cells/mL in 250 mL shaker flasks at a final working volume of 80 mL. During the experiment the cultures were incubated at 37°C with a 10% CO_2 overlay on a shaker platform (120 rpm). At each sampling point 10 mL of supernatant were collected and filtered to remove the cells. The glycosylation of the antibody present in the supernatant was then analyzed as described in the methods (n = 2).

Figure 7.6 shows the galactosylation index (GI) (see Chapter 2.6.5.1) for each culture during the experiment. In all cultures the individual GI remained stable throughout the run. The lowest GI values were observed in the 'Batch' and 'NS' culture at 0.28 and 0.29, respectively. In the 'Galactose' culture the average GI increased to 0.33. A further increase was observed in the 'UG' and 'UMG' cultures with an average GI of 0.37 and 0.40, respectively. The increased GI in the 'UG' and 'UMG' cultures were found to be significantly higher ($P < 0.02$) than what was observed in the 'Batch' and 'NS' culture on days 4, 5, and 6.

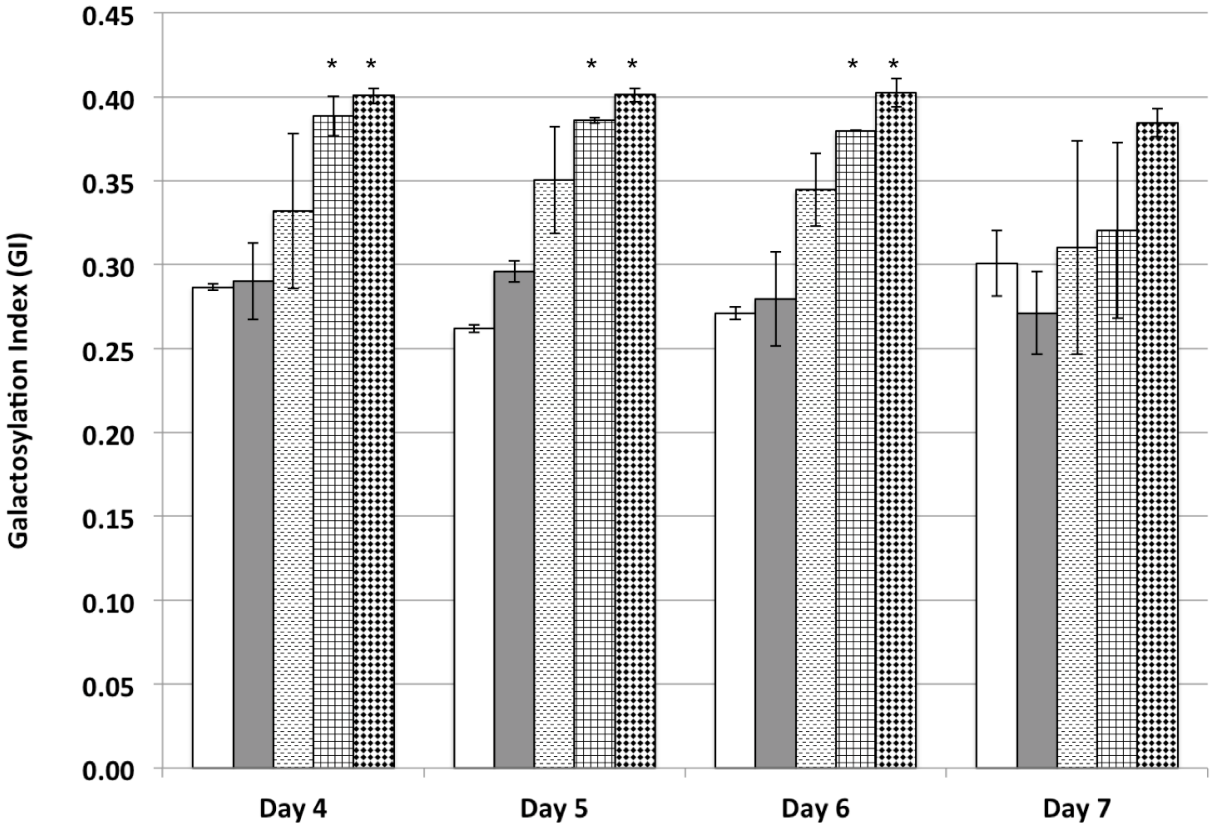

Figure 7.6: The galactosylation indices during a 'Batch' (▭), 'NS' (▭), 'Galactose' (▭), 'UG' (▭), and 'UMG' (▭) fed-batch DP12 cultures. (n = 2; error bars indicate the standard deviation)

* ($P < 0.02$) compared to the 'Batch' and 'NS' culture that day

Figure 7.7 shows the distribution and percentage of the different galactosylated glycan forms (i.e. G0, G1, and G2) that were used to calculate the overall GI during the bioprocess. The percentage of G0 in each culture during the bioprocess is shown in Figure 7.7 (A). As seen in the GI values the individual percentage of G0 glycoforms in each culture did not vary much over time. The highest average percentage of G0 glycoforms at 52.3% and 50.3% was observed in the 'Batch' and 'NS' cultures, respectively. The 'Galactose' culture showed a slightly lower average G0 content at 43.6%. Compared to the 'Batch' and 'NS' culture a lower content was found in the 'UG' and 'UMG' culture at 39.9% and 36.3%, respectively. On day 4, 5, and 6 the G0 content in both the 'UG' and the 'UMG' culture was significantly lower ($P < 0.02$) compared to the 'Batch' culture. On day 5 the G0 content in the 'UG' and 'UMG' culture was also significantly lower ($P < 0.02$) compared to the 'NS' culture. The G1 content in all cultures is shown in Figure 7.7 (B). As observed in the G0 content the average G1 content in each culture stayed stable during the bioprocess. The lowest average in the G1 content was seen in the 'Batch' and 'NS' culture at 39.4% and 42.5%, respectively. A slightly higher G1 content was observed in the 'Galactose', 'UG', and 'UMG' cultures at 45.8, 46.4, and 47.9%, respectively. For the 'UMG' culture the G1 content seemed to slightly increase over time. On day 5 and 6 the G1 content was significantly higher ($P < 0.02$) than the G1 determined for the 'Batch' and 'NS' cultures. Figure 7.7 (C) shows the percentage of the G2 glycans present in each culture during the bioprocess. As previously seen with the other glycoforms the 'Batch' and 'NS' culture contained a stable average G2 content during the experiment at 8.3 and 7.2%, respectively. These values also represented the lowest average G2 percentages found. The 'Galactose' culture had an average G2 content of 10.5% throughout the run. In the 'UG' and 'UMG' cultures a decrease from 16 to 10% and from 17 to 14% in the G2 content was found during the respective

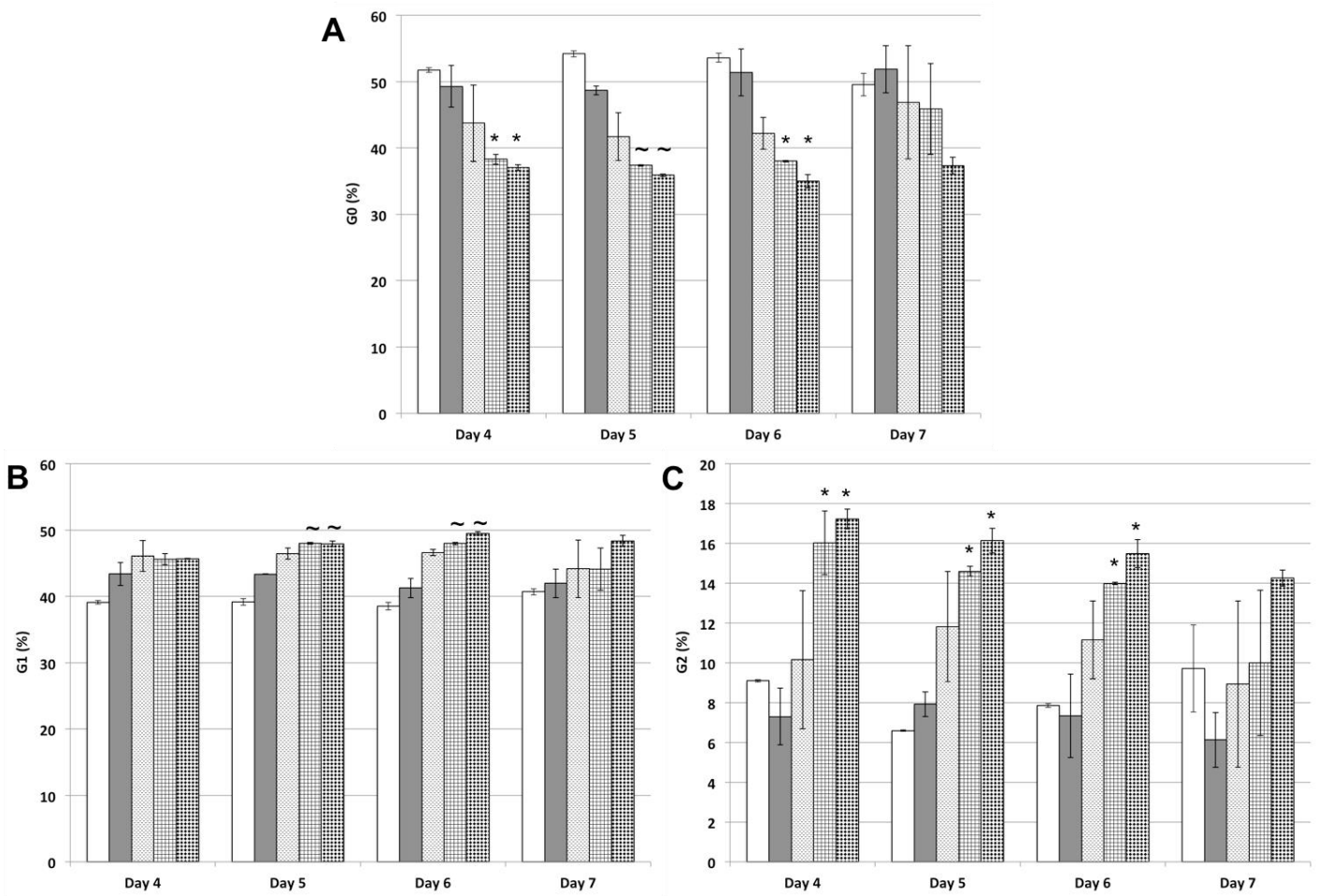

Figure 7.7: The distribution of galactosylation forms present during the 'Batch' (▭) and 'NS' (▭), 'Galactose' (▭), 'UG' (▭), and 'UMG' (▭) fed-batch DP12 cultures. (n = 2; error bars indicate the standard deviation)

* ($P < 0.02$) compared to the 'Batch' culture that day

~ ($P < 0.02$) compared to the 'Batch' and 'NS' cultures that day

run. On day 4, 5, and 6 a significantly higher ($P < 0.02$) G2 content was found in the 'UG' and 'UMG' cultures compared to the 'Batch' culture.

Figure 7.8 shows the fucosylation index (FI) (see Chapter 2.6.5.2) for each culture throughout the bioprocess. In all cultures a decline in the FI was observed starting on day 6. In the 'Batch' culture the FI decreased from 1.0 to 0.86. A lower decrease from 1 to 0.94 and 0.93 was observed in the 'NS' and 'Galactose' cultures, respectively. The lowest decrease was observed in the 'UG' and 'UMG' cultures. On day 7 the FI for the 'Batch' culture was significantly lower ($P < 0.02$) than the FI for all other cultures.

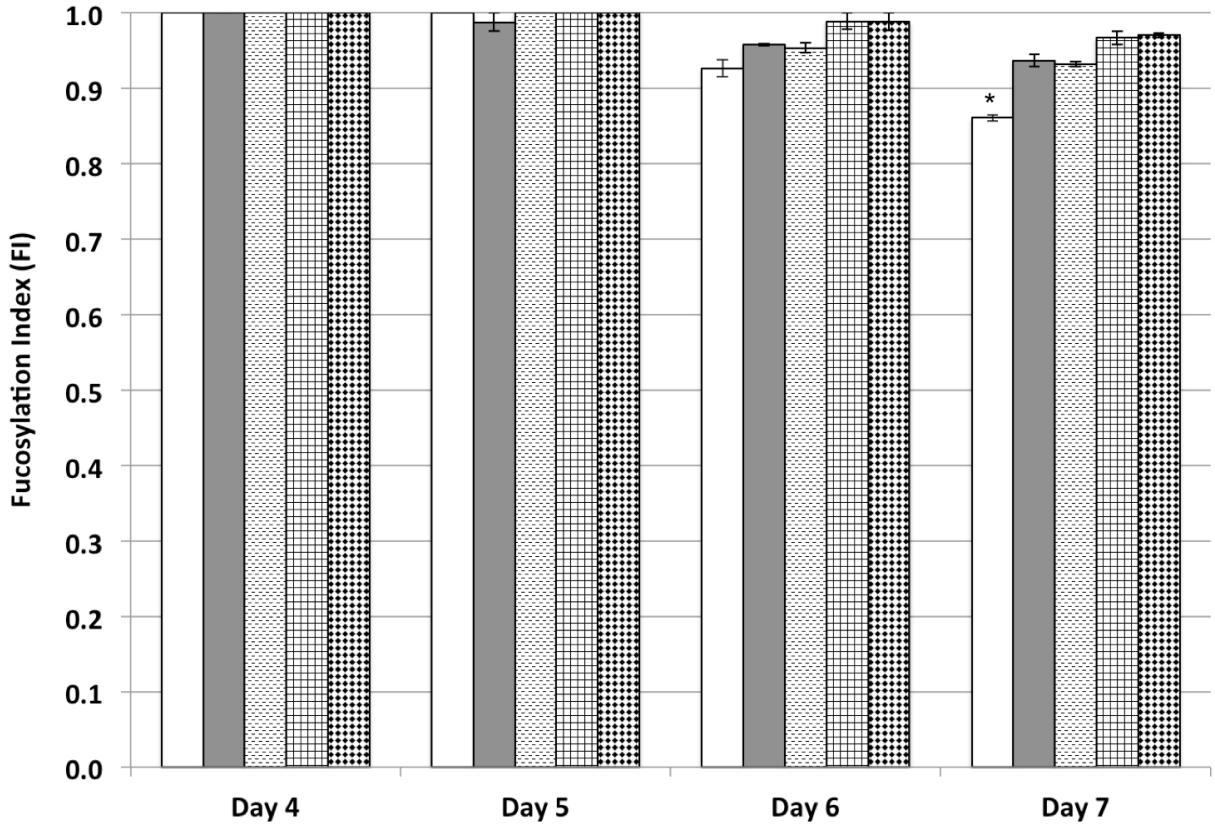

Figure 7.8: The fucosylation indices during the 'Batch' (▭), 'NS' (▭), 'Galactose' (▭), 'UG' (▭), and 'UMG' (▭) fed-batch DP12 cultures. (n = 2; error bars indicate the standard deviation)

* ($P < 0.02$) compared to all other cultures that day

The change in the sialylation index (SI) (see Chapter 2.6.5.3) over time for each culture is shown Figure 7.9. The overall sialylation of DP12 was very low and barely detectable. The 'Batch' culture showed a stable SI of 0.012 with no detectable sialylation on day 5. In the 'NS' culture sialylation was only detected at day 6 (0.005). A similar low level was observed in the 'Galactose' culture. Higher sialylation values were determined for the 'UG' and 'UMG' cultures. However, in the 'UG' and 'UMG' cultures the SI decreased from 0.03 to 0.005 and from 0.04 to 0.01, respectively, over the course of the experiment.

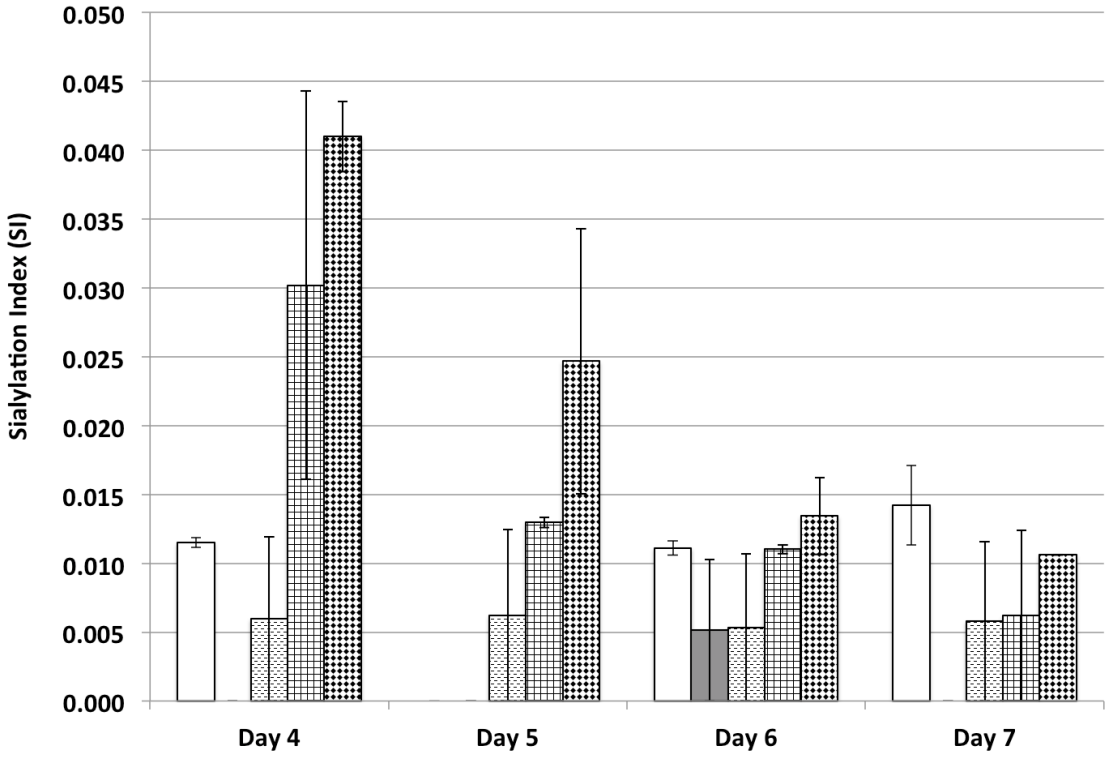

Figure 7.9: The sialylation indices during the 'Batch' ( ), 'NS' ( ), 'Galactose' ( ), 'UG' ( ), and 'UMG' ( ) fed-batch DP12 cultures. (n = 2; error bars indicate the standard deviation)

Overall, the addition of UG and UMG precursor combinations to the CHO-DP12 culture was able to increase and maintain the GI over the time observed. This increase was mainly

observed due to the shift from the G0 to the G1 and G2 glycoforms. In addition, the 'UG' and 'UMG' cultures showed a stable FI for the days observed. An increase in the SI was seen initially with the addition of UG and UMG, but it was not maintained over time. The addition of galactose alone was also able to increase the GI of the DP12 sample, but not to the extent observed in the 'UG' and 'UMG' culture. The addition of galactose resulted in a lower decrease in the FI and a low but stable SI. While the GI remained stable in the 'Batch' and 'NS' culture, the FI showed a decrease over time.

7.2.4 The correlation of the intracellular UDP-Gal pool on the protein galactosylation in DP12 cultures.

The UDP-Gal concentration versus the GI for each experimental run is graphed in Figure 7.10. In the 'Batch' culture the intracellular UDP-Gal was too low to be detected. At this low level the GI was determined at 0.29. In the 'NS' culture UDP-Gal was only detected on day 7 of the culture. However, this did not reflect in a higher GI, which remained on average at 0.29. Compared to the 'Batch' and 'NS' cultures a higher UDP-Gal concentration was seen in the 'Galactose' culture (Figure 6.6). This higher UDP-Gal concentration resulted in a higher GI at 0.35 on day 5 and 6. In the 'UG' and 'UMG' cultures even higher UDP-Gal levels were detected. This increase in the UDP-Gal concentration was also correlated with a significant increase ($P < 0.02$) in the GI to 0.39 compared to the 'Batch' and 'NS' cultures.

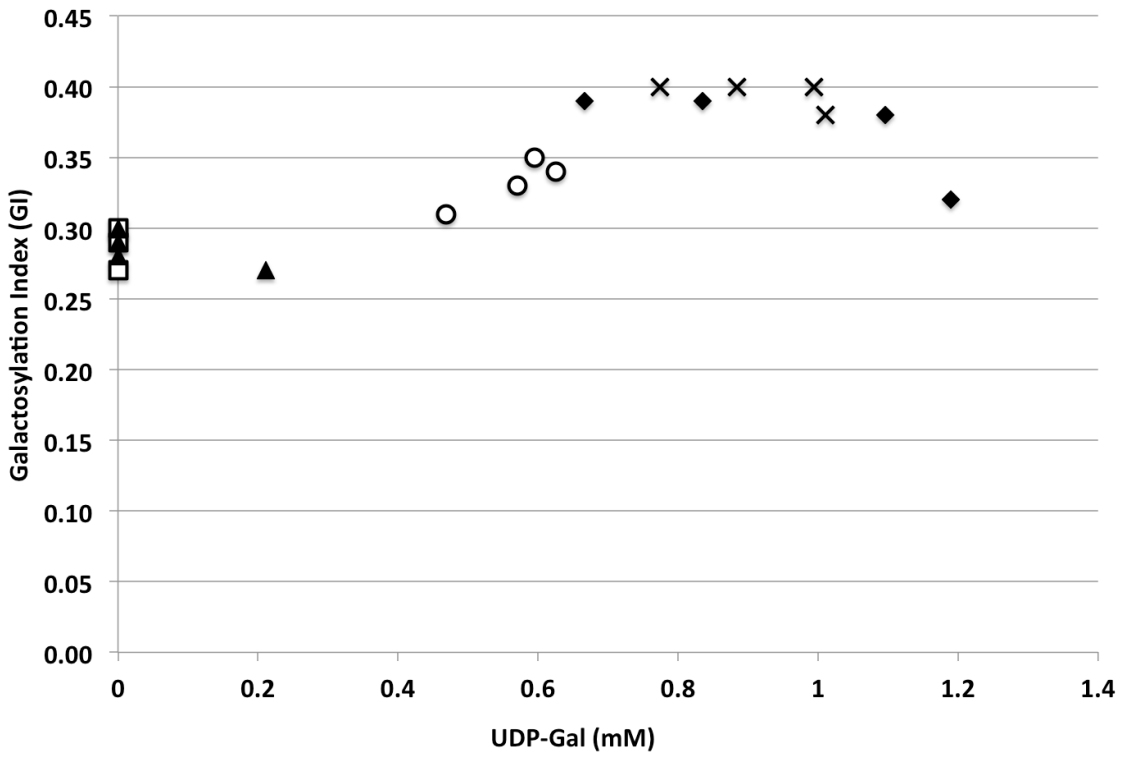

Figure 7.10: The UDP-Gal concentration versus the galactosylation index (GI) during the 'Batch' (□), 'NS' (▲), 'Galactose' (○), 'UG' (◆), and 'UMG' (×) fed-batch DP12 cultures.

7.2.5 Comparison of effects in EG2 and DP12 cultures.

The overviews of the precursor feeding effects on the glycosylation are summarized in Figure 7.11-7.14

In Figure 7.11 the impact of the precursors feedings on the GI in both cultures is shown. It is notable that the GI decreased in the EG2 'Batch', 'NS' and 'Galactose' cultures over time while it remained stable in all other cultures for the EG2 cell line and all DP12 cultures. For both the EG2 and DP12 cultures a small increase in the GI was observed in the 'NS' compared to the 'Batch' culture. By adding galactose to the culture an additional increase of 8.5% and 17.8% was observed for the EG2 and the DP12 culture, respectively. Another increase in the GI compared to the 'Control' was seen after adding galactose in combination with uridine to both

the EG2 and DP12 culture at 23.9% and 21.6%, respectively. By additionally adding manganese to the UG combo the GI was further increased compared to the 'NS' by 25.4% and 37.9% for the EG2 and the DP12 culture, respectively. In the EG2 culture this increase in GI was mainly due to an increase in the G2 and G3 glycoforms for both the 'UG' and 'UMG' cultures. However, in the DP12 culture the increase in the 'UG' and 'UMG' cultures was due to an increase in the G1 and G2 glycoforms.

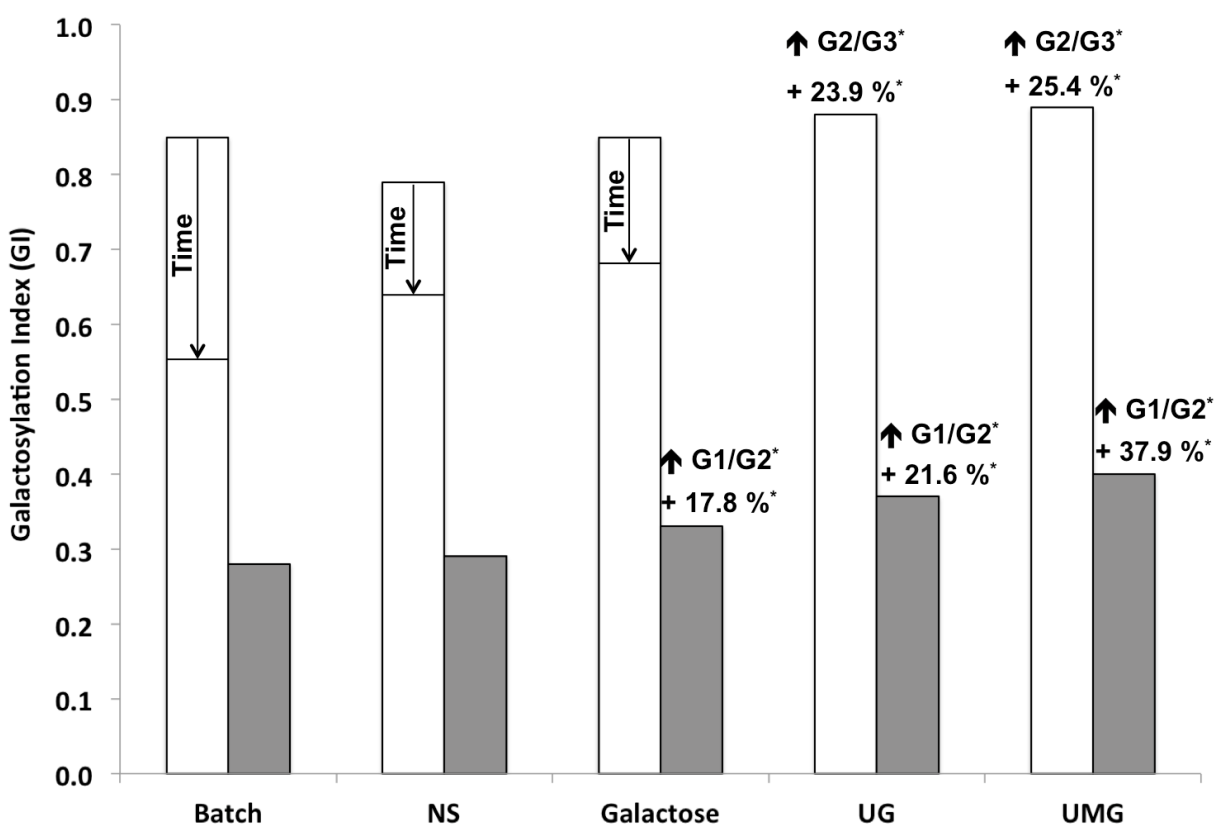

Figure 7.11: Comparison of the effect of the nucleotide sugar precursor feedings on the galactosyaltion index in CHO EG2 (▭) and DP12 (▬) cultures.

***** Increase compared to respective 'NS' culture

Figure 7.12 shows the effect the precursor feedings had on the fucosylation in both cell lines. In the 'Batch' culture the FI decreased over time in the both cell lines. In addition, the FI

also decreased in the DP12 'NS' and 'Galactose' cultures. For all other DP12 cultures the FI only decreased marginally with the highest daily FI detected in the DP12 'UG' and 'UMG' cultures. Under the same conditions the EG2 culture resulted in a lower (0.95 and 0.94) but stable FI.

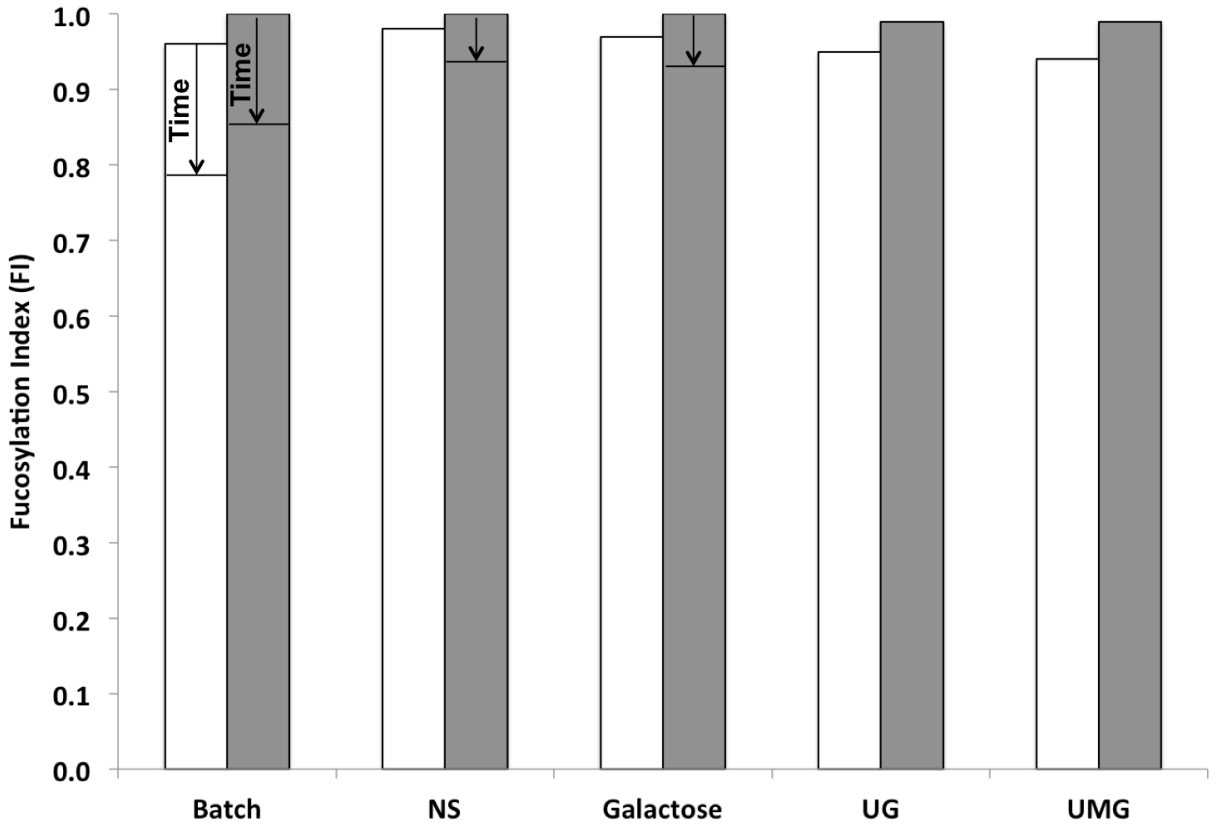

Figure 7.12: Comparison of the effect of the nucleotide sugar precursor feeding on the fucosylation index in CHO EG2 (▭) and DP12 (▬) cultures.

The comparison of the sialylation index in the two cell lines for this study is shown in Figure 7.13. While the SI decreased in the EG2 'Batch', 'NS', and 'Galactose' cultures, it remained stable in those DP12 cultures. On the other hand, the DP12 'UG' and 'UMG' cultures

showed a decreasing SI during the bioprocess while the same cultures remained stable in the CHO-EG2 cultures.

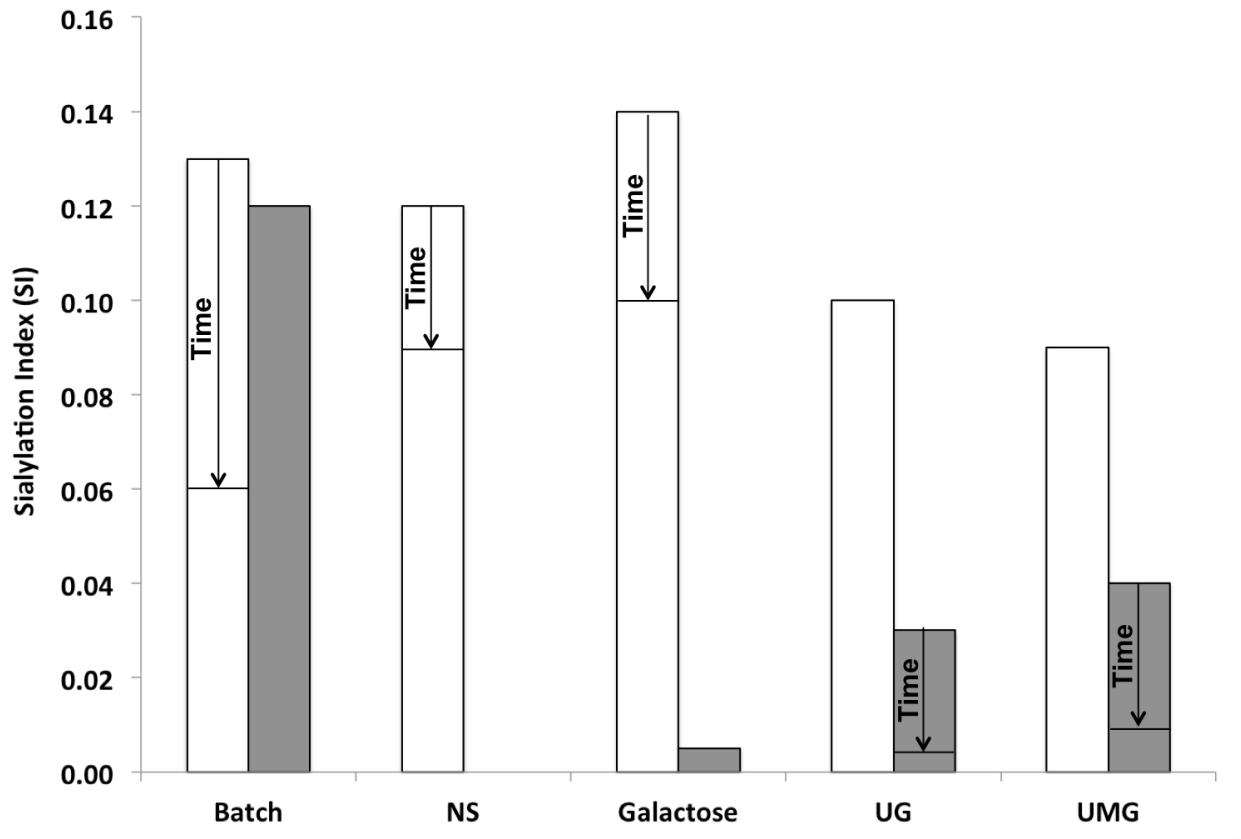

Figure 7.13: Comparison of the effect of the nucleotide sugar precursor feeding on the sialylation index in CHO EG2 (▭) and DP12 (▬) cultures.

The correlation between the intracellular UDP-Gal concentration and the respective galactosylation index for both cell lines are shown in Figure 7.14. In both cell lines the UDP-Gal concentration and GI increased through the addition of galactose. In addition, a further increase in UDP-Gal (in CHO DP12) and GI (both cell lines) was observed when adding uridine + galactose together. While, the addition of manganese did not show a further increase in UDP-Gal a small increase in the GI was observed in both cell lines.

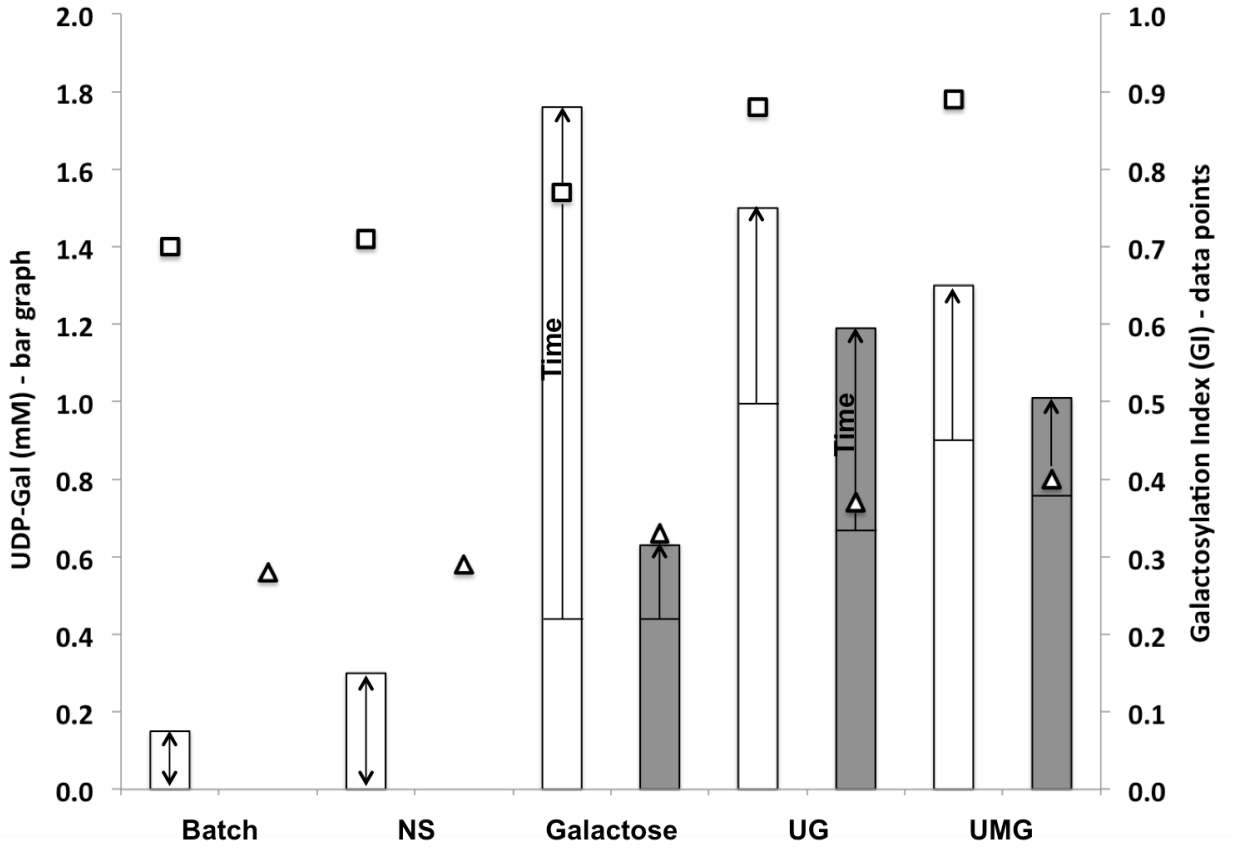

Figure 7.14: Comparison of the effect of the intracellular UDP-Gal pool on the galactosyaltion index in CHO EG2 (▭) and DP12 (▬) cultures.

7.3 Discussion

The objective of this study was to determine the effect of the precursor feedings and the connected intracellular nucleotide sugar pool – especially UDP-Gal – on the antibody glycosylation in two CHO cell lines. A special interest was the change in the galactosylation of two antibodies with a different initial galactosylation index (GI).

Previous studies showed that the addition of galactose, uridine, and manganese in different cell lines, producing different glycoproteins showed varying results without going further into the differences between the cell lines. In this study both cell lines experienced an

increase in the intracellular UDP-Gal concentration, which is the building block necessary for the galactosylation process. As shown in Chapter 6 this increase is caused by the addition of galactose to the basal and feed medium. The further addition of uridine led to a consistent increase in the UDP-Gal concentration throughout the experiment by providing the necessary UTP for galactose activation.

Both antibodies experienced an increase in the galactosylation index when nucleotide sugar precursors were added to the medium. The increase in the GI with the addition of galactose, UG and UMG has previously been shown by other research groups (Kildegaard et al., 2015; Gramer et al., 2011; Wong et al., 2010; Grainger and James, 2013). The increase observed in the EG2 culture from 0.71 in the 'NS' to 0.89 in the 'UMG' culture is comparable with observations done by Liu et al. (2014) in CHO-EG2 batch cultures. While the DP12 culture exhibited a rather low GI in the 'NS' culture (0.29) the UMG feeding strategy allowed for an increase up to a GI value of 0.4. This also agreed with findings by Liu et al. (2014). The large discrepancy in the GI determined for the EG2 and the DP12 glycan pool could be caused by a steric hindrance that would cause difficulty for the galactosyltransferase to add galactose to the glycan in the Fc region of DP12 (Hills et al., 2001; Wormald et al., 1997). It is currently assumed that two mutations in the Fc region of the EG2 molecule could be creating a better access for the galactosyltransferase compared to the DP12.

Another important aspect in the bioprocess is not only the control of the galactosylation of product but also to maintain it throughout the bioprocess. During the experiments it was observed that the GI of the EG2 culture decreased over time in the 'Batch', 'NS', and 'Galactose' culture, while the same cultures for the DP12 cell line were able to maintain their GI. For the 'UG' and 'UMG cultures both cell lines showed increased GI values compared to the

'NS' culture that could be maintained throughout the bioprocess. A similar observation was made by Grainger and James (2013) and Gramer et al. (2011). Furthermore, consistent with the observations in this study Gramer et al. (2011) showed that the addition of UMG at a variety of concentrations did not only show a stabilization of the galactosylation in a culture but even its increase. The stable GI observed in the 'Batch', 'NS', and 'Galactose' cultures of the DP12 cell lines could be explained by the overall low galactosylation, which can be increased and maintained without problems by the cell even with low UDP-Gal concentrations. On the other hand the high starting GI found in the EG2 cultures can only be maintained with a consistent high UDP-Gal concentration – as observed in the 'UG' and 'UMG' cultures.

The galactosylation was not further increased when manganese was added to the EG2 culture. However, in the DP12 culture the addition of manganese further improved the galactosylation showing a synergistic effect as seen by Gramer et al., (2011). Based on the original GI in the DP12 cell line a shift in G0F to G1F and secondarily to G2 and G2F was seen - as observed by Gramer et al. (2011). Since the EG2 culture already had a high GI a shift from G1F to G2 and G2F and secondarily to G3 was observed.

In both cell lines a general decrease in the fucosylation was observed in the 'Batch' culture. Less of a decline was observed in all other cultures with the lowest decline in the 'Galactose' and 'NS' in the EG2 culture and the 'UG' and 'UMG' in the DP12 cultures. Previous studies found that the fucosylation was not affected by low concentration precursor feedings (Kildegaard et al., 2015; Gramer et al., 2010). However, Gramer et al. (2010) found that as the UMG concentration increased a negative effect on the fucosylation was observed. This finding agrees with the observations made for the EG2 experiments while the observations

in the DP12 experiments show a positive effect of UG and UMG feedings on maintaining the fucosylation.

For EG2 a decrease in the sialylation was seen over time in the 'Batch' culture. A slight decrease was also observed in the 'NS' and 'Galactose' cultures, while the sialylation in the 'UG' and 'UMG' cultures were constant but lower than seen in the other cultures. Similar observations towards less sialylated species were made by Wong et al. (2010). The decrease of sialylation in the 'UG' and 'UMG' as well as all others cultures could be partially explained with the increased UDP-GlcNAc content that competes with the CMP-Neu5Ac transport into the Golgi. On the other hand a high sialylation was observed in the beginning of the 'UG' and 'UMG' DP12 cultures, which then decreased over time. This decrease is also correlated to the UDP-GlcNAc competition with CMP-NeuAc as UDP-GlcNAc accumulated over time.

Previous work by Wong et al. (2010) showed that the addition of galactose increased the UDP-Gal concentration in the CHO cell line used. Wong and colleagues also showed that the feeding of galactose in combination with uridine did not further increase the UDP-Gal concentration but did cause a shift in galactosylated species to less sialylated forms. In this work the relationship between the intracellular UDP-Gal concentration and the GI index showed that an initial increase in the UDP-Gal increased the GI. As shown by Wong et al. (2010) in both cell lines the addition of galactose led to an increase in the UDP-Gal concentrations. However, opposite of Wong's results (2010) the addition of uridine and manganese further increased the UDP-Gal concentration in the DP12 'UG' and 'UMG' cultures. Even though the UDP-Gal concentration wasn't further increased in the EG2 culture fed with UG and UMG the GI was slightly increased compared to the 'Galactose' culture. However, since the GI in the 'UMG' EG2 culture was not significantly different to the 'UG' culture it can be assumed that the

additive effect was from the uridine in the EG2 cell line. At the concentration used the manganese did not show a positive impact on the galactosylation in the EG2 culture. In the DP12 cell line the feeding of UG and UMG in combination not only increased the GI but also the UDP-Gal concentration. This indicates that UTP could have been limiting in all other DP12 cultures for the activation of galactose. Hence an increased UDP-Gal pool can be achieved with the addition of uridine as precursor for UTP. In both cell lines a maximum plateau (GI) was reached with the addition of the UG and UMG feeding strategies. Similar plateaus were observed by Gramer et al. (2011) who saw that increasing the UMG concentrations at some point did not further increase the GI. Since the further increased UDP-Gal concentration was not able to promote the increase of the GI, this could be the maximum GI for the respective antibodies under these conditions. With a high UDP-Gal this plateau could be caused by a sterical hindrance in the Fc region hindering the access of the galactosyltransferase or the lack of galactosyltransferase.

7.4 Conclusion

The results of this experiment demonstrate that the addition of galactose alone was able to increase the UDP-Gal concentration and GI in both cell lines but was not able to maintain the GI over time for the highly galactosylated antibody. By feeding uridine in combination with galactose the GI was maintained in both cell lines with a further increase in the UDP-Gal concentration in the DP12 cell line. This showed that uridine was needed in this particular cell line for galactose activation. Adding manganese to the feed allowed for an additional increase in the GI of the DP12 antibody indicating the increase of the galactosyltransferase activity by manganese. The highest increase in the GI for both antibodies compared to the 'NS' culture was

observed in the UMG culture at 25.4% and 37.9% in the EG2 and DP12 culture, respectively. Results also showed that the addition of uridine was able to support the DP12 cell line in the high fucosylation maintenance. Overall the data support the differences seen among cell lines and the effect precursor feedings have on the respective product glycosylation. In both cell lines a threshold limit exists after which a further increase in the UDP-Gal concentration is not correlated to an increase in the galactosylation index under these experimental conditions.

Section B

Summary

Glycosylation is an important part of the secondary post-translational modification of recombinant proteins as the glycan structure has a great impact on the proteins' stability, solubility, and efficacy. Hence the study of glycosylation is important to understand how the glycosylation profile of a recombinant protein can be altered and / or maintained. While many factors can influence the glycosylation profile, the addition of nucleotide sugar precursors has shown to increase certain glycosylation building blocks. These building blocks are part of the nucleotide / nucleotide sugar metabolism, which also contains many metabolites involved in the energetics of the cell. Therefore, it is important to take a more global approach to look at the impact of the precursor feedings on the nucleotide sugar metabolism and subsequent glycosylation.

As the first step in this study the effects of the nucleotide sugar precursors galactose, uridine, and $MnCl_2$ on the cell growth and metabolism of the two cell lines was studied in fed-batch cultures. It was demonstrated that based on the genetic make-up of the cell line the addition of certain precursors – in this case uridine – can have a negative effect on the growth while the viability is maintained. It was also demonstrated that the switch from a batch to a fed-batch culture in general was able to increase the volumetric productivity.

Furthermore the impact of the precursors feedings on the actual glycan building blocks and energy nucleotides was analyzed. Here it was shown that for both cell lines the addition of galactose increased the UDP-Gal pool. This intracellular pool was additionally increased in the DP12 when uridine was added, indicating that UTP is limiting for galactose activation under

normal circumstances. When looking at the energy metabolites – especially the AEC value a continuing decline in the DP12 cultures was seen. This decline was associated with the hypoxanthine present in the regular growth medium. Since the DHFR pathway is not compromised in this cell line the addition of hypoxanthine might have led to an increased level or uric acid in the cells. This increase has previously been connected with changes in the mitochondria and a drop in ATP production.

Lastly a look at he final glycosylation profile of the antibodies of interest showed that while the sole addition of galactose was able increase the GI it was not enough to maintain it over time. However, in combination with uridine the GI was further enhanced and more importantly maintained. In both the EG2 and DP12 culture the GI was increased by 25.4 and 37.9%, respectively, with the addition of precursors to the medium. Nonetheless, the GI could not be increased infinitely as both cell lines exhibited an individual limit for the conditions tested. Furthermore, it was demonstrated that the change from a batch to a fed-batch culture allowed for a better maintainance of the fucosylation in both cell lines.

Chapter 8

Conclusion and Future Work

8.1 Conclusion

During this study, I looked at two important aspects in cell culture monitoring. In the first part of the study I evaluated the use of dielectric measurements to analyze and characterize mammalian cells by comparing them to more commonly used cell density and viability measurements. In biopharmaceutical production it is desirable to extend the duration of a bioprocess to increase the volumetric productivity. Hence, the early detection of cell demise can be useful as these stages may be reversible by an appropriate feeding strategy. However, the right cell culture media composition and feeding strategy is not only important for cell viability but also for the maintaince of the quality of the protein produced by the cell. Thus, in the second part of this study I evaluated the effect of nucleotide / nucleotide sugar precursor feedings on the biopharmaceutical production and glycosylation process.

Both bulk and single cell dielectric measurements are able to detect changes in the cytoplasm conductivity and cell membrane capacitance. This results in the faster detection of cell decline than seen using the trypan blue exclusion method (Braasch et al., 2013). In addition it was shown that the DEP cytometer is able to detect any changes with a higher sensitivity including rare events that might otherwise be masked by the culture. The DEP cytometer can be more sensitive because single cells are analyzed by their displacement in an electrical field with sensitivity of 0.1 μm and at a rate of 5 cells per second. This allows the detection of small changes in dielectric properties enabling multiple subpopulations to be monitored. Hence, the device has the potential of a low-cost, label-free, electronic monitor of physiological changes in

cells. This work also emphasizes and supports the need for single cell dielectric analysis methods to detect rare events in a bioprocess (See Section 4.2.4).

In the batch cultures grown in a controlled bioreactor the decline in cell health was associated with a drop in the AEC value. This drop was related to substrate deprivation towards the end of the culture. However, the cell culture media composition does not only have an impact on cell health but also plays an important part in the glycosylation process. In addition, a loss in cell viability can cause cells to release glycosidases, which have a negative effect on the final protein quality. Hence it is important to look at the overall glycosylation process when assessing media components. While some aspects of the process have been elucidated the process is quite complex and hence difficult to understand or predict. Especially since different cell lines and products are known to show different results.

In the second part of this study I further elucidated some aspects in the glycosylation process by not only looking at the final glycan profile after nucleotide sugar precursor feeding but by also looking at the overall nucleotide sugar profile, cell growth, viability, and productivity in two cell lines producing two very different antibodies. It was shown that additions to the basal or feed medium have a variety of consequences. Hence all these factors should be studied together to determine the best strategy for the recombinant protein of interest. In this case the removal of uridine or a feeding strategy including a later addition of uridine or less frequent feeding might be of interest to maintain growth but also increase and maintain the GI in the EG2 cell lines. The addition of manganese also does not seem needed in this cell line and therefore could be omitted. For the DP12 cell line the hypoxanthine should be removed from the medium to see if the removal will improve the energetic state of the cell. However, the feeding of uridine, galactose, and manganese should be maintained as it resulted in the highest GI for this

antibody. This emphasizes and supports the need for detailed metabolic analysis in the process development.

The achievements of these studies were the elucidation of the dielectric measurements used for cell viability determination and the further understanding of their potential in the detection of changes within the cell (Braasch et al., 2013; Saboktakin-Rizi et al., 2014). This early detection is important in process development to better understand the reason for cell demise so that changes can be made to the process. One of the changes that can be made is the improvement of the cell culture medium to provide optimal conditions for growth and protein glycosylation. The information obtained from the precursor feeding experiments showed that certain additions allowed for glycosylation to be improved and maintained during the bioprocess. However, it also showed that precursors can reach saturation and that some additives such as uridine could have a negative impact on certain cell lines based on their genetic make-up. These aspects need to be taken into consideration to create a medium optimal for growth and production without feeding unnecessary components or unnecessary high concentrations.

8.2 Future Work

8.2.1 Dielectric Measurements

In this work the dielectric measurements for batch and apoptosis cultures have been correlated to changes in the ionic content of the cells. To verify that these changes in the cytoplasm are correlated with the dielectric measurements it would be beneficial to monitor the ion content in the cells and supernatant. This could be done by taking a cell and supernatant sample at each time point to determine the intra- and extracellular ion content.

It would also be interesting to see if starvation and rescue experiments can be performed. It has been shown that dielectric measurements are able to determine cell demise early on and it has been suggested that nutrient feeding could reverse the early stages of apoptosis. Hence, it could be tested whether the early detection can be used to control the feeding strategy. Apoptosis could be artificially induced by starvation. At different timepoints of the dielectric measurements nutrients could be added to the culture to determine if and how the cells dielectric properties change and if cells are able to return to normal growth.

Another important aspect for the dielectric measurements would be the use of another cell line. Seeing that the CHO-DP12 cell line showed a consistent drop in the AEC values and therefore ATP due to hypoxanthine, it would be interesting to see if and how its dielectric properties change throughout the bioprocess. It would also be interesting to compare the growth and dielectric properties of that cell line in the presence and absence of hypoxanthine.

8.2.2 Precursor Feeding

For future work regarding the precursor feeding experiments it would be interesting to explore whether the GI saturation reached in both cell lines is caused by steric hindrance in the Fc region of the antibody. The steric hindrance hypothesis could be tested by developing the protein structure using X-ray crystallography. The structure of both antibodies could then be compared to determine any structural differences in the Fc region.

Based on the assumption that the hypoxanthine in the medium was the reason for the drop in the AEC during the bioprocess, it would be beneficial to repeat the experiment with

medium lacking hypoxanthine. If the hypoxanthine was the reason for the drop in AEC it would be interesting to see if the nucleotide precursor feedings would have a different impact on cell growth and glycosylation.

References

Abu-Absi, S, Xu, S, Graham, H, Dalal, N, Boyer, M, Dave, K. (2014) Cell culture process operations for recombinant protein production: in Mammalian Cell Cultures for Biologics Manufacturing (ed. Weichang Zhou and Anna Kantardjief), 139: 35-68. Advances in Biochemical Engineering / Biotechnology. Springer.

Ahn WS, Antoniewicz MR. (2011) Metabolic flux analysis of CHO cells at growth and non-growth phases using isotopic tracers and mass spectrometry. Metabolic Engineering 13(5): 598–609.

Al-Rubeai M, Emery AN. (1993) Flow cytometry in animal cell culture. Nature Biotechnology 11: 572-579.

Altman SA, Randers L, Rao G. (1993) Comparison of trypan blue dye exclusion and fluorometric assays for mammalian cell viability determinations. Biotechnology Progress 9: 671–674.

St. Amand, MM, Radhakrishnan, D, Robinson, AS, Ogunnaike, BA. (2014) Identification of manipulated variables for a glycosylation control strategy. Biotechnology and Bioengineering 111: 1957-1970.

Ansorge S, Esteban G, Schmid G. (2010) On-line monitoring of responses to nutrient feed additions by multi-frequency permittivity measurements in fed-batch cultivations of CHO cells. Cytotechnology 62: 121–132.

Asami K, Takahashi Y, Takashima S. (1989) Dielectric properties of mouse lymphocytes and erythrocytes. Biochimica et Biophysica Acta (BBA) - Molecular Cell Research 1010: 49–55.

Atkinson AE. (1968) The energy charge of the adenylate pool as a regulatory parameter. Interaction with feedback modifiers. Biochemistry 7: 4030-4034.

Au J, Su M, Wientjes, G. (1989) Extraction of intracellular nucleosides and nucleotides with acetonitrile. Clinical Chemistry 35: 48-51.

Barnabe, N, Butler, M. (1994) Effect of temperature on nucleotide pools and monoclonal antibody production in a mouse hybridoma. Biotechnology and Bioengineering. 44: 1235-1245.

Barnabé N, Butler M. (1998) The relationship between intracellular UDP-N-acetyl hexosamine nucleotide pools and monoclonal antibody production in a mouse hybridoma. Journal of Biotechnology 60: 67-80.

Barnabé N, Butler M. (2000) The effect of glucose and glutamine on the intracellular nucleotide pool and oxygen uptake rate of a murine hybridoma. Cytotechnology 34: 47-57.

Bebbington CR, Renner G, Thomson S, King D, Abrams D, Yarranton GT. (1992) High-Level Expression of a Recombinant Antibody from Myeloma Cells Using a Glutamine Synthetase Gene as an Amplifiable Selectable Marker. Nature Biotechnology 10: 169–175.

Beckmann TF, Kraemer O, Klausing S, Heinrich T, Thuete T, Buentemeyer H, Hoffrogge R, Noll T. (2012) Effects of high passage cultivation on CHO cells: A globalanalysis. Applied Microbiology and Biotechnology 94: 659-671.

Bell A, Wang ZJ, Arbabi-Ghahroudi M, Chang TA, Durocher Y, Trojahn U, Baardsnes J, Jaramillo ML, Li S, Baral TN, O'Connor-McCourt M, MacKenzie R, Zhang J. (2010) Differential tumor-targeting abilities of three single-domain antibody formats. Cancer Letters 289: 81-90.

Bitbol, M, Fellman, P, Zachowski, A, Devaw, PF. (1987) Ion regulation of phosphatidylserine and phosphatidylethanolamine outside-inside translocation in human erythrocytes. Biochimica et Biophysica Acta 904: 268.

Bortner CD, Cidlowski JA. (2003) Uncoupling cell shrinkage from apoptosis reveals that Na+ influx is required for volume loss during programmed cell death. Journal of Biological Chemistry 278: 39176–84.

Bortner CD, Scoltock AB, Sifre MI, Cidlowski JA. (2012) Osmotic stress resistance imparts acquired anti-apoptotic mechanisms in lymphocytes. Journal of Biological Chemistry 287: 6284–95.

Bortner CD, Cidlowski JA. (2002) Apoptotic volume decrease an the incredible shrinking cell. Cell Death and Differentiation 9: 1307–1310.

Braasch, K, Nikolic-Jaric, M, Cabel, T, Salimi, E, Bridges, GE, Thomson, DJ, Butler, M. (2013), The changing dielectric properties of CHO cells can be used to determine early apoptotic events in a bioprocess. Biotechnology and Bioengineering 110 (11): 2902-2914.

Breen, GAM, Scheffler, IE. (1980) Cytoplasmic inheritance of oligomycin resistance in Chinese hamster ovary cells. The Journal of Cell Biology 86: 723-729.

Browne SM, Al-Rubeai M. (2011) Defining viability in mammalian cell cultures. Biotechnology Letters 33:1749.

Budihardjo I, Oliver H, Lutter M, Luo X, Wang X. (1999) Biochemical Pathways of Caspase Activation During Apoptosis. Annual Review of Cell and Developmental Biology 15: 269–290.

Burgener A, Coombs K, Butler M. (2006) Intracellular ATP and total adenylate concentrations are critical predictors of reovirus productivity from Vero cells. Biotechnology and Bioengineering 94: 667-679.

Butler M. (1988) Processes with animal cell and tissue culture. In: Biotechnology V.6b H. J. Rehm and G. Reed (eds.) VCH Verlagsgesellschaft, Weinheim pp.250-316.

Butler M, Jenkins N. (1989) Nutritional aspects of growth of animal cells in culture. Journal of Biotechnology 12: 97-110.

Butler M. (2005) Animal cell cultures: recent achievements and perspectives in the production of biopharmaceuticals. Applied Microbiology and Biotechnology 68: 283–291.

Butler M. 2006. Optimisation of the cellular metabolism of glycosylation for recombinant proteins produced by mammalian cell systems. Cytotechnology 50: 57–76.

Butler M. (2009) Mammalian Cell Lines and Glycosylation: A Case Study, in: G. Walsh (Eds.) Post-translational Modification of Protein Biopharmaceuticals. Wiley-VCH Verlag GmbH & Co. KGaA, Weinheim, pp. 51-77.

Butler, M, Spearman, M, Braasch, K. (2014) Monitoring cell growth, viability and Apoptosis. in Animal Cell Biotechnology – Methods and Protocols (ed. Ralf Poertner), 1104: 169-192. Methods in Molecular Biology. Humana Press.

Caradonna, SJ, Cheng, YC. (1980) The role of deoxyuridine triphosphate nucleotidohydrolase, uracil-DNA glycosylase, and DNA polymerase alpha in the metabolism of FUdR in human tumor cells. Molecular Pharmacology 18: 513–520.

Caro-Maldonado, A, Munoz-Pineda, C. (2011) Dying for something to eat: How cells respond to starvation. The Open Cell Signaling Journal. 3: 42-51.

Carvell JP, Dowd JE. (2006) On-line Measurements and Control of Viable Cell Density in Cell Culture Manufacturing Processes using Radio-frequency Impedance. Cytotechnology 50: 35–48.

Cemazar J, Vrtavcnik D, Amon S, Kotnik T. (2011) Dielectrophoretic Field-Flow Microchamber for Separation of Biological Cells Based on Their Electrical Properties. IEEE Transactions on nanobioscience 10.

Cho, JW, Balasubramanyam, M, Chernaya, G, Gardner, JP, Aviv, A, Reeves, JP, Dargis, PG, Christian, EP. (1997) Oligomycin inhibits store-operated channels by a mechanism independent of its effect on mitochondrial ATP. Biochemistry Journal 324: 971-980.

Clark KJR, Griffiths J, Bailey KM, Harcum SW. (2005) Gene-expressionprofiles for five key glycosylation genes for galactose-fed CHO cellsexpressing recombinant IL-4/13 cytokine trap. Biotechnolology and Bioengineering 90: 568–577.

Crowell CK, Grampp GE, Rogers GN, Miller J, Scheinman RI. (2007) Amino acid and manganese supplementation modulates the glycosylation state of erythropoietin in a CHO culture system. Biotechnolology and Bioengineering 96: 538–549.

Cruz HJ, Freitas CM, Alves PM, et al. (2000). Effects of ammonia and lactate on growth, metabolism, and productivity of BHK cells. Enzyme and Microbial Technology 27: 43–52.

Curi R, Lagranha CJ, Doi SQ, Sellitti DF, Procopio J, Pithon-Curi TC et al (2005) Molecular mechanisms of glutamine action. Journal of Cell Physiology 204: 392–401.

Curling, EMA, Hayter, PM, Baines, AJ, Bull, AT, Gull, K, Strange, PG, Jenkins, N. (1990) Recombinant human interferon-gamma – differences in glycosylation and proteolytic processing lead to heterogeneity in batch culture. Biochemical Journal 272: 333-337.

Dalili, M, Sayles, GD, Ollis, DF. (1990) Glutamine-limited batch hybridoma growth and antibody production: experiment and model. Biotechnolology and Bioengineering 36: 74-82.

Demierre N, Braschler T, Muller R, Renaud P. (2008) Focusing and continuous separation of cells in a microfluidic device using lateral dielectrophoresis. Sensors and Actuators B 132: 388–396.

Dietmair, S, Timmins, N, Gray, P, Nielsen, L, Krömer, J. (2010) Towards quantitative metabolomics of mammalian cells: Development of a metabolite extraction protocol. Analytical Biochemistry 404: 155-164.

Dorai H, Kyung YS, Ellis D, Kinney C, Lin C, Jan D, Moore G, Betenbaugh MJ. (2009) Expression of anti-apoptosis genes alters lactate metabolism of Chinese hamster ovary cells in culture. Biotechnolology and Bioengineering 103(3): 592–608.

Doyle, C, Butler, M. (1990) The effect of pH on the toxicity of ammonia to a murine hybridoma. Journal of Biotechnology 9: 346-352.

Ducommun P, Kadouri A, von Stockar U, Marison IW. (2002) On-line determination of animal cell concentration in two industrial high-density culture processes by dielectric spectroscopy. Biotechnology and Bioengineering 77: 316–323.

Duncan L, Shelmerdine H, Hughes MP, Coley HM, Hübner Y, Labeed FH. (2008) Dielectrophoretic analysis of changes in cytoplasmic ion levels due to ion channel blocker action reveals underlying differences between drug-sensitive and multidrug-resistant leukaemic cells. Physics in Medicine and Biology 53: N1–N7.

Durocher Y, Butler M. (2009) Expression systems for therapeutic glycoprotein production. Current Opinion in Biotechnology 20: 700-707.

Duval, D, Demangel, C, Miossec, S, Geahel, I. (1992) Role of metabolic waste products in the control of cell proliferation and antibody production by mouse hybridoma cells. Hybridoma 3: 311-322.

Ecker DM, Jones SD, Levine HL. (2015) The therapeutic monoclonal antibody market. mAbs 7: 9-14.

Engstrom, W, Zetterberg, A. (1984) The relationship between purines, pyrimidines, nucleotides, and glutamine for fibroblast cell proliferation. Journal of Biological Chemistry 256: 7812-7819.

Fadok, VA, Voelker, DR, Campbell, PA, Cohen, JJ, Bratton, DL, Henson, PM. (1992) Exposure of phosphatidylserine on the surface of apoptotic lymphocytes triggers specific recognition and removal by macrophages. Journal of Immunology 148: 2207-2216.

Faijes M., Mars A.E., Smid E.J. (2007) Comparison of quenching and extraction methodologies for metabolome analysis of Lactobacillus planatarum. Microbial Cell Factories 6: 27.

Fan, Y, Del Val, IJ, Mueller, C, Sen, JW, Rasmussen, SK, Kontoravdi, C, Weilguny, D, Andersen, MR. (2015) Amino acid and glucose metabolism in fed-batch CHO cell culture affects antibody production and glycosylation. Biotech. Bioeng. 112: 521-535.

Feng HT, Wong N, Wee S, Lee MM. (2008) Simultaneous determination of 19 intracellular nucleotides and nucleotide sugars in Chinese Hamster ovary cells by capillary electrophoresis. Journal of Chromatography 870: 131-134.

Flanagan LA, Lu J, Wang L, Marchenko S, Jeon NL, Lee AP, Monuki ES. (2008) Unique Dielectric Properties Distinguish Stem Cells and Their Differentiated Progeny. Stem Cells 26: 656–665.

Florin, L, Lipske, C, Becker, E, Kaufmann, H. (2011) Supplementation of serum free media with HT is not sufficient to restore growth properties of DHFR-/- cells in fed-batch processes – Implication for designing novel CHO-based expression platforms. Journal of Biotechnology 152: 189-193.

Foster KR, Schwan HP. (1989) Dielectric Properties of Tissues and Biological Materials: A Critical Review. Critical Reviews in Biomedical Engineering 17: 25–104.

Freeze, HH, Elbein, AD. (2009) Glycosylation Precursors. In: Varki, A., Cummings, R. D., Esko, J. D., et al., editors. Essentials of Glycobiology. 2nd edition. Cold Spring Harbor (NY): Cold Spring Harbor Laboratory Press.

Frenzel A, Hust M, Schirrmann T. (2013) Expression of recombinant antibodies. Frontiers in Immunology 4: 1-20.

Gagnon Z. (2011) Cellular dielectrophoresis: Applications to the characterization, manipulation, separation and patterning of cells. Electrophoresis 32: 2466–2487.

Geske FJ, Lieberman R, Strange R, Gerschenson LE. (2001) Early stages of p53-induced apoptosis are reversible. , Published online: 22 February 2001; | doi:10.1038/sj.cdd.4400786 8. http://www.nature.com.proxy1.lib.umanitoba.ca/cdd/journal/v8/n2/full/4400786a.html.

Ghaderi D, Zhang M, Hurtado-Ziola N, Varki A. (2012) Production platforms for biotherapeutic glycoproteins. Occurrence, impact, and challenges of non-human sialylation. Biotechnology & Genetic Engineering Reviews 28: 147-175.

Ghirlando, R, Lund, J, Goodall, M, Jefferis, R. (1999) Glycosylation of human IgG-Fc: influences on structure revealed by differential scanning micro-calorimetry. Immunology Letters 68(1): 47-52.

Godard, T, Deslandes, E, Lebailly, P, Vigreux, C, Sichel, F, Poul, J-M, Gauduchon, P. (1999) Early detection of staurosporine-induced apoptosis by comet and annexin V assays. Histochemistry and Cell Biology 112: 155-161.

Grafstrom, RH, Tseng, BY, Goulian, M. (1978) The incorporation of uracil into animal cell DNA *in vitro*. Cell 15: 131-140.

Grainger, RK, James, DC. (2013) CHO Cell Line Specific Prediction and Control of Recombinant Monoclonal Antibody N-Glycosylation. Biotechnology and Bioengineering. 11: 2970-2983.

Gramer MJ, Eckblad JJ, Donahue R, Brown J, Shultz C, Vickerman K, Priem P, van den Bremer ET, Gerritsen J, van Berkel PH. 2011. Modulation of antibody galactosylation through feeding of uridine, manganese chloride, and galactose. Biotechnology and Bioengineering 108 (7): 1591-1602.

Grob, M, O'Brien, K, Jua Chu, J, Chen, D. (2003) Optimization of cellular nucleotide extraction and sample preparation for nucleotide pool analyses using capillary electrophoresis. Journal of Chromatography 788: 103-111.

Hajnoczky, G, Davies, E, Madesh, M. (2003) Calcium signaling and apoptosis. Biochemical and Biophysical Research Communications. 304: 445-454.

Hamers-Casterman C, Atarhouch T, Muyldermans S, Robinson G, Hamers C, Songa EB et al. (1993) Naturally occurring antibodies devoid of light chains. Nature 363: 446-448.

Hardie DG. (2007) AMP-activated/SNF1 protein kinases: conserved guardians of cellular energy. Nature Reviews Molecular Cell Biology 8(10): 774-85.

Harmsen, E, DeTombe, PP, Willem, DeJong, JW, Achterberg, PW. (1984) Enhanced ATP and GTP synthesis from hypoxanthine or inosine after myocardial ischemia. The American Physiological Society. H37-H43.

Harris CM, Todd RW, Bungard SJ, Lovitt RW, Morris JG, Kell DB. (1987) Dielectric permittivity of microbial suspensions at radio frequencies: a novel method for the real-time estimation of microbial biomass. Enzyme and Microbial Biotechnology 9: 181–186.

Hassell, T, Gleave, S, Butler, M. (1991) Growth inhibition in animal cell culture. The effect of lactate and ammonia. Applied Biochemistry and Biotechnology 30: 29-41.

Hayter, PM, Kirkby, NF, Spier, RE. (1992) Relationship between hybridoma growth and monoclonal antibody production. Enzyme and Microbial Technology 14: 454-461.

Hills, AE, Patel, A, Boyd, P, James, DC. (2001) Metabolic control of recombinant monoclonal antibody N-glycosylation in GS-NS0 cells. Biotechnology and Bioengineering 75: 239-251.

Holm-Hansen, O, Karl, DM. (1978) Biomass and adenylate energy charge determination in microbial cell extracts and environmental samples. Methods in Enzymology 57: 73-85.

Hossler, P, Khattak, SF, Li, ZJ. (2009) Optimal and consistent protein glycosylation in mammalian cell culture. Glycobiology 19: 936–949.

Huang, Y, Holzel, R, Pethig, R, Wang, X-B. (1992) Differences in the AC electrodynamics of viable and non-viable yeast cells determined through combined dielectrophoresis and electrorotation studies. Physics in Medicine and Biology 37: 1499–1517.

Hughes, JFM, Bortner, CD, Purdy, GD, Cidlowski, JA. (1997) Intracellular K+ Suppresses the Activation of Apoptosis in Lymphocytes. Journal of Biological Chemistry 272: 30576.

Huijing, F, Slater, EC, (1961) The use of oligomycin as an inhibitor of oxidative phosphorylation. Journal of Biochemistry 2: 493-501.

Jaitovich, AA, Bertorello, AM. (2006) Na+, K+-ATPase: An Indispensable Ion Pumping-Signaling Mechanism Across Mammalian Cell Membranes. Seminars in Nephrology 26: 386–392.

De Jesus, M, Wurm, FM. (2011) Manufacturing recombinant proteins in kg-ton quantities using animal cells in bioreactors. European Journal of Pharmaceutics and Biopharmaceutics 78: 184–188.

Jing, Y, Egan, SE, Qian, YQ, Borys, MC, Abu-Absi, NR, Li, ZJ. (2011) Dextran sulfate inhibits staurosporine-induced apoptosis in Chinese hamster ovary (CHO) cells: Involvement of the mitochondrial pathway. Process Biochemistry 46: 427-432.

Jones, RG, Thompson, CB. (2009) Tumor suppressors and cell metabolism: a recipe for cancer growth. Genes & Development 23(5): 537-48.

Jones, TB. (1995) Electromechanics of Particles. Cambridge University Press.

Kildegaard, HF, Fan, Y, Sen, JW, Larsen, B, Andersen, MR. (2015) Glycoprofiling effects of media additives on IgG produced by CHO cells in fed-batch bioreactors. Biotechnology and Bioengineering DOI 10.1002/bit.25715.

Kim, NS, Lee, GM. (2002) Response of recombinant Chinese hamster ovary cells to hyperosmotic pressure: effect of Bcl-2 overexpression. Journal of Biotechnology 95: 237–248.

Knabben, I, Regestein, L, Grumbach, C, Steinbusch, S, Kunze, G, Büchs, J. (2010) Online determination of viable biomass up to very high cell densities in Arxula adeninivorans fermentations using an impedance signal. Journal of Biotechnology 149: 60–66.

Kochanowski, N., Blanchard, F., Cacan, R., Chirat, F., Guedon, E., Mare, A., Goergen, J. (2006) Intracellular nucleotide and nucleotide sugar contents of cultured CHO cells determined by a fast, sensitive, and high-resolution ion-pair RP-HPLC. Analytical Biochemistry 348: 243-251.

Kochanowski, N, Blanchard, F, Cacan, R, Chriat, F, Guedon, E, Marc, A, Goergen, J-L. (2008) Influence of intracellular nucleotide and nucleotide sugar contents on recombinant interferon-y glycosylation during batch and fed-batch cultures of CHO cells. Biotechnology and Bioengineering 100(4): 721-733.

Koide, N, Nose, M, Muramatsu, T. (1977) Recognition of IgG by Fc receptor and complement: effects of glycosidase digestion. Biochemical and Biophysical Research Communities. 75: 838-844.

Koopman, G, Reutelingsperger, CP, Kuijten, GA, Keehnen, RM, Pals, ST, van Oers, MH. (1994) Annexin V for flow cytometric detection of phosphatidylserine expression on B cells undergoing apoptosis. Blood 84: 1415-1420.

Labeed, FH, Coley, HM, Hughes, MP. (2006) Differences in the biophysical properties of membrane and cytoplasm of apoptotic cells revealed using dielectrophoresis. Biochimica et Biophysica Acta 1760: 922–929.

Lanks, KW, Li, PW. (1988) End products of glucose and glutamine metabolism by cultured cell lines. Journal of Cellular Physiology 135: 151-155.

Lao, MS, Toth, D. (1997) Effects of ammonium and lactate on growth and metabolism of a recombinant Chinese hamster ovary cell culture. Biotechnology Progress 13: 688–691.

Li, J, Wong, CL, Vijayasankaran, N, Hudson, T, Amanullah, A. (2012) Feeding lactate for CHO cell culture processes: Impact on culture metabolism and performance. Biotechnology and Bioengineering 109(5): 1173–1186.

Lim, Y, Wong, NSC, Lee, YY, Ku, SCY, Wong, DCF, Yap, MGS. (2010) Engineering mammalian cells in bioprocessing – current achievements and future perspectives. Biotechnology and Applied Biochemistry 55: 175–189.

Limoli, CL, Hartmann, A, Shephard, L, Yang, C, Boothman, DA, Bartholomew, J, Morgan, WF. (1998) Apoptosis, Reproductive Failure, and Oxidative Stress in Chinese Hamster Ovary Cells with Compromised Genomic Integrity. Cancer Research 58: 3712–3718.

Liu, B, Spearman, M, Doering, J, Lattova, E, Perreault, H, Butler, M. (2014) The availability of glucose to CHO cells affects the intracellular lipid-linked oligosaccharide distribution, site occupancy and the N-glycosylation profile of a monoclonal antibody. Journal of Biotechnology 170: 17-27.

Lucas, BK, Giere, LM, DeMarco, RA, Shen, A, Chisholm, V, Crowley, CW. (1996) High-Level Production of Recombinant Proteins in CHO Cells Using a Dicistronic DHFR Intron Expression Vector. Nucleic Acids Research 24: 1774–1779.

Lundin, A, Hasenson, M, Persson, J et al. (1986) Estimation of biomass in growing cells lines by adenosine triphosphate assay. Methods in Enzymology 133: 27-42.

Martin, SJ. (1995) Early redistribution of plasma membrane phosphatidylserine is a general feature of apoptosis regardless of the initiating stimulus: inhibition by overexpression of Bcl-2 and Abl. Journal of Experimental Medicine 182: 1545–1556.

Mastrangelo, AJ, Hardwick, JM, Zou, S, Betenbaugh, MJ. (2000) Part II. Overexpression of bcl-2 family members enhances survival of mammalian cells in response to various culture insults. Biotechnology and Bioengineering 67: 555–564.

Matsuyama, S, Xu, Q, Velours, J, Reed, JC. (1998) The Mitochondrial F_0F_1-ATPase Proton Pump Is Required for Function of the Proapoptotic Protein Bax in Yeast and Mammalian Cells. Molecular Cell 2: 327–336.

Maxwell, JC. (1881). A Treatise on Electricity and Magnetism Second. Oxford: Clarendon Press. Vol. I. 2 vols.

Mimura, Y, Lund, J, Church, S, Dong, S, Li, J, Goodall, M, Jefferis, R. (2001) Butyrate increases production of human chimeric IgG in CHO-K1 cells whilst maintaining function and glycoform profile. Journal of Immunological Methods 247: 205–216.

Munoz-Pinedo, C, Ruiz-Ruiz, C, Ruiz de Almodovars, C, Palacios, C, Lopez-Rivas, A. (2003) Inhibition of glucose metabolism sensitizes tumor cells to death receptor-triggered apoptosis through enhancement of death inducing signaling complex formation and apical procase-8 processing. Journal of Biological Chemistry 278: 12759-12768.

Nakajima, K., Kitazume, S., Angata, T., Fujinawa, R., Ohtsubo, K., Miyoshi, E., Tanguchi, N. (2010) Simultaneous determination of nucleotide sugars with ion-pair reversed-phase HPLC. Glycobiology 20: 865-871.

Niepel, M, Spencer, SL, Sorger, PK. (2009) Non-genetic cell-to-cell variability and the consequences for pharmacology. Current Opinion in Chemical Biology 13: 556-561.

Nikolic-Jaric, M, Cabel, T, Salimi, E, Bhide, A, Braasch, K, Butler, M, Bridges, GE, Thomson, DJ. (2013) Differential electronic detector to monitor apoptosis using dielectrophoresis-induced translation of flowing cells (DEP cytometry). Biomicrofluidics 7: 024101.

Nyberg, GB, Balcarcel, RR, Follstad, BD, Stephanopoulos, G, Wang, DIC. (1999) Metabolic effects on recombinant interferon-y glycosylation in continuous culture of Chinese hamster ovary cells. Biotechnol. Bioeng. 62: 336-347.

Opel, CF, Li, J, Amanullah, A. (2010) Quantitative modeling of viable cell density, cell size, intracellular conductivity, and membrane capacitance in batch and fed-batch CHO processes using dielectric spectroscopy. Biotechnology Progress 26(4): 1187–1199.

Panayiotidis, MI, Bortner, CD, Cidlowski, JA. (2006) On the mechanism of ionic regulation of apoptosis: would the Na+/K+-ATPase please stand up? Acta Physiologica 187:215.

Pethig, R, Menachery, A, Pells, S, Sousa, PD. (2010) Dielectrophoresis: A Review of Applications for Stem Cell Research. Journal of Biomedicine and Biotechnology 2010: 182581.

Pilbrough, W, Munro, T, Gray, P. (2009) Intraclonal protein expression heterogeneity in recombinant CHO cells. PLoS ONE 12: doi: 10.1371/journal.pone.0008432.

Plagemann, PGW, Wohlhueter, RM. (1984) Nucleoside transport in cultured mammalian cells – multiple form with different sensitivity to inhibition by nitrobenzylthioinosine or hypoxanthine. Biochimica et Biophysica Acta. 773: 39-52.

Qiao, L, Koutsos, M, Tsai, LL, Kosoni, V, Guzman, J, Shiff, SJ, Rigas, B. (1996) Staurosporine inhibits the proliferation, alters the cell cycle distribution and induces apoptosis in HT-29 human colon adenocarcinoma cells. Cancer Letters 107:83–89.

Quek, LE, Dietmair, S, Kromer, JO,Nielsen, LK. (2010) Metabolic flux analysis in mammalian cell culture. Metabolic Engineering 12(2): 161–171.

Räbinä, J., Mäki, M., Savilahti, E., Järvinen, N., Penttilä, L., Renkone, R. (2001) Analysis of nucleotide sugars from cell lysates by ion-pair solid-phase extraction and reversed-phase high–performance liquid chromatography. Glycoconjugate Journal 18: 799-805.

Rao, RV, Niazi, K, Mollahan, P, Mao, X, Crippen, D, Poksay, KS, Chen, S, Bredesen, DE. (2006) Coupling endoplasmic reticulum stress to the cell-death program: a novel HSP90-independent role for the small chaperone protein p23. Cell Death & Differentiation 13: 415–25.

Rijcken, W., Overdijk, B., Van Den Eijnden, D., Ferwerda, W. (1995) The effect of increasing nucleotide-sugar concentrations on the incorporation of sugars into glycoconjugates in rat hepatocytes. Biochemical Journal 305: 865-870.

Ritter, J., Genzel, Y., Reichl, U. (2008) Simultaneous extraction of several metabolites of energy metabolism and related substances in mammalian cells: Optimization using experiental design. Analytical Biochemistry 373: 349-369.

Ryll, T, Jager, V, Wagner, R (1991) Variations in the ratios and concentrations of nucleotide triphosphates and UDP-sugars during a perfused batch cultivation of hybridoma cells: In Animal Cell Culture and Production of Biologicals. R. Sasaki and K. Ikura (eds.) Kluwer Academic Pub., Norwell, Ma., pp.307-317.

Ryll, T., Wagner, R. (1991) Improved ion-pair high-performance liquid chromatographic method for the quantification of a wide variety of nucleotides and sugar-nucleotides in animal cells. Journal of Chromatography 570: 77-88.

Ryll, T., Wagner, R. (1992) Intracellular ribonucleotide pools as a tool for monitoring the physiological state of in vitro cultivated mammalian cells during production processes. Biotechnology and Bioengineering 40: 934–946.

Saboktakin Rizi, B, Braasch, K, Salimi, E, Butler, M, Bridges, GE, Thomson, DJ. (2014) Monitoring the dielectric response of single cells following mitochondrial adenosine triphosphate synthase inhibition by oligomycin using a dielectrophoretic cytometer. Biomicrofluidics. 8: Doi: 10.1063/1.4903221.

Sanchez-Lozada, LG, Lanaspa, MA, Cristobal-Garcia, M, Garcia-Arroyo, F, Soto, V, Cruz-Robles, D, Nakagawa, T, Yu, M-A, Kang, D-H, Johnson, RJ. (2012) Uric acid-induced endothelial dysfunction is associated with mitochondrial alterations and decreased intracellular ATP concentrations. Nephron Experimental Nephrology 121: e71-e78.

Scarlett, JL, Sheard, PW, Hughes, G, Ledgerwood, EC, Ku, HH, Murphy, MP. (2000) Changes in mitochondrial membrane potential during staurosporine-induced apoptosis in Jurkat cells. FEBS Letters. 475: 267-272.

Schilling, BM, Gangloff, S, Kothari, D, Leister, K, Matlock, L, Zegarelli, SG, Joosten, CE, Basch, JD, Sakhamuri, S, Lee, SS. (2008) Production quality enhancements in mammalian cell culture process for protein production. US Patent 7,332,303.

Schnell, JR, Dyson, HJ, Wright, PE. (2004) Structure, dynamics, and catalytic function of dihydrofolate reductase Annual Review of Biophysics and Biomolecular Structure 33: 119–140

Schwan, HP. 1957. Electrical Properties of Tissue and Cell Suspensions. In: . Advances in Biological and Medical Physics. New York: Academic Press Inc., Vol. V, pp. 147–209.

Scoltock, AB, Cidlowski, JA. (2004) Activation of intrinsic and extrinsic pathways in apoptotic signaling during UV-C-induced death of Jurkat cells: the role of caspase inhibition. Experimental Cell Research. 297: 212-223.

Sebastian, S, Settleman, J, Reshkin, SJ, Azzariti, A, Bellizzi, A, Paradiso, A. (2006) The complexity of targeting EGFR signaling in cancer: from expression to turnover. Biochimica et Biophysica Acta 1766: 120-139.

Sellick, CA, Hansen, R, Maqsood, AR, Dunn, WB, Stephens, GM, Goodacre, R, Dickson, AJ. (2009) Effective quenching process for physiologically valid metabolite profiling of suspension cultured mammalian cells. Analytical Chemistry 81: 174-183.

Sellick, CA, Hansen, R, Stephens, GM, Goodacre, R, Dickson, AJ. (2011) Metabolite extraction from suspension-cultured mammalian cells for global metabolite profiling. Nature Protocols 6: 1241-1249.

Shchepina, LA, Pletjushkina, OYu, Avetisyan, AV, Bakeeva, LE, Fetisova, EK, Dzyumov, DS, Saprunova, VB, Vyssokikh, MYu, Chernyak, BV, Skulachev, VP. (2002) Oligomycin, inhibitor of F0 part of H+-ATP-synthase, suppresses the TNF-induced apoptosis. Oncogene 21: 8149–8157.

Simon, L, Karim, MN. (2002) Control of starvation-induced apoptosis in Chinese hamster ovary cell cultures. Biotechnology and Bioengineering 78: 645–657.

Span, PN, Pouwels, MJ, Olthaar, AJ, Bosch, RR, Hermus, RMM, Sweep, CGJ. (2001) Assay for hexosamine pathway intermediates (uridine diphosphate-N-acetyl amino sugars) in small samples of human muscle tissue. Tech Briefs 47: 944–946.

Spearman, M, Butler, M. (2015) Glycosylation in cell culture: in Animal Cell Culture, Cell Engineering (ed. Al-Rubeai). Springer. Pp. 237-258.

Strober, W. (2001) Trypan blue exclusion test of cell viability. Current Protocols in Immunology Appendix 3:Appendix 3B.

Tey, BT, Singh, RP, Piredda, L, Piacentini, M, Al-Rubeai, M. (2000) Influence of Bcl-2 on cell death during the cultivation of a Chinese hamster ovary cell line expressing a chimeric antibody. Biotechnology and Bioengineering 68: 31–43.

Tibayrenc, P, Preziosi-Belloy, L, Ghommidh, C. (2011) On-line monitoring of dielectrical properties of yeast cells during a stress-model alcoholic fermentation. Process Biochemistry 46: 193–201.

Tomiya, N, Ailor, E, Lawrence, SM, Betenbaugh, MJ, Lee, YC. (2001) Determination of nucleotides and sugar nucleotides involved in protein glycosylation by high-performance anion-exchange chromatography: Sugar nucleotide contents in cultured insect cells and mammalian cells. Analytical Biochemistry 293: 129-137.

Trimarchi, JR, Liu, L, Smith, PJS, Keefe, D. (2000) Noninvasive measurement of potassium efflux as an early indicator of cell death in mouse embryos. Biology of Reproduction. 63: 851-857.

Val, IJd, Kyriakopoulos, S, Polizzi, KM, Kontorvadi, C. (2013) An optimized method for extraction and quantification of nucleotides and nucleotide sugars from mammalian cells. Analytical Biochemistry doi:10.1016/j.ab.2013.09.005.

Vermes, I, Haanen, C, Reutelingsperger, C. (2000) Flow cytometry of apoptotic cell death. Journal of Immunological Methods 243: 167-190.

Volmer, M, Northoff, S, Scholz, S, Thute, T, Buntemeyer, H, Noll, T. (2011) Fast filtration for metabolome sampling of suspended animal cells. Biotechnology Letters 33: 495-502.

Walsh G. 2003. Biopharmaceutical benchmarks 2003. Nature Biotechnology 21: 865-870.

Walsh G. 2010. Biopharmaceutical benchmarks 2010. Nature Biotechnology 28: 917–924.

Webley, SD, Welsh, SJ, Jackman, AL, Aherne, GW. (2001) The ability to accumulate deoxyuridine triphosphate and cellular response to thymidylate synthase (TS) inhibition. British Journal of Cancer 85: 446–452.

Weibl, KE, Mor, J-R, Fiechter, A. (1974) Rapid sampling of yeast cells and automated assays of adenylate, citrate, pyruvate and glucose-6-phosphate pools. Analytical Biochemistry 348: 243-251.

Wesolowski, J, Alzogaray, V, Reyelt, J, Unger, M, Juarez, K, Urrutia, M, Cauerhff, A, Danquah, W, Rissiek, B, Scheuplein, F, Schwarz, N, Adriouch, S, Boyer, O, Seman, M, Licea, A, Serreze, DV, Goldbaum, FA, Haag, F, Koch-Nolte, F. (2009), Single domain antibodies: promising experimental and therapeutic tools in infection and immunity. Medical Microbiology and Immunology. 198: 157-174.

Winchester, B. 2005. Lysosomal metabolism of glycoproteins. Glycobiology 15:1R–15R.

Winder, CL, Dunn,WB, Schuler, S, Boradhurst, D, Jarvis, R, Stephens, GM, Goodacre, R. (2008) Global metabolic profiling of *Escherichia coli* culture: an evaluation of methods for quenching and extraction of intracellular metabolites. Analytical Chemistry 80: 2939-2948.

Witsell, DL, Casey, CE, Neville, MC. (1990) Divalent-cation activation of galactosyltransferase in native mammary golgi vesicles. Journal of Biological Chemistry 265(26): 15731–15737.

Wlodkowic, D, Telford, W, Skommer, J, Darzynkiewicz, Z. (2011) Apoptosis and Beyond: Cytometry in studies of programmed cell death. Methods in Cell Biology 103: 55-98.

Wong, AW, Baginski, TK, Reilly, DE. (2010a) Enhancement of DNA uptake in FUT8-deleted CHO cells for transient production of afucosylated antibodies. Biotechnology and Bioengineering 106: 751-763.

Wong, NS, Yap, MG, Wang, DI. (2006) Enhancing recombinant glycoprotein sialation through CMP-sialic acid transporter over expression in Chinese Hamster Ovary cells. Biotechnology and Bioengineering 93: 1005-1016.

Wong, NSC et al. (2010b) An investigation of intracellular glycosylation activities in CHO cells: effects of nucleotide sugar precursor feeding. Biotechnology and Bioengineering 107: 321-336.

Wormald, MR, Rudd, PM, Harvey, DJ, Chang, SC, Scragg, IG, Dwek, RA. (1997) Variations in oligosaccharide–protein interactions in immunoglobulin G determine the site-specific glycosylation profiles and modulate the dynamic motion of the Fc oligosaccharides. Biochemistry 36: 1370–1380.

Wurm, FM. (2004) Production of recombinant protein therapeutics in cultivated mammalian cells. Nature Biotechnology 22: 1393–1398.

Yun, CY, Liu, S, Lim, SF, Wang, T, Chung, BYF, Teo, JJ, Chuan, KH, Soon, ASC, Goh, KS, Song, Z. (2007) Specific inhibition of caspase-8 and -9 in CHO cells enhances cell viability in batch and fed-batch cultures. Metabolic Engineering 9: 406-418.

Zou, H, Li, Y, Liu, X, Wang, X. (1999) An APAF-1.cytochrome c multimeric complex is a functional apoptosome that activates procaspase-9. Journal of Biological Chemistry 274: 11549–11556.

Zwelling, LA, Altschuler, E, Mayes, J, Hinds, M, Chan, D. (1991) The effect of staurosporine on drug-induced, topoisomerase IImediated DNA cleavage in human leukemia cells. Cancer Chemotherapy and Pharmacology 29: 48–52.

Appendix A

Optimal quenching, extraction and HPLC method for nucleotide / nucleotide sugar analysis*

A.1 Introduction

While most nucleotides and nucleotide sugars are very stable in the cell, others such as ATP have a very rapid turnover rate (1 – 2 sec) (Weibl et al., 1974). This means that the cell metabolism has to be stopped immediately after sampling to obtain an accurate measurement of [ATP] and other metabolites for the bioprocess at that moment in time. Previously reported quenching methods have included a rapid decrease of culture temperature to values below 0° C to inactivate the metabolism (Grob et al., 2003) combined with the use of various chemicals (Winder et al., 2008; Faijes et al., 2007). Other studies have shown that quenching with a low salt solution at 0°C was able to sufficiently quench the culture sample (Dietmair et al., 2010). Several comparative studies using mammalian cells (Dietmair et al., 2010; Sellick et al., 2009) have been performed of which only one focused explicitly on the retrieval of nucleotides and nucleotide sugars involved in glycosylation (Val et al., 2013). Val et al. (2013) reported that they found no need for quenching, which is most likely due to the fact that they extracted the samples immediately after removing them from the culture. However, this is not always feasible especially if multiple or large samples have to be taken. They also did not report the AEC, which is particularly sensitive to the method of quenching and a good indicator for how

* The content of this chapter was included in a paper:
Braasch, K., Villacres, C., and Butler, M. (2015), Evaluation of quenching and extraction methods for nucleotide / nucleotide sugar analysis: in Glyco-Engineering: Methods and Protocols (ed. Alexandra Castilho), Methods in Molecular Biology. Humana Press.

efficiently the metabolism is stopped during sampling.

The choice of an extraction method depends on the metabolite of interest. It is important to choose an efficient extraction procedure that can effectively cause cell lysis and release the intracellular content. Commonly, strong acidic extraction solvents such as perchloric, trichloroacetic, formic acid or tetra butyl-ammonium sulphate have been used for nucleotide extractions (Kochanowski et al., 2006; Sellick et al., 2011). However, degradation of nucleoside triphosphates can occur. Acetonitrile (ACN) (Grob et al., 2003; Au et al., 1989; Feng et al., 2008; Ryll and Wagner, 1991), ethanol (Nakajima et al., 2010; Grob et al., 2003) and methanol (Ritter et al., 2008; Grob et al., 2003) have also been used as organic solvents for the extraction of nucleotides. ACN acts as an effective protein denaturant; causing cell membrane damage that allows the nucleotides and nucleotide sugars to pass through (Grob et al., 2003). Cell exposure to ethanol and methanol causes less damage to the cell membranes compared to acetonitrile (ACN), but requires longer periods of exposure. Hence, low nucleotide yields have been reported when using ethanol (Tomiya et al., 2001; Grob et al., 2003). A different approach to the extraction of nucleotides / nucleotide sugars has been described by Räbinä et al. (2001). This group used a graphitized carbon containing solid-phase extraction (SPE) column (Envi^{TM}-Carb column) taking advantage of the negatively charged nature of the nucleotides and nucleotide sugars. The column binds the nucleotide sugars tightly and allows for subsequent elution with an ion-pairing reagent such as triethylammonium acetate (TEAA) in combination with an elution solvent such as ACN (Räbinä et al., 2001).

Extracted intracellular metabolites have been analyzed by a variety of methods including capillary electrophoresis (CE) (Grob et al., 2003), high-performance liquid chromatography (HPLC), ion-pair reverse-phase high-performance liquid chromatography (RP-HPLC) (Nakajima

et al., 2010; Räbinä et al., 2001; Kochanowski et al., 2006; Ryll and Wagner, 1991) and anion-exchange chromatography (HPAEC) (Tomiya et al., 2001; Val et al., 2013). However, none of the methods has enabled the separation of all nucleotide and nucleotide sugars involved in glycosylation. While the optimized method by Val et al. (2013) (based on Tomiya et al. (2001)) provides a faster chromatography method not all peaks are separated and absorbance is measured using two UV detectors (Val et al., 2013).

A.2 Quenching

Two quenching methods, 60% methanol / 0.85% ammonium bicarbonate "Methanol/AMBIC" (pH 7.4, -20°C, based on Sellick et al. (2009)) and 0.9% NaCl "NaCl" (0.5°C, based on Dietmair et al. (2010)), were compared to control samples ("Control") for which cells were harvested by centrifugation without cooling or quenching. During this study the focus was on the recovery of the nucleotides and the adenylate energy charge (AEC) value. Since the cells were in mid-exponential phase of growth when samples were taken, their high viability would be reflected by high AEC values, expected to be between 0.85-0.95 (Atkinson, 1968). The results show that the "Methanol/AMBIC" method (Sellick et al., 2009; Sellick et al., 2011) was the most effective in resulting in a high AEC value (0.87), which was in the range expected for cells in mid-exponential phase (Figure A.1). In comparison the AEC values determined from the "Control" and "NaCl" quenching procedures were 18% lower. The AEC values of "NaCl" quenched samples showed no significant difference to the AEC values of the "Control". The higher AEC value in the "Methanol/AMBIC" method suggests a higher recovery of ATP and hence more efficient quenching compared to the "NaCl" quenching and "Control" method.

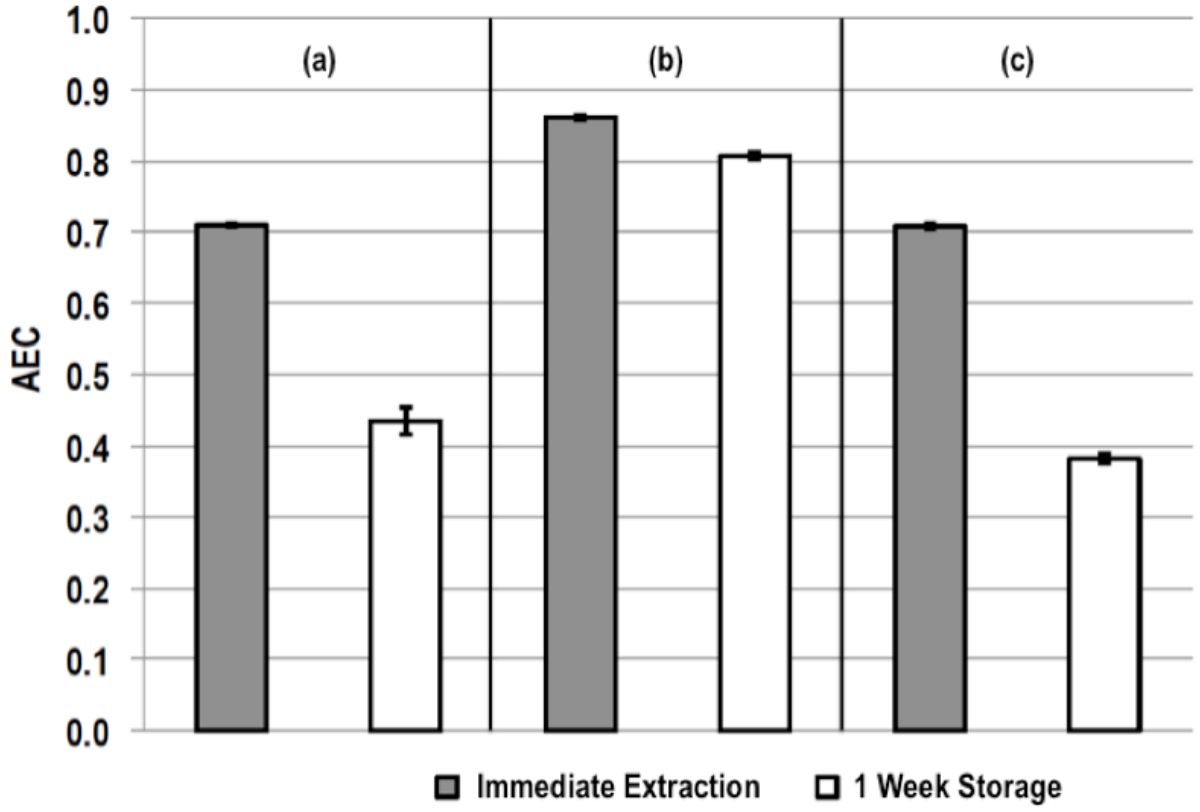

Figure A.1: Comparison of adenylate energy charge (AEC) values determined for (a) Control (no quenching, 37°C), (b) 60% Methanol / 0.85% Ammonium bicarbonate (AMBIC) (pH 7.4, -20°C), and (c) 0.9% NaCl (0.5°C) quenching following immediate or 1-week delayed extraction (n = 2).

In addition, the stability of the quenched samples to retain the initial [ATP] over a 1-week storage period was determined. The "Methanol/AMBIC" quenching procedure was also the most effective in retaining the stability of the samples with only a 7% decrease in AEC after one week storage at -70°C. In comparison the "Control" and "NaCl" samples showed a decrease in the AEC value of 39% and 47% respectively. This suggests that the "Methanol/AMBIC" quenching method minimized ATP breakdown and stabilized cell samples resulting in higher and expected AEC values compared to the alternative methods. Therefore the "Methanol/AMBIC" method was chosen as the preferred quenching protocol.

A.3 Extraction

Four extraction methods were tested to compare the recovery of nucleotide / nucleotide sugars as determined from the sum of integrated peak areas assigned from standard HPLC runs (fmol/cell; Figure A.2). The extraction methods included the use of a solid-phase extraction column (3 mL) "Envi^{TM}-Carb column" (Räbinä et al., 2001), "Cold Methanol" (100%, ice-cold) (Sellick et al., 2009), "Cold Acetonitrile" (50%, ice-cold) (Dietmair et al., 2010) and a "Methanol/Chloroform" procedure (70% methanol, chloroform) based on (Ryll and Wagner, 1991). Figure A.2 shows the recoveries obtained from the combination of the 3 quenching methods with each of the 4 extraction methods. The lowest recovery of nucleotides (~5 fmol/cell) was obtained using "Cold Methanol". In comparison the other three extraction methods resulted in an average recovery of 12-15 fmol/cell. While these three extraction methods showed similar overall recoveries, the "Cold Acetonitrile" method showed higher variability of values (Figure A.2), a clear disadvantage for quantitative analysis. However, the "Envi^{TM}-Carb column" and "Methanol/Chloroform" methods not only showed similar extraction recoveries but also similar variability between samples, with slightly lower variability for the "Envi^{TM}-Carb column" (Figure A.2). Therefore, our preferred method of extraction is the "Envi^{TM}-Carb column" protocol. This provides high recovery of nucleotides with low variability and can be adapted for analysis of multiple samples.As indicated by the star (☼) in Figure A.2 our preferred methods for the recovery of nucleotides and nucleotide sugars is the combination of "Methanol/AMBIC" quenching and "Envi^{TM}-Carb Column" extraction.

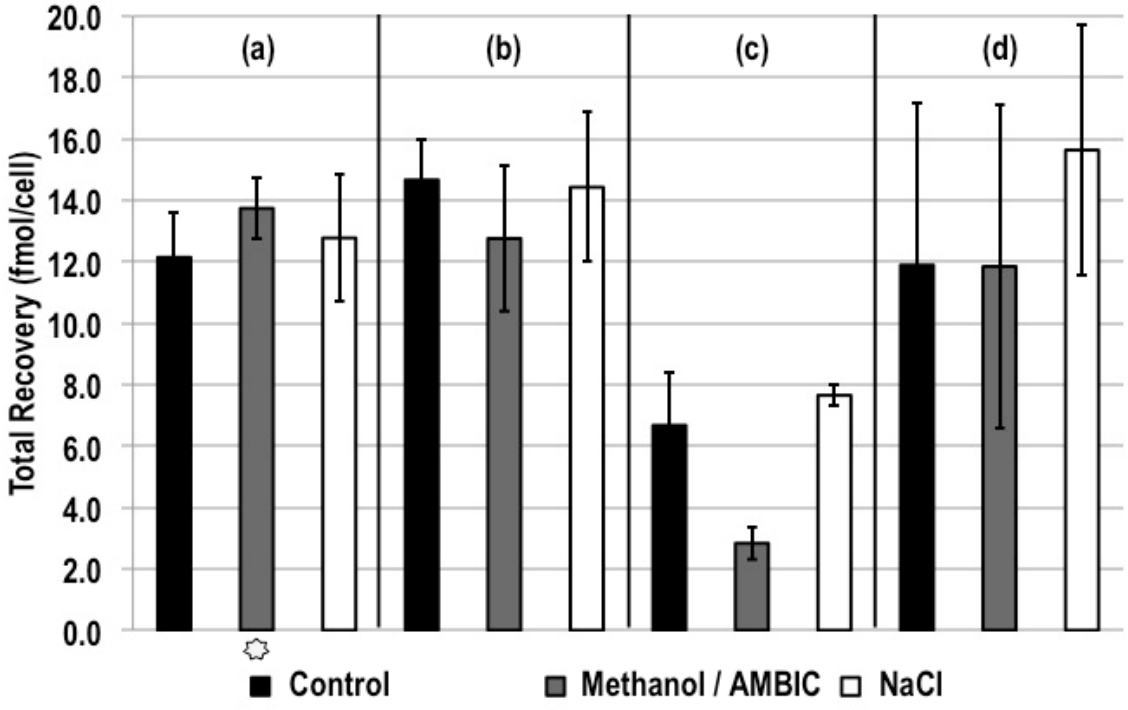

Figure A.2: Comparison of the total nucleotide / nucleotide sugar recovery for quenched and unquenched samples using the following extraction methods (a) an Envi^{TM}-Carb Column, (b) 70% Methanol / Chloroform, (c) 100% ice-cold Methanol and (d) 50% ice-cold Acetonitrile. The values for immediate extraction and after a 1-week delay were averaged (n = 4).
☼ The combination of "Methanol/AMBIC" quenching and "Envi^{TM}-Carb Column" extraction was chosen for the most efficient and reproducible nucleotide / nucleotide sugar extraction process.

A.4 HPLC Analysis

An HPLC method for separation and quantitative analysis of nucleotides extracted from cells was optimized based on a previously published HPAEC method by Tomiya et al. (2001). The original method by Tomiya et al. (2001) allowed for an efficient separation and quantification of nucleotides / nucleotide sugars in the extracted sample, except for CTP with ADP, which co-elute as one peak. This presented a problem for the determination of AEC values, which are important for the viability measurements. To separate CTP and ADP the elution gradient was modified to be more gradual. While this allowed for the separation of CTP

and ADP, CTP is now co-eluting with UDP-GlcNAc. Although UDP-GlcNAc is an important precursor for glycosylation precursor determination the co-elution with CTP is not that much of a disadvantage. An increase in its concentration can be seen due to an overall increase in the peak area of CTP and UDP-GlcNAc since the CTP concentration is not expected to fluctuate very much. Although 30 min longer than the method previously reported (Tomiya et al., 2001), the modification resulted in a better baseline separation allowing more accurate identification and quantification. In addition, the extra 30 min includes 15 min of column re-conditioning to ensure consistent runs. Overall this method allowed the efficient separation and quantification of 18 nucleotides / nucleotide sugars in the extracted sample, except for UDP-GlcNAc and CTP which co-elute as one peak. The original method reported co-elution of CTP with ADP. Our modification allows separation of these nucleotides permitting the calculation of the AEC value for each sample.

A.5 Conclusion

These methods were selected for the sampling, extraction and analysis of intracellular nucleotide and nucleotide sugar pools in CHO cells cultured in suspension. The final protocol was chosen based on the comparison of two quenching protocols and a control (no quenching) in combination with four extraction protocols found in the literature. Special attention was paid to the AEC values, the overall extraction of the metabolites of interest and the methods overall reproducibility. Based on the results it was determined that the "Methanol/AMBIC" quenching with the "Envi^{TM}-Carb column" is the best combination for an efficient and reproducible nucleotide / nucleotide sugar analysis. A modified HPLC analytical method based on Tomiya et al. (2001) was determined optimal for the analysis of extracted samples.